AARHUS
UNIVERSITY

Ph.D. Thesis

Mitigating gaseous emissions following land application of manure slurry in growing crops

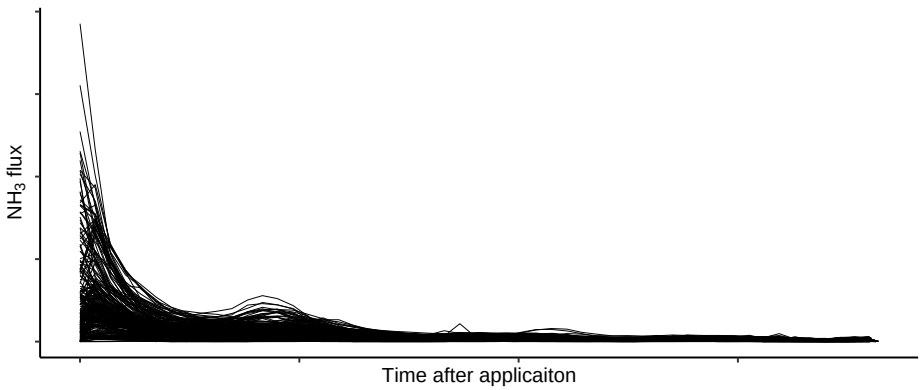

Johanna Pedersen
Department of Engineering
Aarhus University

September 2020

Johanna Pedersen
Aarhus University
Department of Engineering
Finlandsgade 12, 8200 Aarhus N.
Denmark
jp@eng.au.dk

ISBN: 978-87-7507-493-8
DOI: 10.7146/aul.397

This Doctor of Philosophy (Ph.D.) thesis was submitted to the Graduate School of Technical Sciences (GSTS) at Aarhus University, Denmark as part of the requirements for obtaining a Ph.D. degree in Engineering. The Ph.D. study was partly funded by the Danish Agricultural Agency, the Ministry of Environment and Food of Denmark through the *Grønt Udviklings- og Demonstrationsprogram (GUDP)* project *New technology for land spreading of slurry in growing crops* (Danish: *Ny Udbringningsmetode af Gylle i voksende Afgrøder, NUGA*) and partly by GSTS.

The research described in this thesis was conducted from August 2017 to September 2020 under the supervision of Associate Professor Anders Feilberg, and co-supervision of Senior Advisor Tavs Nyord and Honorary Associate Professor Sasha Hafner at the Air Quality Engineering group at the Department of Engineering, Aarhus University at the facilities in Aarhus and Foulum. As a part of the Ph.D. two external research stays were carried out at Agro Intelligence ApS, Aarhus, Denmark (November 2018 – December 2018) and at Agassiz Research and Development Centre, Agassiz, British Colombia, Canada (May 2019 – July 2019), the last under supervision of Research Scientist Shabtai Bittman.

Thesis submitted:
September 30 th 2020

Main Supervisor:
Anders Feilberg
Associate Professor
Department of Engineering
Aarhus University
af@eng.au.dk

Co-supervisors:
Tavs Nyord
Senior Advisor
Department of Engineering
Aarhus University
tavs.nyord@eng.au.dk

Sasha Hafner
Honorary Associate Professor
Department of Engineering
Aarhus University
sasha@hafnerconsulting.com

Acknowledgements

I would like to gratefully acknowledge the funding from GUDP under the Danish Agricultural Agency, the Ministry of Environment and Food of Denmark and GSTS that made this Ph.D. research possible, and the financial support for my research stay at Agassiz Research and Development Center from Fondation Idella, GSTS, and Knud Højgaards Fond.

Firstly, I would like to express my sincere gratitude to my three supervisors, Associate Professor Anders Feilberg, Senior Advisor Tavs Nyord, and Honorary Associate Professor Sasha Hafner for their guidance and support. You have continuously encouraged, motivated, and inspired me these last three years. You have always guided me through uncertainties and challenges when needed. I am grateful for the many things you have taught me and for always keeping your 'doors open'.

During my research stays at AgroIntelli and Agassiz Research and Development Center I spend time with a lot of good colleagues. Their time and collaboration is much appreciated. Particularly, I would like to thank Research Scientist Shabtai Bittman who hosted my research stay at Agassiz. Thank you for welcoming me into your research group. I have enjoyed our many discussions which has brought great value to my work. Two experiments were conducted in collaboration with Associate Professor Sofia Delin and Ph.D. student Karin Andersson from the Swedish Agricultural University at their facilities. Even though the visits were short, the outcomes were great due to their significant contributions. Senior Researcher Rodrigo Labouriau from the Department of mathematics deserves a big thank you for the very fruitful collaboration and discussions on data treatment.

The NUGA-collaboration with Associate Professor Bo Melander and Ph.D. student Margaret Rose Mc Collough from Aarhus University and Søren Mejlstrup Jensen, Research and Development Manager, Samson Agro A/S has been very valuable. Many useful discussions have brought new insights and ideas that was used during the Ph.D. research, thank you for that.

Thank you to all my great colleagues in Air Quality Engineering and at L30

in Foulum. It was the talks with you, coffees, laughs, good advices, and help when needed along the way that made the Ph.D. time enjoyable.

To the technical staff who has accompanied me countless hours out in the field, especially Heidi Grønbæk, Peter Storegård Nielsen, and Per Wiborg Hansen, I would like to express my gratitude. Regardless of sun, rain or freezing cold weather it has always been nice to be out in the field with you and the mood was always good. When things went wrong and failed repeatedly, there was always energy to try again or creativity to find new solutions. I have really appreciated both your flexibility, commitment, and company. Thank you.

Thank you to Kamma, David, and Leon for careful proofreading of the thesis.

The people who deserves the biggest thank you is my family and friends. Without your moral support and practical help, I would not have succeeded. Thank you to my parents and sisters for making it possible to have long working days with fieldwork, attending conferences etc. Especially a big thank you to my mother, Anne, for enabling the research stay in Canada by coming with us, and for helping during the COVID-19 lockdown.

Finally, thank you to Leonora for being exactly who you are.

Contents

Abstract

The agricultural sector contributes substantially to global pollution, as it accounts for a significant amount gaseous emission of ammonia (NH_3), greenhouse gases, volatile organic compounds (VOC), and hydrogen sulfide (H_2S). Agriculture accounts for 75% of the global NH_3 emission with the primary sources being production units for livestock, storage facilities and land application of animal manure. Regardless of continuously updated legislation and regulations, Denmark does not meet the targeted NH_3 reduction agreed upon in the National Emission Ceilings Directive from the European Union.

Field application of liquid animal manure (slurry) accounts for 28% of the NH_3 emissions in Denmark. For decades research has been carried out in order to mitigate these emissions. Several factors affect the emission, such as soil, slurry, and crop type and conditions, meteorological conditions, and application method and rate. Furthermore, all of the parameters interact with each other, making it difficult to isolate and quantify singular effects. Different strategies are applied in order to mitigate emissions, including manure treatment prior to application, optimal field management (crop rotation allowing direct soil injection), timing of application, and low emission application techniques. In growing cereal crops most low emission application techniques apply slurry at the surface in bands.

Although extensive research has been carried out, there is still a knowledge gap concerning the interaction effects. There is a need for a high precision measurement method that can quantify NH_3 emission patterns and relatively small differences in cumulative emission in order to document the effects.

The research in this Ph.D. thesis examines the mechanisms that have an impact on NH_3 emission from surface applied manure in growing crops in order to investigate which circumstances will lead to successful or unsuccessful abatement using both well known and new application techniques. For this purpose, a system of dynamic chambers and online measurements of NH_3 flux with Cavity Ring-Down Spectroscopy was developed. A series of field experiments were conducted with this system under a large variety of conditions. The measuring system allow for NH_3 flux measurements with a low variation, high time resolution, and long

measuring periods. In addition, a new method for quantification of the exposed surface area (ESA) of the slurry at the soil surface over time has been developed. It is demonstrated that the method can be used to gain further knowledge about the slurry-soil interaction after surface application of slurry.

The results presented show that the interaction between soil type and application technique is important when assessing the low emission application techniques in terms of their success in reducing emission. Measurements of ESA proved useful as an explanatory variable to explain why different slurry treatments mitigate the emission under certain circumstances but not under other. The ESA results also highlights the importance of gaining further knowledge about slurry infiltration into the soil after application and characterization of increased dry matter in the air-slurry boundary layer including quantification of a possible crust formation.

Air temperature is known to have an important effect on NH_3 emission. Analysis of data from 19 experiments reveals a positive response of cumulative NH_3 emission to the temperature at application up to a temperature of approximately 14°C. After this, a further increase in temperature does not change the cumulative NH_3 emissions. It is hypothesized that the absence of temperature effect over a certain point is caused by an increased resistance of NH_3 transport due to increased dry matter at the slurry-air interface.

When combining a Proton Transfer Reaction Time-of-Flight Mass Spectrometer with the dynamic chambers, it is possible to measure, identify, and quantify emissions of non-methane VOC and H_2S after field application of manure. The system allows for precise measurements of the emission dynamics over time and estimations of the odor activity value.

Resumé

Landbrugssektoren bidrager væsentligt til global forurening, da den tegner sig for en betydelig mængde emissioner af ammoniak (NH_3), drivhusgasser, flygtige organiske forbindelser (VOC) og hydrogensulfid (H_2S). Landbruget tegner sig for 75% af den globale NH_3 emission, og de primære kilder er produktionsenheder til husdyr, lagerfaciliteter til husdyrgødning og udbringning af husdyrgødning på marker. Trods løbende opdatering af lovgivning og regler på området, overholder Danmark ikke NH_3 reduktionsmålet aftalt i det nationale emissionsloftdirektiv (eng: National Emission Ceilings Directive (NEC)) fra den Europæiske Union.

Udbringning af flydende husdyrgødning (gylle) tegner sig for 28% af NH_3 emissionerne i Danmark. I årtier er der udført forskning for at reducere disse emissioner. Flere faktorer påvirker emissionerne, såsom jordforhold, gylle og afgrøde type og betingelser, meteorologiske forhold, samt udbringningsmetode og mængde. Derudover er der interaktioner imellem de forskellige parameter, hvilket gør det vanskeligt at isolere og kvantificere enkeltvirkninger. Forskellige strategier anvendes for at mindske emissionerne, herunder behandling af gyllen inden udbringning, optimeret markdrift (sædskifte, der muliggør gylle nedfældning), timing af udbringning og lavemissions-udbringningsmetoder. Typisk er lavemissions-
udbringningsmetoder i voksende afgrøder metoder hvor udbringningsmetoden placere gyllen i smalle bånd på jordoverfladen.

Selvom der er udført omfattende forskning, er der stadig et videns gab om vekselvirkningerne mellem jord, gylle og afgrøde. Der er behov for en målemetode med høj præcision, der kan kvantificere NH_3 emissions-dynamikken over tid, med relativt små forskelle i kumulativ emission, for at dokumentere effekterne.

Forskningen i nærværende Ph.d. afhandling undersøger de mekanismer, der har indflydelse på NH_3 emissionen fra gylle overfladeudbragt i voksende afgrøder. Det bliver undersøgt hvilke omstændigheder, der fører til vellykket eller mislykket reduktion af gasemissionerne med kendte og nye udbringningsmetoder. Et system bestående af dynamiske kamre og online NH_3 fluxmålinger med *Cavity Ring-Down Spectroscopy* blev udviklet til formålet. En række felteksperimenter blev

udført med systemet under en stor variation af betingelser. Målesystemet muliggør målinger i lange perioder med lav variation og høj tidsopløsning. Derudover er der udviklet en ny metode til kvantificering af det eksponerede overfladeareal (ESA) af gyllen på jordoverfladen over tid. Det demonstreres, at metoden kan bruges til at få yderligere viden om gylle-jord-interaktionen efter overfladeudbringning af gylle.

Resultaterne viser at interaktionen imellem jord type og udbringningsmetoden er vigtigt ved brug af lavemissions udbringningsmetoder. Målinger af ESA viste sig nyttige som en forklarende variabel til at belyse, hvorfor forskellige behandlingsformer af gyllen kan reducere emissionerne under visse omstændigheder, men ikke under andre. Målingerne af ESA fremhæver vigtigheden af at få yderligere viden om gyllens infiltration i jorden efter udbringning og karakterisering af øget tørstof i gylle-luftgrænselaget grundet infiltration, inklusiv kvantificering af en mulig skorpedannelse.

Det er veletableret at lufttemperaturen har en høj effekt på NH_3 emissionen. Analyse af data fra 19 eksperimenter afslører en positiv respons på kumulative NH_3 emissioner af lufttemperaturen på udbringningstidspunktet til og med en temperatur på ca. 14°C, derefter påvirkede en yderligere temperaturstigning ikke den kumulative NH_3 emission. Det antages, at fraværet af temperatureffekten over et bestemt punkt er forårsaget af en reduceret hastighed af NH_3-transport grundet øget tørstofindhold i gylle-luft grænselaget.

Ved at kombinere en *Proton Transfer Reaction Time-of-Flight Mass Spectrometer* med de dynamiske kamre var det muligt at måle, identificere, og kvantificere emissioner af ikke-methan VOC og H_2S efter udbringning af gylle. Systemet gav nøjagtige målinger af emissionsdynamikken over tid og mulighed for at give et skøn af lugtaktivitetsværdien.

Nomenclature

AD	Anaerobic digestion
ALFAM	Ammonia loss from field-applied animal slurry
(aq)	Denotes that the compound is in the liquid phase
bLS	backward Lagrangian Stochastic
CH_4	Methane
CO_2	Carbon dioxide
CO_3^{2-}	Carbonate
$CO(NH_3)_2$	Urea
CRDS	Cavity Ring-Down spectroscopy
DM	Dry matter
E	Electric field strength
EF	Emission Factor
ESA	Exposed Surface Area
E/N	Reduced electric field
(g)	Denotes that the compound is in the gas phase
GC	Gas Chromatography
GHG	Green-house gases
H^+	Hydrogen ion
HCO_3^-	Bicarbonate
H_3O^+	Hydronium
H_2S	Hydrogen sulfide
IHF	Integrated horizontal flux
IR	Infrared
K_H	Henry's law constant
K_N	Equilibrium constant
M	Compound in air being analyzed
MH^+	Product ion
m/z	mass-to-charge
MS	Mass Spectroscopy/Spectrometer
N	Gas number density

NH_3	Ammonia
NH_4^+	Ammonium
NMVOC	Non-methane volatile organic compounds
NO_2	Nitrogen dioxide
O_2	Oxygen
OTV	Odor threshold value
p_A	Partial pressure of the gas in the gas layer
PAS	Photoacoustic spectroscopy
pK_a	Logarithmic acid dissociation
PTR	Proton Transfer Reaction
R	Gas constant
T	Temperature
TAN	Total ammoniacal nitrogen (NH_4^+, NH_3)
TIC	Total inorganic carbon (CO_2, HCO_3^+, CO_3^{2+})
TOF	Time-of-Flight
Torr	Unit of pressure
Townsend (Td)	Unit of E/N ratio
VFA	Volatile fatty acids (C2-C5 acids)

Chapter 1

Introduction

1.1 Air pollution from agriculture

The demand for agricultural products is expected to increase by 15% during the next decade, due to a growing global population alongside increasing incomes [1–3]. The expanding and increasingly intensive agricultural sector has a high impact on the environment. It imposes an international environmental challenge, through its high demand on water and land resources, use of fertilizer and pesticides, and gaseous emissions [1, 3, 4]. While increasing its output due to growing demands, the agricultural sector needs to minimize its environmental impacts [3, 4]. It is expected that the global agricultural land use will remain at approximately 40% of the terrestrial area in the future [2, 4]. Therefore, the increased output must be obtained by higher productivity through greater yields, improved production intensity and new technological advances [1–4].

During the production of livestock, animal manure is an unavoidable by-product. Liquid animal manure (slurry) can be valuable if utilized correctly, as it contains nutrients that can be recycled for crop growth, and consequently it can be an alternative or addition to synthetic fertilizer. Slurry however is a large contributor to air pollution (Figure 1.1) by emission of ammonia (NH_3) [5], greenhouse gases (GHG) [6], non-methane volatile organic compounds (NMVOC) [7, 8], hydrogen sulfide (H_2S) [9], and particulate matter [10]. Such emissions occur throughout the livestock production chain, at the production sites, storage facilities, and after land application of the slurry.

To protect the environment the European countries have agreed upon emission reduction goals of NH_3, GHG, NMVOC, sulphur oxides (SO_x), nitrogen oxides (NO_x), and particulate matter [12]. In order to reach these goals reductions in emissions from agriculture is required, including emissions from field-

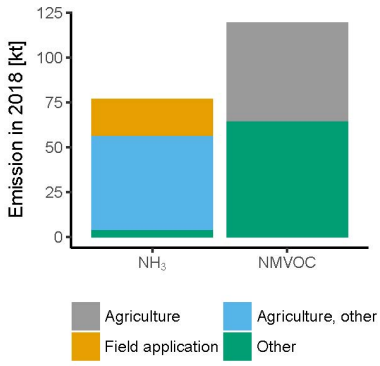

Figure 1.1: *Reported NH_3 and NMVOC emissions in Denmark, year 2018. Data from [11].*

applied slurry. Successfully reducing agricultural emission requires that the whole "manure-chain" (from animal house to field application) is considered, to avoid replacing emissions mitigated at the production site or storing facility with emissions during field application.

1.2 Ammonia emission from field-applied slurry

Ammonia is one of the most significant contributors to acidification of the terrestrial environment, and accounted for the highest share of acidifying potential in the EU-28 countries in 2014 [13]. Ammonia emission contribute to nitrogen deposition which can negatively impact sensitive habitats through eutrophication [14]. Additionally, NH_3 reacts with NO_x and SO_x to form particulate matter [1], which can have severe health impacts on humans. Nitrogen loss to the atmosphere (as NH_3) represents a loss of a valuable nutrient in the plant production chain [1].

Agriculture is the main source of atmospheric NH_3 in the EU-28 countries [13] and accounts for 75% of global NH_3 emission [15]. In Denmark agriculture accounts for 95% of the total NH_3 emissions, with animal slurry applied to soils accounting for approximately 27% of the total (Figure 1.1) [11]. Denmark has committed to reduce NH_3 emissions by 24% by 2020, with no further reduction until 2030 [12]. However, in 2018 (latest reported numbers) the obtained reduction of 15% fell short (Figure 1.2). This is a clear indication that the reduction target will be unachievable, and that immediate action is needed in order to reduce emissions to meet Denmark's emissions target.

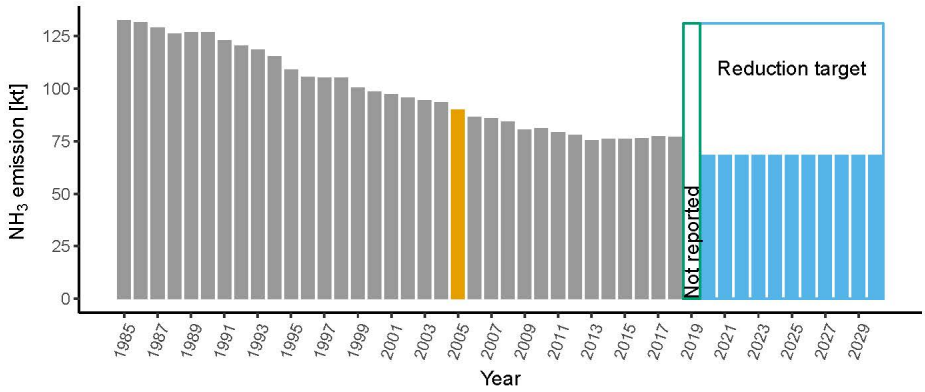

Figure 1.2: *Ammonia emission in Denmark from 1985 to 2018 and the reduction target from 2020 and forth. The reduction target is 24% compared to 2005 (marked with orange) [12]. Data from [11].*

1.3 Mitigation technologies for slurry application in growing crops

Ammonia emission from slurry application is influenced by many factors (Figure 1.3) such as application technique, soil parameters, slurry characteristics, and meteorological conditions [16]. Emissions can be reduced by minimizing the contact area between slurry and the atmosphere, which can be achieved by field application techniques that reduces the exposed slurry area [16–18]. This is most efficiently obtained by incorporation or direct soil injection of the slurry, as these techniques bypass infiltration [18]. Even though these technologies reduce NH_3 emissions and thereby increase the amount of NH_4^+ available for the plants, a higher yield is not observed due to damage of the roots during application [17–22].

In Denmark, approximately 39 million metric tons (oral communication, Mette Hjorth Mikkelsen, March 2020) of animal slurry is field-applied annually, and approximately 35% of this is applied to winter crops [23]. Therefore, low emission application strategies for growing crops is a key contribution to reducing NH_3 emissions from field applied manure.

In growing crops, surface application techniques that reduce the exposed surface area of the slurry can be used. These allow for low emission application, without reducing the crop yield [17]. Common surface application techniques are trailing hoses and trailing shoes. On soil with cereal crops trailing hoses apply the slurry between the rows of plants in narrow bands, whereas the trailing shoes

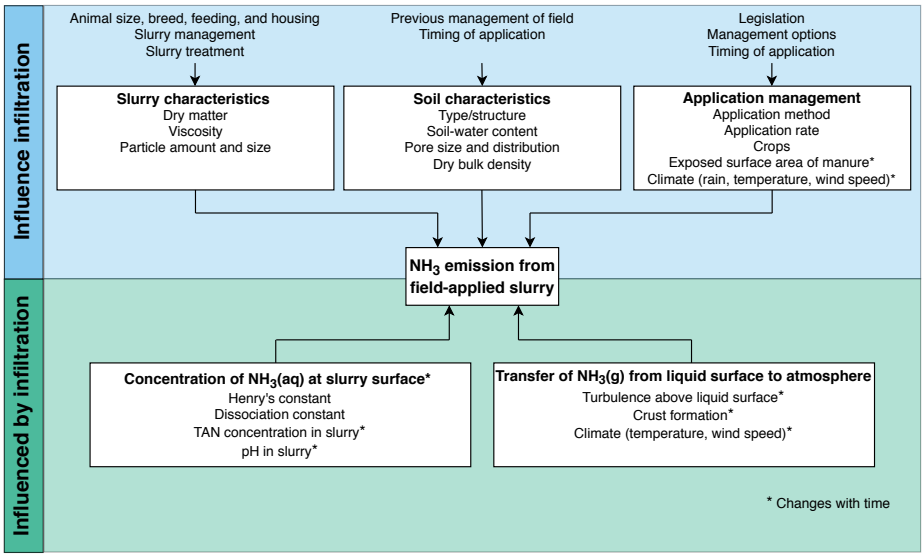

Figure 1.3: *Factors affecting NH_3 emission from field applied slurry.*

create a slit in the soil for the slurry to be deposited in. On grass fields no slits are created with the trailing shoes, but the slurry is typically placed in narrow bands on top of the grass sward or a little below compared to trailing hoses [17].

1.4 Non-methane volatile organic compounds and hydrogen sulfide emissions from field-applied slurry

Non-methane volatile organic compounds and H_2S also contribute to air pollution, with NMVOC acting as a precursors to ozone production in the troposphere. Increased ambient levels of ozone has been found to cause negative health effects for humans by inducing respiratory problems, it has been linked to premature human mortality and it causes reduced crop yield [24]. In addition, tropospheric ozone is a powerful GHG [25].

It is estimated that agriculture account for 46% of the total NMVOC emissions in Denmark (Figure 1.1) [11]. This national emission calculation does not specify the size of the fraction of emissions from animal slurry applied to soil.

Regardless of the large contribution to air pollution, measurements of NMVOC and H_2S after field application of slurry has only been attempted in a few studies

[7, 8, 26–29]. The reported emission factors are highly uncertain as they are estimated by indirect approaches based on scarce data [30]. In addition, NMVOC and H_2S are sources of odor nuisance in local surroundings [31]. In order to gain more knowledge about the impact of NMVOC from agriculture, and how these can be mitigated, measurements from field-applied slurry are urgently required.

1.5 Key challenges

To summarize, several key challenges and knowledge gaps were identified at the initiation of this Ph.D. study and have been addressed:

- A lack of a sufficiently precise method for identification of relatively small differences in cumulative NH_3 emission (<30%) between application techniques.
- Limited knowledge on temporal evolution of emissions of NH_3 and NMVOC.
- A lack of methods for quantifying the effects of the exposed surface area and infiltration and the interaction between these and slurry characteristics.
- The challenge of comparing related field emission experiments performed under different climatic conditions and on different soils.
- Quantification of single factors contributing to variations in emission data from field experiments.

1.6 Thesis overview

The present Ph.D. thesis consist of an introduction, a chapter with background and theory, three scientific papers, two paper drafts, a chapter with miscellaneous findings, followed by a chapter with major findings, conclusions, and perspectives.

The preceding introduction presents the subject and underlines the significant challenges regarding mitigating emissions from field-applied slurry, which leads to the hypotheses and objectives of the research conducted. The background and theory chapter provide state of the art knowledge and the most important findings from previous research as well as theory behind measurement methods and gas analysis techniques, thereby laying the foundation of the research in this thesis. Chapters 3-8 are the peer-reviewed papers, paper drafts, and miscellaneous findings, which is the outcome of the research activities carried out during the Ph.D. study. Major findings throughout the research conducted, and future research perspectives can be found in Chapter 9.

1.7 Hypotheses and objectives

The main aim of this project has been to examine which mechanisms has the greatest impact on processes controlling NH_3 loss from slurry land-applied in growing crops. This has been achieved by investigating which parameters affect the emissions and mitigation of these, in order to gain a better understanding of which circumstances will lead to successful or unsuccessful abatement with known and new application techniques. A dynamic chamber (wind tunnel) system with online Cavity Ring-Down Spectroscopy (CRDS) measurements of NH_3 was selected as the general assessment tool (*measurement system* here forth). An obstacle for development of low NH_3 emission techniques has been the absence of an easy to use and valid method with high time resolution that makes it possible to investigate emission dynamics in order to determine relative differences between techniques. This work creates a better framework for further development of low emission application techniques of slurry in growing crops.

More specifically, four hypothesis with objectives were formed:

- Hypothesis I: The measurement system can be used to measure NH_3 flux after field application of slurry with very low variation and can therefore be used to measure the effect of different low emission application techniques by accurately quantifying relative small differences.
  - Objective I-I: Optimize and evaluate the measuring system to obtain high time resolution measurements of relative emission of NH_3 after field application of slurry, under conditions as true to life as possible.
  - Objective I-II: Measure NH_3 emission after field application of slurry in growing crops and identify key parameters influencing the emission, with a focus on application of slurry at the soil surface.
- Hypothesis II: Exposed surface area of the slurry on the soil surface and infiltration of slurry into the soil after field application can be used as an explanatory variable for NH_3 emission.
  - Objective II-I: Develop a method to quantify ESA of slurry on the soil surface and infiltration of slurry into the soil after field application as a function of time under conditions as true to life as possible.
  - Objective II-II: Measure ESA and infiltration simultaneously with NH_3 emissions from field applied slurry to investigate if they can be used as an explanatory variables.
- Hypothesis III: Increased knowledge about the effect of temperature on NH_3 emission after field application of slurry can be obtained by analysis of data from multiple field experiments.

  - Objective III-I: Use the measuring system to measure NH_3 emission from field applied slurry with varying climate conditions, application techniques, and slurry- and soil properties.
  - Objective III-II: Use statistical modelling to analyze which temperature has the highest effect on cumulative NH_3 emission from field applied slurry and investigate the response pattern.

- Hypothesis IV: The measuring system can be combined with a PTR-TOF-MS in order to measure NMVOC and H_2S flux after field application of slurry, which will increase the understanding of the emission dynamics and improve the sparse knowledge of the area.
  - Objective IV-I: Optimize and evaluate the system for high time resolution measurements of relative emissions of NMVOC and H_2S after field application of slurry.
  - Measure NMVOC and H_2S emissions from field-applied slurry in growing crops and provide new data.

1.8 Publications

1.8.1 Papers

Published

Paper I: Pedersen, J., Feilberg, A., Kamp, J. N., Hafner, S., Nyord, T., 2020. Ammonia emission measurement with an online wind tunnel system for evaluation of manure application techniques. Atmos. Environ. 230. https://doi.org/10.1016/j.atmosenv.2020.117562 (Chapter 3).

Paper VI: Foldager, F. F.; Pedersen, J.; Skov, E. H.; Evgrafova, A.; Green, O., 2019. Lidar-based 3d scans of soil surfaces and furrows in two soil types. Sensors (Switzerland) 19, 1-13. https://doi.org/10.3390/s19030661 (Appendix 1).

Submitted

Paper II: Pedersen, J., Nyord, T., Hansen, M. J., Feilberg, A. 2020, Emissions of VOC and H_2S from field-applied manure by PTR-TOF-MS and wind tunnels. Science of the Total Environment, in review September 2020 (Chapter 4).

Paper III: Pedersen, J., Andersson, K., Feilberg, A., Delin, S., Nyord, T., The effect of surface exposed area on ammonia emission from separated, unseparated, and digested cattle manure. Biosystems Engineering, in review September 2020 (Chapter 5).

Drafts

Paper IV: Pedersen, J., Nyord, T., Feilberg, A., Labouriau, R., Hunt, D., Bittman, S. Working title: Effect of reduced exposed surface area and enhanced infiltration on ammonia emission from untreated and separated cattle slurry (Chapter 6).

Paper V: Pedersen, J., Nyord, T., Feilberg, A., Labouriau, R. Analysis of the effect of air temperature on ammonia emission from band applied slurry (Chapter 6).

Paper VII: Lemes, Y. M., Pedersen, J., Fontaine, D., Møller, H. B., Erikesen, J., Sørensen, P., Nyord, T., Feilberg, A. Effect of catch crop addition, dilution of manure and anaerobic digestion on ammonia and odours emissions from land-applied manure (not included in thesis).

1.8.2 Conference contributions

Published

Pedersen, J., Feilberg, A., Nyord, T., February 2019. Application of PTR-TOF-MS for measurement of odor release from slurry application in field trials using dynamic chambers. Abstract and Poster. PTR-MS conference, Innsbruck, Austria.

Pedersen, J., February 2020. Effects on ammonia and odor emissions when using alternatives to trailing hoses for field application of manure. Oral presentation. Plantekongres, Herning, Denmark.

Submitted[1]

Pedersen, J., Feilberg, A, Andersson, K., Delin, S., Nyord, T, 2021. Surface exposed area over time after field application of manure. Abstract for oral presentation. Ramiran, Cambridge, United Kingdom.

Andersson, K., Delin, S., Pedersen, J., Nyord, T., 2021. Ammonia emissions from cattle slurry application on a Swedish clay soil – effects of slurry treatment and application method. Abstract for oral presentation. Ramiran, Cambridge, United Kingdom.

[1] Abstracts were submitted for Ramiran 2020, that was to be held in September 2020. The conference was postponed to 2021 due to COVID-19.

Chapter 2

Background

This chapter contains background information and theory about gaseous emissions after field application of slurry. The first section of the chapter addresses the general theory of emissions from a liquid to the atmosphere. The following section is a short review of the different factors that influence the emissions. Lastly, different measurement methods are described, with a focus on the methods used during the work for this thesis.

This Ph.D. project addresses how NH_3 emissions from field-applied slurry in growing crops may be reduced by different application techniques, and which factors are most important for retention of NH_3 as a valuable nutrient. Therefore, this chapter will focus on theory and background of NH_3 emissions from slurry and application techniques related to application in growing crops.

When slurry is applied on land, several gasses are emitted. Information about the solubility and odor threshold value (OTV) for NH_3, H_2S, and selected NMVOC can be found in Table 2.1. The concentration levels are highly variable, as the concentrations depends on many factors such as climatic conditions, soil and slurry properties, and measurement approach. The NMVOC after field application of slurry has only been measured with static or dynamic chambers, which are inadequate for absolute emission measurements. Therefore, the concentrations presented in the table are included with the intention of showing the broad ranges and are not meant to be perceived as absolute values. Dynamic chambers are in general assessed to be more realistic and may still provide indications of the magnitude of emissions.

Table 2.1: *Measured concentration levels after field application of slurry, Henry's law constant (K_H), and odor threshold values (OTV) for NH_3, H_2S, and selected NMVOC.*

Compound	Mass [g mol^{-1}]	Measured concentration levels right after application [ppb][a]	$K_{H,298K}$ [mol kg^{-1} bar^{-1}][c]	OTV
Ammonia	17.03	>2000[b]	67.8	1500[g]
Methanol	32.04	<1 – 5	220	33000[g]
Hydrogen sulfide	34.1	<1 - 100	0.1[k]	0.8[h]
Acetaldehyde	44.05	<1 – 20	13.8	1.5[g]
Methanethiol	48.11	<1 – 30	0.31	0.03[h]
Acetone	58.08	<1 - 200	28.3	42000[g]
Trimethylamine	59.11	<1 – 7	9.5	0.08[h]
Acetic acid	60.05	2 – 170	6300	8.3[h]
Dimethyl sulfide	62.13	<1 – 3	0.56	2.3[h]
2-Butanone	72.11	<1 – 11	17.7	440[g]
Propionic acid	74.08	<1 – 34	4733	5.7[h]
2,3-Butanedione	86.09	<1 – 14	65.5	0.06[h]
Butanoic acid	88.11	<1 - 115	3300	0.23[h]
Phenol	94.11	<1 - 140	2900	8.4i
C5 carboxylic acids	102.13	<1 – 60	2200[d], 1200[e,f]	0.2[g], 0.09[f,h]
4-Methylphenol	108.13	<1 - 300	1300	0.02[h]
C6 carboxylic acids	116.16	<1 - 13	1300[k]	0.6[g,i], 0.4[g,j]
Indole	117.15	<1	1129	0.06[h]
4-Ethylphenol	122.16	1 - 15	1218	0.4[h]
Skatole	131.17	<1 - 30	1022	0.003[h]

[a]From [7, 8, 26–29] except NH_3. [b]Jesper Kamp, oral communication, July 2020.
[c]From [27], unless otherwise stated. [d]Pentanoic acid. [e]From [32]. [f]Isovaleric acid.
[g]From [33]. [h]Calculated mean from [34]. [i]Hexanoic acid. [j]Iso hexanoic acid. [k]From [35]

2.1 Processes of gaseous emission from liquid slurry

When gaseous compounds are emitted from liquid slurry to the atmosphere, both diffusive and convective mass transport is involved. As the total ammoniacal nitrogen (TAN) concentration, slurry properties (e.g. crust formation), and ambient air conditions (e.g. wind speed and temperature) all affect the emission potential, and these varying with time, the emissions from a slurry surface has to be considered as a dynamic system. The emissions from which can be described by three steps (Figure 2.1) [32, 35]:

1. Transportation of the compound in the slurry to the air-liquid boundary

layer of the slurry by diffusion.

2. Transfer of the gas over the air-liquid boundary layer.
3. Transport into the atmosphere from the interface by convection.

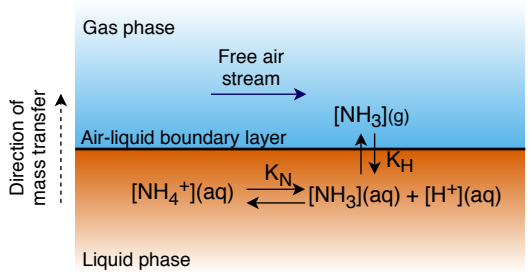

Figure 2.1: *Mechanism related to NH_3 release from manure. $[NH_3]_g$ is the free NH_3 in the gaseous phase, $[NH_3]_{(aq)}$ is the free NH_3 in the liquid phase, $[NH_4{}^+]_{(aq)}$ is the free $NH_4{}^+$ in the liquid phase, K_H is Henry's constant and K_N is the equilibrium constant for $NH_4{}^+/NH_3$. Free after [36, 37].*

Diffusion is driven by the concentration gradient of the compounds and convection is the transport of the compound caused by movements of air or liquid containing the compound. The significance of the two processes on the emissions is determined by the local conditions [32]. Convection often yields in a faster transport compared to diffusion [32]. For relatively water-soluble compounds emitted from field-applied slurry, the air-side resistance above the emitting surface practically determines the overall emission rate. This is due to high convection caused by turbulence intensity, which is created by the velocity of air [35, 38, 39]. This effect on the NH_3 and NMVOC emissions has been found in several studies [5, 40, 41]. As the concentration of TAN in the slurry, slurry properties (e.g. dry matter content), and ambient air conditions continuously change over time, the emission potential will change as well.

Directly above the emitting surface, the differences in concentrations of the emitting compound drives the release from the surface of the liquid layer to the air phase. Henry's law can be used to describe the partitioning of the compound between the liquid and gas phase (Equation 2.1). A high Henry's law constant (K_H (M atm^{-1}) or H (mol$_{(aq)}$ L^{-1} / mol$_{(g)}$ L^{-1})) indicate a high solubility of the gas in the liquid phase, whereas a low Henry's law constant indicates a low solubility in the liquid phase [32].

$$K_H = \frac{[A]_{(aq)}}{p_A} \text{ or } H = \frac{[A]_{(aq)}}{[A]_{(g)}} = \frac{[A]_{(aq)}}{p_A} RT = K_H RT \tag{2.1}$$

$[A]_{(aq)}$ is the concentration of the compound in the liquid phase, $[A]_{(g)}$ is the concentration of the compound in the gas phase, p_A is the partial pressure of the gas in the gas layer, R is the gas constant and T is the temperature.

Only the uncharged compounds are emitted from the liquid layer. The concentration of the uncharged species can be calculated from the total concentration, pH, and equilibrium constant (Equation 2.2, NH_3 as example). Thereafter Henry's law can be used to calculate the concentration in the gas phase directly above the emitting surface (Equation 2.3, NH_3 as example) [32].

$$[NH_3]_{(aq)} = \frac{[TAN]_{(aq)}}{1 + [H^+]_{(aq)}/K_N} \tag{2.2}$$

$$[NH_3]_{(g)} = \frac{1}{H_{NH3}} \frac{[TAN]_{(aq)}}{1 + [H^+]_{(aq)}/K_N} \tag{2.3}$$

$[NH_3]_{(aq)}$ is the concentration of NH_3 is the liquid phase, $[NH_3]_{(g)}$ is the concentration of NH_3 is the gas phase, TAN is the concentration of total ammoniacal nitrogen in the liquid phase (TAN = NH_4^+ + NH_3), $H^+_{(aq)}$ is the concentration of hydrogen ions in the liquid phase, K_N is the equilibrium constant for NH_4^+/NH_3, and H_{NH3} is the Henry's law constant of NH_3 ($mol_{(aq)}$ $L^{-1}/mol_{(g)}$ L^{-1}), all concentrations are in mol L^{-1}.

The proton activity in the slurry is buffered by total inorganic carbon (TIC = CO_2 + HCO_3^- + CO_3^{2-}), TAN, and volatile fatty acids (VFA = C_2 – C_5 acids). The concentration of these changes with time after slurry application, due to infiltration and emission. At low pH there is a higher emission potential for acidic compounds, such as VFA and H_2S, and at higher pH the emission potential is higher for basic compounds, such as NH_3. Emission of these compounds will affect the proton activity in the slurry, resulting in changes of the slurry pH [32, 38]. Emission of NH_3 will lead to a net increase in the amount of hydronium (H_3O^+) in the slurry, resulting in a decrease of pH, whereas emission of acetic compounds will increase pH as the concentration of H_3O^+ in the slurry will decrease [32, 38]. Emission of carbon dioxide (CO_2) will also increase pH as it is acidic in aqueous solution [38, 42]. At neutral pH, inorganic carbon is mainly present as HCO_3^- in equilibrium with dissolved CO_2, which in turn is in equilibrium with gaseous CO_2. From Le Chatelier's principle it is seen that loss of CO_2 leads to consumption of H^+ (higher pH):

$$H^+(aq) + HCO_3^+(aq) \rightleftharpoons CO_2(aq)(+H_2O(aq)) \rightleftharpoons CO_2(g) \tag{2.4}$$

After application of slurry the liquid fraction will start to infiltrate into the soil and liquid will evaporate, changing the physical and chemical properties of the remaining emitting layer at the soil surface [35]. Over time, only the solid fraction of the slurry will remain at the soil surface. The rate and magnitude

of this infiltration is controlled by several soil- and slurry parameters as well as climatic conditions [40, 43, 44]. When the slurry dries out at the surface, a crust is formed. The crust formation can be rapid or slow, depending on the climatic conditions as both wind speed, temperature, solar radiation, and rainfall rate will have an effect. When the crust is formed it functions as a physical barrier between the compounds in the slurry and the atmosphere, hence reducing the emissions [45]. This occurs if the main mode of transport from the bulk liquid to the surface is by molecular diffusion in the liquid phase, which is expected for relatively water-soluble compounds with low vapor pressure and high affinity to dry matter (relative to the gas-phase). This is opposed to porous gas-phase transport in the dry crust, which may be more prevalent for relatively volatile compounds with lower surface affinity.

2.2 Ammonia emission from field-applied slurry

For several decades, researchers have investigated what influences NH_3 emission from field-applied slurry, and how emission can be mitigated. Large advancements have been made, and many countries have continuously updated their legislation to reduce national emissions and to reach reduction targets.

Regardless of the major advantages in NH_3 emission research in recent decades, the wide variation and associated uncertainty in emission factors and reduction potential of different techniques remains a significant challenge [18, 46]. There are unanswered questions regarding the magnitude of influence of the different parameters affecting the emissions [18, 46] Especially the interaction between the slurry and soil is an area with a clear knowledge gap.

2.2.1 The effect of slurry properties

Slurry is a complex mixture of animal feces and urine, with different amounts of bedding materials, spilt feed, and water used for cooling down the animals and/or washing the floors [48]. Slurry contains organic matter: carbohydrates, lignin, VFA, organic liquids, and proteins, and elements from the animal diets: nitrogen, phosphorous, potassium, sodium, calcium, magnesium, manganese, iron, zinc, copper, and others [49, 50].

The chemical and physical characteristics of the excreted slurry depends on the livestock (breed, size, sex etc.), diet composition, and environmental factors [49]. After excretion, slurry management at the livestock production site and during storage will affect the final properties of the slurry [49–51]. Due to high variability in the design of the livestock production and storing facilities, methods of slurry collection and handling, as well as differences in climate, the slurry properties at the time of field application can vary greatly [52–54].

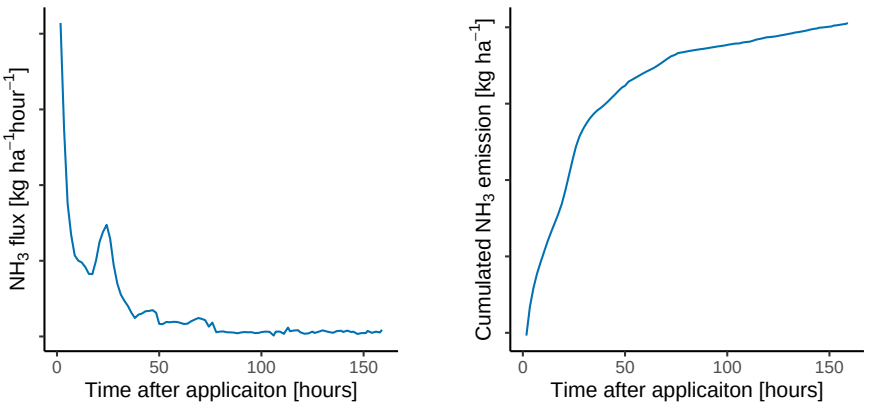

Figure 2.2: *a: Typical pattern of NH_3 emission flux after surface application of liquid slurry to a field. b: Usual pattern of cumulative NH_3 emission after surface application of liquid slurry to a field.*

Depending on the livestock category and management, 4-45% of the nitrogen in the livestock feed is transformed into animal protein. The remaining nitrogen is excreted as organically bound nitrogen, primarily in the form of urea ($CO(NH_3)_2$) in urine [48, 50]. Urea is hydrolyzed right after excretion by the enzyme urease to NH_3, NH_4^+, and bicarbonate (HCO_3^-) (Equation 2.5). Urease is present in abundant amounts, as bacteria present in the feces produce it. Therefore, almost all urea is hydrolyzed rapidly after urine excretion [48].

$$CO(NH_3)_2 + 2H_2O \leftrightarrow NH_3 + NH_4^+ + HCO_3^- \tag{2.5}$$

The combined amount of NH_3 and NH_4^+ is called total ammoniacal nitrogen (TAN). An instant equilibrium occur between the two, and the dissociation is highly dependent on pH, as there will be a 10-fold increase in NH_3 in the slurry each time pH increase by one (Equations 2.2 and 2.3) [35, 55].

pH in the slurry is primarily buffered by TAN, VFA, and TIC. Carbon dioxide (CO_2) is produced via microbial decomposition, which contributes significantly to the TIC pool [35]. After field application of slurry high emissions of CO_2 and NH_3 occur [35]. Due to a much lower solubility of CO_2 in water compared to NH_3, it will emit rapidly [38, 56]. The rapid CO_2 emission increases pH of the slurry, which will result in higher emission of NH_3. After a period of 24-48 hours pH will decline due to buffering capacity of the soil and slurry [35, 50].

The amount of dry matter (DM) in the slurry has been found to have a high

effect on the NH_3 emission in several studies. A higher emission is observed from slurries with higher DM content [40, 44, 57–59], as it reduces infiltration by sealing soil pores [35, 43]. High viscosity has also been found to increase emissions [35]. An exponential correlation between viscosity and DM can be observed for both cattle and pig slurry, with a generally higher viscosity from cattle slurry compared to pig slurry at the same DM content [60, 61]. Anaerobically digested (AD) slurry has not been found to exhibit the same correlation pattern, most likely due to co-digestion of other substrates with the slurry [61].

Different slurry handling practices are used before field application in order to reduce NH_3 emission, with the most common ones being separation, AD, and acidification, all of which will alter both the physical and chemical properties of the slurry.

Separation splits the slurry into a solid and a liquid fraction, which gives a higher flexibility of slurry management and nutrient utilization [50, 54]. Lower NH_3 emissions has been reported from the liquid fraction [62–64], which has been attributed to faster infiltration caused by lower DM content and viscosity [50, 61, 65].

Anaerobic digestion of slurry produces biogas (CO_2 and methane (CH_4)) through microbiological degradation of organic matter. The production of CH_4 is the primary goal, as it is utilized as an energy source [66, 67]. During AD of slurry, other substrates, such as straw, slaughterhouse waste products, and food waste, can be added for co-digestion. As the organic matter in the slurry is converted into biogas, a fraction of the organic N is mineralized to NH_4^+, increasing the overall TAN concentration in the digestate compared to the undigested slurry [54, 65]. Furthermore, the AD process reduces the DM content of the slurry [50, 54, 65], and increases pH [65]. Different results have been reported concerning the emissions of NH_3 from field applied digested slurry compared to untreated slurry. Some studies have found that the low DM compensates for the higher pH by increasing infiltration, and therefore NH_3 emission from digested slurry is not higher than that of untreated slurry [68, 69]. This is in contrast to [62, 64, 70], who found higher emission from digested slurry compared to untreated slurry.

Acidification is used to decrease the concentration of NH_3 relative to NH_4^+ in the slurry, by lowering the slurry pH (Equation 2.2). The acidification can be performed at the livestock production house, in the storage tank, or immediately before application to soil. The most commonly used acid is sulfuric acid, and the pH of the slurry is typically lowed to approximately 5.5 for storage acidification [71]. During field acidification Danish law requires that pig and cattle slurry is acidified to pH $<$6.4 [72]. Acidification has been found to reduce NH_3 emission from field-applied slurry in several studies [63, 73–77].

2.2.2 The effect of soil properties and infiltration

It is widely recognized that soil type and conditions highly effect NH_3 emission from field-applied slurry, as it influences the infiltration rate [40, 58, 77–79]. Slurry infiltration reduces NH_3 emission by reducing the TAN concentration at the soil surface, thereby lowering the emission potential [35].

Soil can be described as a three phase system comprising of a soil, a liquid, and a gaseous phase [80]. The soil phase mainly consists of inorganic components (sand, silt, clay, gravel, and stone), and the relative amounts of these can be used to classify the soil type. Furthermore, the soil phase constitutes organic components of degraded and decomposed plant materials. The combination of the three phases gives a complex non-stationary heterogeneous system. The size and amount of macro and micro pores are continuously varying which influences the infiltration capacity of the soil, as the relative sizes of the three phases are constantly changing as they depends on climate, vegetation, and animal and human activities [80, 81].

The soil-water content has been linked to the infiltration of the slurry and thereby NH_3 emissions in several studies. Some studies concludes that a lower soil-water content decreases NH_3 emissions by increasing infiltration [82, 83], whereas other studies find that the emissions are lowest at a higher soil-water content, and attributes this to the dryer soil being hydrophobic [58]. Slurry type (and hence viscosity) as well as soil type has also been found to have a significant effect on slurry infiltration into the soil, and thereby the NH_3 emission [43, 59].

2.2.3 The effect of surface application technique

Comprehensive research has been conducted showing how different surface application techniques, such as trailing hoses and trailing shoes [18, 58, 69, 84–86], and incorporation techniques [58, 87, 88], reduce NH_3 emission compared to broadcast application. Incorporation of the slurry into the soil is by far the most efficient reduction technique, but it is not suitable in growing crops as it can reduce crop yield [22], leaving surface application as the best option when applying slurry in growing crops. Optimal surface application prevent deposition of slurry on the crops, minimize ESA and increase infiltration.

While surface application undoubtedly has lower emissions compared to broadcast, there is still a large variation in collected data and contradictory results when it comes to comparing trailing hoses and trailing shoes. These differences concerning whether trailing shoes or trailing hoses are the most efficient application method for mitigating NH_3 emission in growing crops are most likely due to differences in all the other parameters affecting the emission. As trailing shoes require a higher draft force it is a more costly application technique [88], therefore it is desirable to know which emission abatement approach is the most cost

effective.

2.2.4 The effect of timing of application

Climatic conditions, such as air and soil temperature, wind speed and rainfall during slurry application and in the following period influences the emission. These factors cannot be controlled in field experiments but will be determined by the timing of the application.

Ambient temperature has been correlated with the flux in several studies [40, 77–79, 89]. Besides directly increasing the NH_3 emission, increasing temperatures will cause more evaporation of water from the slurry, which will increase the TAN concentration in the slurry-liquid and thereby give a higher emission potential [35]. Solar radiation has been positively correlated to NH_3 emission [45], whereas air temperature did not have a significant effect, but the study speculates that a higher temperature and low humidity resulted in crust formation which reduced NH_3 emission. Rainfall suppresses the NH_3 flux rates [35, 79, 89–91] by transporting the slurry liquid, and thereby the TAN, into the soil. Wind speed has also been recognized as having a large influence on NH_3 emission [5, 40, 57], as higher wind speeds cause higher turbulence at the soil surface, hence driving the transport of NH_3 from the liquid-gas interface into the atmosphere.

2.2.5 Models for prediction of ammonia emission from field-applied slurry

Measurements of NH_3 emissions are expensive and laborious, and as only one or two of the parameters influencing the emissions can be studied at once the resulting data has limitations. As both timing (i.e. climatic conditions during the measuring period), and soil and slurry conditions will vary between experiments if not performed at the exact same time, it complicates comparison of results between experiments and thereby makes it difficult to draw general conclusions. Modelling can be used to overcome some of the challenges arising due to the limitations of experimental measurements and can be used for calculating or estimating emission factors (EF) and absolute emission on a regional level.

Several different modelling approaches can be used, and depending on the required output some are better suited than others [92]. Models can give information about what factors have the biggest influence on ammonia emissions and their magnitude, which can be used to develop management strategies in order to mitigate emissions. Moreover, models can calculate emission factors used for national inventory reporting and legislative purposes. An important consideration is how much detail the models should be able to describe and their level of complexity. Especially the latter point will usually affect how simple it is to use

the model. Ammonia emission models can be general or region-specific [16, 92].

Both empirical [40, 93], semi-empirical [16], and mechanistic (process-based) [94] models have been used to describe the NH_3 emission after field application of slurry. The mechanistic models usually provides more accurate data [92], but have a higher complexity and require more input variables including variables for which there are not data, e.g. infiltration rate, compared to empirical models [16, 92].

Volt'Air

Volt'Air is a mechanistic model developed by Génermont and Cellier (1997) [94]. The model estimates the NH_3 emission by simulating the influence of various factors, such as transfer and equilibria of NH_3 in the topsoil, and between the soil and atmosphere. The model consists of six sub-models. Three of the sub-models concern the transfers and equilibria between TAN species and the other three simulates heat and water transfer in the soil layer. The input data includes meteorological data and soil and slurry information. Furthermore, the model requires a pH measurement of the slurry after field application. If this is not provided, an empirical adjustment is performed to reflect the pH increase after application [94].

The model was implemented by Smith et al. (2009) [95], who validated the model results against data from wind tunnel trails. They showed that the model was most sensitive against pH, which is in agreement with Génermont and Cellier (1997) [94]. They found a reasonable agreement between the model predictions and empirical data, with an overall underestimation by the model. Within the first 24 hours after slurry application the NH_3 emission was underestimated by 29.5% [95].

ALFAM1

Søgaard et al. (2002) [93] published the first ALFAM (Ammonia Loss from Field-applied Animal Slurry) model. The ALFAM model is an NH_3 loss rate model where empirical European NH_3 emission data has been collected and statistically modelled with a non-linear regression procedure. They describe the emission mathematically, with loss rates as the response variable and several multiplicative sub-models. The model finds that the variables which significantly affect the emission are soil-water content, air temperature, wind speed, slurry type, DM and TAN content of slurry, application method and rate, slurry incorporation, and measuring technique.

Huijsmans et al. (2018)

Huijsmans et al. (2018) [40] statistically analyzed empirical data from several experiments measuring NH_3 emission after application of liquid cattle slurry to grassland with logistic regression models. They modelled regression models for eight shifts, which were the amount of measuring intervals used in the field experiments. In each shift the response variable was the NH_3 emission, expressed as the percentage still present at the start of the shift. The models were developed separately for broadcast spreading, band application (trailing shoes), and shallow injection.

They found that wind speed, air temperature, soil type, TAN and DM content of the slurry, application rate, and grass height were significant explanatory variables, with wind speed and air temperature being the most important. They did not see an effect of pH, which they assign to a small variation in pH within the experiments.

ALFAM2

An updated ALFAM model (ALFAM2) was made by Hafner et al. (2019) [16]. They added data to the original ALFAM database and made a semi-empirical dynamic model for predicting NH_3 emission from field-applied slurry. The model identified a fast and slow pool from where emission take place. The fast pool occurs when the slurry is in direct contact with the atmosphere and the slow pool is the fraction of slurry from where emission is not occurring due to infiltration or other processes. The model tracks the mass of TAN, and its partitioning between the slow and fast pool. The model has several primary parameters with values linked to a set of predictor variables, such as weather conditions, slurry DM, and application technique. They identified seven important variables controlling the NH_3 emission: slurry DM, application method and rate, incorporation, air temperature, wind speed, and rainfall rate, with the most important being application technique. A high variation occurs with the model, mainly due to overall differences between test organizations. This may be explained by methodological biases, or differences in emission due to local soil properties or other factors not included in the model. The authors suggest that improving the model requires linking the infiltration rate to soil properties. The results also highlight the need for one or more commonly accepted and verified reference methods.

2.3 Non-methane volatile organic compounds and hydrogen sulfide emissions from field-applied slurry

Only a few studies have measured NMVOC and H_2S from field-applied slurry [7, 8, 26–29, 96], leaving a huge knowledge gap regarding quantification of the amounts which result in high uncertainties regarding the effect on the environment. Emissions of NMVOC and H_2S are undoubtedly highly affected by soil and slurry properties as well as timing and method of application, like emission of NH_3. Therefore, research is highly needed to enlighten the research area.

2.4 Measurements of ammonia, non-methane volatile organic compounds, and hydrogen sulfide from field-applied slurry

2.4.1 Measurement methods for ammonia

Different methods can be used to measure NH_3 emissions from field-applied slurry, the most common being micrometeorological methods [45, 64, 84, 85, 90, 97–100] and different designs of static and dynamic chambers [45, 58, 64, 78, 86, 90, 101–110]. Dynamic chambers are often referred to as wind tunnels.

For accurate absolute flux measurements, integrated horizontal flux (IHF) micrometeorological methods are frequently used because they do not influence the emission process. This allows for measurements from big plots where slurry can be applied with farm machinery and an unmodified measurement environment. To calculate the average NH_3 emission rate using the IHF method horizontal fluxes are calculated from NH_3 concentration measurements and wind speed at different heights, usually by collecting NH_3 with passive flux samplers. The average NH_3 emission rate is calculated from the horizontal fluxes. The emission rate can also be calculated from average differences in measurements downwind and upwind at one height (ZINST method, special case of IHF method), or by measuring the NH_3 concentration and wind speed using the backward Lagrangian Stochastic (bLS) dispersion technique [5, 97, 111–113].

Micrometeorological methods can be challenging, as they require large horizontally homogeneous field plots with no objects (trees, houses, etc.) within several 100 meters [114, 115], to ensure undisturbed wind profiles. Therefore, the number of replicates is often practically limited. It is necessary to have a uniform emission source which requires a fast even slurry application, which can be challenging within a large experimental plot [5, 97, 111].

The dynamic chamber designs used in most studies were originally designed by Lockyer et al. (1984) [102]. These tunnels have an experimental area under a transparent canopy of 2 x 0.5 m, with the height of the canopy being 0.4 m. The tunnel section is connected to a metal duct with a fan. The air flow is recorded with an anemometer and can be adjusted manually. The NH_3 concentration is sampled from the air entering and leaving the tunnel by absorption flasks with acid (acid scrubbers), which are subsequently analyzed in a laboratory [102]. A drawback of using acid scrubbers is that it often lead to very high variation in data. Within triplicates coefficient of variation above 100% has been observed [64, 78, 86, 106, 107, 110].

The unique appeal and great advantage of dynamic chambers is that the measurement technique allows for replicates, making them advantageous for comparative studies [5, 97, 111, 116]. If a low variation is achieved, small differences in NH_3 emission rates from e.g. different low emission application techniques can be detected. The replicates are possible because the dynamic chambers only require small plot areas and can be placed next to each other without emissions from one plot influencing the others. They are also not sensitive to obstacles in the area, as opposed to micrometeorological methods. Variation between studies using dynamic chamber measurements may occur if many different designs are used, which leads to high variations in the velocity profiles within the chambers [117]. This has to be taken into consideration when comparing data obtained with different wind tunnel systems.

However, the dynamic chambers modify the measurement environment and have been found to both under- and overestimate NH_3 emissions compared to micrometeorological measurements. The deviation between the two measuring techniques has been assigned to differences in air flow within the emission chamber compared to ambient conditions. In two studies [90, 116], the air flow inside the emission chamber was adjusted continuously to match the ambient wind speed outside the tunnels, whereas in parallel experiments the emission rate was measured with micrometeorological mass balance method. Both studies found that there was no significant difference in the measurements between the two measurement techniques in periods without rainfall. Other studies have made similar experiments comparing IHF and ZINST to dynamic chambers, with a fixed air flow inside the emission chambers of 1 m s^{-1}. Two of these studies measured comparable emission from the two methods [111, 113]. In one of the studies, the ambient wind speed was similar to the air speed inside the emission chamber [113], for the other study the ambient wind speed was not reported [111]. Two other studies found a poor correlation between the dynamic chamber measurements and and IHF measurements [97, 116]. In one of the studies the ambient wind speeds varied a lot, and were at times three times higher than the air speed inside the chamber [116]. For the other study the ambient wind

speeds were not reported [97]. Presumably the experiments that obtained a good correlation between the measuring techniques and a fixed air flow inside the emission chambers obtained approximately the same turbulence at the soil surface and that the air speed inside the chambers were close to the ambient wind speeds. These experiments show that air flow inside the emission chamber is a crucial operating parameter and must be chosen with great consideration.

2.4.2 Measurement methods for non-methane volatile organic compounds

A limited amount of studies have attempted to measure the complex matrix of NMVOC and H_2S emitted after field application of slurry. Most studies used a variation of static or dynamic chambers [7, 8, 26–29, 96]. Only one study was found using a micrometeorological method for measurements of a NMVOC (methanol) after field application of slurry [118].

No standard measuring technique exists, and various designs of dynamic and static chambers have been used. One study tested static chambers, and found that these had a critical error in sample collection [8]. The studies using dynamic chambers for sample collection of NMVOC and H_2S emissions has a large variation in design and operation condition [7, 27, 28, 96, 119]. Successful collection of gas samples after slurry application to soil with dynamic chambers has been obtained in several studies [7, 27, 28, 96]. Feilberg et al. (2015) [7] and Parker et al. (2013) [28] found that dynamic chambers were suitable for measuring relative differences between treatments. Non-methane volatile organic compound emission has been shown to depend on the air flow rate inside the emission chamber, making this one of the most important operating parameters [41].

2.4.3 Dynamic chamber flow rate

The emissions of NH_3 and NMVOC measured with dynamic chambers are positively correlated with the air flow rate inside the emission chamber [5, 27, 120, 121]. This correlation is caused by slurry-to-air mass transfer of several components being mainly restricted by the air side resistance (for more information, see Section 2.1) [27, 41, 121, 122].

Several studies found that a higher air flow rate inside the emission chamber increase the emission flux, until a certain point [5, 120, 121, 123].

The optimal air flow inside the emission chamber should be sufficiently high to provide both mixing within the tunnel and turbulence above the emitting surface to reduce laminar film boundary [120]. The air flow is typically reported as an average air velocity in the longitudinal dimension of the emission chamber and is either measured in a single point (usually in the middle) of the chamber using an

anemometer or calculated from the volumetric flow rate through the chamber. A single measurement or report of the air flow is not sufficient to gain knowledge of the velocity profiles and variations within the chamber or at the emitting surface as variations throughout the chamber in both longitudinal and vertical directions will occur [124].

2.4.4 Gas analysis methods

Several gas analysis methods for measurements of NH_3, NMVOC, and odor have been developed. When choosing a measuring method several theoretical and practical aspects have to be considered: purpose of measurements (absolute or relative measurements), accuracy, sample interval, sample handling from measuring site to results, concentration range of the compounds during the measuring period, scale (size and dimensions of emitting area), and cost.

This section is a short overview and description of the most commonly used measurement techniques that can be used to measure NH_3, NMVOC, and odor from field-applied slurry. An elaboration of methods used during this research follow: Cavity Ring-Down Spectroscopy (CRDS) and acid impingers for measurement of NH_3, and Proton Transfer Reaction Time-of-Flight Mass Spectroscopy (PTR-TOF-MS) for measurement of NMVOC and H_2S.

Ammonia can be measured with a range of methods, depending on the application. Absorption by an acid medium is the simplest approach. In this method, the NH_3 reacts with the acid and forms aquesous NH_4^+. Thereafter, the sample can be analyzed for its NH_4^+/NH_3 concentration. Scrubbers where the air is bubbled through an acid is commonly used. Other methods include denuders coated with acid or containing an acid medium and acid coated filters. The disadvantage of these methods is the time averaging, and labor-intensive continuous replacement of samplers if near-continuous measurements are wanted. The sampling can be passive or active. In passive sampling NH_3 is transported to the acidic medium through diffusion (passive ventilation), whereas active sampling uses convective flow transport [112, 125].

Different online continuous absorption spectroscopy methods can also be used to measure NH_3, such as Infrared (IR) Photoacoustic Spectroscopy (PAS) and CRDS. As the methods characterize molecular structures they provide information of functional groups, which makes them well suited for identification and measurements of known trace gases in the atmosphere, but less suited for measurements of unknown compounds [126]. Such instruments typically have a high investment cost, but are very advantageous as they can provide accurate and sensitive measurements with a high time resolution [112, 127, 128].

In a IR PAS instrument the gas absorbs energy from the IR radiation in a sealed cell. This causes the cell pressure to increase and decrease, which cre-

ates an acoustic signal that can be detected and converted to a voltage. The voltage is proportional to the concentration of the gas [129]. Recent work [130] has shown that there can be severe interferences from non-target gases, such as NMVOC, on NH_3 measurements by IR PAS due to absorption of IR light at similar wavelengths from the different compounds. These interferences can give very inaccurate results during agricultural measurements where vast quantities of NMVOC is emitted alongside NH_3 [130].

Cavity Ring-Down Spectroscopy measures the 'ring-down' time of a pulsed laser in a cavity due to absorbance by the target gas. The time to reach a certain amount of the original light intensity is measured and used to calculate the concentration of the compound. The technique provides accurate and continuous measurements with a high sensitivity, and is often used to monitor small inorganic compounds in the atmosphere [125, 126, 128, 131, 132].

Odor is very complex to measure as it consists of a broad range of compounds in varying amounts and the sensory perception is very subjective [47]. It can be measured with an olfactometric analysis whereas odorous compounds, NMVOC and H_2S, can be measured using different technologies, such as GC-MS and PTR-MS.

Odor is commonly measured with olfactometric analysis [8, 96, 124]. For olfactometric analysis, the odorous air is assessed by a panel being introduced to decreasing dilutions of the sample, and information about the dilution at which the sample can be detected is used to calculate an odor concentration value [122]. The advantage of olfactometry is that the result is a quantitative odor concentration value that can be linked to the odor experienced by the human nose. A disadvantage is that the individual compounds and concentrations of these are not assessed in the measurements. Olfactometric analysis has been identified to give strongly biased results, due to sampling and storage leading to discrimination and loss of sample compounds [133–136]. Furthermore, olfactometry is associated with high uncertainty and poor repeatability associated with variation due to panel selection even if this is based on a common reference compound [137].

Non-methane volatile organic compounds are usually measured using Gas Chromatography coupled to Mass Spectrometry (GC-MS). With regard to detection of a wide range of compounds, it is unsurpassed by other techniques [126]. Gas Chromatography Mass Spectroscopy separates the compounds chromatographically based on their volatility, and thereafter the individual compounds are identified and quantified by MS analysis. Most of these measuring techniques require sample preparation prior to analysis. Additionally, pre-concentration of the NMVOC might be needed in order to achieve acceptable detection limits, but this has a drawback of giving a poorer time resolution [138] and limits the applicability for very volatile and reactive compounds (e.g. H_2S). The GC-MS analysis can be labor- and time consuming and often gives results of high vari-

ability [139–141].

In recent years PTR-MS has successfully been used for high time resolution chemical measurements of NMVOC from applied slurry [7, 8, 26, 27] and livestock production facilities [34, 133, 142–144]. It has been shown that PTR-MS provides more comprehensive results of quantitative measurements of NMVOC and sulfur compounds compared to olfactometric analysis and GC-MS without sampling discrimination, and with high sensitivity and selectivity [8]. Proton Transfer Reaction Mass Spectroscopy has the added benefit that there are no sampling challenges as the measurements can be performed online in real-time [126]. Proton Transfer Reaction Mass Spectroscopy uses soft chemical ionization by H_3O^+ to ionize the trace compounds in the gas with a higher proton affinity than water. The mass-to-charge (m/z) ratio of the protonated compounds are subsequently quantified with a mass detector [145, 146].

Proton Transfer Reaction Mass Spectroscopy can also be used to measure NH_3 as it has a higher proton affinity than water. Intrinsic ions at m/z 18 are produced in the ion source, making the instrumental background contribution significant, typically at a few hundred ppb. The intrinsic background is relatively stable, which makes it possible to correct the samples for background values, but the resulting detection limit is in the range of 20-50 ppb, which is high compared to CRDS where a detection limit of 0.7 ppb can be obtained [130].

Ammonia measurements with Cavity Ring-Down Spectroscopy

Cavity Ring-Down Spectroscopy is a very sensitive, direct, and continuous absorption technique that measures the rate of absorption of light at a narrow wavelength. Cavity Ring-Down Spectroscopy has an improved detection sensitivity compared to other ultraviolet spectroscopies due the extended optical path length [126]. The absorption of a narrow range light pulse being coupled into an optical cavity with highly reflective mirrors is measured. The light is reflected between the mirrors and can have an absorption path length of several kilometers. After each reflection a minor fraction of the light pulse leaks out of the cavity (Figure 2.3). The cavity cell requires precise temperature and pressure conditions. When a gas sample with NH_3 is placed inside the cavity, it absorbs some of the light being pulsed back and forward between the two mirrors, giving a faster decay in the amount of light in the cavity as it makes fewer passes between the mirrors. The ring-down time is the time it takes for the light to reach a certain fraction of the original intensity. The ring-down times are used to calculate the concentration of NH_3 in the gas from known spectroscopic constants, making it a direct quantitative measurement, hence calibrations are in principle not required. A high sensitivity can be obtained, as the ring-down time is independent of fluctuations in the light pulses into the cavity. As samples can flow directly into the cavity chamber without sampling or pre-concentration the

measurements have a high time response, even for sticky gases such as NH_3. The accuracy, high repeatability, and low detection limit of 0.7 ppb [130] is unique compared to other measurement techniques [112, 125, 128, 131, 132].

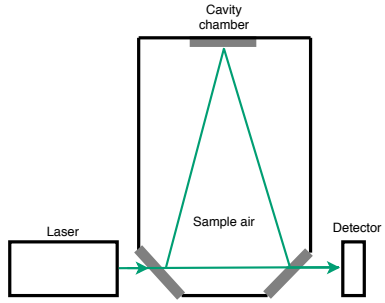

Figure 2.3: *A schematic of the CRDS analyzer, after [147].*

The G2103 analyzer from Picarro (G2103 NH_3 Concentration Analyzer, Picarro, CA, USA) used during this Ph.D. research measures absorption from 6548.5 to 6549.2 cm^{-1}, and the cavity is controlled at 140 Torr and 45°C [148]. A small interference on NH_3 measurements with the G2103 from water vapor was found by Martin et al. (2016) [148], due to spectral line broadening. Models produced after this finding correct for the interference. A study by Kamp et al. (2019) [149] found that the water vapor interference on NH_3 emission measured with CRDS without the correction is negligible under common conditions. Furthermore, they tested the interference of nitrogen dioxide (NO_2), CH_4 and 10 NMVOC commonly found in livestock buildings on NH_3 measurements, and found that it was negligible [149]. It was shown that the G2103 has an excellent linearity over a large range of NH_3 concentrations, both in laboratory and field calibrations [149].

Cavity Ring-Down Spectroscopy has been used to measure NH_3 after field application of slurry [150] and from animal production facilities [151].

Ammonia measurements with acid scrubbers

Acid impingers are usually used to measure NH_3 emission from dynamic chamber systems [78, 86, 102, 121]. Air from the inlet and outlet of the emission chamber are bubbled through a container with acid through an impinger, which allows for small bubbles of air to be distributed throughout the acid (Figure 2.4). When the NH_3 gets in contact with the acid it is rapidly converted to NH_4^+ and contained in the acid solution. The acid is collected, and later quantified for its NH_4^+ content in the laboratory by colorimetry, a selective electrode, or titrimetry [112].

The advantage of scrubbers is their high trapping efficiency, relatively low

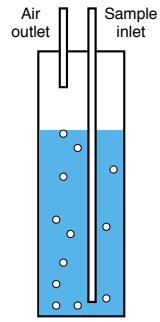

Figure 2.4: *Schematic of an acid scrubber typically used with dynamic chamber systems.*

equipment cost, and simplicity. Furthermore, no significant effect of acid strength, air flow rate, or duration of sampling interval has been found on the collection of NH_3 [97, 112]. The disadvantage is that the acid has to be changed manually for each measuring point, making the method laborious. The average time-resolution is high (median $>$ 11 hours [46]), which leads to poor knowledge of emission dynamics [112]. Furthermore, quantification requires very accurate control of the sampling flow rate, which may be influenced by climatic conditions, throughout the sampling period.

Non-methane volatile organic compound measurements with Proton Transfer Reaction Time-of-Flight Mass Spectroscopy

Proton Transfer Reaction Time-of-Flight Mass Spectroscopy makes it possible to simultaneously and continuously measure compounds in air that has a higher proton affinity than a proton donor (most commonly water) such as the majority of NMVOC. It is an online measurement technique, that provides real-time measurements with a rapid response time and high sensitivity.

The PTR-MS consist of three main parts (Figure 2.5) [145, 146]:

1. A discharge ion source.
2. A drift-tube reactor.
3. Mass spectrometer.

The discharge ion source consists of a hollow cathode discharge with a continuous inflow of water vapor. Here electron impact reactions produce ionic and neutral fragments of the water vapor. After the ion source, a small intermediate source-drift region is used to convert the ions from the hallow-cathode to

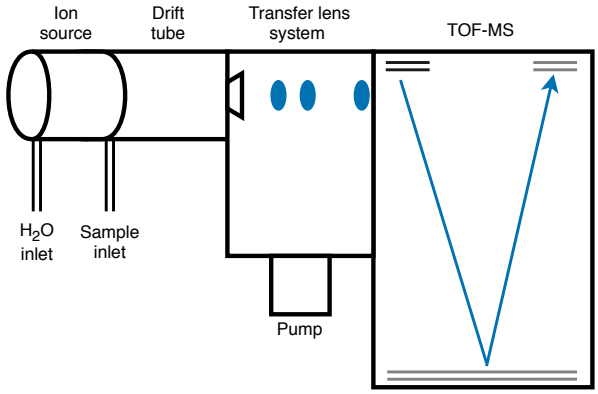

Figure 2.5: *Schematic of the PTR-TOF-MS, after [152].*

H_3O^+. Some impurities, mainly of dioxygenyl (O_2^+) and nitrosonium (NO^+) will be produced from the air back streaming from the drift tube to the ion source. These impurities are unwanted as they can undergo charge-transfer reactions with some of the compounds in the air being analyzed with a much harder ionization method. The H_3O^+ signal can be increased or decreased depending on the voltages applied on the chamber elements. A higher H_3O^+ signal can be obtained, but simultaneously a higher fraction of impurities will be produced [138, 145, 146].

The H_3O^+ is transported to the drift tube which consist of stainless-steel rings separated by Teflon rings. The Teflon rings ensures that the steel rings are electrically isolated and seals the vacuum. A homogeneous electric field is established inside the drift tube. Inside the drift tube water clustering can occur, which is unwanted as it can interfere with the mass spectra. The clustering can be minimized by optimizing the drift tube voltage which affect the mean collisional energy between reactant ions and neutrals, which can be described by the E/N number (E is the electric field strength (V cm^{-1}) and N is the gas number density (cm^{-3})). Increasing E/N ratio results in more energetic collisions between the reagent ions and neutrals. This yields in lower cluster ion formation, but also results in higher fragmentation. In the drift-tube H_3O^+ react with the compounds in the air phase entering the PTR-MS, and compounds with a higher proton affinity than water (~697 kJ mol^{-1}) is ionized (Equation 2.6) [138, 145, 146].

After the drift-tube the protonated compounds (product ions) and the reagent are measured by mass spectrometry [138, 145, 146]. In the Time-of-Flight Mass Spectrometry (TOF-MS) a batch of ions are introduced to a flight tube. The

ions are separated based on the time it takes for them to reach a detector. The main advantages are 1) that a TOF-MS measures all masses at once and 2) that a higher mass resolution is obtained, which makes it possible to distinguish nominally isobaric compounds [138, 145, 152] such as acetone and glyoxal.

Water as a proton donor gives a soft ionization, which result in very low fragmentation of the product ions. In the cases of no fragmentation, the product ion is equal to the compound mass plus one (Equation 2.6) [145]. If the product ion only has a proton affinity marginally higher than water, the reverse reaction can occur and needs to be considered (Equation 2.7). The collision rate coefficient (k) of the reverse reaction is very small compared to the forward reaction, but the concentration of H_2O in the drift tube is high compared to the concentration of M [145, 146].

$$H_3O^+ + M \xrightarrow{k} MH^+ + H_2O \tag{2.6}$$

$$MH^+ + H_2O \xrightarrow{k} H_3O^+ + M \tag{2.7}$$

Where M is the compound in the air being analyzed, k is the collision rate coefficient, MH^+ is the product ion [145].

The collision rate coefficient needs to be known in order to quantify the mass spectra obtained with the PTR-MS. It can be calculated from known polarizability and permanent dipole moments of the molecule by methods described in [153].

Each ion has a mass dependent transmission efficiency (mass discrimination) that needs to be considered when concentrations are calculated from the mass spectra [145]. The transmission efficiency can be measured with a standard gas mixture, containing compounds with masses covering the expected mass range of NMVOC to be analyzed [27].

The main advantages of the PTR-MS is that no sampling preparation is required, and the measurements can be made in real-time [145]. Furthermore, the common constituents of air all have proton affinities lower than water, meaning that they will not be measured and possibly complicate the mass spectra [154]. A disadvantage is that there is no direct identification of the compounds being analyzed, as it is the mass of the product ion that is determined. With TOF-MS the higher mass resolution allows for determination of the atomic molecular formula making identification less challenging. If cluster ions and fragmentation of the product ions occur, the mass spectra can be challenging to interpret [145].

Chapter 3

Paper I

J. Pedersen, A. Feilberg, J. N. Kamp, S. Hafner, T. Nyord. Ammonia emission measurement with an online wind tunnel system for evaluation of manure application techniques. *Atmospheric Environment*, volume 230, 1 June 2020, 117562

Atmospheric Environment 230 (2020) 117562

Contents lists available at ScienceDirect

Atmospheric Environment

journal homepage: http://www.elsevier.com/locate/atmosenv

Ammonia emission measurement with an online wind tunnel system for evaluation of manure application techniques

Johanna M. Pedersen, Anders Feilberg, Jesper N. Kamp, Sasha Hafner, Tavs Nyord *

Aarhus University, Dept. of Engineering, Denmark

HIGHLIGHTS

- A system consisting of dynamic chambers and online measurement of ammonia was developed.
- The system allows for precise measurements with an average CV of 13% among triplicates.
- Ammonia emission abatement with trailing shoe was found to depend on soil type.
- Applying slurry at soil surface gave a large reduction in emissions.

GRAPHICAL ABSTRACT

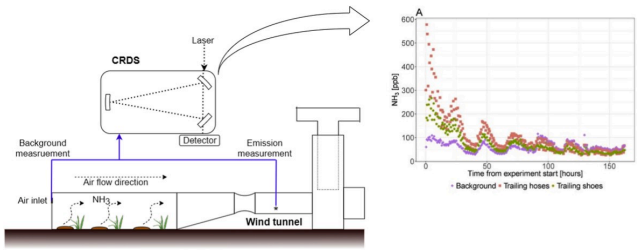

ARTICLE INFO

Keywords:
Wind tunnels
Dynamic chambers
Trailing hose
Trailing shoe
Band application

ABSTRACT

Field application of liquid manure contributes substantially to atmospheric ammonia. Low emission application methods are commonly used to reduce ammonia transfer to the atmosphere. To document which application method results in lower ammonia volatilization there is a need for high precision measurements to ensure that small differences in total emission and emission patterns can be quantified. This paper presents the evaluation and application of a new system of dynamic chambers (wind tunnels) with online cavity ring down spectroscopy measurements of ammonia. The system allows for high time resolution of 104 min throughout the measuring period (≥90 h) when testing two treatments and one reference in triplicates. Measurement variability is low with a coefficient of variation of 13 ± 8% within triplicates. The system was used to investigate the effect of trailing shoes compared to trailing hoses on different soil and crop types, where the expected differences in ammonia volatilization are low. The results show that when applying pig slurry on coarse sand a significant reduction of 47 ± 20% was obtained, whereas the reduction when applied on loamy sand and sandy loam was lower and occasionally insignificant. During ten experiments on three different soil types, an overall average reduction of ammonia volatilization from using trailing shoes compared to trailing hoses was found to be 19 ± 12%. Furthermore, the importance of correct use of trailing hoses was examined by comparing with application above the crop canopy. Application at the ground surface gave an ammonia emission reduction of 40 ± 13% compared to application 20 cm above the canopy.

* Corresponding author. Aarhus Universitet, Finlandsgade 10, 8200, Aarhus N, Denmark.
E-mail address: tavs.nyord@eng.au.dk (T. Nyord).

https://doi.org/10.1016/j.atmosenv.2020.117562
Received 20 December 2019; Received in revised form 1 April 2020; Accepted 22 April 2020
Available online 27 April 2020

1. Introduction

Intensive livestock production yields vast quantities of manure, a valuable by-product if utilized correctly due to the content of important nutrients. Good manure handling practices are important to ensure proper use of the nutrients and reduce the risk of polluting the surroundings. Emissions from manure include greenhouse gases, ammonia, and odor. The main sources of emissions are livestock production units, storage facilities, and land application. These contribute to environmental pollution due to nitrogen deposition, acidification, global warming (Eurostat, 2017; Haisler and Jacobsen, 2017), and formation of particles (Walker et al., 2006), which are associated with negative health impacts (Eurostat, 2017). The emissions depend on several factors such as meteorological conditions, soil and slurry conditions, crop type, application method, timing of application, and the interactions of these parameters.

Agriculture is the main source of ammonia emissions in the EU-28 countries (Eurostat, 2017) and accounts for 75% of the global NH3 emissions (Van Vuuren et al., 2011). Nitrification of ammonia is one of the most important contributors to acidification of the environment, and accounted for the highest share of acidifying potential in the EU-28 countries in 2014 (Eurostat, 2017). In addition, chronic deposition of nitrogen is linked to reduction of biodiversity in e.g. grasslands (Stevens et al., 2010). Mitigating ammonia emissions is a key strategy for preventing environmental acidification. The EU-28 countries have committed to reduce emission of ammonia from agriculture in order to reduce the environmental impact of food production (Haisler and Jacobsen, 2017). Reducing emissions from field application is an essential step towards overall ammonia reduction, since field application contributes 42% (Eurostat, 2017) of total agricultural ammonia emissions in the EU.

2. Ammonia emissions

Extensive research has been done on ammonia emissions from field-applied slurry. Different measuring methods have been used, of which the most common are micrometeorological methods (Häni et al., 2016; Misselbrook et al., 2005a; Pacholski et al., 2006; Mannheim et al., 1995); enclosure methods using various designs of static and low-flow dynamic chambers (Parker et al., 2013); and wind tunnels, arguably a type of dynamic chamber, but with high and primarily longitudinal air flow (Bell et al., 2015; Lockyer, 1984; Mannheim et al., 1995; Rochette et al., 2008; Sommer and Misselbrook, 2016).

Wind tunnels require smaller plots than micrometeorological methods, which makes it possible to have more replicates. Because they modify the measurement environment and have been observed to overestimate ammonia emissions compared to micrometeorological mass balance measurement techniques (Misselbrook et al., 2005b; Sommer and Misselbrook, 2016), they may not be suitable for determining absolute emission under natural conditions. Nonetheless, the small area footprint required and the possibility to make unbiased replications make the wind tunnel method an appealing option for comparative measurements if designed correctly (Misselbrook et al., 2005a, 2005b; Sommer and Misselbrook, 2016). With wind tunnels, ammonia is typically captured by bubbling exhaust air through acid impingers and later quantified (Bell et al., 2015; Lockyer, 1984; Rochette et al., 2008; Smith and Watts, 1994). This method is laborious, as the acid impingers have to be changed manually and acid solutions saved and later analyzed in a laboratory, leading to limited time resolution (median $>$ 11 h (ALFAM2)) and little information about the ammonia emission dynamics. The design of the wind tunnels strongly affects results, with air flow or air velocity being recognized as the most important factor in several studies, as higher values result in higher measured fluxes (Eklund, 1992; Smith and Watts, 1994; Sommer and Misselbrook, 2016). Eklund (1992) argued that the optimal air velocity depends on the tunnel design and the source of emissions. The air flow should be sufficiently high to provide realistic levels of turbulence above the emitting surface. Despite this knowledge, limited effort has been brought into investigating air flow. Two different approaches have been used: setting the air flow to a constant value (Bell et al., 2015; Bhandral et al., 2009; Smith et al., 2000) or adjusting the air flow so average air velocity matches ambient wind speed during the experiment or short measurement intervals (Braschkat et al., 1997; Mannheim et al., 1995). In wind tunnel studies air flow is commonly reported as average air velocity in the longitudinal dimension [m s^{-1}]. This value is either calculated from the volumetric flow rate and cross-sectional area (i.e., the average air velocity) or measured at one point in the emission chamber using an anemometer. Considerable variations in air velocity throughout the tunnel chamber will undoubtedly occur (Jiang et al., 1995). A single report of air flow does not provide any knowledge of the velocity profile and potential variations throughout the chamber or at the soil surface where the emissions occur.

Several factors influence ammonia emission from field applied slurry including total ammoniacal nitrogen (TAN) concentration (Huijsmans et al., 2018), incorporation into soil (Hafner et al., 2019; Rodhe et al., 2004; Smith et al., 2000), application technique (Hafner et al., 2019; Rodhe et al., 2004; Smith et al., 2000), application rate (Hafner et al., 2019; Huijsmans et al., 2018), slurry pH (Sommer and Olesen, 1991), slurry dry matter (Hafner et al., 2019; Huijsmans et al., 2018; Sommer et al., 2006), air temperature (Bell et al., 2015; Hafner et al., 2019; Huijsmans et al., 2018), wind speed (Hafner et al., 2019; Huijsmans et al., 2018; Misselbrook et al., 2005b), rainfall rate and timing (Hafner et al., 2019; Martínez-Lagos et al., 2013), crop conditions (Huijsmans et al., 2018; Smith et al., 2000), and soil type and conditions (Bell et al., 2015; Huijsmans et al., 2018; Smith et al., 2000). The soil conditions influence infiltration together with manure dry matter and application technique. Infiltration is often considered to be highly important for emissions (de Jonge et al., 2004; Hafner et al., 2019; Misselbrook et al., 2005b; Rochette et al., 2008).

Although comprehensive research has been conducted on ammonia emissions from field-applied slurry, a number of questions remain concerning the factors that influence emission and the relative importance of these. The primary aim of this study was to develop and evaluate a new wind tunnel system with online measurements. Online measurements allow for higher time resolution and insight into temporal ammonia emission dynamics. As a part of the wind tunnel evaluation, the air-side mass transfer velocities (Lee et al., 2004; Schwarzenbach et al., 2003) in the wind tunnel system have been compared to outside conditions via measuring the evaporation of a pure liquid (ethanol). The air-side transfer velocities are assumed to depend only on the turbulence intensity (at the same temperature) and therefore reflect whether turbulence intensities in the wind tunnels are comparable to natural outside conditions. A similar approach was used by Parker et al. (2013). A secondary aim was to use the new system to examine the interaction between soil type and ammonia volatilization from slurry application with trailing shoes and trailing hoses. The objectives were to: (i) Optimize a wind tunnel system measuring ammonia with continuous online measuring technique, (ii) Develop a method for evaluation of the air exchange rate (turbulence intensity) in the emission chamber, (iii) Conduct comprehensive tests on the effect of trailing shoes and trailing hoses on ammonia emissions by including soil type as a factor, and (iv) Illustrate the importance of correct use of slurry application methods by measuring ammonia emissions from slurry applied by trailing hoses at the grass canopy and from 20 cm above the grass canopy.

3. Materials and methods

3.1. Measuring system

3.1.1. Wind tunnels

Emissions were measured using nine wind tunnels operated as dynamic chambers with a continuous and constant air flow (Fig. 1). The

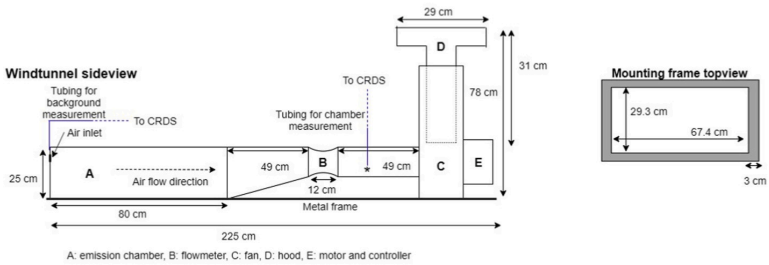

Fig. 1. Sketch of wind tunnels, not to scale.

wind tunnels consisted of a rectangular open-bottomed stainless steel chamber (80 × 40 × 25 cm). The chamber was connected to a fan (SEAT 20 (tunnel 1) and SEAT 25 (tunnel 2–9), SEAT ventilation, Verniolle, France) via a steel duct. An orifice flow meter (FMU 80-63, Lindab, Haderslev, Denmark), where the volumetric flow is calculated from measured pressure drop, was included in the duct. Each fan was run by an electric motor (MS 71B-B34, BUSCK, Kållered, Sweden) and a frequency converter (ATV12H037M2, Schneider Electric, Rueil-Malmaison, France). A micro manometer (5825, DP-CALCTM, Shoreview, MN, USA) was used to measure the air flow through the tunnel, which was manually adjusted with the frequency converter to an air exchange rate of 25 min^{-1}. The air exchange rate corresponds to a calculated mean air velocity of 0.33 m s^{-1} in the emission chamber. Resistance of the air flow through the chamber and stabilization of the fans was increased by having a small air-inlet (33.5 × 1.3 cm) into the tunnels and a hood at the air exit of the fan. The small inlet prevents back-flow which might lead to false emission measurements due to erroneously high background concentrations. To control the amount of slurry for each tunnel and avoid leaks, a seal between the soil and tunnel was obtained by a metal frame inserted 40 mm into the soil for the tunnel to be mounted on. The frame gave a plot area of 0.2 m^2.

Air from the tunnels was drawn through 8 mm PTFE tubing with a minimum flow rate of 0.9 L min^{-1} to a channel selection manifold consisting of 19 on/off valves (P/N 038T2S24-54-4, Bio-Chem Fluidics, Boonton, NJ, USA) with a valve for each sampling tube. The tubing was heated to approximately 40 °C by heating cables and insulation pipes. The valve manifold was controlled by a custom-built data logger. Air was drawn from each valve for 8 min. A cavity ring down spectroscopy (CRDS) instrument (G2103 NH3 Concentration Analyzer, Picarro, CA, USA) was connected to the valve manifold for continuously measuring ammonia.

3.1.2. Instrumentation

The recovery of ammonia throughout the system was tested in the field with a standard ammonia gas (11.3 ppm, Linde, Surrey, UK) added to the tube inlets. The recovery of ammonia within the 8 min of measurement interval measured at several occasions out in the field was minimum 90%. In experiments A and B, a leakage in the connection to the CRDS was discovered at the completion of experiment B. The data in experiments A and B has therefore been corrected for the decreased recovery measured onsite with the reference gas.

3.1.3. Selection of air flow rate

To assess the air-side mass transfer velocity (mass transfer coefficient) and hence turbulence intensity, evaporation rates of ethanol inside the tunnels were compared to outside evaporation at the same time. Nine petri dishes (78 mm diameter) were placed evenly in a three x three grid on the soil surface within the tunnel frame. 20 mL of ethanol (≥96% (v/v)) were added to the petri dishes. The tunnels were placed on top of the frames and run with a fixed air exchange rate for one or two h. Three tunnels were used for each air exchange rate. Simultaneously, six to nine petri dishes were placed next to the tunnels to measure evaporation outside. Evaporations with six different air exchange rates, from 15 to 47 min^{-1}, were measured (data not included). Based on these, an air exchange rate of 25 min^{-1} was chosen for all the experiments (see section 3.1.1. for discussion of this). Thereafter several experiments were performed with different ambient temperature and wind speed conditions on three tunnels with an air exchange rate of 25 min^{-1}. During these experiments, the average temperatures ranged from 6 to 17 °C and the average wind speed ranged from 2.7 to 7.5 m s^{-1} (Fig. S1).

3.2. Experimental setup and site

3.2.1. Soil

Field trials were performed in spring and summer 2018 at different sites at Research Center Foulum (Aarhus University, Tjele, Denmark). Experiments with winter wheat crops and bare soil were performed in an experimental field facility established in 1993 (Nyord et al., 2010). The facility has three soil types: coarse sand (Ortic Haplohumod), loamy sand (Typic Hapledult), and sandy loam (Typic Agrudalf) with clay contents of 4, 9, and 18% respectively (Chen et al., 2013). Experiments on clover grassland were performed on two different fields at Research Center Foulum, both with the same loamy sand soil as in the experimental field facility (the soil was established in 2015). Soil-water contents and dry bulk densities were determined gravimetrically using 100 cm^3 soil cores taken at 0–5 cm depth and 1:1 water pH was determined using the standard method (USDA, 2009). Each experiment required a soil plot of approximately 16 × 2.5 m. The tunnels were placed adjacent to each other, and differences between blocks of the same soil type were expected to be small. All soil information and analysis can be found in Table 1.

3.2.2. Slurry

Cattle and pig slurry was sampled from concrete slurry storage tanks at Aarhus University Foulum.

Analyses were performed using standard methods for dry matter content (APHA, 1999), total nitrogen (AOAC, 1999), and TAN (IS, 1984). All analysis results and application rates during the experiments can be found in Table 2.

3.2.3. Slurry application

To investigate application by trailing shoes a metal frame on wheels was constructed (Fig. 2a). Three trailing shoes (Bomech B. V., Albergen, The Netherlands) were mounted to the frame, with a distance of 25 cm between them. The force on each shoe was adjusted to the soil, with a maximum force at the end of each trailing shoe of approximately 117 N based on the maximum possible force typically applied on a commercial slurry tanker boom. The slits were obtained at a constant speed of approximately 2 km h^{-1}. The resulting slits from running the metal frame with the trailing shoes differed greatly in size and geometry due to the different pressure applied, soil-water content, and crops.

At the start of the experiments a pre-determined volume of the slurry

Table 1
Soil properties for all the experiments and force on each trailing shoe when applicable. Standard deviations are displayed in parenthesis ($n = 3$).

Exp	Soil	Crops	Dry bulk density [g cm^{-3}]	Water content [g g^{-1}]	pH	Force on trailing shoe [N]
A	Coarse sand	Winter wheat	1.41 (0.08)	0.09 (0.004)	4.5	78
B	Loamy sand	Winter wheat	1.32 (0.07)	0.13 (0.01)	4.4	88
C	Sandy loam	Winter wheat	1.41 (0.06)	0.17 (0.01)	6.3	98
D	Loamy sand	Grass	1.15 (0.08)	0.15 (0.01)	4.9	117
E	Loamy sand	Grass	1.15 (0.08)	0.21 (0.01)	4.8	117
F	Coarse sand		1.41 (0.08)	0.11 (0.004)	4.5	88
F	Loamy sand		1.32 (0.07)	0.18 (0.01)	4.9	108
F	Sandy loam		1.41 (0.06)	0.18 (0.01)	6.4	117
G	Coarse sand		1.41 (0.08)	0.08 (0.002)	4.6	
G	Loamy sand		1.32 (0.07)	0.13 (0.01)	5.5	
G	Sandy loam		1.41 (0.06)	0.14 (0.005)	6.8	
H	Loamy sand	Grass	1.61 (0.08)	0.15 (0.01)	5.9	117
I	Loamy sand	Grass	1.61 (0.08)	0.19 (0.01)	6.1	
J	Loamy sand	Grass	1.61 (0.08)	0.20 (0.02)	6.2	

Table 2
Slurry properties for all the experiments. Standard deviations are displayed in parenthesis ($n = 2$).

Exp	Type	Application rate		Dry matter [%]	Total N [g L^{-1}]	Ammoniacal N [g L^{-1}]	pH
		[kg m^2]	[g NH_4-N m^{-2}]				
A	Pig	4.5	10.00 (0.14)	3.87 (0.05)	2.62 (0.42)	2.22 (0.03)	7.19 (0.04)
B	Pig	4.5	9.90 (0.38)	3.84 (0.09)	3.45 (0.23)	2.20 (0.08)	7.04 (0.03)
C	Pig	4.5	10.11 (0.44)	3.40 (0.18)	2.92 (1.07)	2.25 (0.10)	7.10 (0.08)
D	Cattle	3.5	9.77 (0.44)	9.04 (0.01)	5.07 (0.17)	2.79 (0.13)	6.94 (0.01)
E	Cattle	3.5	9.90 (0.68)	8.96 (0.02)	4.61 (1.04)	2.83 (0.19)	6.94 (0.01)
F	Pig	4.5	5.21 (0.55)	3.17 (0.27)	1.71 (0.10)	1.16 (0.12)	7.30 (0.01)
G	Pig	4.5	5.64 (0.08)	3.02 (0.01)	1.85 (0.04)	1.25 (0.02)	7.64 (0.01)
H	Cattle	3.5	9.51 (0.05)	8.63 (0.02)	4.26 (0.27)	2.72 (0.01)	6.83 (0.01)
I	Cattle	4.5	15.77 (0.06)	6.76 (0.01)	3.05 (0.04)	3.50 (0.14)	7.37 (0.04)
J	Cattle	4.5	15.93 (0.87)	6.78 (0.07)	3.02 (0.16)	3.54 (0.19)	7.33 (0.04)

(Table 2) was applied manually by a hose attached to a watering can (as done by (Bell et al., 2015; Misselbrook et al., 2005b; Wulf et al., 2002)) evenly in the three slits when mimicking application by trailing shoes, at the soil surface when mimicking application by trailing hoses, or from 20 cm above the grass canopy when mimicking application by trailing hoses used with a distance between the trailing hoses and the ground.

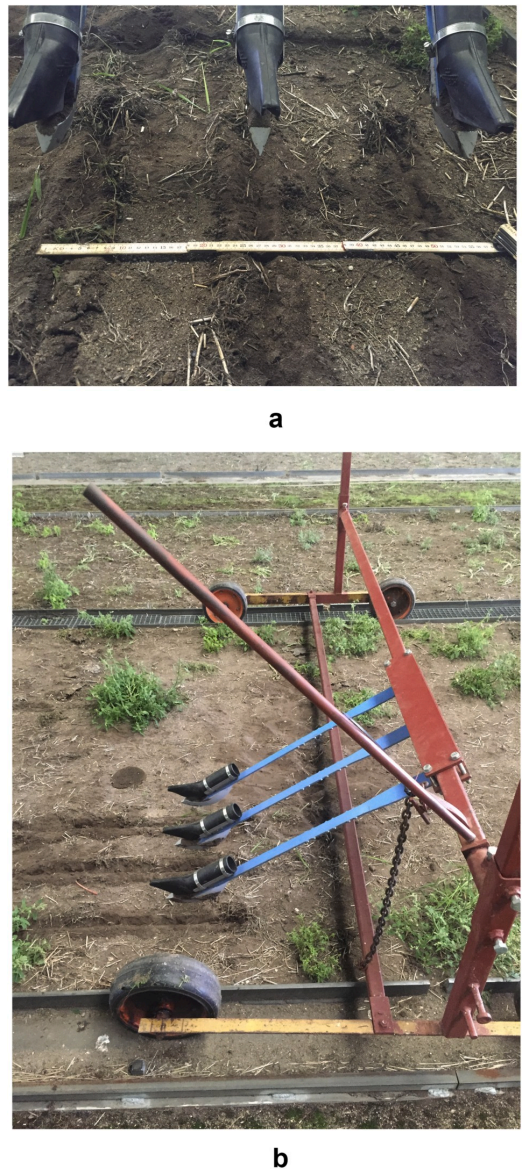

Fig. 2. (a) Metal frame with Bomech trailing shoes attached. (b) Slits made by Bomech trailing shoes on coarse sandy soil.

The slurry was thoroughly stirred before the amount needed was removed and applied.

3.2.4. *Meteorological data*

A weather station (Theis CLIMA, Göttingen, Germany with a Campbell CR10xB data logger, Campbell Scientific, INC, UT, USA) was continuously measuring ambient air temperature (Hygro-Thermo Transmitter-compact, THEIS CLIMA) and soil temperature (Temperature Transmitter, Theis CLIMA) 5 cm from the soil surface in 10 min intervals. Average weather data can be found in Table 3.

Table 3
Soil and air temperature during all experiments. Averages of the first 6 and 24 h after application and total experimental period. Soil temperatures are measured at 5 cm depth.

	Air temperature [°C]			Soil temperature [°C]		
Exp	6 h avg.	24 h avg.	Total avg.	6 h avg.	24 h avg.	Total avg.
A	25.1	18.9	15.1	20.4	17.6	15.9
B	22.6	17.6	18.2	19.8	16.8	16.7
C	21.9	20.2	20.4	17.3	16.8	16.8
D[a]	15.7	12.8	15	NA	16.3	17.1
E	22.5	17	16.9	24.1	18.6	18.3
F[b]	21.6	19.3	17.6	19.2	18.5	17.5
G[b]	23.5	19.6	15.6	18.5	17.7	15.7
H	15.9	14.7	15.7	19.4	17.5	17.7
I	10.4	9.2	10.4	10.7	9.1	10.6
J	15	12.9	15	12.1	11.1	12.1

[a] Soil temperature is missing for the first 10 h.
[b] Soil temperature measured in loamy sand.

3.3. Data treatment

The experiments varied in duration from 90 to 157 h. To compare the accumulated emissions they were calculated for 90 h. For all of the experiments, most of the emissions had occurred at this time (minimum 83% of total emissions during the measuring period, data not included). For the experiments with data for >90 h the emissions were at such a low level that no differences in ammonia emissions from the different treatments were observed (data and analysis not included).

The volatilization flux of ammonia in units of g m^{-2} min^{-1} was calculated from the concentration, the air flow in the tunnel, and the area of the soil surface covered by the tunnel (Equations (1) and (2)).

$$F_{NH3} = (C^*q) / A \quad (1)$$

where F_{NH3} is the flux (g min^{-1} m^{-2}), C is the concentration (g L^{-1}), q is the volumetric air flow rate (2016 L min^{-1}), and A is the area of the soil surface within the tunnel (0.2 m^2).

Concentration was converted to units of g L^{-1} and corrected for background concentration by Equation (2):

$$C = P / (R^*T)/(c_o - c_i) \ ^*M \quad (2)$$

where C is the ammonia concentration (g L^{-1}) (average of the last 30 s of a measuring cycle), P is the pressure (1 atm), R is the gas constant (0.08206 L atm K^{-1} mol^{-1}), T is the temperature (K), c_o is the outlet concentration (ppb), c_i is the inlet (background) concentration (ppb), and M is the molar mass of ammonia (17.03 g mol^{-1}).

To calculate emission the flux between two measurements was taken as the value calculated by equation (1) at the beginning of the 104 min interval (i.e., a left Riemann sum). When concentrations are not significantly higher than the background, they are set to 0.

During five of the experiments, an error occurred in the sampling system, resulting in loss of emission data. The missing data spans from 4 h (E) to 16.6 h (F) (Fig. S3). The missing data were estimated to obtain more correct cumulative emission calculations. Linear interpolation was used to estimate the data if the ambient air temperature was either increasing or decreasing during the period. If the temperature was increasing followed by a decreasing or vice versa, a minimum or maximum was estimated based on the time of day, the temperature and the temperature-emission ratio in the dataset. Then linear interpolation was used from the points right before and after the missing data and the estimated maximum or minimum. The standard deviations of the missing data were calculated from the highest coefficient of variation in the data before and after the missing data.

3.3.1. Statistics

Single factor or two factor analysis of variance (ANOVA) was used to test for differences among application methods. Within each block, one tunnel with each treatment was present and randomly assigned. Data were analyzed with an ANOVA, with the cumulative emission after 90 h as the response variable and an individual plot in a single wind tunnel as an observational unit. Subsequently, Tukey's test, with a confidence interval of 95%, was used to investigate which treatments were significantly different. Only a single soil type was used in Experiments A, B, and C (Table 1). Data from these three experiments were analyzed together in a two-way factorial ANOVA with soil type and application method as the independent variables, based on the assumption that differences (including any interactions) among experiments were primarily related to soil type. Experiments F and G were analyzed separately with one-way ANOVA with soil type as the independent variable. Experiments D and E were analyzed together with a one-way ANOVA with application method as the independent variable and experiment as a blocking variable. Due to a large difference in emissions from experiment H compared to I and J, the results from H were analyzed separately with a one-way ANOVA with application method as the independent variable. Experiments I and J were analyzed together with a one-way ANOVA with application method as the independent variable and experiment as a blocking variable.

A paired *t*-test was used to test the average reduction of ammonia emissions using trailing shoes compared to trailing hoses in all the experiments.

Graphics include error bars representing one standard deviation.

4. Results and discussion

4.1. Evaluation of wind tunnels

4.1.1. Air exchange rate

Theoretically, ammonia emissions from an aqueous surface are expected to be determined almost completely by air-side resistance due to its relatively low partitioning into the gas phase (Hafner et al., 2012; Schwarzenbach et al., 2003) partly as a result of the rapid equilibrium between NH_3 and NH_4^+. Consequently, the emission is expected to depend on turbulence intensity, which in turn is related to air velocity. Observations indeed support that emissions are highly depending on air velocity (Huijsmans et al., 2018; Misselbrook et al., 2005c; Sommer and Misselbrook, 2016), and wind tunnel air exchange rate is therefore an important operating parameter. The optimal air exchange rate inside the tunnel should create turbulence at the soil surface comparable to what is found outside the tunnels, and should be relatively homogeneous throughout the tunnel. Parker et al. (2013) presented a methodology based on evaporation of water for standardizing and comparing different evaporation chambers and correlate the emissions within the chamber to field conditions. Inspired by this method, evaporation measurements of ethanol inside and outside the emissions chambers were used as a method for rapid and quantitative evaluation of the sweep air flow. Ethanol was chosen rather than water vapor, since it evaporates more quickly and has a low atmospheric concentration (compared to water).

Based on testing several different air exchange rates, 25 min^{-1} was chosen as the optimal. It gave rather homogeneous evaporation throughout the soil surface in the emission chamber, and the evaporations were close to the evaporations outside the tunnels. Evaporation tests at different days allowed to test under several different weather conditions. Under these very different weather conditions, the emissions inside and outside the tunnels where in the same range (Fig. 3) with an average difference of 11 ± 7%. The air exchange rate of 25 min^{-1} corresponds to a calculated mean air velocity of 0.33 m s^{-1} in the emission chamber. Jiang et al. (1995) did extensive testing of velocity profiles with an anemometer within a wind tunnel emission chamber of the same dimensions as the ones used in this paper. They found that a velocity of 0.33 m s^{-1} gave the most stable velocity profile throughout the chamber.

It was assumed that the air flow through the tunnel was constant during the experiments. The air flows were measured and adjusted right

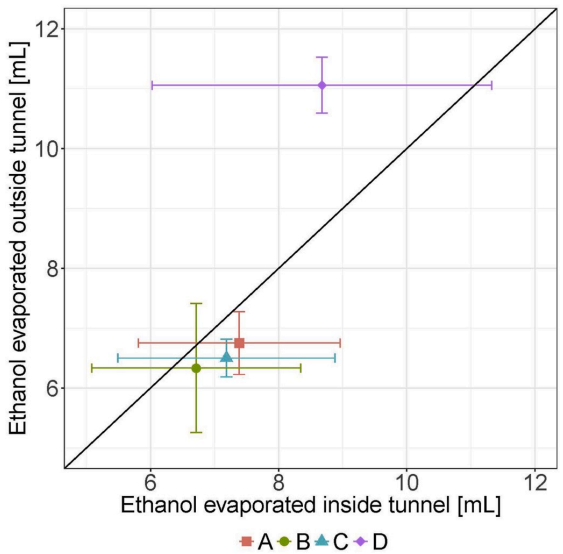

Fig. 3. Average evaporation of nine petri dishes inside a wind tunnel emission chamber ($n = 3$) compared to average emission from six petri dishes outside of wind tunnel. Standard deviations are displayed as error bars ($n = 27$ for inside measurements, $n = 6$ for outside measurements). The letters indicate test days with different weather conditions.

after slurry application and measured at the end of the experiment. Slight changes occurred, assigned to changes in the ambient wind speed. On two occasions, the difference compared to the air flow at the time of application was 7%, but in all other cases, the variations were within 5%.

It is concluded that the wind tunnel design and air flow rate used in this study provides a good simulation of outside turbulence intensities.

4.1.2. Sampling system

Online CRDS measurement provides data with a 104 min time resolution with one control and two treatments in triplicates (nine tunnels in total). This time resolution is very high throughout the measuring period compared to experiments with manually sampling (Bell et al., 2015; Rochette et al., 2008; Sommer et al., 2006). The conditions inside the dynamic chamber are in principle different from real field conditions, therefore the absolute emission values cannot necessarily be translated to outside emissions. As the effect of air velocity (turbulence at the soil surface) compared to ambient conditions are not very different, it might be possible to correct the chamber measurements in the future to yield absolute emission data. This has not been investigated further in this paper. Low variation in the results (Section 3.2) indicates that the method gives reliable quantitative data, which can be used to compare different application methods, slurry types or soil types. 23 sets of measured triplicates give an average coefficient of variation of 13 ± 8%. The variation is low compared to the literature (Nyord et al., 2012; Rochette et al., 2013), which is necessary when examining methods with expected effects in a lower range, such as trailing shoes compared to trailing hose. The system allows for experiments under realistic agricultural conditions with continuous measurements over long periods providing comprehensive datasets with details of the emission dynamics, such as diurnal patterns (Fig. 4).

The sampling system typically requires 5–8 min to reach a stable reading of both high and low concentrations. The response time depends on the internal surface temperature and ammonia concentration differences. In the first cycle of ammonia measurements, the concentration in most cases increased close to linearly due to the rapidly increasing emissions shortly after slurry application (Fig. S2). It cannot, however, be completely ruled out that the sampling system (tunnels, tubes, fitting, valve-block, etc.) needed more time to equilibrate in the first measurement cycle, which would have resulted in a minor underestimation of the first data point. From the second measuring cycle, all tunnels reached stable readings with a sampling time of 8 min (Fig. S2).

High emission measurements result in false high background

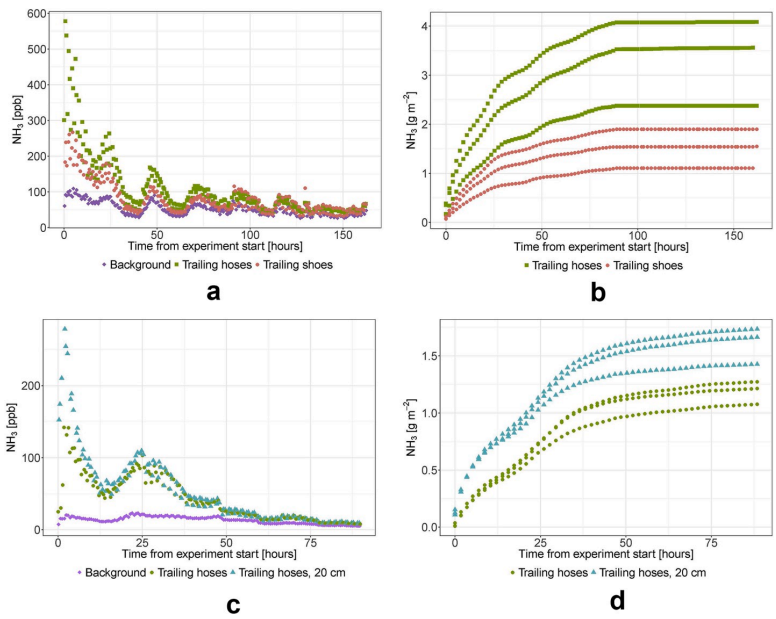

Fig. 4. Outlet ammonia concentration and accumulated loss of nitrogen due to ammonia volatilization during experiment A and I.

measurements as the system did not have time to reach a stable background reading. With emission measurements of 700 ppb before a background measurement, the underestimation of the ammonia concentration is approximately 3.5%, whereas an emission measurement of 300 ppb before a background measurement will lead to an underestimation of 1%. Generally, only very few measurements are above 300 ppb (Fig. 4), and it only occurred during the first couple of cycles. Therefore, the slightly higher background readings have a very limited effect on the overall results.

4.2. Ammonia emissions from surface applied slurry in growing crops

Ten experiments were performed testing the effect of trailing shoes compared to trailing hoses. In three experiments (A, B, and C) the two application methods were tested against each other on three soil types with winter wheat crops (Figs. 5a and 4). Two experiments (F and G) were conducted in which each application method was tested across the three soil types simultaneously (Fig. 5b). Trailing hoses and trailing shoes were compared on a clover grass field in two identical experiments (D and E) (Fig. 6a) and the last three experiments focused on comparing trailing hoses used correctly and trailing hoses applying slurry 20 cm above the grass canopy (H, I, and J) (Figs. 6b and 4).

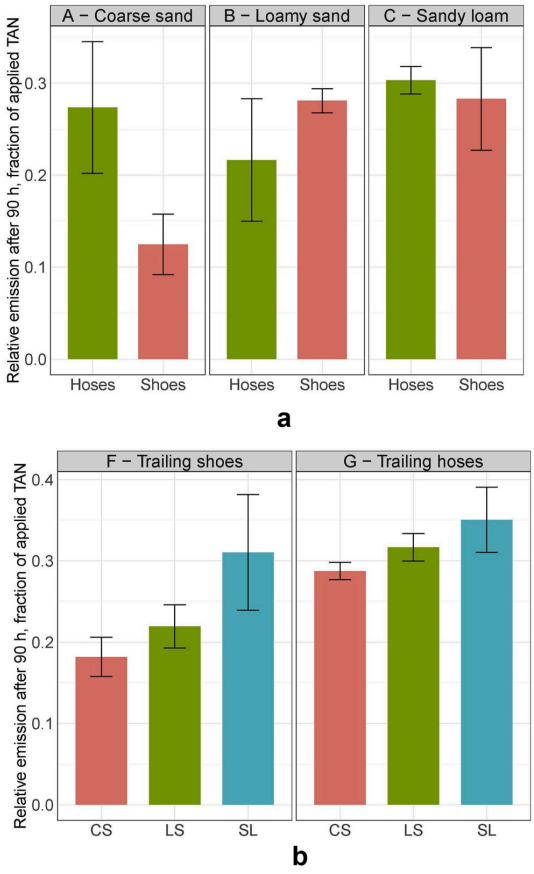

Fig. 5. Effect of slurry application method for pig slurry applied to coarse sand, loamy sand and sandy loam soils. Standard deviations are displayed as error bars ($n = 3$ for emission measurements and $n = 2$ for NH4-N analysis). (a) Three experiments varying soil type with trailing shoes (Shoes) and trailing hoses (Hoses). (b) Two experiments varying application method on three different soil types: coarse sand (CS), loamy sand (LS) and sandy loam (SL).

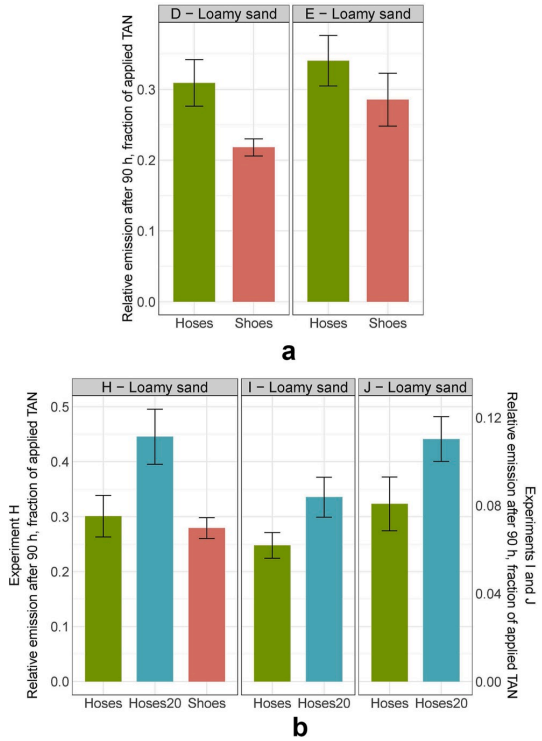

Fig. 6. Effect of slurry application method for cattle slurry applied to loamy sand soil with clover grass. Standard deviations are displayed as error bars ($n = 3$ for emission measurements and $n = 2$ for NH4-N analysis). (a) Two experiments with trailing shoes (Shoes) and trailing hoses (Hoses). (b) Three experiments with trailing hoses and trailing hoses lifted 20 cm (Hoses20) above the grass canopy. H includes trailing shoes.

Comparing trailing hoses to trailing shoes on the same soil with winter wheat (A, B, and C) a significant difference in the ammonia volatilizations was only found on coarse sand with a reduction of 56 ± 20% (A) ($p < 0.05$) (Fig. 5). Testing trailing shoes across three different soil types (F), significantly higher ammonia volatilization was found on sandy loam compared to loamy- and coarse sand ($p < 0.05$) (Fig. 5). The pattern of ammonia volatilization from trailing hoses across three soil types (G) was the same as with trailing shoes (F), but the soil type effect was markedly lower (Fig. 5). When trailing shoes are used on bare soils or soil with cereal crops it is used to create a slit for the slurry to be contained in. The intent is to create a lower surface area between the slurry and air, hence lowering the emissions compared to trailing hoses. On soils with high clay content, a higher mechanical force is needed in order to create the slit. Under certain conditions, slits might not be obtained as the force applied on each shoe is limited by the construction and weight of the boom. This limitation can explain why the abatement obtained on coarse sand is more efficient with an average reduction of 47 ± 20% compared to the loamy sand and sandy loam (average reductions of 2 ± 10 and 9 ± 3% respectively) (A, B, C, F, and G). Hence, the reduction of ammonia volatilization from slurry applied by trailing shoes is highly dependent on the soil type.

Air temperature has been observed to be one of the most important factors for ammonia emissions (Bell et al., 2015; Huijsmans et al., 2018; Martínez-Lagos et al., 2013). Relatively large variations in air temperatures occurred for experiments A, B, and C with an average air temperature of 15.1 °C and 20.4 °C during A and C, respectively. The high

average air temperature during C was due to short periods with hot temperatures (above 27 °C). The average soil temperatures, as well as the 6 and 24 h averages of both air and soil temperature, were very similar, (Table 3). It is assumed that the experiments can be compared as most of the emissions occur during the first 24 h after application.

When applying slurry on grass fields with trailing shoes no slits are created due to the grass. When the trailing shoes move across the grass the force of the shoes ensures that the slurry is applied on top or a little below the surface of the grass. This presumably results in a lower surface exposed area of slurry and creates better conditions for slurry infiltration compared to trailing hoses. Lower ammonia volatilization was found in three experiments testing trailing shoes against trailing hoses on loamy sand with clover grass with an average reduction of 17 ± 4% (D, E, and H) (Fig. 6). The reduction is significant in two of the three experiments (D and E) ($p < 0.05$), but low compared to the reduction found on sandy soil with winter wheat (Figs. 5 and 6). The lower ammonia volatilization from trailing shoes compared to trailing hoses on grass is in contrast with findings by Smith et al. (2000). They found that the reduction of ammonia emissions by trailing shoes and trailing hoses compared to broadcast spreading was almost identical, 23% and 25% respectively, when applying cattle slurry onto grasslands of four different soil types. Häni et al. (2016) reported that no significant difference in reduction obtained by the two methods was found after application of neither pig nor cattle manure on grassland. The difference in the effect of trailing shoes in experiment H compared to D and E can most likely be assigned to soil conditions, as the slurry properties and air temperatures are similar. The water contents of the soils were in the same range, but the dry bulk density of the soil used in experiment H is much higher than for the soil used in experiment D and E (Table 1). When the soil types and soil water contents are the same, the higher dry bulk density must correspond to a lower amount of air-filled pores. This could hinder infiltration during experiment H compared to the field used in experiment D and E. The main function of trailing shoes is to open the soil surface and expose slurry to porous soil and reduce slurry application to plant foliage. A low soil porosity (high bulk density) is therefore expected to limit the mitigation effect of trailing shoes, since the difference in infiltration rate of shoe versus hose will be diminished.

On average, a significant reduction of 19 ± 12% (paired *t*-test, $p < 0.05$) is found when using trailing shoes compared to trailing hoses during the eight experiments with these two application methods. This agrees with a review by Webb et al. (2010) who found a greater reduction of ammonia volatilization from trailing shoes compared to trailing hoses looking at averages reported in literature. They discuss the large variation in data, which is partly due to the limited amount of reported emissions after application with trailing shoes. Misselbrook et al. (2002) and Wulf et al. (2002) also reported a higher reduction from trailing shoes compared to trailing hoses. However, Misselbrook et al. (2002) only compared the two application methods directly in one out of 27 experiments, whereas in 26 experiments the application methods were compared one by one to broadcast spreading. The other experiments in the study compared either trailing hoses or trailing shoes to broadcast spreading. Contrary to this, Rochette et al. (2008) found significantly higher ammonia volatilization from trailing shoes compared to trailing hoses from pig slurry applied on a clay loam with grass. They assign this unexpected result to a decrease in the infiltration rate caused sealing of the soil surface by the trailing shoes. The variation in reported results can most likely be attributed to factors like soil type, soil and slurry properties, and meteorological conditions, all affecting the infiltration rate of the slurry and thereby the rate of emission. Other challenges also exist, such as the large variation in methods used and the variability of these. Additionally, a large variation in trailing shoe designs exist which has a huge effect on the slits created. The practical implementation of the application method when applying the slurry can also influence results. The majority of articles reports the application of slurry by trailing hoses at the soil surface, however Rodhe et al. (2006) and Smith et al. (2000) reports that the trailing hoses applied slurry 3–10 and 5 cm above ground, respectively, which is assumed to have a significant effect on the emissions.

To avoid tear on the trailing hoses and protect the boom construction it is normal practice in Denmark (observation) to raise the hoses above the crop. In three experiments (H, I and J), all on loamy sand with clover grass, significantly higher ammonia volatilization was observed by using trailing hoses raised 20 cm above grass canopy compared to application at the grass canopy surface ($p < 0.05$). The average increase is 40 ± 13% (Fig. 6). The emission is substantially larger in H compared to I and J. Several factors could cause this. The soil-water content in H is lower than in the other experiments. This could cause lower infiltration rates of the slurry, hence higher emissions as found by Smith et al. (2000). They attribute a lower infiltration to the hydrophobicity of dry soil. These findings are in contrast to findings by de Jonge et al. (2004) and Sommer and Jacobsen (1999) who found that lower soil-water content increased infiltration. The average soil temperature is 5–7 °C higher during experiment H (Table 3), which will cause higher emissions. The lower values of slurry and soil pH during experiment H (Tables 1 and 2), leads to a larger fraction of TAN to be on the ammonium form, which consequently should result in reduced emissions. Conversely, the lower dry matter content of the slurry and higher slurry application rates in I and J could enhance infiltration and thereby lower emissions as observed by Huijsmans et al. (2018) and Häni et al. (2016). This effect should be investigated further in order to draw conclusions.

5. Conclusions

A new system of wind tunnels and online measurements was used to measure the ammonia emissions from band applied liquid slurry. From ten experiments, it was concluded: (i) The wind tunnel set up with online measurements of ammonia allows for precise and repeatable results of ammonia emissions when comparing different treatments or soil types. The online measurements ensure a high time resolution of 104 min, an overall low variation within treatments (coefficient of variation of 13 ± 8%), long measuring times and comprehensive datasets which shows the emissions dynamics over time. (ii) The method for evaluating turbulence intensity in the emission chamber and the effect of turbulence at the soil surface throughout the chamber can be used as a support tool to choose the most realistic air exchange rate. (iii) Trailing shoes were found to give lower ammonia emissions when used on coarse sand, whereas only a weak and varying effect was found for application on loamy sand with and without clover grass and for application on sandy loam. The average reduction of ammonia emissions from trailing shoes compared to trailing hoses was 19 ± 12%. (iv) A high emission reduction can be obtained by correct use of trailing hoses, i.e. by ensuring that the slurry is applied right at the soil surface and hence avoiding splashing.

When choosing the application method with the objective of ammonia abatement, the soil type should be taken into consideration. The results in this study help explain why previous research studies have found different effects of trailing shoes.

6. Funding

This work was funded by the Ministry of Environment and Food of Denmark as a green development and demonstration program (GUDP) with the project title *New application method for slurry in growing crops*.

Declaration of competing interest

The authors declare that they have no known competing financial interests or personal relationships that could have appeared to influence the work reported in this paper.

CRediT authorship contribution statement

Johanna M. Pedersen: Conceptualization, Methodology, Formal

analysis, Investigation, Writing - original draft, Visualization. **Anders Feilberg:** Conceptualization, Methodology, Validation, Writing - review & editing, Supervision, Funding acquisition. **Jesper N. Kamp:** Methodology, Writing - review & editing. **Sasha Hafner:** Methodology, Validation, Writing - review & editing, Supervision. **Tavs Nyord:** Conceptualization, Methodology, Validation, Writing - review & editing, Supervision, Project administration, Funding acquisition.

Acknowledgements

We would like to acknowledge the technical staff Heidi Grønbæk, Jens Kr Kristensen, Per Wiborg Hansen, and Peter Storegård Nielsen for their skillful assistance with development of the measuring system, carrying out measurements and laboratory analysis.

Appendix A. Supplementary data

Supplementary data to this article can be found online at https://doi.org/10.1016/j.atmosenv.2020.117562.

References

The ALFAM2 Project. Measurements of ammonia emissions from field applied slurry. Online database. https://biotransformers.shinyapps.io/ALFAM2/. (Accessed 24 October 2019).

American Public Health Association, 1999. Standard Methods for the Examination of Water and Wastewater.

Association of Official Analytical Chemists, 1999. Official Methods of Analysis of AOAC International, sixteenth ed. (Washington, D. C).

Bell, M.J., Hinton, N.J., Cloy, J.M., Topp, C.F.E., Rees, R.M., Williams, J.R., Misselbrook, T.H., Chadwick, D.R., 2015. How do emission rates and emission factors for nitrous oxide and ammonia vary with manure type and time of application in a Scottish farmland? Geoderma 264, 81–93. https://doi.org/10.1016/j.geoderma.2015.10.007.

Bhandral, R., Bittman, S., Kowalenko, G., Buckley, K., Chantigny, M.H., Hunt, D.E., Bounaix, F., Friesen, A., 2009. Enhancing soil infiltration reduces gaseous emissions and improves N uptake from applied dairy slurry. J. Environ. Qual. 38, 1372–1382. https://doi.org/10.2134/jeq2008.0287.

Braschkat, J., Mannheim, T., Marschner, H., 1997. Estimation of ammonia losses after application of liquid cattle manure on grassland. Pflanzenernähr. Bodenk. 160, 117–123.

Chen, Y., Munkholm, L.J., Nyord, T., 2013. A discrete element model for soil–sweep interaction in three different soils. Soil Tillage Res. 126, 34–41. https://doi.org/10.1016/j.still.2012.08.008.

de Jonge, L.W., Sommer, S.G., Jacobsen, O.H., Djurhuus, J., 2004. Infiltration of slurry liquid and ammonia volatilization from pig and cattle slurry applied to harrowed and stubble soils. Soil Sci. 169, 729–736. https://doi.org/10.1097/01.ss.0000146019.31065.ab.

Eklund, B., 1992. Practical guidance for flux chamber measurements of fugitive volatile organic emission rates. J. Air Waste Manag. Assoc. 42, 1583–1591. https://doi.org/10.1080/10473289.1992.10467102.

Eurostat, 2017. Agri-environmental Indicator – Ammonia Emissions, pp. 1–11.

Hafner, S.D., Montes, F., Alan Rotz, C., 2012. The role of carbon dioxide in emission of ammonia from manure. Atmos. Environ. 66, 63–71. https://doi.org/10.1016/j.atmosenv.2012.01.026.

Hafner, S.D., Pacholski, A., Bittman, S., Carozzi, M., Chantigny, M., Génermont, S., Häni, C., Hansen, M.N., Huijsmans, J., Kupper, T., Misselbrook, T., Neftel, A., Nyord, T., Sommer, S.G., 2019. A flexible semi-empirical model for estimating ammonia volatilization from field-applied slurry. Atmos. Environ. 199, 474–484. S1352231018308069.

Haisler, J., Jacobsen, S.M., 2017. Forsk 2025 – Fremtidens Løfterige Forskningsområder. Ministry of Higher Education and Science, Denmark. Technical report.

Huijsmans, J.F.M., Vermeulen, G.D., Hol, J.M.G., Goedhart, P.W., 2018. A model for estimating seasonal trends of ammonia emission from cattle manure applied to grassland in The Netherlands. Atmos. Environ. 173, 231–238. https://doi.org/10.1016/j.atmosenv.2017.10.050.

Häni, C., Sintermann, J., Kupper, T., Jocher, M., Neftel, A., 2016. Ammonia emission after slurry application to grassland in Switzerland. Atmos. Environ. 125, 92–99. https://doi.org/10.1016/j.atmosenv.2015.10.069.

IS, 1984. International Standard, 1984. Water Quality - Determination of Ammonium - Part 1: Manual Spectrometric Method.

Jiang, K., Bliss, P.J., Schulz, T.J., 1995. The development of a sampling system for determining odor emission rates from areal surfaces: Part 1. Aerodynamic Performance. J. Air Waste Manag. Assoc. 45, 831–832. https://doi.org/10.1080/10473289.1995.10467424.

Lee, J.F., Chao, H.P., Chiou, C.T., Manes, M., 2004. Turbulence effects on volatilization rates of liquids and solutes. Environ. Sci. Technol. 38, 4327–4333. https://doi.org/10.1021/es0353964.

Lockyer, D.R., 1984. A system for the measurement in the field of losses of ammonia through volatilization. J. Sci. Food Agric. 35, 837–848. https://doi.org/10.1002/jsfa.2740350805.

Mannheim, T., Braschkat, J., Marschner, H., 1995. Comparison of the wind tunnel and the IHF method under field conditions. Z. Pflanzenernähr. Bodenk 158, 215–219.

Martínez-Lagos, J., Salazar, F., Alfaro, M., Misselbrook, T., 2013. Ammonia volatilization following dairy slurry application to a permanent grassland on a volcanic soil. Atmos. Environ. 80, 226–231. https://doi.org/10.1016/j.atmosenv.2013.08.005.

Misselbrook, T.H., Nicholson, F.A., Chambers, B.J., Johnson, R.A., 2005a. Measuring ammonia emissions from land applied manure: an intercomparison of commonly used samplers and techniques. Environ. Pollut. 135, 389–397. https://doi.org/10.1016/j.envpol.2004.11.012.

Misselbrook, T.H., Nicholson, F.A., Chambers, B.J., 2005b. Predicting ammonia losses following the application of livestock manure to land. Bioresour. Technol. 96, 159–168. https://doi.org/10.1016/j.biortech.2004.05.004.

Misselbrook, T.H., Scholefield, D., Parkinson, R., 2005c. Using time domain reflectometry to characterize cattle pig slurry infiltration into soil. Soil Use Manag. 21, 167–172. https://doi.org/10.1079/SUM2005316.

Misselbrook, T.H., Smith, K.A., Johnson, R.A., Pain, B.F., 2002. Slurry application techniques to reduce ammonia emissions: results of some UK field-scale experiments. Biosyst. Eng. 81, 313–321. https://doi.org/10.1006/bioe.2001.0017.

Nyord, T., Hansen, M.N., Birkmose, T.S., 2012. Ammonia volatilisation and crop yield following land application of solid-liquid separated, anaerobically digested, and soil injected animal slurry to winter wheat. Agric. Ecosyst. Environ. 160, 75–81. https://doi.org/10.1016/j.agee.2012.01.002.

Nyord, T., Kristensen, E.F., Munkholm, L.J., Jørgensen, M.H., 2010. Design of a slurry injector for use in a growing cereal crop. Soil Tillage Res. 107, 26–35. https://doi.org/10.1016/j.still.2010.01.001.

Pacholski, A., Cai, G., Nieder, R., Richter, J., Fan, X., Zhu, Z., Roelcke, M., 2006. Calibration of a simple method for determining ammonia volatilization in the field - comparative measurements in Henan Province, China. Nutrient Cycl. Agroecosyst. 74, 259–273. https://doi.org/10.1007/s10705-006-9003-4.

Parker, D., Ham, J., Woodbury, B., Cai, L., Spiehs, M., Rhoades, M., Trabue, S., Casey, K., Todd, R., Cole, A., 2013. Standardization of flux chamber and wind tunnel flux measurements for quantifying volatile organic compound and ammonia emissions from area sources at animal feeding operations. Atmos. Environ. 66, 72–83. https://doi.org/10.1016/j.atmosenv.2012.03.068.

Rochette, P., Angers, D.A., Chantigny, M.H., Gasser, M.O., MacDonald, J.D., Pelster, D.E., Bertrand, N., 2013. NH3 volatilization, soil concentration and soil pH following subsurface banding of urea at increasing rates. Can. J. Soil Sci. 93, 261–268. https://doi.org/10.4141/cjss2012-095.

Rochette, P., Guilmette, D., Chantigny, M.H., Angers, D., MacDonald, J.D., Bertrand, N., Parent, L.É., Côté, D., Gasser, M.O., 2008. Ammonia volatilization following application of pig slurry increases with slurry interception by grass foliage. Can. J. Soil Sci. 88, 585–593. https://doi.org/10.4141/CJSS07083.

Rodhe, L., Pell, M., Yamulki, S., 2006. Nitrous oxide, methane and ammonia emissions following slurry spreading on grassland. Soil Use Manag. 22, 229–237. https://doi.org/10.1111/j.1475-2743.2006.00043.x.

Rodhe, L., Rydberg, T., Gebresenbet, G., 2004. The influence of shallow injector design on ammonia emissions and draught requirement under different soil conditions. Biosyst. Eng. 89, 237–251. https://doi.org/10.1016/j.biosystemseng.2004.07.001.

Schwarzenbach, R.P., Gschwend, P.M., Imboden, D.M., 2003. Environmental Organic Chemistry, second ed. Wiley-Interscience, John Wiley & Sons, Inc, Canada.

Smith, K.A., Jackson, D.R., Misselbrook, T.H., Pain, B.F., Johnson, R.A., 2000. Reduction of ammonia emission by slurry application techniques. J. Agric. Eng. Res. 78, 233–243. https://doi.org/10.1006/jaer.2000.0639.

Smith, R.J., Watts, P.J., 1994. Determination of odour emission rates from cattle feedlots: Part 2, evaluation of two wind tunnels of different size. J. Agric. Eng. Res. 58, 231–240. https://doi.org/10.1006/jaer.1994.1053.

Sommer, S.G., Jacobsen, O.H., 1999. Infiltration of slurry liquid and volatilization of ammonia from surface applied pig slurry as affected by soil water content. J. Agric. Sci. 132, 297–303. https://doi.org/10.1017/S0021859698006261.

Sommer, S.G., Jensen, L.S., Clausen, S.B., Søgaard, H.T., 2006. Ammonia volatilization from surface-applied livestock slurry as affected by slurry composition and slurry infiltration depth. J. Agric. Sci. 229–235. https://doi.org/10.1017/S0021859606006022.

Sommer, S.G., Misselbrook, T.H., 2016. A review of ammonia emission measured using wind tunnels compared with micrometeorological techniques. Soil Use Manag. 32, 101–108. https://doi.org/10.1111/sum.12209.

Sommer, S.G., Olesen, J.E., 1991. Effects of dry matter content and temperature on ammonia loss from surface-applied cattle slurry. J. Environ. Qual. 20, 679–683. https://doi.org/10.2134/jeq1991.00472425002000030029x.

Stevens, C.J., Dupr, C., Dorland, E., Gaudnik, C., Gowing, D.J., Bleeker, A., Diekmann, M., Alard, D., Bobbink, R., Fowler, D., Corcket, E., Mountford, J.O., Vandvik, V., Aarrestad, P.A., Muller, S., Dise, N.B., 2010. Nitrogen deposition threatens species richness of grasslands across Europe. Environ. Pollut. 158, 2940–2945. https://doi.org/10.1016/j.envpol.2010.06.006.

USDA, 2009. Soil survey field and laboratory methods manual, 2009. U.S. Dep. Agricult. https://doi.org/10.13140/RG.2.1.3803.8889.

Van Vuuren, D., Bouwman, L.F., Smith, S.J., Dentener, F., 2011. Global projections for anthropogenic reactive nitrogen emissions to the atmosphere: an assessment of scenarios in the scientific literature. Curr. Opin. Environ. Sustain. 3, 359–369. https://doi.org/10.1016/j.cosust.2011.08.014.

Walker, J.T., Robarge, W.P., Shendrikar, A., Kimball, H., 2006. Inorganic PM2.5at a U.S. agricultural site. Environ. Pollut. 139, 258–271. https://doi.org/10.1016/j.envpol.2005.05.019.

Webb, J., Pain, B., Bittman, S., Morgan, J., 2010. The impacts of manure application methods on emissions of ammonia, nitrous oxide and on crop response - a review. Agric. Ecosyst. Environ. 137, 39–46. https://doi.org/10.1016/j.agee.2010.01.001.

Wulf, S., Maeting, M., Clemens, J., 2002. Application technique and slurry co-fermentation effects on ammonia, nitrous oxide, and methane emissions after spreading. J. Environ. Qual. 31, 1789. https://doi.org/10.2134/jeq2002.1795.

Supporting Information

Ammonia emission measurement with an online wind tunnel system for evaluation of manure application techniques

Johanna Pedersen, Anders Feilberg, Jesper N. Kamp, Sasha Hafner, Tavs Nyord*

Aarhus University, Dept. of Engineering, Denmark

*Corresponding author email: tavs.nyord@eng.au.dk

S1. Weather conditions during evaporation experiments

To ensure that the ethanol did not get diluted the experiments were performed when there was no rainfall. The specific ambient air temperatures and wind speeds during the four experiments can be seen in Figure S1.

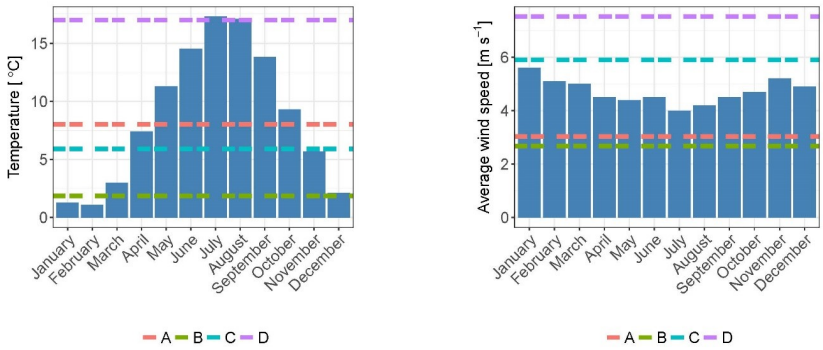

Figure S1: *Temperature (left) and wind speed (right) during the evaporation experiments compared to monthly averages in Denmark from (DMI 2013). The letters indicate different test days.*

S2. Saturation of the wind tunnel system

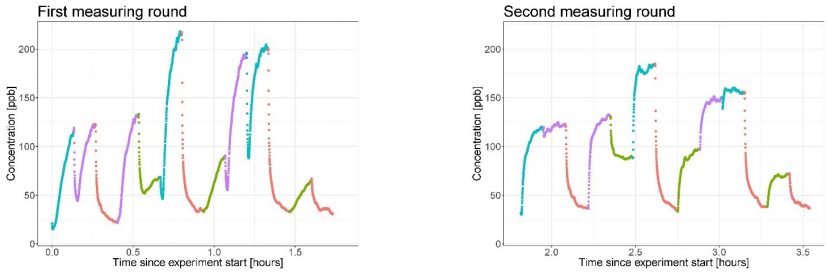

Figure S2: *Raw data of ammonia emissions measured with wind tunnels and CRDS. Colors indicate different application techniques, red is background measurements. First (left) and second (right) measuring cycle on all nine tunnels and four backgrounds.*

S3. Plots of data from all experiments

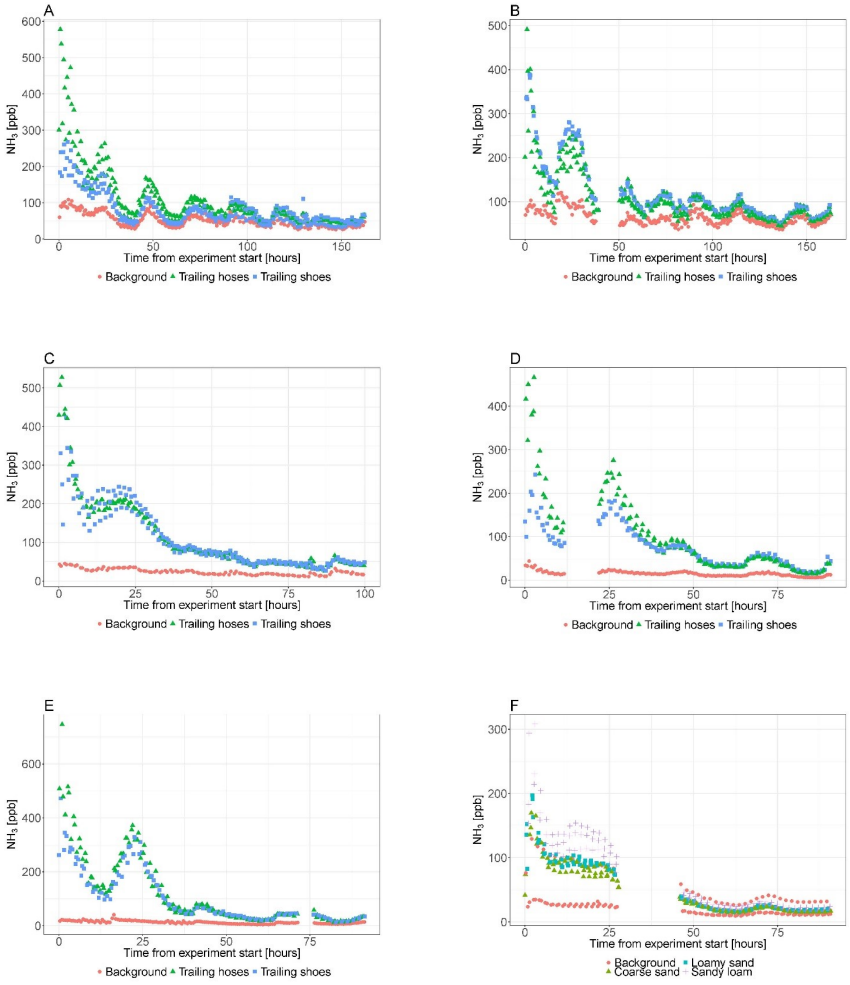

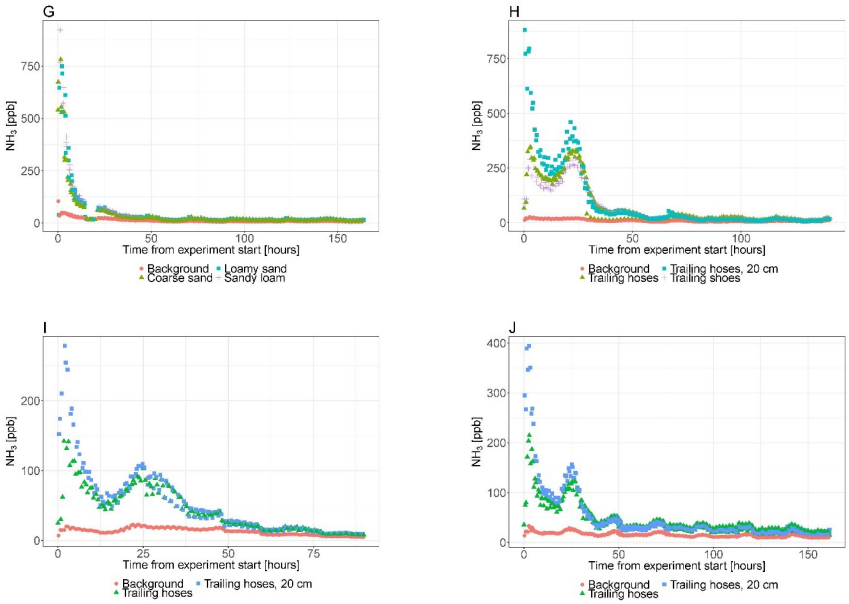

Figure S3: *Ammonia concentrations measured in wind tunnel chambers with CRDS after application of pig (experiment A, B, C, F, G) and cattle (experiment D, E, H, I, J) manure.*

References

Wang, P. R., 2013. Teknisk Rapport 12-23. Referenceværdier. Måneds- og årskort 2001 – 2010, Danmark for temperatur, relativ luftfugtighed, vindhastighed, globalstråling og nedbør.

Chapter 4

Paper II

J. Pedersen, T. Nyord, M. J. Hansen, A. Feilberg. Emissions of NMVOC and H_2S from field-applied manure measured by PTR-TOF-MS and wind tunnels. *Atmospheric Environment*, in review September 2020

Emissions of NMVOC and H_2S from field-applied manure measured by PTR-TOF-MS and wind tunnels

Johanna Pedersen, Tavs Nyord, Michael J. Hansen, Anders Feilberg*

Aarhus University, Dept. of Engineering, Denmark
*Corresponding author email: af@eng.au.dk, Address: Aarhus University, Finlandsgade 10, 8200 Aarhus N, Denmark, +45 30896099

Keywords: Dynamic chambers, Odor emission, Odor activity value, Air pollution, Trailing hoses, Trailing shoes

Abstract

Field application of animal manure is a source of volatile organic compounds (VOC) and hydrogen sulfide (H_2S) emission that contribute to air pollution and odor nuisance in local surroundings. In this study the non-methane volatile organic compounds (NMVOC) and H_2S emission and odor activity dynamics over time after field application of pig and cattle manure were investigated. Furthermore, three different application techniques, trailing hoses, trailing shoes, and trailing hoses applying manure 20 cm above canopy, was compared. With a flexible system combining dynamic chambers and Proton Transfer Reaction Time-of-Flight Mass Spectroscopy (PTR-TOF-MS), H_2S and 22 different NMVOC were measured, identified, and quantified. From pig manure high amounts of H_2S was measured right after application, resulting in high odor activity values (OAV). During the first ten hours 4-methylphenol accounted for most of the cumulative emissions and OAV. Carboxylic acids were emitted for a longer period, and accounted for most of the long-term emissions and OAV. Acetic acid alone accounted for 33-57% of the total cumulative emissions. Trailing shoes were found to reduce NMVOC emission under certain conditions. It is suggested to use updated ratios from this study to calculate NMVOC emissions relative to ammonia emissions. The average ratios of cumulated NMVOC emission divided by cumulated ammonia emission 90 hours after application of pig manure is 1.15±0.55 and 0.72±0.26 for trailing hoses and trailing shoes respectively, whereas the same numbers for cattle manure is 0.43±0.11 and 0.18±0.04.

1 Introduction

Field application of manure contributes to air pollution due to emissions of ammonia (Eurostat, 2017), volatile organic compounds (VOC) (Feilberg et al., 2015, 2011) and hydrogen sulfide (H_2S) (Feilberg et al., 2017). Of these emissions, only ammonia emission has been studied and quantified extensively in a vast number

of investigations and by using a variety of methods. During the last decades, an extensive amount of studies have focused on reduction of ammonia and greenhouse gas emissions from field applied manure (Montes et al., 2013; Nielsen et al., 2016; Sommer and Misselbrook, 2016). Many of the studies have investigated different manure application techniques, as it is one of the most important factors for reduction of ammonia emission (Hafner et al., 2019). Different techniques can be used for surface application of manure slurry, and it has been shown that trailing shoes on certain soil types reduce ammonia emission compared to trailing hoses (Pedersen et al., 2020). On bare soils with cereal crops, the trailing shoes can create a slit for containing the slurry, which can lower emissions by reducing the surface area between slurry and air. Trailing hoses on the contrary, apply the slurry at the soil surface without any manipulation of the soil resulting in a larger surface area due to spreading out. For VOC and volatile sulfur compounds (VSC), on the other hand, there is a scarcity of reports available and their contributions have been estimated only by indirect approaches based on limited data (EMEP/EEA, 2016). In addition to their general air pollution contribution, these compounds are sources of odor nuisance in local surroundings (Hanna et al., 2000). Only a few studies (Feilberg et al., 2015, 2011, 2010b; Liu et al., 2018; Parker et al., 2013a; Woodbury et al., 2016) have attempted to measure the complex matrix of VSC and VOC emitted after field application of manure, resulting in very limited quantitative data (EMEP/EEA, 2016; Nielsen et al., 2016). In Denmark, agriculture has been estimated to account for 37% of the total non-methane VOC (NMVOC) emission by extrapolating data from a limited number of studies (Nielsen et al., 2016), and this contribution is associated with great uncertainty.

The European countries have committed to reduce the emission of NMVOC (Union, 2016). However, the knowledge of NMVOC emission from field application of manure is so limited, that it is not possible to calculate emission factors (EMEP/EEA, 2016). The emission of NMVOC from manure application are estimated as a fraction of the emission from a pig house, and assumed to have the same ratio as ammonia emissions based on a single pig house study by Feilberg et al. (2010b) (EMEP/EEA, 2016; Feilberg et al., 2010b). For estimating accurate NMVOC emission factors and identifying mitigation measures, more research into this area is acutely needed.

The most common technique used for identification and quantification of NMVOC are gas chromatography (GC) with different detectors, such as mass spectrometry (MS) or flame ionization detection (FID) (Ni et al., 2012). Most of these techniques require time-consuming procedures with variation in sampling, preparation, and analysis, often producing results with high variability (Ni et al., 2012; Parker et al., 2013b). To quantify odor, olfactometry has commonly been used, but these too have been identified to give poor results, as the sampling,

storage, and analysis may result in potential discrimination and loss of sample compounds (Kasper et al., 2018a, 2018b, 2017).

Proton Transfer Reaction Mass Spectroscopy (PTR-MS) has been proven as a successful tool for online measurements of VSC and NMVOC from field applied manure (Feilberg et al., 2015, 2011, 2010a; Liu et al., 2018) and livestock production facilities (Feilberg et al., 2010b; Hansen et al., 2016, 2012; Ngwabie et al., 2008). PTR-MS benefit from being an online measurement technique with the possibility for measuring a broad range of NMVOC and VSC compounds (Feilberg et al., 2011). PTR-MS can provide quantitative results for a large suite of NMVOC based on a calculated sensitivity if mass discrimination factors are determined based on a suitable mixture of compounds with known concentrations and known proton-transfer rate constants. According to Sekimoto et al. (2017), the accuracy is within 20% when using consolidated proton-transfer rate constants for determining concentrations of unknowns. Liu et al. (2018) reported an accuracy within ±12% for 11 typical livestock manure VOC when comparing calculated PTR-MS concentrations with concentrations from a known source. Fragmentation patterns and influence of water clusters in the PTR-MS drift tube must be taken into account when using this approach (Cappellin et al., 2012; Sekimoto et al., 2017).

Different types of static and dynamic chambers has been used to measure gaseous emission from field-applied manure. Feilberg et al. (2011) tested a static flux chamber for sample collection, and found that the flux chamber technique had critical errors. Other studies have used various designs of dynamic chambers with a huge variation in physical characteristics and operating conditions to collect samples from surfaces emitting NMVOC and VSC (Feilberg et al., 2015; Hudson and Ayoko, 2008a; Liu et al., 2018; Parker et al., 2013a).

The selection of air flow in dynamic chamber flux measurements critically influences the absolute emissions of compounds for which the manure-to-air mass transfer is limited primarily by the air side resistance (Hudson and Ayoko, 2008b; Liu et al., 2018; Parker et al., 2009; Smith and Watts, 1994). Currently, there is no generally accepted approach for correcting emission data obtained by dynamic chamber methods to obtain absolute emissions valid for open fields. Dynamic chambers are therefore mostly suitable for relative comparisons of e.g. the effects of different treatments on emission. Since no micrometeorological studies of NMVOC and VSC emissions from manure application have been published, however, dynamic chamber data is still useful for indicating the magnitude of absolute emissions. A range of different air velocities have been used (Feilberg et al., 2015; Liu et al., 2018; Parker et al., 2013a, 2009), which should be kept in mind when comparing data from different studies.

The primary aim of the study was to identify and quantify the emission from field-applied manure based on dynamic chamber measurements. The objectives

were to: (i) Study the emission dynamics over time of VSC, NMVOC, and odor activity value (OAV) after field application of pig and cattle manure. (ii) Investigate the effect of application technique on emission after application of manure by trailing hoses, trailing shoes, and trailing hoses applying manure 20 cm above canopy. For this purpose, a flexible system combining dynamic chambers and PTR-TOF-MS (TOF: Time-of-Flight) for measurements of VSC and NMVOC has been designed.

2 Experimental

Emission of VSC and NMVOC were measured during six experiments. The three first experiments (A, B, and C) were performed on three different soil types with winter wheat crop. The last three experiments (D, E, and F) were performed on two different loamy sand fields with clover grass. During each experiment, VSC and NMVOC emitted from manure applied by trailing hoses or trailing shoes were measured. The last experiment (F) include the use of trailing hoses raised 20 cm above the grass canopy (trailing hoses 20 cm). The application of trailing hoses 20 cm above the surface was tested, since it has been reported (T. Nyord, personal communication) to be a common practice by farmers in order to reduce wear of the hoses. All experiments varied the application techniques in triplicates. An overview of the experiments can be found Table 1.

Table 1: *Overview of experiments*

Experiment	Soil	Manure	Application technique[1]	Measuring time (hours)
A	Coarse sand			120
B	Loamy sand	Pig	TS, TH	90
C	Sandy loam			45
D			TS, TH	115[2]
E	Loamy sand	Cattle		70[3]
F			TS, TH, TH20	100

[1]TS: trailing shoes, TH: trailing hoses, TH20: trailing hoses 20 cm.
[2]Data estimated for following hours: 10.4-21.9;37.4-42.7; 61.7-66.9.
[3]Data estimated for following hours: 15.6-22.6; 58.9-64.2.

2.1 Dynamic chamber setup

The measurement system has been described in detail by Pedersen et al. (2020) including a thorough description of the system, evaluation of air flow within the emission chamber, and ammonia emission data. The air flow within the emission chamber was chosen based on experiments evaluating the air turbulence (caused by air exchange) at the soil surface by measuring evaporation of ethanol in pure liquid form inside the tunnels relative to the outside evaporation of ethanol, as the emissions of most compounds are expected to be dependent on air turbulence. Ethanol was chosen as the solvent since it is quickly evaporated and flushed from the wind tunnel system. Details of ethanol evaporation experiments are provided in Pedersen et al. (2020). The following is a short description of the system. The measuring system consisted of nine wind tunnels with a constant air flow. The wind tunnels consisted of a rectangular open-bottomed stainless steel chamber (80 cm length, 40 cm wide, and 25 cm high) connected to a fan, and a motor with a frequency converter via a steel duct. To avoid leaks and ensure the correct amount of manure within a plot, each tunnel was mounted on a metal frame inserted into the soil. The plot area was 0.2 m^2. Backflow of air through the inlet (due to inhomogeneous turbulence) was prevented by using an air inlet with a reduced slit opening of 33.5 x 1.3 cm. An air exchange rate inside the emission chamber of 25 min^{-1} was used, which corresponds to a nominal air velocity of 0.33 m s^{-1}. From the tunnels, sample air was drawn into a channel selection manifold consisting of 19 on/off valves using 8 mm PTFE (polytetrafluoroethylene) tube heated to approximately 40°C. The length of the tubing from the tunnels to the selection manifold varied between four and 10 meters. The flow in these tubes were minimum 1 L min^{-1}. From the manifold, a split-flow of the sample air was analyzed in a continuous cycle by PTR-TOF-MS (PTR-TOF 4000, Tracer VOC Analyzer, IONICON Analytik, Innsbruck, Austria) and another split flow was analyzed continuously by a ring down spectroscopy instrument (CRDS) (G2103 NH_3 Concentration Analyzer, Picarro, CA, USA) for ammonia concentration. The tubing between the selection manifold and analytical instruments was approximately three meters. Three tubes for background measurements were evenly distributed between the tunnels. Furthermore, one 20 m tube was placed outside of the experimental plot for measurements of field background. The measuring time for each measurement point was 8 minutes, resulting in a time resolution for each single tunnel of 104 minutes. The 8-minute measurement intervals were sufficient to get a stable reading of both high and low concentrations. As a test of recovery throughout the system and estimation of wall loss, the recovery of ammonia throughout the wind tunnel system was measured during several occasions in the field. This was done by adding a standard gas (11.3 ppm ammonia, Linde, Surrey, UK) at the tube inlets. At all occasions, the recovery was minimum 90% within the 8 minute measurement interval. Liu et al. (2018) showed that wall

losses of sulfur compounds, which are known to be sticky, were negligible in similar wind tunnels. A weather station logged air and soil temperature in 10-minute intervals during the experiments (Table S1).

At the start of the experiments, the manure was applied inside the wind tunnel frame. Application took approximately 20 seconds. The tunnels were placed on the frames immediately after and measurements started.

2.2 Measurements and data treatment

A high sensitivity PTR-TOF-MS operated with H_3O^+ as the primary ion was used to measure the VSC and NMVOC. PTR-TOF-MS is an online chemical ionization technique for detection of compounds with a proton affinity higher than water (691 kJ mol^{-1}) by Time-of-Flight Mass Spectrometry (Blake et al., 2009; de Gouw and Warneke, 2007). The drift tube conditions in the present study were set to a pressure of 2.4 mbar, a voltage of 600V, and temperature of 80°C giving a E/N of 140 Td. The instrument was operated in full scan mode from m/z 5 to 200. The inlet temperature was 80°C and the air flow into the instrument was 400 mL min^{-1}. Measurements were recorded every five seconds during A, B, and C and every 10 seconds during D, E, and F.

A mass transmission curve was measured as described by Liu et al. (2018) (details of composition and concentrations can be found in Table S4) and a H_2S humidity-dependent calibration was performed as described by Feilberg et al. (2010b). The proton-transfer rate constants were calculated with the method described by Su (1994), Cappellin et al. (2012) and Sekimoto et al. (2017) with polarization and dipole moments found or estimated based on recent literature (Cappellin et al., 2012; Sekimoto et al., 2017) (Table S5). Quantification of concentration was done as reported and validated by Liu et al. (2018). Fragmentations have been assigned, based on known fragmentation patterns from literature (Feilberg et al., 2015, 2011, 2010a; Hansen et al., 2016, 2012). Ion fragments of carboxylic acids (corresponding to loss of H_2O) were included in the concentration determinations in order to avoid bias due to variations in the fragmentation rate (e.g. caused by humidity (Feilberg et al., 2010b)).

For each detected compound, a mean of the last 30 seconds of measurements per measurement cycle (8 minutes) was used for further calculations. For the sulfur compounds, the emission during the first 8 minutes right after application was calculated separately, and added to the cumulative emission, since peaks of emission occurred during this time for these compounds, leading to an underestimation if not included. An average of the background measurements ($n = 3$) was subtracted for each measurement cycle before further calculations. Compounds lower than the detection limit (three times the standard deviation of the background measurements) were set to zero.

The fluxes (F_n [mg m^{-2} min^{-1}]) were calculated from the concentrations

(C_n), the air flow in the emission chamber (q) and the area of soil surface covered by the tunnel (A) (Equation 1).

$$F_n = (C_n * q)/A \qquad \text{Equation 1}$$

Due to software failure and temporary power cuts to the system, sections of data was lost during D and E (Table 1). These data were estimated in order to calculate a more representative cumulative emission. A linear interpolation between the data points right before and after the missing data was used for the estimation. This might have led to small over- or underestimation. During the second night of experiment B, very low emission was measured for all compounds. After approximately 50 hours, very low concentrations of carboxylic acid were measured in experiment A, in contrast to experiment B in which carboxylic acids contribute to emissions in the whole measuring period of 90 hours. As no failures have been found that could cause measurement errors in any of the cases, the data is included as it is.

Odor activity value is an estimation of odor based on measured odorants, and can be used to assess the relative influence of the individual compounds on the total odor nuisance of a complex odor mixture. In order to use OAV as a quantitative measurement, it is assumed that OAV for the individual odorants is additive and that no synergistic or antagnostic effects take place between the odorants. The OAV was calculated from the concentrations (C_n) of the odorant and the odor threshold (OTV) values from literature (Hansen et al., 2018; Nagata, 2003; Ruth, 1986; van Gemert, 2003) (Table 2) (Equation 2).

$$\sum OAV_n = \sum_{n=1}^{n} \frac{C_n}{OTV_n} \qquad \text{Equation 2}$$

An estimation of the odor emission rate (E [OAV h^{-1} m^{-2}]) is calculated from the OAV, the air flow in the emission chamber (q), and the area of soil surface covered by the tunnel (A) (Equation 3), as done by Hudson and Ayoko (2008b).

$$F_{odor} = (OAV * q)/A \qquad \text{Equation 3}$$

During experiment A air samples for supplementary screening with GC/MS were taken and analyzed as described by Feilberg et al. (2010b). Right after slurry application, one sample per tunnel was collected in adsorption tubes packed with a TenaxTA/Carbograph 5D combination, at a flowrate of 200 mL min^{-1} for five minutes.

2.2.1 Statistics

To test for differences among application methods, a single factor analysis of

variance (ANOVA) was used. The design of each experiment was a complete randomized block design with three blocks. Each block had each treatment randomly assigned. An individual plot in a single wind tunnel was used as the observational unit. For total NMVOC emission, the cumulative emission after 45 and 90 hours were used as the response variables. For OAV the OAV right after manure application as well as after 24 and 48 hours were used as the response variables. To investigate which treatments were significantly different, a Tukey's test with a confidence interval of 95% was used on the cumulative NMVOC emission or OAV value.

2.3 Experimental setup and site

2.3.1 Soil

The experiments were performed at Research Center Foulum (Aarhus University, Tjele, Denmark) in spring and summer 2018. A, B, and C were performed in an experimental field facility with winter wheat crops on a coarse sand (Orthic Haplohumod), loamy sand (Typic Hapledult), and sandy loam (Typic Agrudalf) respectively. D, E, and F were performed on two different loamy sand fields (Typic Hapledult) with clover grass (established in 2015). Dry bulk densities and soil-water contents were determined gravimetrically using 100 cm^3 soil cores at 0-5 cm depth. Soil pH was determined in a solution of 1:1 water and soil according to the standard method (USDA, 2009). Soil information and analysis can be found in Table S2. During each experiment, a soil plot of approximately 2.5 x 16 meters was used. It was assumed that differences in soil within the same area were insignificant.

2.3.2 Manure

Cattle and pig manure was sampled from concrete manure storage tanks at Aarhus University Foulum. Standard methods were used to analyze the dry matter content (American Public Health Association, 1999) and ammoniacal nitrogen (Association of Official Analytical Chemists, 1999). Volatile fatty acids were analyzed using GC (HP 6850 Series GC system, Agilent Technologies, Santa Clara, CA, USA) as done by Dalby et al. (2018). Manure properties can be found in Table S3. The dry matter contents were found to be 3.67 (0.23) and 8.87 (0.19) g kg^{-1} for pig and cattle manure respectively, and the pH values were 7.11 (0.08) and 6.90 (0.06) respectively.

2.3.3 Manure application

A metal frame on wheels with three trailing shoes (Bomech B.V., Albergen, The Netherlands) was used to create sweeps for application by trailing shoes. The trailing shoes had a distance of 25 cm between them, and a constant speed of approximately 2 km h^{-1} was used to create the sweeps. The force applied on each

trailing shoe was adjusted to the soil. The maximum possible force was 117 N, based on the force a typical commercial slurry tanker boom can provide. During experiments A, B, and C, the force measured at the end of the individual trailing shoe was adjusted to approximately 88 N. For D, E, and F it was adjusted to approximately 117 N. Manure was applied manually with a hose attached to a watering can. A pre-determined volume of manure for each tunnel was added to the can. The manure was spread evenly in three bands at the soil surface to mimic application by trailing hoses, in three bands 20 cm above the grass canopy when mimicking trailing hoses used with a distance of 20 cm from the grass canopy, or in the three sweeps created by the trailing shoes on the frame when mimicking trailing shoe application. For A, B, and C 45 metric ton ha^{-1} pig manure was applied, and for experiment D, E, and F 35 metric ton ha^{-1} cattle manure was applied. The application rates were chosen based on standard Danish practice.

3 Results and discussion

Real-time measurements of NMVOC and VSC emission from field-applied manure were successfully obtained with a system of dynamic chambers and PTR-TOF-MS. It was possible to calculate total NMVOC and VSC emission with an average variation of 18±8% within treatments. The environment inside the dynamic chambers differed from real field conditions by having a constant air flow, no precipitation, and no solar radiation. The lack of precipitation and solar radiation could affect the plant growth and microbial communities in the soil, possibly leading to a change in their natural emission of NMVOC. The conditions are identical in all tunnels and the relative differences will not be affected by this. NMVOC emission from the air entering the tunnels is measured by the background measurements, which is subtracted from the tunnel measurements. No measurements were made without slurry addition, hence the contribution from crops and soil to the emissions is not clear. Other studies looking at emissions from winter wheat (Bachy et al., 2020; Gonzaga Gomez et al., 2019; Potard et al., 2017) and different types of grass (Bamberger et al., 2010; Custer and Schade, 2007; Miresmailli et al., 2013; Ruuskanen et al., 2011) could indicate that the contribution of methanol from the crops could be significant. Additional compounds found in these studies that were also identified in the present study include alcohol fragments, acetaldehyde, acetone, acetic acid, 2-butanone, cyclohexene, and butanoic acid, but all in low concentrations compared with the fluxes measured in the present study. Furthermore, the overall flux (μg C m^{-2} h^{-1}) reported in all studies except one (Gonzaga Gomez et al., 2019) is between 60 and 3000 times lower than the average flux measured in the present study. It is assumed that the NMVOC emissions from the plants are insignificant compared to the high emissions from applied manure. As there is a general decrease in the NMVOC with time, it indicates that there are no significant amount of NMVOC released

from the plants due to stress. A list of additional detected mass-to-charge (m/z) values that were not included in further analysis can be found in Table S6 together with approximate concentration levels in the extended field background and the tunnels. These masses have not been included in further analysis due to the extremely low concentrations and the lack of unambiguous compound assignment. The concentrations of all compounds found in this background were close to the concentrations measured in the tunnel backgrounds. Furthermore, manure was applied manually in small plots. Despite these disadvantages, the low variation indicates that the method gives reliable quantitative data, which can be used for relative comparison of different manure applications. The system allows for continuous measurements over long periods, showing the emission dynamics over time. The setup takes advantage of the low detection limit and the full scan option of the PTR-TOF-MS, thereby enhancing the likelihood of detecting all compounds of interest from the complex manure matrix.

3.1 Identification and dynamics of compounds

A total of 23 compounds were assigned to the measured m/z values based on previous experiments with pig or cattle manure (Feilberg et al., 2015, 2011, 2010b, 2010a; Hansen et al., 2016, 2012; Liu et al., 2018). The concentrations of the compounds were determined from signal counts, transmission factors, and proton-transfer rate constants. The m/z values, formula, assigned compound, and OTV can be found in Table 2. In addition to the 23 compounds listed in Table 2, one fragment, m/z 46.026, was measured. As the contribution of this compound maximum was 0.3% of the total cumulative emission after 90 hours it was excluded from further calculations. It is speculated that the fragment might be formamide. m/z 41.038 can be a fragment of both 2-propanol and 2-butanol (Brown et al., 2010). From the GC/MS measurements, the relative contribution of 2-propanol and 2-butanol to m/z 41.038 is estimated to be 65% and 35%, respectively (data not shown). As the fragment from acetic acid (m/z 43.017) is much larger and overlap with the fragment from 2-propanol (m/z 43.052) this fragment is highly overestimated. Therefore, based on work by Brown et al. (2010) it is assumed that the true amount of the 2-propanol fraction (m/z 43.052) will be approximately 0.3 times the amount of 2-propanol fraction from m/z 41.038.

An overview of the emission trend and variation can be seen in Figures 1, 2, and S1, showing the average concentration after trailing hose application over time from each experiment. Clear diurnal patterns can be observed, especially for carboxylic acids. Formic acid emissions are quite low and therefore do not show the same clear trend as the other carboxylic acids. The pK_a of formic acid is one unit lower than the other carboxylic acids, which limits the emission by approximately one order of magnitude. During manure storage anaerobic conditions occur (Cooper and Cornforthb, 1978), which lead to a rapid break down

of formic acid by methanogens (Page et al., 2014). This is expected to cause a low amount of formic acids in the manure prior to application. A fast decrease (within 24 hours after manure application) can be observed for the three phenol compounds. A very rapid decrease (within minutes after manure application) is observed for H_2S and methanethiol, which were above the detection limit in two of the experiments with pig manure (B and C). As the sulfur compounds exhibited a very fast decay, the initial 10-20 seconds of emissions possibly have not been captured by the measurements leading to an underestimation (Feilberg et al., 2015). During experiment A, no H_2S and methanethiol was detected. It is assumed that all H_2S was emitted before the chambers were closed. During this experiment, it took approximately one-two minutes from manure application to the chambers were mounted on the frames. However, the results shows that reduced sulfur compounds will only have a very short-term influence on the emission from application of manure. The patterns of emission correlates with findings in previous studies (Feilberg et al., 2015; Liu et al., 2018; Parker et al., 2013a), but none of them have measured beyond 37 hours. The same compounds and emission patterns are found for both manure types (Figures 1 and 2).

Only a few other studies have been published with quantification of VSC and NMVOC emission from field applied manure (Feilberg et al., 2015, 2011, 2010a; Liu et al., 2018; Parker et al., 2013a; Woodbury et al., 2016). In all of these studies the compounds: acetic acid, propionic acid, butanoic acid, C5 carboxylic acids/pentanoic acid, phenol, 4-ethylphenol, and 4-methylphenol were identified and measured. Two of the studies used GC/MS for NMVOC analysis and only measured seven compounds (Parker et al., 2013a; Woodbury et al., 2016). The studies using PTR-MS measured between 12 and 17 compounds (Feilberg et al., 2015, 2011, 2010a; Liu et al., 2018). The compounds found in the present study that was not included in the other studies using PTR-MS were only found in very small amounts, which could explain why they have not been identified before.

Feilberg et al. (2015) and Parker et al. (2013a), who used dynamic chambers, and Feilberg et al. (2011) and Feilberg et al. (2010a), who used static chambers, reported emission measurements in the same ranges for pig manure right after field application as found during A, B, and C. They are in contrast to emissions reported by Liu et al. (2018), who reported emission measurements that is between ten and 40 times higher for propanoic-, acetic-, butanoic -, and C5 carboxylic acids right after manure application. During none of the experiments in this study does the fraction of carboxylic acids emitted compared to the amount in the manure exceed 10% (Table S3 and S7), whereas Liu et al. (2018) estimates that a very large fraction of carboxylic acids will emit from field applied manure to the atmosphere. Lower slurry pH or higher air and soil temperatures could results in higher emissions, but as it is not the case in Liu et al. (2018) it is not possible to conclude why the differences occur. It is assumed that the higher

Table 2: *Detected masses (m/z) and assigned compounds after field application of 45 metric ton ha^{-1} pig manure to winter wheat and metric 35 ton ha^{-1} cattle manure to clover grass. Chemical formula based on exact mass, and odor threshold values (OTV) are included.*

m/z	Formula	Assigned compound[a]	OTV [ppb]	Group
33.032	CH_4O	Methanol	33000[b]	Other
34.995	H_2S	Hydrogen sulfide	0.8[c]	VSC
41.038	C_3H_4	Alcohol fragment	26000[bd] / 220[be]	Other
43.052	C_3H_6	Alcohol fragment	26000[d]	Other
45.033	C_2H_4O	Acetaldehyde	1.5[b]	Other
47.013	CH_2O_2	Formic acid	4400[f]	Carboxylic acid
49.011	CH_4S	Methanethiol	0.03[c]	VSC
59.049	C_3H_6O	Acetone	42000[b]	Other
60.075	C_3H_9N	Trimethylamine	0.08[c]	Other
61.024 + 43.017	$C_2H_4O_2$	Acetic acid	8.3[c]	Carboxylic acid
63.026	C_2H_6S	Dimethylsufide	2.3[c]	VSC
69.067	C_5H_8	Isoprene	48[b]	Other
73.06	$C_4H_8O_2$	2-Butanone	440[b]	Other
75.041 + 57.066	$C_3H_6O_2$	Propionic acid	5.7[c]	Carboxylic acid
79.05	C_6H_6	Benzene	2700[b]	Other
83.075	C_6H_{10}	Cyclohexene	180[g]	Other
87.058	$C_4H_6O_2$	2,3-Butanedione	0.06[c]	Other
89.056 + 71.075	$C_4H_8O_2$	Butanoic acid	0.23[c]	Carboxylic acid
95.047	C_6H_6O	Phenol	8.4[c]	Phenol
101.05	$C_5H_8O_2$	Acetyl acetone	10[h]	Other
103.067 + 85.07	$C_5H_{10}O_2$	C5 carboxylic acids	0.2[c]	Carboxylic acid
109.058	C_7H_8O	4-Methylphenol	0.02[c]	Phenol
123.066	$C_8H_{10}O$	4-Ethylphenol	0.4[c]	Phenol

[a]Information about compounds assignment in comparison to other studies can be found in S2.1 Compound assignment. [b]From Nagata (2003). [c]Calculated mean from Hansen et al. (2018). [d]For 2-propanol. [e]For 2-butanol. [f]Estimated based on van Gemert (2003). [g]From van Gemert (2003). [h]From Ruth (1986).

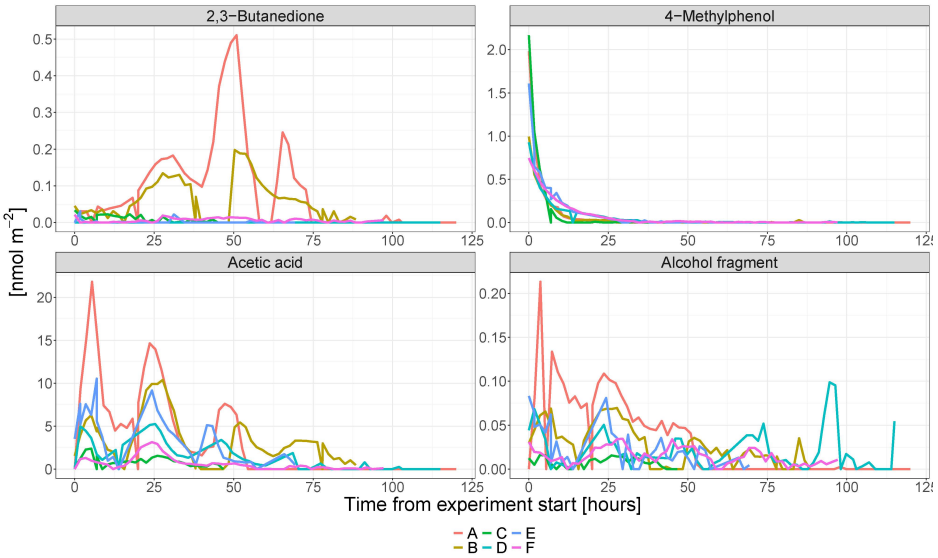

Figure 1: *Flux trends and variation from selected compounds measured after field application of 45 metric ton ha^{-1} pig manure to winter wheat and 35 metric ton ha^{-1} cattle manure to clover grass by trailing hoses. All data from all six experiments, each line represents the average of three wind tunnels. Timespan of the different experiments can be found in Table 1. Plots for compounds not shown here can be found in supporting information (Figure S1).*

emission in Liu et al. (2018) was caused by the higher air velocity within the emission chamber. The mass transfer process of carboxylic acids from a liquid phase to a gas phase is gas-film controlled, and thereby highly depends on the air turbulence above the emitting surface (Schwarzenbach et al., 2003). The nominal air velocity used by Liu et al. (2018) was more than double of what was used in other studies with dynamic chamber for NMVOC measurements (Feilberg et al., 2015; Parker et al., 2013a, 2009), including the present study. The air velocity inside the emission chambers used in the present study has been thoroughly evaluated in order to obtain a field-like turbulence at the emission surface, as described in more detail by Pedersen et al. (2020).

3.2 Total emission and effect of application method

A high variation is observed in total cumulated NMVOC emissions within the same manure type, with a generally higher emission observed from pig manure compared to cattle manure (Table 3). In one out of three experiments with pig

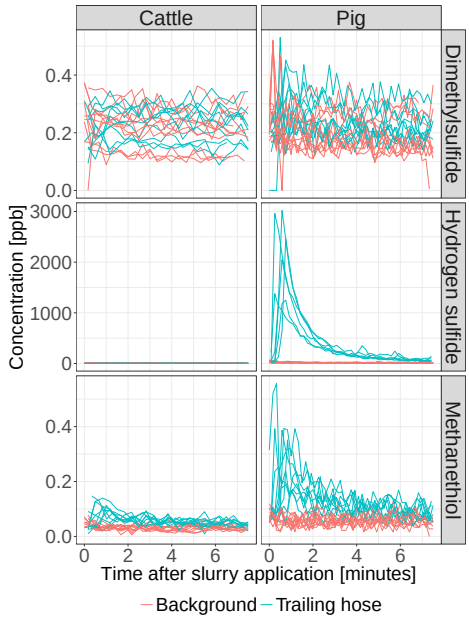

Figure 2: *Three detected VSC the first eight minutes after field application of 45 metric ton ha^{-1} pig manure to winter wheat and 35 metric ton ha^{-1} cattle manure to clover grass by trailing hoses. Data from all six experiments, each line represents a wind tunnel.*

manure, a significant (P=0.0207) reduction in cumulative NMVOC emission emitted after application by trailing shoes compared to trailing hoses (A, 93±41%) was found. The NMVOC emission from the two application techniques were not significantly different for experiment B and C. This complies with the ammonia emissions during the same experiments, reported by Pedersen et al. (2020). The differences were assigned to soil type and conditions hindering the trailing shoes in creating a slit for the manure and assumedly lowering infiltration during experiment B and C. Using trailing shoes instead of trailing hoses when applying cattle manure on loamy sand with clover grass gave an average reduction of cumulated NMVOC emission during 90 hours of 52±19% respectively (two (P=0.0161 and P = 0.0311) out of three significant). A grass crop hinders the trailing shoe in creating a slit in the soil. Here the force of the trailing shoes ensures that the slurry is applied directly at the top or a little below the surface of the grass. Consequently, the area of slurry exposed to air compared to trailing hoses is reduced, which results in lower emissions (Pedersen et al., 2020). As there is no contact between the trailing shoe and the soil, the effect of soil type is expected to be low

Table 3: *Cumulative emissions of NMVOC after field application of 45 metric ton ha^{-1} pig manure to winter wheat and 35 metric ton ha^{-1} cattle manure to clover grass by trailing hoses. Cumulative emissions are calculated after 45 and 90 hours. The standard deviations are displayed in parenthesis (n = 3).*

	Cumulated NMVOC emission [mg m^{-2}]					
Experiment	A	B	C	D	E	F
	45 hours					
TS[1]	458.84	1563.47	519.50	151.04	507.28	367.41
	(164.81)	(155.46)	(43.95)	(33.49)	(83.20)	(53.65)
TH[1]	2352.48	1343.59	441.95	776.16	1219.85	490.44
	(588.51)	(191.73)	(85.88)	(122.34)	(245.24)	(79.80)
TH20[1]	-	-	-	-	-	1782.07
	-	-	-	-	-	(244.40)
	90 hours					
TS[1]	522.58	2125.59	-	266.78	-	450.92
	(193.97)	(242.71)	-	(51.78)	-	(64.18)
TH[1]	2641.43	1968.26	-	1018.39	-	649.45
	(602.25)	(269.96)	-	(153.34)	-	(115.66)
TH20[1]	-	-	-	-	-	2192.17
	-	-	-	-	-	(312.05)

[1]TS: trailing shoes, TH: trailing hoses, TH20: trailing hoses 20 cm.

on a grass field. During experiment F, trailing hoses 20 cm above canopy was found to significantly (P=0.0062) increase the total accumulated NMVOC emission during 90 hours with 338±77%. The trend in NMVOC emission reduction and increase by using trailing shoes and trailing hoses 20 cm above canopy from cattle manure on loamy sand also complies with the ammonia emission reported by Pedersen et al. (2020). The reductions and increases are, however, much higher for NMVOC than for ammonia. The reduction of ammonia was found to be 17±4% by using trailing shoes instead of trailing hoses, and a 40±13% increase was found for using trailing hoses 20 cm above canopy compared to trailing hoses applied at the grass canopy (Pedersen et al., 2020). The reduction or increase in total NMVOC emission is caused primarily by a reduction or increase in the carboxylic acids.

During the first ten hours, a large amount of 4-methylphenol was emitted from both manures. This was also observed by Feilberg et al. (2015), Liu et al. (2018), and Parker et al. (2013a). Taking the chemical equilibria in the aqueous phase at the pH and temperature conditions present during the experimens into account, it can be calculated that phenols partition to a much higher degree into the air phase compared to carboxylic acids, which explains the faster emissions of phenols whereas carboxylic acid emissions remain for several days. After ten hours, nearly ~100 and ~70% of the emitted NMVOC from pig and cattle manure respectively were carboxylic acids (Figures 3 and S2 and Table S7). Carboxylic acids represent

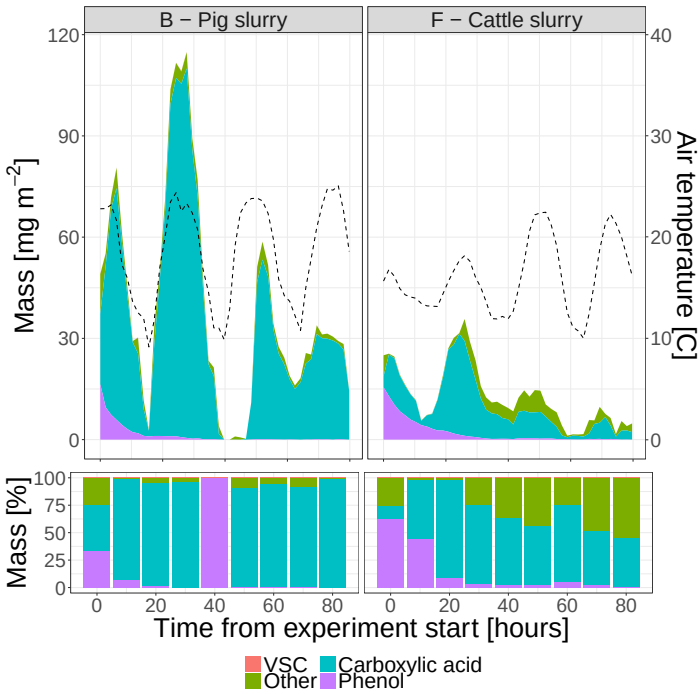

Figure 3: *Total NMVOC emission after field application of 45 metric ton ha^{-1} pig manure to winter wheat and 35 metric ton ha^{-1} cattle manure to clover grass by trailing hoses. Figures for experiment A, C, D, and E can be found in supplementary material (Figure S4).*

the biggest contribution to the total accumulated NMVOC emission, ranging from 58 – 90% of the total emitted mass, where acetic acid alone accounted for between 33 – 57% (cumulative emissions 45 and 90 hours after manure application with trailing hoses from all six experiments, Table S7). This agrees with previous publications (Feilberg et al., 2015; Liu et al., 2018; Parker et al., 2013a) that found contributions from carboxylic acids to total NMVOC emission from land applied pig manure to be in the same range.

Due to a lack of reported data and NMVOC emission factors, it has been suggested that approximations of NMVOC emissions can be calculated based on ammonia emissions, as these has been widely studied and reported (EMEP/EEA, 2016; Feilberg et al., 2010b). The data from these experiments show that there is considerable variation in the ratio of NMVOC emission compared to ammonia emission, both within manure types and application technique. Before extensive research within the area has been conducted, it is suggested that the new ratios from the present study is used, as it is the best available data. The average ratios of cumulated NMVOC emission divided by cumulated ammonia emission 90 hours after application of pig manure is 1.15±0.55 and 0.72±0.26 for trailing hoses and trailing shoes respectively, whereas the same numbers for cattle manure is 0.43±0.11 and 0.18±0.04 (Table S7). Using these new ratios to calculate yearly NMVOC emission after field application of cattle and pig manure by trailing hoses in Denmark gives a total emission of ~5000 metric ton/year, which is approximately 80% higher than the emission calculated when using data from the national inventory (see Table S8). According to this estimate, manure application contributes ~4% of the total NMVOC emissions in Denmark. The big difference between yearly NMVOC emissions calculated using ratios from this study and ratios from the national inventory clearly shows that the national inventory most likely underestimates the NMVOC emissions from field-applied manure.

3.3 Odorant assessment and effect of application method

High OAV of approximately 2000 were calculated for B and C right after manure application due to the occurrence of H_2S, which dominated the OAV and account for more than 90% of the cumulated OAV in the minutes right after manure application (Figure 4, left). After the initial 8 minutes, when H_2S was only present in small amounts, 4-methylphenol accounted for most of the OAV from pig manure during the first ten hours. This corresponds with the findings by Parker et al. (2013a) who observed that 4-methylphenol accounted for 79.5% of the summed NMVOC the first 24 hours after pig manure application. The long term OAV was caused by carboxylic acids and 2,3-butanedione. OAV for cattle manure (Figure 4, right) was dominated by 4-methylphenol during the first 30 hours, which is in contrast with findings by Woodbury et al. (2016) who

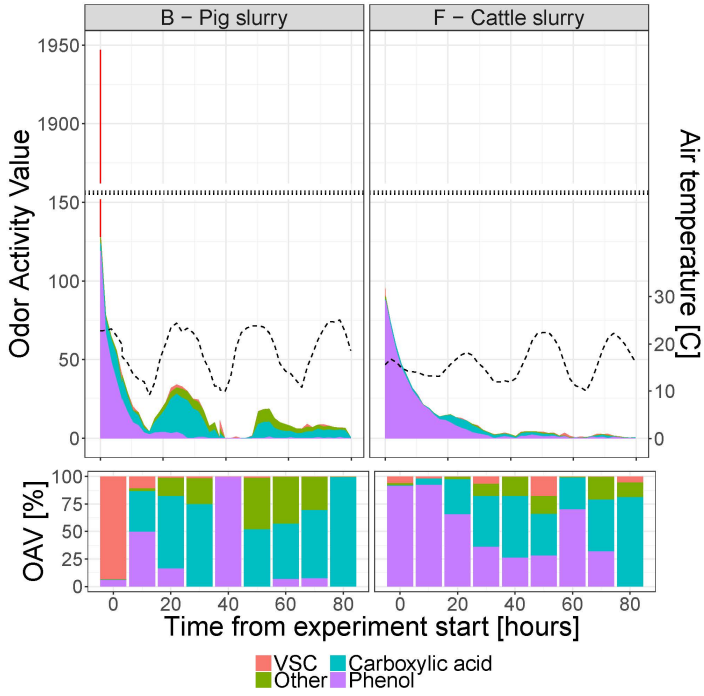

Figure 4: *Total OAV after field application of 45 metric ton ha^{-1} pig manure to winter wheat and 35 metric ton ha^{-1} cattle manure to clover grass by trailing hoses. Figures for experiment A, C, D, and E can be found in supplementary material (Figure S5). The short initial VSC emission is seen as a thin red vertical line to the left in experiment B.*

only attributes 4-methylphenol 5.9% of the OAV after field application of cattle manure. They measured high amounts of dimethyl disulfide and dimethyl trisulfide, which together accounted for more than 40%. These high amounts reported by Woodbury et al. (2016) has not been reported in any of the other studies. No emissions of dimethyl disulfide and dimethyl trisulfide were observed during these experiments, or during the two most recent studies measuring NMVOC from field applied manure using PTR-MS (Feilberg et al., 2015; Liu et al., 2018). It has been proven that methanethiol easily reacts and forms dimethyl disulfide during sampling with sorbent tubes (Andersen et al., 2012). It is unclear whether Woodbury et al. (2016) has corrected for the transformation, but leaving dimethyl disulfide and dimethyl trisulfide out from their results, the relative contribution from 4-methylphenol would be closer to the findings in the present study. Approximately 30 hours after application of cattle manure, the OAV became very low, and carboxylic acids contributed increasingly to the total OAV (Figure 4, right).

Odor emission rates right after manure application was found to be between 443±93 and 4170±683 OAV h^{-1} m^{-2} and 143±57 and 320±86 OAV h^{-1} m^{-2} for pig and cattle manure applied with trailing hoses, respectively. Right after manure application, a significantly (P=0.0022) lower odor emission after application with trailing shoes compared to trailing hoses was found for one experiment with pig manure (A, 63±30%). During four of the other experiments trailing shoes also resulted in numerically lower odor emission compared to trailing hoses (C, D, E, and F), but the differences were not significant. Manure applied by trailing hoses 20 cm above canopy on clover grass gave a significant (P=0.0022) increase in odor emission of 326±141% right after application and at noon the following day compared to trailing hoses and trailing shoes. During all the experiments no significant differences in odor emission was observed for the different application techniques after 48 hours, where all values where low (maximum 33 for pig manure and 4 for cattle manure) (Table S9).

3.4 Final remarks

NMVOC and OAV dynamics after field application can successfully be measured with the system of dynamic chambers and PTR-TOF-MS. The low variation of 18±8% within treatments for cumulative emissions allows for investigation of different treatments, such as manure application technique. Trailing shoes resulted in lower emission during some of the experiments compared to trailing hoses. Trailing hoses used 20 cm above canopy gave a large increase in NMVOC emissions and OAV. The effect of using different application techniques on NMVOC emission was bigger than the effect on ammonia. New average ratios for calculation of cumulated NMVOC emissions relative to ammonia emission has been presented based on both manure type and slurry application technique. In ad-

dition to soil type and manure application technique, ambient air temperature and slurry parameters are expected to influence the NMVOC emissions from field-applied manure. The experiments presented in this study is not enough to draw any conclusions of the effect of these parameters, therefore, more research is highly needed within this area.

Funding source
This work was funded by the Ministry of Environment and Food of Denmark as a green development and demonstration program (GUDP) with the project title New application method for slurry in growing crops.

Acknowledgement
The authors would like to acknowledge the technical staff Heidi Grønbæk, Jens Kr. Kristensen, Per Wiborg Hansen, and Peter Storegård Nielsen for their skillful assistance with development of the measuring system, carrying out measurements, and laboratory analysis. The authors would like to express gratitude to Mette Hjorth Mikkelsen for her invaluable help with accessing national emission inventory data.

References

American Public Health Association, 1999. Standard methods for the examination of water and wastewater.

Andersen, K.B., Hansen, M.J., Feilberg, A., 2012. Minimisation of artefact formation of dimethyl disulphide during sampling and analysis of methanethiol in air using solid sorbent materials. J. Chromatogr. A 1245, 24–31. https://doi.org/10.1016/j.chroma.2012.05.020

Association of Official Analytical Chemists, 1999. Official methods of analysis of AOAC international, 16th ed. AOAC, Washington, D. C.

Bachy, A., Aubinet, M., Amelynck, C., Schoon, N., Bodson, B., Delaplace, P., De Ligne, A., Digrado, A., du Jardin, P., Fauconnier, M.L., Mozaffar, A., Müller, J.F., Heinesch, B., 2020. Dynamics and mechanisms of volatile organic compound exchanges in a winter wheat field. Atmos. Environ. 221, 117105. https://doi.org/10.1016/j.atmosenv.2019.117105

Bamberger, I., Hörtnagl, L., Schnitzhofer, R., Graus, M., Ruuskanen, T.M., Müller, M., Dunkl, J., Wohlfahrt, G., Hansel, A., 2010. BVOC fluxes above mountain grassland. Biogeosciences 7, 1413–1424. https://doi.org/10.5194/bg-7-1413-2010

Blake, R.S., Monks, P.S., Ellis, A.M., Blake, R.S., Monks, P.S., Ellis, A.M., 2009. Proton-Transfer Reaction Mass Spectrometry. Chem. Rev. 109, 861–896. https://doi.org/10.1021/cr800364q

Brown, P., Watts, P., Märk, T.D., Mayhew, C.A., 2010. Proton transfer reaction mass spectrometry investigations on the effects of reduced electric field and reagent ion internal en-

ergy on product ion branching ratios for a series of saturated alcohols. Int. J. Mass Spectrom. 294, 103–111. https://doi.org/10.1016/j.ijms.2010.05.028

Cappellin, L., Karl, T., Probst, M., Ismailova, O., Winkler, P., Soukoulis, C., Aprea, E., Märk, T.D., Gasperi, F., Biasioli, F., 2012. On quantitative determination of volatile organic compound concentrations using proton-transfer-reaction-time-of-flight-mass-spectrometry. Environ. Sci. Technol. 4, 1–4.

Cooper, P., Cornforthb, I.S., 1978. Volatile fatty acids in stored animal slurry. J. Sci. Food Agric. 29, 19–27.

Custer, T., Schade, G., 2007. Methanol and acetaldehyde fluxes over ryegrass. Tellus, Ser. B Chem. Phys. Meteorol. 59, 673–684. https://doi.org/10.1111/j.1600-0889.2007.00294.x

Dalby, F.R., Hansen, M.J., Feilberg, A., 2018. Application of proton-transfer-reaction mass spectrometry (PTR-MS) and 33S isotope labeling for monitoring sulfur processes in livestock waste. Environ. Sci. Technol. 52, 2100–2107. https://doi.org/10.1021/acs.est.7b04570

de Gouw, J., Warneke, C., 2007. Measurements of volatile organic compounds in the earth's atmosphere using proton-transfer-reaction mass spectrometry. Mass Spectrom. Rev. 26, 223–257. https://doi.org/10.1002/mas

EMEP/EEA, 2016. EMEP/EEA air pollutant emission inventory guidebook 2016. Technical guidance to prepare national emission inventories. 3.B Manure management. European Environment Agency.

Eurostat, 2017. Energy, transport and environment indicators 2017 edition. https://doi.org/10.2785/889945

Feilberg, A., Bildsoe, P., Nyord, T., 2015. Application of PTR-MS for measuring odorant emissions from soil application of manure slurry. Sensors (Switzerland) 15, 1148–1167. https://doi.org/10.3390/s150101148

Feilberg, A., Dorno, N., Nyord, T., 2010a. Odour emissions following land spreading of animal slurry assessed by proton-transfer-reaction mass spectrometry (PTR-MS). Chem. Eng. Trans. 23, 111–116. https://doi.org/10.3303/CET1023019

Feilberg, A., Hansen, M.J., Liu, D., Nyord, T., 2017. Contribution of livestock H2S to total sulfur emissions in a region with intensive animal production. Nat. Commun. 8, 1–7. https://doi.org/10.1038/s41467-017-01016-2

Feilberg, A., Liu, D., Adamsen, A.P.S., Hansen, M.J., Jonassen, K.E.N., 2010b. Odorant emissions from intensive pig production measured by online proton-transfer-reaction mass spectrometry. Environ. Sci. Technol. 44, 5894–5900. https://doi.org/10.1021/es100483s

Feilberg, A., Nyord, T., Hansen, M.N., Lindholst, S., 2011. Chemical evaluation of odor reduction by soil injection of animal manure. J. Environ. Qual. 40, 1674–82. https://doi.org/10.2134/jeq2010.0499

Gonzaga Gomez, L., Loubet, B., Lafouge, F., Ciuraru, R., Buysse, P., Durand, B., Gueudet, J.C., Fanucci, O., Fortineau, A., Zurfluh, O., Decuq, C., Kammer, J., Duprix, P., Bsaibes, S.,

Truong, F., Gros, V., Boissard, C., 2019. Comparative study of biogenic volatile organic compounds fluxes by wheat, maize and rapeseed with dynamic chambers over a short period in northern France. Atmos. Environ. 214. https://doi.org/10.1016/j.atmosenv.2019.116855

Hafner, S.D., Pacholski, A., Bittman, S., Carozzi, M., Chantigny, M., Génermont, S., Häni, C., Hansen, M.N., Huijsmans, J., Kupper, T., Misselbrook, T., Neftel, A., Nyord, T., Sommer, S.G., 2019. A flexible semi-empirical model for estimating ammonia volatilization from field-applied slurry. Atmos. Environ. 199, 474–484. https://doi.org/S1352231018308069

Hanna, H.M., Bundy, D.S., Lorimor, J.C., Mickelson, S.K., Melvin, S.W., Erbach, D.C., 2000. Manure incorporation equipment effects on odor, residue cover, and crop yield. Appl. Eng. Agric. 16, 621–627.

Hansen, M.J., Jonassen, K.E.N., Løkke, M.M., Adamsen, A.P.S., Feilberg, A., 2016. Multivariate prediction of odor from pig production based on in-situ measurement of odorants. Atmos. Environ. 135, 50–58. https://doi.org/10.1016/j.atmosenv.2016.03.060

Hansen, M.J., Kasper, P.L., Adamsen, A.P.S., Feilberg, A., 2018. Key odorants from pig production based on improved measurements of odor threshold values combining olfactometry and proton-transfer-reaction mass spectrometry (PTR-MS). Sensors (Switzerland) 18. https://doi.org/10.3390/s18030788

Hansen, M.J., Liu, D., Guldberg, L.B., Feilberg, A., 2012. Application of proton-transfer-reaction mass spectrometry to the assessment of odorant removal in a biological air cleaner for pig production. J. Agric. Food Chem. 60, 2599–2606. https://doi.org/10.1021/jf300182c

Hudson, N., Ayoko, G.A., 2008a. Odour sampling. 2. Comparison of physical and aerodynamic characteristics of sampling devices: A review. Bioresour. Technol. 99, 3993–4007. https://doi.org/10.1016/j.biortech.2007.03.043

Hudson, N., Ayoko, G.A., 2008b. Odour sampling 1: Physical chemistry considerations. Bioresour. Technol. 99, 3982–3992. https://doi.org/10.1016/j.biortech.2007.04.034

Kasper, P.L., Hansen, M.J., Feilberg, A., 2018a. Impact of saturation effects during dynamic olfactometry on low-concentration environmental odour samples. Chem. Eng. Trans. 68, 37–42. https://doi.org/10.3303/CET1868007

Kasper, P.L., Mannebeck, D., Oxbøl, A., Nygaard, J. V., Hansen, M.J., Feilberg, A., 2017. Effects of dilution systems in olfactometry on the recovery of typical livestock odorants determined by PTR-MS. Sensors (Switzerland) 17. https://doi.org/10.3390/s17081859

Kasper, P.L., Oxbøl, A., Hansen, M.J., Feilberg, A., 2018b. Mechanisms of loss of agricultural odorous compounds in sample bags of Nalophan, Tedlar, and PTFE. J. Environ. Qual. 47, 246–253. https://doi.org/10.2134/jeq2017.07.0289

Liu, D., Nyord, T., Rong, L., Feilberg, A., 2018. Real-time quantification of emissions of volatile organic compounds from land spreading of pig slurry measured by PTR-MS and wind tunnels. Sci. Total Environ. 639, 1079–1087. https://doi.org/10.1016/j.scitotenv.2018.05.149

Miresmailli, S., Zeri, M., Zangerl, A.R., Bernacchi, C.J., Berenbaum, M.R., Delucia, E.H., 2013. Impacts of herbaceous bioenergy crops on atmospheric volatile organic composition and potential consequences for global climate change. GCB Bioenergy 5, 375–383.

https://doi.org/10.1111/j.1757-1707.2012.01189.x

Montes, F., Meinen, R., Dell, C., Rotz, A., Hristov, A.N., Oh, J., Waghorn, G., Gerber, P.J., Henderson, B., Makkar, H.P.S., Dijkstra, J., 2013. Mitigation of methane and nitrous oxide emissions from animal operations: II. A review of manure management mitigation options. Am. Soc. Anim. Sci. 5070–5094. https://doi.org/10.2527/jas2013-6584

Nagata, Y., 2003. Measurement of odor threshold by triangle odor bag method. Odor Meas. Rev. 118–127.

Ngwabie, N.M., Schade, G.W., Custer, T.G., Linke, S., Hinz, T., 2008. Abundances and flux estimates of volatile organic compounds from a dairy cowshed in Germany. J. Environ. Qual. 37, 565–573. https://doi.org/10.2134/jeq2006.0417

Ni, J.Q., Robarge, W.P., Xiao, C., Heber, A.J., 2012. Volatile organic compounds at swine facilities: A critical review. Chemosphere 89, 769–788.
https://doi.org/10.1016/j.chemosphere.2012.04.061

Nielsen, O.-K., Plejdrup, M.S., Winther, M., Nielsen, M., Hjelgaard, K., Fauser, P., Mikkelsen, M.H., Albrektsen, R., Thomsen, M., 2016. Emissionsfremskrivning 2015-2030. Danish Centre for Environment and Energy, Aarhus University, Denmark.

Page, L.H., Ni, J.Q., Heber, A.J., Mosier, N.S., Liu, X., Joo, H.S., Ndegwa, P.M., Harrison, J.H., 2014. Characteristics of volatile fatty acids in stored dairy manure before and after anaerobic digestion. Biosyst. Eng. 118, 16–28. https://doi.org/10.1016/j.biosystemseng.2013.11.004

Parker, D., Gilley, J., Woodbury, B., Kim, K.H., Galvin, G., Bartelt-Hunt, S.L., Li, X., Snow, D.D., 2013a. Odorous VOC emission following land application of swine manure slurry. Atmos. Environ. 66, 91–100. https://doi.org/10.1016/j.atmosenv.2012.01.001

Parker, D., Ham, J., Woodbury, B., Cai, L., Spiehs, M., Rhoades, M., Trabue, S., Casey, K., Todd, R., Cole, A., 2013b. Standardization of flux chamber and wind tunnel flux measurements for quantifying volatile organic compound and ammonia emissions from area sources at animal feeding operations. Atmos. Environ. 66, 72–83. https://doi.org/10.1016/j.atmosenv.2012.03.068

Parker, D.B., Cole, A.N., Casey, K.D., Galvin, G., Ormerod, R., Paris, C.S., Caraway, E.A., Rhoades, M.B., 2009. Wind tunnels vs. flux chambers: Area source emission measurements and the necessity for VOC and odour correction factors. Proc. 19th Int. Clean Air Environ. Conf., Perth, Aust. 6–9.

Pedersen, J.M., Feilberg, A., Kamp, J.N., Hafner, S., Nyord, T., 2020. Ammonia emission measurement with an online wind tunnel system for evaluation of manure application techniques. Atmos. Environ. 230. https://doi.org/10.1016/j.atmosenv.2020.117562

Potard, K., Monard, C., Le Garrec, J.L., Caudal, J.P., Le Bris, N., Binet, F., 2017. Organic amendment practices as possible drivers of biogenic Volatile Organic Compounds emitted by soils in agrosystems. Agric. Ecosyst. Environ. 250, 25–36.
https://doi.org/10.1016/j.agee.2017.09.007

Ruth, J.H., 1986. Odor thresholds and irritation levels of several chemical substances: A review. Am. Ind. Hyg. Assoc. 47. https://doi.org/10.4103/ijccm.IJCCM$_2$06$_1$7

Ruuskanen, T.M., Müller, M., Schnitzhofer, R., Karl, T., Graus, M., 2011. Europe PMC Funders Group Eddy covariance VOC emission and deposition fluxes above grassland using PTR-TOF. Atmos. Chem. Phys. 11. https://doi.org/10.5194/acp-11-611-2011.Eddy

Schwarzenbach, R.P., Sxchwend, P.M., Imboden, D.M., 2003. Environmental organic chemistry, second edi. ed. Wiley-Interscience, John Wiley Sons, Inc. Canada.

Sekimoto, K., Li, S.M., Yuan, B., Koss, A., Coggon, M., Warneke, C., de Gouw, J., 2017. Calculation of the sensitivity of proton-transfer-reaction mass spectrometry (PTR-MS) for organic trace gases using molecular properties. Int. J. Mass Spectrom. 421, 71–94. https://doi.org/10.1016/j.ijms.2017.04.006

Smith, R.J., Watts, P.J., 1994. Determination of odour emission rates from cattle feedlots: Part 2, Evaluation of two wind tunnels of different size. J. Agric. Eng. Res. 58, 231–240. https://doi.org/10.1006/jaer.1994.1053

Sommer, S.G., Misselbrook, T.H., 2016. A review of ammonia emission measured using wind tunnels compared with micrometeorological techniques. Soil Use Manag. 32, 101–108. https://doi.org/10.1111/sum.12209

Su, T., 1994. Parametrization of kinetic energy dependences of ion-polar molecule collision rate constants by trajectory calculations. J. Chem. Phys. 100, 4703. https://doi.org/10.1063/1.466255

Union, E., 2016. Directive (EU) 2016/2284 of the European Parliament and of the council - of 14 December 2016 - on the reduction of national emissions of certain atmospheric pollutants, amending Directive 2003/35/EC and repealing Directive 2001/81/EC, Official Journal of the European Union. https://doi.org/ http://eur-lex.europa.eu/pri/en/oj/dat/2003/l$_2$85/$l_2$8520031101en00330037.*pdf*

USDA, 2009. Soil survey field and laboratory methods manual 407. https://doi.org/10.13140/RG.2.1.3803.8889

van Gemert, L.J., 2003. van Gemert - Compilations of odour threshold values in air, water and other media. Boelens Aroma Chemical Informatoin Service, Huizen, The Netherlands.

Woodbury, B.L., Gilley, J.E., Parker, D.B., Marx, D.B., Eigenberg, R.A., 2016. Emission of volatile organic compounds as affected by rate of application of cattle manure. Trans. ASABE 59, 885–895. https://doi.org/10.13031/trans.59.11374

Supporting Information

Emissions of NMVOC and H_2S from field-applied manure measured by PTR-TOF-MS and wind tunnels

Johanna Pedersen, Tavs Nyord, Michael J. Hansen, Anders Feilberg*

Aarhus University, Dept. of Engineering, Denmark

*Corresponding author email: af@eng.au.dk

S1 Weather, soil, and manure data

Table S1: *Soil and air temperature during all experiments. Soil temperature is measured at 5 cm depth.*

	Air temperature [°C]			Soil temperature [°C]		
Experiment	6 h avg.	24 h avg.	Total avg.	6 h avg.	24 h avg.	Total avg.
A	25.1	18.9	15.1	20.4	17.6	15.9
B	22.6	17.6	18.2	19.8	16.8	16.7
C	21.9	20.2	20.4	17.3	16.8	16.8
D*	15.7	12.8	15.0	NA	16.3	17.1
E	22.5	17.0	16.9	24.1	18.6	18.3
F	15.9	14.7	15.7	19.4	17.5	17.7

*Soil temperature is missing for the first 10 hours.

Table S2: *Soil properties for all experiments and force on each trailing shoe. Clay contents are from (Chen et al., 2013). Standard deviations are displayed in parenthesis (n = 3).*

Experiment	Soil	Clay content [%]	Crops	Dry bulk density [g cm^{-3}]	Water content [g g^{-1}]	pH	Force on trailing shoe [N]
A	Coarse sand	4	Winter wheat	1.41 (0.08)	0.09 (<0.01)	4.5	78
B	Loamy sand	9		1.32 (0.07)	0.13 (0.01)	4.4	88
C	Sandy loam	18		1.41 (0.06)	0.17 (0.01)	6.3	98
D	Loamy sand	9	Grass	1.15 (0.08)	0.15 (0.01)	4.8	117
E					0.21 (0.01)		
F				1.61 (0.08)	0.15 (0.01)	5.9	

Table S3: *Pig (experiment A, B, and C) and cattle (experiment D, E, F) manure properties for all experiments. Standard deviations are displayed in parenthesis (n = 2). N: Nitrogen, TAN: total ammoniacal nitrogen, VFA: volatile fatty acids.*

Experiment	Total N [g L^{-1}]	TAN [g L^{-1}]	Acetic acid [mg L^{-1}]	Propionic acid [mg L^{-1}]	Butyric acid [mg L^{-1}]	Iso-butyric acid [mg L^{-1}]	Isovaleric acid [mg L^{-1}]	Pentanoic aicd [mg L^{-1}]	Iso caproic acid [mg L^{-1}]	Hexanoic acid [mg L^{-1}]	Total VFA
A	2.62 (0.42)	2.22 (0.03)	3580 (42)	1200 (17)	369 (9)	1514 (28)	675 (16)	455 (6)	17 (1)	596 (16)	8401 (135)
B	3.45 (0.23)	2.20 (0.08)	3965 (7)	1234 (2)	420 (4)	1386 (0)	730 (6)	453 (5)	17 (0)	561 (7)	8767 (13)
C	2.92 (1.07)	2.25 (0.10)	3780 (123)	1071 (29)	397 (11)	903 (22)	693 (19)	269 (171)	15 (1)	421 (13)	7549 (388)
D	5.07 (0.17)	2.79 (0.13)	8396 (299)	2981 (87)	483 (8)	1290 (32)	381 (234)	225 (1)	9 (0)	41 (29)	13806 (632)
E	4.61 (1.04)	2.83 (0.19)	8077 (7)	2859 (8)	494 (6)	1252 (2)	554 (5)	216 (3)	9 (1)	47 (3)	13507 (19)
F	4.26 (0.27)	2.72 (0.01)	8443 (34)	2981 (17)	514 (2)	1286 (5)	570 (1)	218 (0)	9 (1)	46 (1)	14068 (60)

S2 Transmission gas information

Table S4: *Properties for the certified gas standard mixture used for the gas transmission curve. The gas standard was custom-prepared from Linde Gas, Surrey, UK.*

Compound	m/z	k[a] x 10^9 [cm^3 $molecules^{-1}$ s^{-1}]	Gas concentration [ppb]
Benzene	79	1.93	95.32
Toluene	93	2.08	98.93
Styrene	105.07	2.27	104.48
Chlorobenzene	113	2.43	80.82
Trimethylbenzene	121	2.42	118.47
Dichlorobenzene	147	2.21	63.23
Trichlorobenzene	181	2.18	41.71
Dibromobenzene	237	2.50	59.31

[a] k values calculated on method from Su (1994).

S3 Rate constants and compound assignment

S3.1 Compound assignment

Hansen et al. (2016) and Feilberg et al. (2010) identified m/z 73 as C4 carbonyls. Feilberg et al. (2010) wrote that it is primarily 2-butanon. Both Feilberg et al. (2015), Feilberg et al. (2011), Liu et al. (2018), and Hansen et al. (2012) identified it as 2-butanon, which was used in this study. m/z 101 has not been found in the literature, therefore there is some uncertainty in the identification of the compound. The OTV for the assigned compound (acetyl acetone) is from older literature, but as it was only present in small amounts in all the experiments the effect on total NMVOC emissions and OAV were insignificant. Feilberg et al. (2010), Feilberg et al. (2015), Hansen et al. (2012), and Liu et al. (2018) identified m/z 103 as C5 carboxylic acid (with the largest amount being pentanoic acid), the rest of the studies identified it as pentanoic acid (Feilberg et al., 2011; Parker et al., 2013; Woodbury et al., 2016).

Table S5: *Assigned compounds, used polarizability and dipole moments and calculated rate constants.*

m/z	Assigned compound	Polarizability [10^{-24} cm^3]	Dipole moment [Debye]	k[a] x 10^9 [cm^3 $molecules^{-1}$ s^{-1}]
33.032	Methanol[b]	3.21	1.65	2.14
34.995	Hydrogen sulfide[b]	3.75	0.98	1.57
41.038	Alcohol fragment[b]	6.87[c]/8.73[d]	1.64[c]/1.62[d]	2.11[c]/2.16[d]
43.052	Alcohol fragment[b]	6.87[c]	1.64[c]	2.11[c]
45.033	Acetaldehyde[b]	4.58	2.88	3.04
47.013	Formic acid[b]	3.37	1.55	1.91
49.011	Methanthiol[b]	5.32	1.58	2.05
59.049	Acetone[b]	6.39	3.11	3.25
60.075	Trimethylamine[e]	7.64	0.68	1.76
61.024 + 43.017	Acetic acid[b]	5.13	1.79	2.14
63.026	Dimethylsufide[b]	7.46	1.6	2.12
69.067	Isopren[b]	10.3	0.72	1.95
73.06	2-Butanone[b]	8.17	2.96	3.18
75.041 + 57.066	Propionic acid[e]	7.11	1.4	1.92
79.05	Benzen[b]	10.4	0	1.93
83.075	Cyclohexene[b]	10.48	0.32	1.93
87.058	2,3-Butanedione[e]	8.82	2.8	3.03
89.056 + 71.075	Butanoic acid[e]	9.25	1.4	2.05
95.047	Phenol[b]	11.18	1.27	2.14
101.05	Acetyl acetone[e]	10.81	2.8	3.06
103.067 + 85.067	C5 Carboxylic acid[e,f]	11.24	1.4	2.17
109.058	4-Methylphenol[b]	13.89	1.3	2.32
123.066	4-Ethylphenol[e]	15.04	1.3	2.38

[a]k values calculated on method from Su (1994). [b]Polarizability and dipole moment from Cappellin et al. (2012). [c]For 2-propanol. [d]For 2-butanol. [e]Polarizability and dipole moment estimated based on Sekimoto et al. (2017). [f]Pentanoic acid and 3-methylbutanoic acid.

S4 Additional peaks not included in analysis

Table S6: *m/z values, concentration level in background and tunnel measurements (no difference between the concentration measured in the background and tunnels), suggested compound or atomic formula with corresponding theoretical mass (when applicable), and comments on detected peaks that were not included in further data analysis.*

m/z	ppb*	Suggested compound**	Theoretical mass	Comment
31.0125	0.03	Formaldehyde	31.017841	
42.0383	0.08	13C C_3H_5 isotopomer	42.041931	
44.0197	0.06	13C isotopomer of C_2H_2O (fragment from HAc)	44.021196	
45.9947	0.06	NO_2^+ from O_2^+ ionization	45.992351	
49.9932	0.19	CH_3Cl from O_2^+	49.991751	Atmospheric abundance ca 0.6 ppb, not protonated by H_3O^+
62.0309	0.04	HAc 13C isotopomer	62.031761	
81.0615	0.10	C_6H_8	81.069876	Unknown
85.0758	0.09	$C_4H_8N_2$	85.075976	Unknown
97.0893	0.18	$C_6H_{10}N$	97.088601	Unknown
99.0664	0.19			Unknown
111.077	0.26	$C_7H_{10}O$	111.080476	
113.073	0.05			Unknown
115.089	0.05	$C_5H_{10}N_2O$	115.086576	
117.081	0.22			Unknown
123.066	0.06			Unknown
127.064	0.11	$C_7H_{10}S$	127.057576	
129.073	0.12	Naphthalene ($C_{10}H_8$)	129.069876	Ubiquitous in atmosphere in ppt levels
137.08	0.13	C_9H_9F	137.076076	

*Average ppb values in the long background.

**Criteria: the difference between m/z and theoretical mass should be below 0.01.

S5 Cumulative emissions

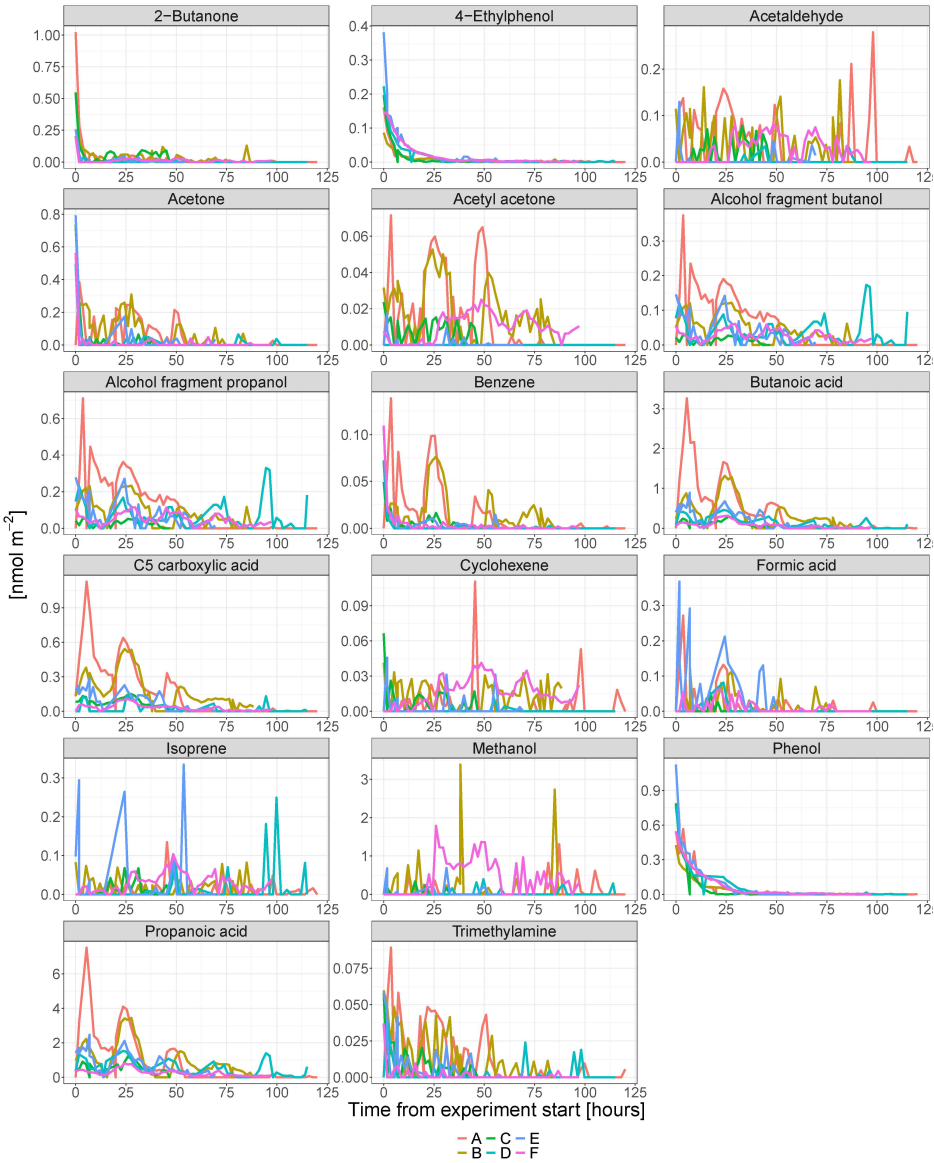

Figure S1: *Flux trends and variation from compounds not presented in the main manuscript measured after field application of 45 metric ton ha^{-1} pig manure to winter wheat and 35 metric ton ha^{-1} cattle manure to clover grass by trailing hoses. All data from all six experiments, each line represents the average of three wind tunnels. Timespan of the different experiments can be found in Table 1.*

Table S7: *Cumulative VSC and NMVOC emissions after field application of 45 metric ton ha^{-1} pig manure to winter wheat and 35 metric ton ha^{-1} cattle manure to clover grass by trailing hoses. Ammonia emissions are from (Pedersen et al., 2020). Standard deviations are displayed in parenthesis (n = 3).*

		45 h [mg m^{-2}]					
		A		B		C	
m/z	Compound	Trailing shoes	Trailing hoses	Trailing shoes	Trailing hoses	Trailing shoes	Trailing hoses
33.032	Methanol	6.90 (1.02)	4.19 (7.26)	4.17 (6.85)	14.90 (19.13)	7.20 (10.81)	2.79 (2.04)
34.995	Hydrogen sulfide	0.00 (0.00)	0.00 (0.00)	49.54 (11.49)	66.02 (21.85)	98.07 (48.77)	115.76 (18.94)
41.038	Alcohol fragment[a]	9.66 (1.57)	27.57 (2.3)	15.75 (1.1)	13.95 (3.21)	5.4 (4.92)	2.86 (0.26)
41.038	Alcohol fragment[b]	14.9 (2.42)	43.51 (3.55)	24.28 (1.7)	21.5 (4.95)	8.33 (7.59)	4.41 (0.39)
43.052	Alcohol fragment[b]	4.47 (0.72)	12.75 (1.07)	7.28 (0.51)	6.45 (1.48)	2.5 (2.28)	1.32 (0.12)
45.033	Acetaldehyde	3.59 (1.54)	8.25 (1.86)	2.59 (0.76)	4.92 (3.90)	12.21 (16.01)	2.74 (1.57)
47.013	Formic acid	0.00 (0.00)	4.91 (3.97)	6.98 (2.13)	2.81 (1.49)	0.55 (0.62)	0.47 (0.43)
49.011	Methanthiol	0.21 (0.06)	0.31 (0.03)	0.19 (0.04)	0.22 (0.03)	0.24 (0.05)	0.24 (0.05)
59.049	Acetone	15.54 (0.91)	17.84 (0.66)	17.42 (0.95)	22.91 (4.61)	16.74 (13.14)	7.76 (0.62)
60.075	Trimethylamine	1.58 (0.28)	4.12 (0.55)	4.23 (0.31)	3.50 (0.54)	1.09 (0.60)	1.50 (1.18)
61.024 + 43.017	Acetic acid	196.43 (155.53)	1247.20 (542.64)	815.92 (141.71)	669.65 (175.04)	183.04 (10.20)	145.24 (72.04)
63.026	Dimethylsufide	0.13 (0.04)	0.99 (0.37)	1.39 (0.28)	1.21 (0.45)	3.17 (0.07)	2.17 (0.70)
69.067	Isoprene	2.34 (2.95)	2.70 (2.26)	0.80 (0.64)	3.44 (2.81)	6.15 (8.04)	2.19 (1.32)
73.06	2-Butanon	10.34 (1.95)	15.83 (2.41)	10.75 (0.48)	13.54 (4.04)	18.97 (16.93)	12.38 (4.69)
75.041 + 57.07	Propionic acid	85.76 (49.32)	467.04 (195.97)	327.71 (54.10)	277.24 (64.48)	123.72 (17.65)	110.79 (43.05)
79.05	Benzene	0.34 (0.29)	7.23 (4.73)	6.91 (2.40)	4.87 (2.17)	0.89 (0.58)	1.38 (1.18)
83.075	Cyclohexene	1.93 (1.93)	2.16 (1.99)	0.64 (0.21)	2.70 (2.58)	6.09 (7.59)	1.94 (1.00)
87.058	2,3-Butandion	20.58 (6.81)	25.70 (9.06)	9.53 (1.38)	13.12 (2.41)	5.56 (2.52)	2.54 (0.41)
89.056 + 71.074	Butyric acid	25.11 (18.61)	251.41 (105.39)	161.67 (30.78)	130.21 (34.34)	33.78 (5.57)	34.23 (14.83)
95.047	Phenol	11.03 (2.90)	31.38 (6.71)	22.14 (0.97)	21.70 (1.63)	19.52 (6.62)	24.40 (1.08)
101.05	Acetyl acetone	3.78 (2.30)	7.17 (1.52)	4.55 (1.00)	6.07 (2.00)	4.50 (3.44)	2.21 (1.27)
103.067 + 85.07	C5 carboxylic acids	21.89 (9.16)	114.40 (44.43)	81.37 (11.89)	69.95 (16.61)	21.39 (4.08)	22.58 (7.00)
109.058	4-Methylphenol	20.27 (4.52)	50.32 (11.43)	32.66 (1.50)	33.79 (4.53)	33.74 (19.29)	49.16 (4.92)
123.066	4-Ethylphenol	2.06 (0.47)	6.50 (1.43)	4.55 (0.40)	4.94 (0.78)	4.71 (2.05)	6.64 (0.48)
	Ammonia	1009.50 (275.41)	2141.93 (598.11)	2060.43 (57.44)	1565.54 (494.26)	2332.26 (491.14)	2557.49 (79.50)
	Total NMVOC	458.84 (164.81)	2352.48 (588.51)	1563.47 (155.46)	1343.59 (191.73)	519.50 (43.95)	441.95 (85.88)
	Total N	830.24 (226.51)	1761.57 (491.90)	1694.55 (47.45)	1287.54 (406.49)	1918.11 (403.92)	2103.34 (65.39)

Total C	236.43 (68.07)	1131.24 (245.69)	750.02 (65.22)	652.14 (80.40)	275.39 (28.48)	237.58 (37.18)
C/N	0.28 (0.11)	0.64 (0.23)	0.44 (0.04)	0.51 (0.17)	0.14 (0.03)	0.11 (0.02)
NMVOC/NH3 ratio	0.45 (0.21)	1.10 (0.41)	0.76 (0.08)	0.86 (0.30)	0.22 (0.05)	0.17 (0.03)

[a]From 2-butanol. [b]From 2-propanol.

		45 h [mg m^{-2}]						
		D		E		F		
m/z	Compound	Trailing shoes	Trailing hoses	Trailing shoes	Trailing hoses	Trailing shoes	Trailing hoses	Trailing hoses, 20cm
33.032	Methanol	0.53 (0.50)	0.52 (0.48)	7.75 (4.06)	6.24 (0.81)	54.99 (19.51)	40.74 (31.63)	72.56 (36.49)
34.995	Hydrogen sulfide	0.32 (0.56)	0.62 (0.56)	2.00 (2.02)	1.07 (0.97)	5.26 (2.74)	3.45 (1.48)	5.34 (2.23)
41.038	Alcohol fragment[a]	1.2 (0.32)	5.31 (2.06)	4.81 (0.36)	8.64 (1.36)	3.39 (0.3)	6.62 (3.52)	16.18 (2.39)
41.038	Alcohol fragment[b]	1.89 (0.49)	8.19 (3.18)	7.41 (0.55)	13.33 (2.1)	5.23 (0.46)	10.2 (5.42)	24.94 (3.69)
43.052	Alcohol fragment[b]	0.57 (0.15)	2.46 (0.95)	2.22 (0.16)	4 (0.63)	1.57 (0.14)	3.06 (1.63)	7.48 (1.11)
45.033	Acetaldehyde	0.94 (1.36)	0.46 (0.62)	1.12 (0.49)	0.48 (0.30)	0.35 (0.25)	2.94 (3.72)	6.32 (0.97)
47.013	Formic acid	0.36 (0.62)	1.73 (0.42)	4.18 (1.42)	10.22 (3.92)	2.91 (2.86)	2.39 (1.40)	13.44 (5.74)
49.011	Methanthiol	0.04 (0.03)	0.03 (0.03)	0.09 (0.06)	0.10 (0.03)	0.07 (0.00)	0.05 (0.06)	0.14 (0.05)
59.049	Acetone	2.94 (1.45)	4.76 (2.24)	10.96 (0.65)	10.46 (2.83)	2.32 (0.71)	4.51 (0.98)	7.92 (1.15)
60.075	Trimethylamine	0.36 (0.27)	0.52 (0.42)	0.88 (0.16)	1.63 (0.68)	0.48 (0.21)	0.50 (0.11)	1.97 (0.98)
61.024 + 43.017	Acetic acid	51.52 (27.13)	428.08 (115.60)	237.24 (78.98)	697.99 (235.79)	137.96 (48.18)	183.91 (63.80)	951.60 (231.49)
63.026	Dimethylsufide	0.05 (0.09)	0.56 (0.46)	0.29 (0.15)	0.69 (0.43)	0.22 (0.10)	0.17 (0.10)	1.20 (0.54)
69.067	Isoprene	0.34 (0.59)	0.16 (0.27)	6.74 (4.32)	8.24 (0.80)	1.37 (0.93)	4.48 (5.70)	1.46 (0.47)
73.06	2-Butanon	1.92 (0.49)	2.08 (0.66)	3.17 (0.16)	4.17 (0.78)	3.43 (1.72)	3.52 (0.86)	6.06 (1.51)
75.041 + 57.07	Propionic acid	33.65 (18.25)	160.30 (35.25)	88.53 (21.17)	208.50 (59.40)	45.90 (10.66)	78.21 (32.92)	288.40 (60.28)
79.05	Benzene	0.57 (0.31)	0.80 (0.27)	1.37 (0.01)	1.86 (0.28)	1.37 (0.07)	1.70 (0.13)	2.93 (0.60)
83.075	Cyclohexene	0.34 (0.45)	0.13 (0.23)	1.48 (1.08)	0.77 (0.50)	0.49 (0.40)	2.94 (4.10)	2.14 (0.88)
87.058	2,3-Butandion	0.00 (0.00)	0.00 (0.00)	0.81 (0.62)	0.59 (0.27)	0.19 (0.15)	1.56 (1.55)	2.60 (0.38)
89.056 + 71.074	Butyric acid	10.06 (4.71)	60.65 (15.63)	34.89 (8.77)	86.76 (26.58)	23.82 (5.66)	33.18 (7.31)	135.31 (28.29)
95.047	Phenol	20.19 (2.02)	38.14 (4.90)	32.24 (5.68)	44.50 (7.58)	27.11 (1.52)	35.06 (2.95)	63.85 (7.41)
101.05	Acetyl acetone	0.00 (0.00)	0.00 (0.00)	0.28 (0.31)	0.34 (0.22)	0.12 (0.19)	2.11 (3.30)	0.39 (0.31)
103.067 + 85.07	C5 carboxylic acids	1.98 (2.10)	9.79 (3.18)	14.56 (3.90)	36.18 (10.04)	9.35 (0.84)	14.28 (2.55)	53.22 (8.85)
109.058	4-Methylphenol	17.28 (3.71)	40.57 (7.50)	36.56 (8.23)	57.90 (10.32)	35.23 (3.42)	45.62 (3.86)	93.61 (12.82)
123.066	4-Ethylphenol	4.29 (1.44)	10.92 (1.99)	9.72 (2.03)	16.26 (3.36)	9.53 (1.76)	12.68 (2.40)	28.35 (4.34)
	Ammonia	1652.28 (151.96)	2429.53 (303.93)	2429.53 (303.56)	2996.56 (300.63)	2385.20 (167.71)	2654.41 (200.76)	3974.06 (427.75)
	Total NMVOC	151.04 (33.49)	776.16 (122.34)	507.28 (83.20)	1219.85 (245.24)	367.41 (53.65)	490.44 (79.80)	1782.07 (244.40)

Total N	1358.87 (124.98)	1998.10 (249.96)	1998.10 (249.96)	2464.44 (247.24)	1961.65 (137.93)	2183.05 (165.11)	3268.36 (351.79)
Total C	84.11 (14.80)	377.89 (50.74)	257.02 (34.84)	584.47 (100.49)	188.25 (21.80)	257.56 (34.18)	864.17 (100.28)
C/N	0.06 (0.01)	0.19 (0.03)	0.13 (0.02)	0.24 (0.05)	0.10 (0.01)	0.12 (0.02)	0.26 (0.04)
NMVOC/NH3 ratio	0.09 (0.02)	0.32 (0.06)	0.21 (0.04)	0.41 (0.09)	0.15 (0.02)	0.18 (0.03)	0.45 (0.08)

[a]From 2-butanol. [b]From 2-propanol.

		90 h [mg m^{-2}]								
		A		B		D		F		
m/z	Compound	Trailing shoes	Trailing hoses	Trailing shoes	Trailing hoses	Trailing shoes	Trailing hoses	Trailing shoes	Trailing hoses	Trailing hoses, 20 cm
33.032	Methanol	7.14 (1.03)	11.63 (11.19)	5.23 (8.70)	26.13 (36.45)	2.92 (2.60)	4.81 (2.66)	87.85 (35.80)	81.05 (53.68)	108.88 (58.38)
34.995	Hydrogen sulfide	0.00 (0.00)	0.00 (0.00)	59.27 (10.64)	69.70 (21.62)	3.98 (3.78)	4.52 (4.80)	9.80 (1.40)	10.88 (3.45)	12.23 (3.93)
41.038	Alcohol fragment[a]	10.05 (1.57)	29.66 (2.43)	19.96 (1.61)	18.9 (2.89)	6.17 (3.17)	10.13 (4.41)	4.42 (0.7)	10.96 (8.01)	20.92 (3.02)
41.038	Alcohol fragment[b]	15.49 (2.42)	45.72 (3.74)	30.76 (2.48)	29.13 (4.46)	9.52 (4.88)	15.62 (6.8)	6.82 (1.08)	16.9 (12.35)	32.25 (4.65)
43.052	Alcohol fragment[b]	4.65 (0.73)	13.72 (1.12)	9.23 (0.74)	8.74 (1.34)	2.85 (1.46)	4.69 (2.04)	2.05 (0.32)	5.07 (3.71)	9.68 (1.39)
45.033	Acetaldehyde	3.79 (1.74)	10.63 (3.81)	3.93 (1.07)	8.50 (5.95)	1.67 (1.87)	0.76 (1.03)	0.56 (0.25)	7.48 (10.71)	10.40 (1.31)
47.013	Formic acid	0.28 (0.26)	5.63 (2.91)	7.84 (2.78)	3.98 (1.91)	0.46 (0.79)	1.73 (0.42)	3.10 (2.98)	2.71 (1.26)	15.02 (6.07)
49.011	Methanthiol	0.15 (0.10)	0.15 (0.02)	0.28 (0.07)	0.36 (0.07)	0.09 (0.01)	0.06 (0.04)	0.11 (0.03)	0.10 (0.06)	0.20 (0.07)
59.049	Acetone	16.89 (1.18)	21.24 (1.29)	20.31 (1.68)	26.90 (4.78)	3.88 (3.08)	5.44 (2.17)	2.36 (0.76)	5.11 (1.49)	8.39 (1.13)
60.075	Trimethylamine	1.82 (0.48)	4.99 (0.45)	4.67 (0.56)	4.12 (0.76)	0.87 (0.92)	0.73 (0.67)	0.53 (0.23)	0.56 (0.14)	2.15 (1.14)
61.024 + 43.017	Acetic acid	228.99 (184.68)	1416.72 (555.65)	1160.45 (226.63)	1036.46 (249.21)	73.73 (45.52)	551.28 (139.50)	164.65 (50.84)	216.61 (77.71)	1195.43 (295.12)
63.026	Dimethylsulfide	0.18 (0.06)	1.43 (0.60)	1.63 (0.49)	1.53 (0.38)	0.26 (0.08)	0.83 (0.37)	0.44 (0.30)	0.36 (0.06)	1.55 (0.67)
69.067	Isoprene	2.37 (2.95)	4.21 (2.80)	2.19 (1.03)	6.86 (3.97)	2.19 (3.79)	1.77 (1.66)	2.08 (1.44)	11.07 (15.62)	2.42 (0.41)
73.06	2-Butanon	10.34 (1.95)	16.60 (2.46)	12.52 (1.69)	15.38 (3.61)	2.11 (0.74)	2.32 (0.83)	5.10 (2.45)	4.96 (2.05)	7.53 (2.26)
75.041 + 57.07	Propionic acid	92.11 (53.29)	513.93 (199.54)	431.57 (73.82)	396.34 (85.84)	90.38 (20.35)	234.14 (57.19)	58.05 (13.83)	112.77 (58.97)	352.71 (71.78)
79.05	Benzene	0.42 (0.33)	8.15 (5.40)	8.45 (3.02)	6.80 (2.01)	0.61 (0.28)	0.87 (0.33)	1.42 (0.02)	1.85 (0.13)	3.10 (0.50)
83.075	Cyclohexene	1.96 (2.00)	2.24 (1.94)	1.60 (0.45)	5.70 (4.94)	0.46 (0.56)	0.31 (0.15)	0.91 (0.81)	7.61 (11.17)	3.24 (1.31)
87.058	2,3-Butandion	35.50 (11.57)	39.19 (14.28)	30.17 (6.14)	27.86 (6.25)	0.00 (0.00)	0.00 (0.00)	0.24 (0.21)	3.01 (3.68)	3.26 (0.67)
89.056 + 71.074	Butyric acid	28.41 (19.70)	273.26 (1077.23)	203.17 (41.53)	177.79 (37.98)	20.94 (20.94)	78.76 (24.10)	26.77 (5.12)	39.45 (7.28)	162.62 (35.73)

95.047	Phenol	11.09 (2.89)	31.82 (6.89)	23.01 (1.09)	22.66 (2.11)	20.62 (2.17)	38.54 (4.67)	27.55 (1.15)	36.71 (5.26)	64.52 (7.48)
101.05	Acetyl acetone	5.45 (2.78)	9.61 (2.39)	7.87 (2.77)	9.75 (3.22)	0.01 (0.02)	0.00 (0.00)	0.12 (0.19)	5.60 (9.15)	0.40 (0.33)
103.067 + 85.07	C5 carboxylic acids	22.98 (9.32)	123.84 (45.11)	103.11 (14.62)	94.41 (20.17)	4.61 (4.87)	13.05 (5.72)	10.38 (0.41)	18.90 (6.57)	63.55 (10.49)
109.058	4-Methylphenol	20.38 (4.57)	50.52 (11.36)	32.80 (1.57)	34.43 (3.91)	17.88 (3.79)	41.17 (7.48)	35.62 (3.33)	47.00 (5.06)	94.57 (13.15)
123.066	4-Ethylphenol	2.13 (0.55)	6.55 (1.47)	4.85 (0.48)	5.54 (1.03)	4.55 (1.61)	11.38 (1.98)	9.77 (1.77)	13.60 (3.15)	29.40 (4.51)
	Ammonia	1246.96 (328.32)	2734.86 (714.01)	2776.36 (73.78)	2140.10 (652.86)	2131.68 (68.12)	3022.26 (291.65)	2654.44 (179.95)	2860.05 (357.79)	4235.96 (475.16)
	Total NMVOC	522.58 (193.97)	2641.43 (602.25)	2125.59 (242.71)	1968.26 (269.95)	266.78 (51.78)	1018.39 (153.34)	450.92 (64.18)	649.45 (115.66)	2192.17 (312.05)
	Total N	1025.53 (270.02)	2249.22 (587.22)	2283.34 (60.68)	1760.07 (536.93)	1753.14 (56.02)	2485.58 (239.86)	2183.07 (147.99)	2352.17 (294.25)	3483.76 (390.78)
	Total C	268.94 (79.76)	1266.03 (251.36)	1008.50 (100.70)	942.58 (112.04)	146.84 (22.81)	493.46 (64.68)	226.65 (25.76)	344.11 (52.98)	1049.93 (127.45)
	C/N	0.26 (0.10)	0.56 (0.18)	0.44 (0.05)	0.54 (0.18)	0.08 (0.01)	0.20 (0.03)	0.10 (0.01)	0.15 (0.03)	0.30 (0.05)
	NMVOC/NH3 ratio	0.42 (0.19)	0.97 (0.33)	0.77 (0.09)	0.92 (0.31)	0.13 (0.02)	0.34 (0.06)	0.17 (0.03)	0.23 (0.05)	0.52 (0.09)

[a]From 2-butanol. [b]From 2-propanol.

S6 NMVOC emission

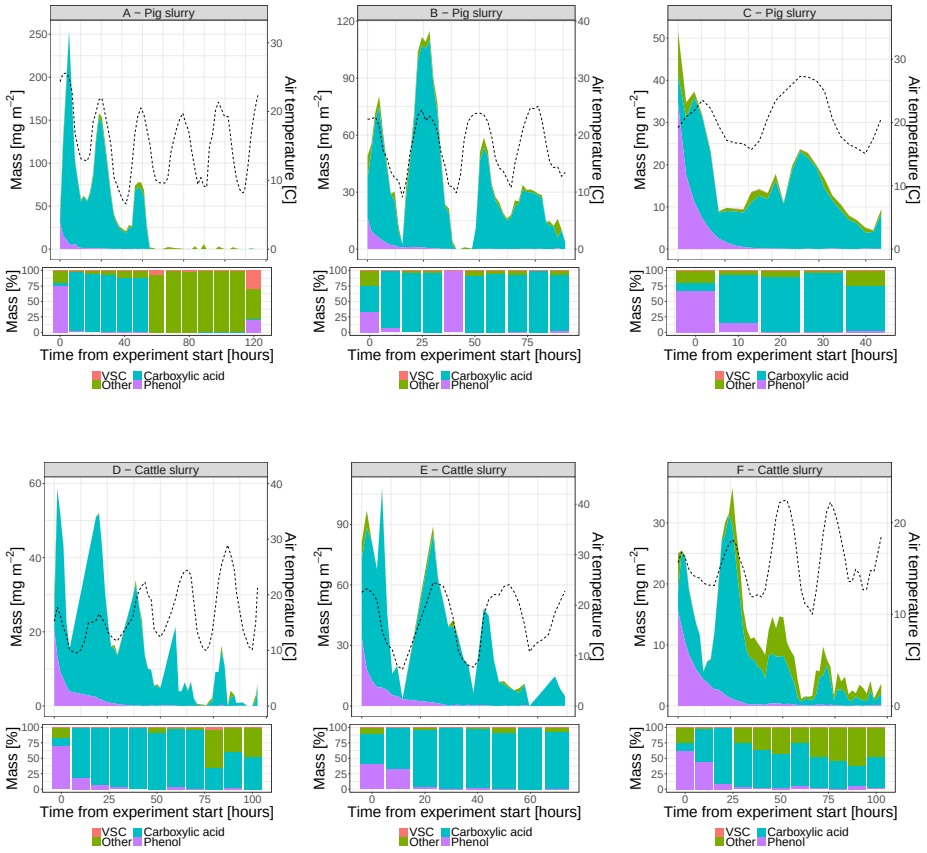

Figure S2: *Average emission of NMVOC over time after field application of 45 metric ton ha^{-1} pig manure to winter wheat and 35 metric ton ha^{-1} cattle manure to clover grass by trailing hoses.*

S7 Total NMVOC emission estimates from field applied manure in Denmark

Table S8:. *Estimations of yearly NMVOC emissions in Denmark from trailing hose applied cattle and pig manure based on numbers from national inventories and this study. Total reported NMVOC emission in Denmark in 2018 was ~120.000 metric ton (Nielsen and Plejdrup, 2020). TH = Trailing hoses.*

		Dairy cows	Finisher pigs	Sows	Piglets	Calculation	Total
Mass of manure field applied[a]	M [metric ton]	17,257,439	10,528,287	5,843,612	4,222,971		37,852,309
Fraction applied by TH[a]	$F_{applied,th}$	0.23	0.63	0.63	0.63		
Mass of manure applied by TH	$M_{applied,th}$ [metric ton]	3,969,211	6,632,821	3,681,476	6,632,821	$M_{applied,TH} = M * F_{applied,TH}$	20,916,328
Amount of manure pr. animal pr. year[b]	M_{animal} [metric ton manure/animal unit/year]	26.7[cd]	0.51[d]	3.88[d]	0.09[d]		
Number of animals produced	A [units/year]	148,660	13,005,531	948,834	73,698,009	$A = M_{applied,TH} * M_{animal}{}^{-1}$	
Emission of NH_3 after field application pr. animal[a]	$E_{NH3,application}$ [kg NH_3 /animal unit/year]	13.06	0.21	1.65	0.03		
Emission of NH_3 after field application by TH	$E_{NH3,application,TH}$ [metric ton NH_3]	1,941	2,678	1,566	2,211	$E_{NH3,application} = E_{NH3,application} * A$	8,396
Emission of NMVOC pr. animal pr. year[a]	$E_{NMVOC,application}$ [kg NMVOC /animal unit-year]	5.82	0.03	0.80	0.01		
Based on data from national inventory:							
NMVOC/NH_3 emission fraction after field application of manure	$F_{NMVOC/NH3}$	0.45	0.16	0.48	0.33	$F_{NMVOC/NH3} = E_{NMVOC,application} * E_{NH3,application}{}^{-1}$	
National yearly NMVOC emission due to field application of manure	$E_{NMVOC,tot}$ [metric ton NMVOC/year]	865	427	759	737	$E_{NMVOC,tot} = F_{NMVOC/NH3} * E_{NH3,application,TH}$	2,788
Based on data from this study:							
NMVOC/NH_3 emission fraction due to field application of manuree	$F_{NMVOC/NH3}$	1.15	0.4	0.4	0.4		
National yearly NMVOC	$E_{NMVOC,tot}$ [metric ton NMVOC/year]	2,233	1,152	673	951	$E_{NMVOC,tot} = F$ NMVOC/NH_3 * $E_{NH3,application,TH}$	5,008
Difference between NMVOC emission estimation from this study and national inventory [%]		158	170	-11	29		

[a]Oral communication, Mette Hjorth Mikkelsen. Data based on the Danish national emission inventory, reported on 18th of June 2020.
[b]From Lund et al. (2019). [c]One dairy cow-year, large breed.
[d]Numbers are from conventionally produced animals. [e]From Table S7.

S8 OAV

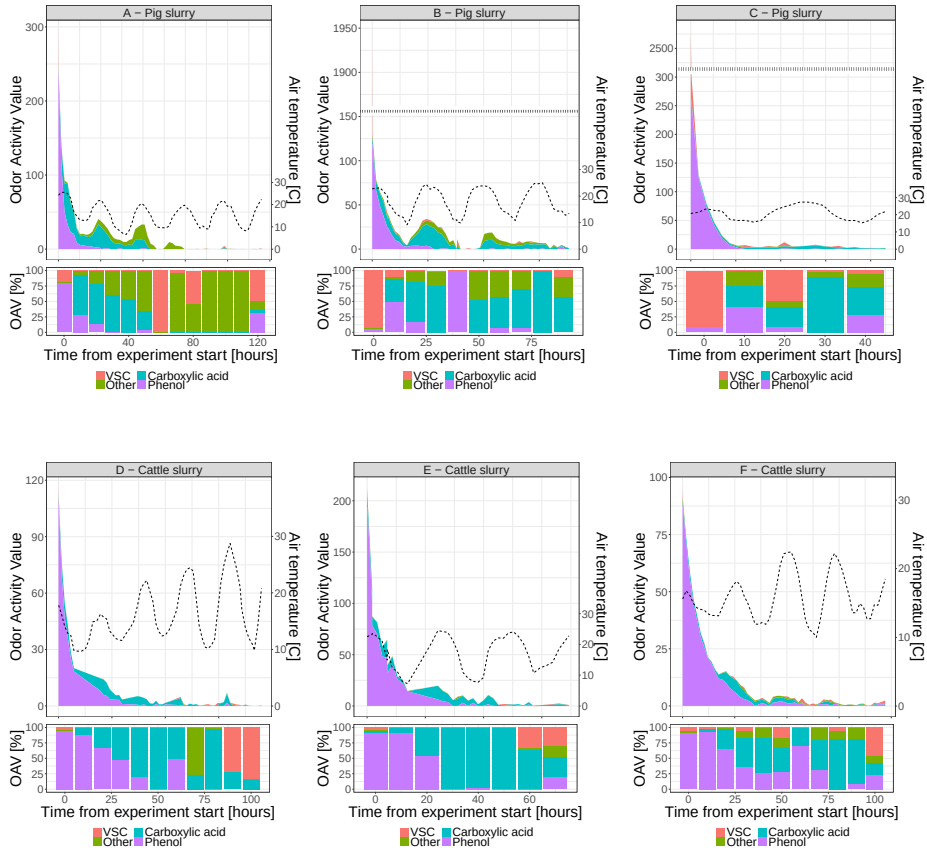

Figure S3: *Average OAV over time after field application of 45 metric ton ha^{-1} pig manure to winter wheat and 35 metric ton ha^{-1} cattle manure to clover grass by trailing hoses.*

Table S9: *Odor emission (E) value right after slurry application, after 24 hours, and after 48 hours. Standard deviations are displayed in parenthesis (n = 3).*

	Odor emission * 10^{-3} (OAV h^{-1} m^{-2}) (mean)								
	0 hours			24 hours			48 hours		
Experiment	TS[1]	TH[1]	TH20[1]	TS	TH	TH20	TS	TH	TH20
A	163.5 (70.5)	443 (93)		14 (6)	56 (9)		38 (14)	50 (15)	
B	2966 (111)	2921 (1401)		51 (8)	51 (11)		26 (11)	26 (12)	
C	2972 (1410)	4170 (683)		12 (8)	8 (8)				
D	25 (47)	174 (47)		5 (8)	2 (6)		2 (8)	6 (9)	
E	215 (77)	320 (86)		18 (5)	30 (5)		2 (2)	2 (2)	
F	99 (42)	143 (57)	465 (75)	15 (3)	20 (3)	45 (5)	2 (2)	6 (3)	8 (18)

[1]TS: trailing shoes, TH: trailing hoses, TH20: trailing hoses 20 cm.

References

Cappellin, L., Karl, T., Probst, M., Ismailova, O., Winkler, P., Soukoulis, C., Aprea, E., Märk, T.D., Gasperi, F., Biasioli, F., 2012. On quantitative determination of volatile organic compound concentrations using proton-transfer-reaction-time-of-flight-mass-spectrometry. Environ. Sci. Technol. 4, 1–4.

Chen, Y., Munkholm, L.J., Nyord, T., 2013. Selection of design parameters for a slurry injection tool. Trans. Asabe 56, 1653–1663. https://doi.org/10.13031/trans.56.10237

Feilberg, A., Bildsoe, P., Nyord, T., 2015. Application of PTR-MS for measuring odorant emissions from soil application of manure slurry. Sensors (Switzerland) 15, 1148–1167. https://doi.org/10.3390/s150101148

Feilberg, A., Liu, D., Adamsen, A.P.S., Hansen, M.J., Jonassen, K.E.N., 2010. Odorant emissions from intensive pig production measured by online proton-transfer-reaction mass spectrometry. Environ. Sci. Technol. 44, 5894–5900. https://doi.org/10.1021/es100483s

Feilberg, A., Nyord, T., Hansen, M.N., Lindholst, S., 2011. Chemical evaluation of odor reduction by soil injection of animal manure. J. Environ. Qual. 40, 1674–82. https://doi.org/10.2134/jeq2010.0499

Hansen, M.J., Jonassen, K.E.N., Løkke, M.M., Adamsen, A.P.S., Feilberg, A., 2016. Multivariate prediction of odor from pig production based on in-situ measurement of odorants. Atmos. Environ. 135, 50–58. https://doi.org/10.1016/j.atmosenv.2016.03.060

Hansen, M.J., Liu, D., Guldberg, L.B., Feilberg, A., 2012. Application of proton-transfer-reaction mass spectrometry to the assessment of odorant removal in a biological air cleaner for pig production. J. Agric. Food Chem. 60, 2599–2606. https://doi.org/10.1021/jf300182c

Liu, D., Nyord, T., Rong, L., Feilberg, A., 2018. Real-time quantification of emissions of volatile organic compounds from land spreading of pig slurry measured by PTR-MS and wind tunnels. Sci. Total Environ. 639, 1079–1087. https://doi.org/10.1016/j.scitotenv.2018.05.149

Lund, P., Hellwing, A.L.F., Børsting, C.F., 2019. Normtal for husdyrgødning 2019. https://doi.org/.1037//0033-2909.I26.1.78

Nielsen, O.-K., Plejdrup, M., 2020. National emission inventories - Denmark 2020 submission [WWW Document]. Submiss. Danish Emiss. data.

Parker, D., Ham, J., Woodbury, B., Cai, L., Spiehs, M., Rhoades, M., Trabue, S., Casey, K., Todd, R., Cole, A., 2013. Standardization of flux chamber and wind tunnel flux measurements for quantifying volatile organic compound and ammonia emissions from area sources at animal feeding operations. Atmos. Environ. 66, 72–83. https://doi.org/10.1016/j.atmosenv.2012.03.068

Pedersen, J.M., Feilberg, A., Kamp, J.N., Hafner, S., Nyord, T., 2020. Ammonia emission measurement with an online wind tunnel system for evaluation of manure application techniques. Atmos. Environ. 230. https://doi.org/10.1016/j.atmosenv.2020.117562

Sekimoto, K., Li, S.M., Yuan, B., Koss, A., Coggon, M., Warneke, C., de Gouw, J., 2017. Calculation of the sensitivity of proton-transfer-reaction mass spectrometry (PTR-MS) for organic trace gases using molecular properties. Int. J. Mass Spectrom. 421, 71–94. https://doi.org/10.1016/j.ijms.2017.04.006

Su, T., 1994. Parametrization of kinetic energy dependences of ion-polar molecule collision rate constants by trajectory calculations. J. Chem. Phys. 100, 4703. https://doi.org/10.1063/1.466255

Woodbury, B.L., Gilley, J.E., Parker, D.B., Marx, D.B., Eigenberg, R.A., 2016. Emission of volatile organic compounds as affected by rate of application of cattle manure. Trans. ASABE 59, 885–895. https://doi.org/10.13031/trans.59.11374

Chapter 5

Paper III

J. Pedersen, K. Andersson, A. Feilberg, S. Delin, S. Hafner, T. Nyord. The effect of exposed surface area on ammonia emission from untreated, separated, and digested cattle manure. *Biosystems Engineering*, in review September 2020.

The effect of exposed surface area on ammonia emission from untreated, separated, and digested cattle manure

Johanna Pedersen[a], Karin Andersson[b], Anders Feilberg[a], Sofia Delin[b], Sasha Hafner[c], Tavs Nyord[a]*

[a]Aarhus University, Dept. of Engineering, Denmark
[b]Swedish University of Agricultural Sciences, Sweden
[c]Hafner Consulting LLC, Reston, VA, USA 20191
*Corresponding author email: tavs.nyord@eng.au.dk, Address: Aarhus University, Finlandsgade 12, 8200 Aarhus N, Denmark, +45 20605533

Keywords: Wind tunnels, Band application, Manure surface pH, Normalized emission, Ammonia volatilization

Abstract

Ammonia (NH_3) emissions from land-applied manure contribute to nitrogen deposition, acidification, and formation of fine particles in the atmosphere. Optimal management and field application techniques can reduce emission. A reduction in contact area between the manure and the atmosphere is expected to reduce NH_3 emission. The objectives of this study were to develop a method for quantifying the exposed surface area (ESA) of field-applied manure over time, and determine the degree to which ESA explains differences in NH_3 emission. Two experiments were conducted in which untreated, separated, and digested manure was applied in bands on two different soils with spring oats stubble. Emission data were obtained from online wind tunnel measurements and manure characteristics such as surface pH, viscosity, and particle size distribution were measured. The new ESA method relies on fluorescent dye added to the manure slurry prior to field application, followed by imaging. The results show that the ESA measurements can give new insight into the soil-manure interactions after manure application, and help explain why some types of manure and application techniques lead to successful abatement under some circumstances, but not under others. Furthermore, a pH-, TAN-, temperature-, and ESA-normalized NH_3 emission is estimated, which helps to identify the effects of infiltration.

1 Introduction

Agriculture causes air pollution by emission of ammonia (NH_3), greenhouse gases, volatile organic compounds, odorous compounds, and airborne particles (Aneja et al., 2009). Emissions from livestock production occur throughout the production chain: production sites, storage facilities, and land spreading of manure.

Ammonia emissions from land-spread manure contribute to nitrogen deposition, acidification (Aneja et al., 2009), and formation of fine particles (PM2.5) (Walker et al., 2006) in the atmosphere. Several factors influence emission, including application technique, soil- and manure parameters, and ambient air temperature (Hafner et al., 2018).

Ammonia emission from manure can be reduced with optimal handling practices and field application techniques (Hafner et al., 2019; Sommer and Hutchings, 2001). In principle, NH_3 emission can be reduced by reducing the contact area between the applied manure and the atmosphere (Hafner et al., 2019; Webb et al., 2010). Low emission application technologies have been developed in order to reduce the exposed surface area (ESA) from which emissions occur. Several studies have described the influence of soil attributes, including inherent characteristics and conditions, on NH_3 emissions from field applied manure (e.g. Bell et al., 2015; Huijsmans et al., 2018; Martínez-Lagos et al., 2013). Other studies identify infiltration of manure to be of high importance for NH_3 emission (e.g. de Jonge et al., 2004; Misselbrook et al., 2005; Rochette et al., 2008; Sommer et al., 2004; Sommer and Jacobsen, 1999), but quantifying the effect of infiltration has remained a challenge. Together with manure characteristics, soil characteristics determine the ESA of the manure.

Different methods can be used to quantify a liquid distribution, including the use of inert tracers or dyes. A tracer is not desirable as it averages out the spatial concentration (Aeby, 1998). To obtain a better spatial resolution, dyes and imaging have been used. Imaging methods are relatively cheap since no chemical analysis is needed, although some dyes are costly. Once the method is developed, data analysis can be performed relatively rapidly. Dyes that can easily be detected must be carefully chosen. Fluorescent compounds may be suitable because with the right technique they can be detected even in dark manure. The dye should be soluble in the manure and not change the hydraulic characteristics. The dye should preferably be non-toxic, mobile in soil to the same extent as the bulk liquid, and should be independent of pH and temperature. Aeby et al. (1998) developed a method to detect and quantify water distribution in the vertical direction in soil using the fluorescent dye Acid Yellow 7 (AY7) and imaging. The method has subsequently been used by Aeby et al. (2001), Rosenbom et al. (2008), Stadler et al. (2000), and Vanderborght et al. (2002). In the current study, a method for quantification of ESA was developed based on the work by Aeby (1998) in order to quantify the changes in ESA of manure on the soil surface over time. The method quantifies the area by the light emitted from the fluorescent compound AY7 added to the manure prior to application.

In order to utilize ESA as a parameter to explain differences in NH_3 emission, two experiments were conducted. The ESA and NH_3 emissions were examined for three different cattle manure batches applied to spring oats stubble with trailing

hoses. The batches were selected in order to obtain different infiltration characteristics and included 1) untreated manure, 2) anaerobically digested manure, and 3) the liquid fraction of solid-liquid separated manure. Anaerobic digestion and solid-liquid separation are two common manure treatment strategies. Anaerobic digestion is a fermentation process where organic matter is converted to carbon dioxide and methane, which can be utilized as an energy source (Nasir et al., 2012; Sakar et al., 2009). Other substrates, such as food waste, slaughter house waste products, and straw can be added for co-digestion with manure. Solid-liquid separation is used to provide a higher flexibility in manure management, nutrient utilization and storage capacity. Manure dry matter is generally decreased by both digestion and separation (Hjorth et al., 2010; Masse et al., 2005). Anaerobic digestion increases the total ammonical nitrogen (TAN) content and pH of the manure due to mineralization of organic nitrogen (Masse et al., 2005). These changes in manure characteristics affect NH_3 emission after field application.

The main goal of this work was to determine if measurements of manure ESA after field application can be used to explain differences in NH_3 emission. Objectives were to: (i) Investigate if AY7 and imaging techniques can be used to quantify ESA after field application of manure, and set up a simple mathematical model to describe the change over time, (ii) Measure ESA and NH_3 emission from untreated, digested, and separated cattle manure applied by trailing hoses on two different soil types, (iii) Evaluate if NH_3 emission can be explained by ESA, surface pH of manure after application, viscosity, and particle size distribution. The hypotheses were: (i) Separated manure will yield the lowest NH_3 emissions due to high infiltration, (ii) The high pH of digested manure will be counterbalanced by the low dry matter leading to minimal change in emission, (iii) Ammonia emissions will generally be lower for soil with a higher sand content due to faster infiltration.

2 Materials and methods

Two experiments were performed measuring NH_3 emissions, changes in manure surface pH, and manure ESA from digested, separated, and untreated cattle manure on silty clay (experiment A) and sandy loam (experiment B) soil, both situated in the west part of Sweden (58°N, 13°E). A field area of approximately 20 x 20 meters was used for all the experiments. It is assumed that the soil and crop variability within the area was insignificant.

2.1 Ammonia measurements

2.1.1 The wind tunnel system

Nine wind tunnels were used to measure NH_3 emission after field application of manure. A detailed description and an evaluation of the system is presented in

(Pedersen et al., 2020), and only a short description is given in the following. A rectangular stainless steel emission chamber (80 x 40 x 25 cm) with a small air inlet (33.5 x 1.3 cm) was connected to a fan, motor, and frequency converter via a steel duct. The air flow through the emission chamber was manually adjusted to an air exchange rate of 25 min^{-1}, corresponding to a calculated mean air speed of 0.33 m s^{-1}. The tunnels were mounted on frames (29.3 x 67.4 cm) that was inserted into the soil in order to control the amount of manure in each plot, and prevent leaks. The plot area of each tunnel was 0.2 m^2. Three background measurements were equally distributed among the tunnels, measuring NH_3 concentrations in the air entering the tunnels. From each tunnel, and the background sampling points, air was drawn for 8 minutes to a channel selection manifold, giving a time resolution of each wind tunnel of 104 minutes. Ammonia concentrations were measured continuously with a Cavity Ring-Down Spectroscopy (CRDS) instrument (G2103 NH_3 Concentration Analyzer, Picarro, CA, USA). During experiment A, air temperature inside and outside a tunnel were logged continuously, and a maximum difference of 2°C occurred, with the higher temperature being observed outside the tunnels. In addition to the continuous measurements five point measurements of the temperature inside and outside the tunnels showed an average difference of 0.4°C.

A standard gas (CALGAZ, 10±1 ppm NH_3) was used to test the recovery of NH_3 by the sampling system from the tube inlet at the wind tunnels to the CRDS. Within 8 minutes >90% of the standard gas concentration was recovered throughout the sampling system.

A weather station at each site logged ambient air temperature continuously throughout both experiments.

2.1.2 Data treatment and statistics

Average NH_3 emission flux F (g m^{-2} min^{-1}) in each measurement interval was calculated separately for each wind tunnel from the concentration C (g m^{-3}), the air flow q (m min^{-1}) in the emission chamber, and the soil area covered by the wind tunnel A (m^2) (Equation 1).

$$F_{NH3} = (C*q)/A \qquad \text{Equation 1}$$

Cumulative emission was calculated using the trapezoidal rule.

Differences among application methods were tested with a single factor analysis of variance (ANOVA). The two experiments were analyzed separately. The nine tunnels were divided into three blocks, each containing one tunnel with each treatment, with a randomized block design. A single wind tunnel was used as observational unit and the cumulative NH_3 emission after 90 hours was used as the response variable. Tukey's test (confidence interval of 95%) was used to investigate differences among treatments.

2.2 Exposed surface area

2.2.1 System for measurement of manure exposed surface area

A setup consisting of dark chambers, UV light, and a camera was used to measure ESA over time. The fluorescence compound AY7 was added to the manure (45 mmol L^{-1}) prior to field application. Further information about AY7 can be found in the supporting material S1.1 Information about Acid yellow 7. The setup with dark chambers ensured that the manure with AY7 was exposed only to the ultra violet (UV) light needed for excitation of the fluorescence compound, and that the area used for quantification was constant during the experiment. For quantification a set of pictures was taken: (a) an intensity picture to correct for inhomogeneous light distribution (Aeby et al., 2001; Rosenbom et al., 2008), and (b) intensity pictures of the manure on the soil surface. One picture was taken right after manure application, and then every 0.5 hours for ten hours during experiment A and every hour for 12 hours during experiment B.

Nine plastic barrels (49 cm diameter, 52 cm height) with the bottoms cut out were used as dark chambers. A piece of plywood (60 cm diameter, 1 cm thickness) with a rectangular opening (35 x 29 cm) was attached to the bottom (Figure 1). The dark chambers were held in place in the field by two large nails inserted into two holes in the plywood on the outside of the barrels. During the experiments, lids were kept on the dark chambers to avoid UV light from the sun to cause photodecomposition of the dye molecules, resulting in a decrease of the fluorescence. One lid was modified so that four UV light bulbs (36-Watts EV LED Bulb, Par38 Spotlight E27 Medium Base, YeeSite, China) with a UV wavelength of 395 – 410 nm, was mounted around a camera (Sony Alpha A7sii mirrorless digital camera, Sony, Japan) with a wide angle lens (Sony FE 28 mm, F2.0, Sony, Japan). To only capture the emission light, a long pass filter (LP515/52 Yellow-Orange Longpass filter, Midopt, IL, USA) was used with the lens. The dark chambers and the lid with the camera and lights were marked so that the lid was placed in the same position for each picture. Pictures of pink fluorescence cardboard (Tutein & Koch ApS, Denmark) used to determine the spatial intensity distribution were taken once at the beginning of the experiment with ISO-400, f18, a shutter speed of 1/250 seconds and no flash. The camera settings for the fluorescence pictures were ISO-400, f18, a shutter speed of 0.5 seconds, and no flash.

2.2.2 Data treatment

All the image processing was performed in MatLab (R2018a, Mathworks).
The following process was done on each set of pictures from each dark chamber:

a The pictures (JPG format, 4240 x 2832 pixels) were corrected for non-uniform lighting with the spatial intensity distribution pictures (Aeby et al., 2001;

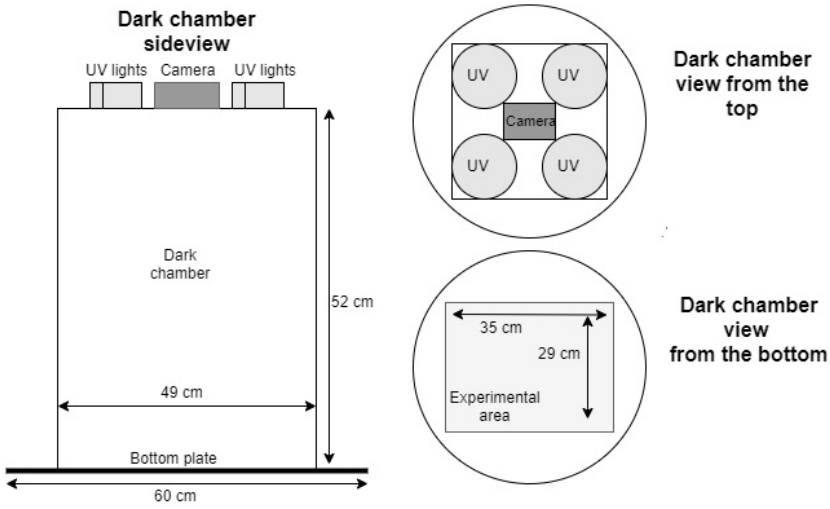

Figure 1: *Dark chamber setup. Sketch is not to scale.*

Rosenbom et al., 2008).

b A mask was created with the picture taken right after manure application (0 h) by manually drawing around the manure in the picture. Everything outside the mask was set to an RBG value of 0. The mask were applied to all the subsequent pictures from the same dark chamber (1 h , 2 h... etc.). The masks were used in order to avoid unnecessary disturbance from crop residues in the pictures.

c The pictures were converted to grayscale.

d The pictures were converted to black and white pictures using a threshold of 0.7 based on several preliminary tests. At this threshold, the pixels with manure became white and the pixels without manure became black

e The amount of white pixels in each picture was counted and the ESA was calculated with the standard curve (Figure S1).

The values of fractional area coverage obtained with steps a-e were fitted to a model (Equation 2).

$$ESA = a*e^{-b*t}+c \qquad \text{Equation 2}$$

Where a (m^2 m^{-2}) is the total reduction in ESA from the initial area after application until stagnation in ESA, b (h^{-1}) is a parameter that describes how

fast the ESA changes after manure application, t is time (h), and c is the area of manure at the soil surface at $t = \infty$ (m^2 m^{-2}). Fitting was done using nonlinear regression (nls()) function in R (version 3.4) (R Core Team, 2018).

During experiment A, an error occurred when taking the picture six hours after application, most likely because the lid with UV lights and camera was not closed well enough when the pictures was taken, allowing daylight to enter. The additional light presumably inflated ESA measurements and therefore these pictures were excluded. During experiment B, the ESA of all three manure types increased between application and the first picture one hour after application due to spreading out. As the model describes the decrease in ESA following maximum spreading, the first measurement after application was excluded.

2.3 Ammonia equilibrium calibration

The ratio of observed NH_3 concentration in the air after manure application relative to the equivalent gas phase equilibrium concentration (${C_g}^{eq}$) of NH_3 (denoted R_C, Equation 3) can be used to compare emission data from different sources since this ratio is independent of surface pH, TAN concentration, and temperature. Due to the expected pH gradient near the manure surface (Feilberg et al., 2015; Hafner et al., 2017, 2013), it is pertinent that surface pH is either measured directly or estimated. ${C_g}^{eq}$ is estimated based on measured or assumed values of these parameters (pH, temperature and [TAN]) for the specific manure. Relative differences in R_C between treatments will indicate differences in emission potential that are not caused by differences in pH, temperature and TAN content, which can normally not be kept constant between treatments. This may enable identification of other effects on emission such as infiltration or the surface area of the manure patches or bands on the soil surface (see below). R_C gives a momentary indication of the actual emission relative to the emission potential.

$$R_C = \frac{C_{g,b}}{C_g^{eq}} = \frac{C_{g,b}}{D_{aw} * [TAN^*]} \qquad \text{Equation 3}$$

Where R_C is the observed NH_3 concentration in the air after manure application relative to equilibrium concentration, $C_{g,b}$ is the measured gas phase (bulk) concentration, ${C_g}^{eq}$ is the theoretical gas phase concentration at equilibrium, TAN^* is the estimated TAN concentration corrected for measured loss of NH_3 in the specific time intervals, and D_{aw} is the equilibrium air-water distribution of TAN (Schwarzenbach et al., 2003):

$$D_{aw} = \frac{[NH_3]_g}{([NH_3]_{aq} + [NH_4^+]_{aq})} = K_{aw}*(1-\alpha) \qquad \text{Equation 4}$$

In equation 4, K_{aw} is the dimensionless air-water distribution of free NH_3, which is calculated from the temperature-specific Henry's law constant ($K_{aw} = K_H/RT$),

and α represents the equilibrium distribution between NH_3 and NH_4^+ at the specific surface pH (Schwarzenbach et al., 2003):

$$\alpha = \frac{1}{1 + 10^{(pH - pK_a)}} \qquad \text{Equation 5}$$

Temperature dependency of R_C is included due to the temperature dependencies of the Henry's law constant and the dissociation constant of NH_4^+ (pK_a in Equation 5). The dependency of R_C on surface pH is included via α. Ideally, a correction should be included for NH_4^+ activity based on ionic strength (Hafner and Bisogni, 2009). Because the ionic strength of the manure (drying over time) is not known, this correction has not been included, but it is assumed that the correction would be similar for the treatments in this study (untreated, digested, separated).

The equilibrium gas phase concentration of NH_3 (${C_g}^{eq}$ in Equation 3) used to calculate R_C represents the potential of the manure to emit NH_3 at the specific temperature, pH, and initial TAN content. Differences in R_C between manure applications occur due to differences in 1) TAN infiltration rate, 2) ESA and 3) liquid-to-air mass transfer coefficient. Due to the low D_{aw} of NH_3 at neutral pH, the resistance to mass transfer of NH_3 is usually considered to be dominated by the air-side resistance (Feilberg and Sommer, 2013). The overall mass transfer coefficient is therefore mainly determined by air-side resistance (Schwarzenbach et al, 2003), which can be assumed to be independent of manure characteristics. It should be noted, however, that at surface pH>8 and if the liquid diffusion pathway exceeds the stagnant air film pathway, there may be some influence of the liquid resistance, which is something that needs further investigation. For interpreting the experimental results presented in this paper, it has been assumed that the mass transfer resistance is dominated by the air-side resistance and that the liquid properties do not affect the resistance significantly. Hence, R_C for different slurries should be close to identical if the TAN content varies only due to emission to air. Observed differences in R_C for different slurries can therefore be ascribed to changes in the amount of liquid TAN available for emission (other than evaporation, i.e. infiltration) or differences in the emitting manure surface area. To summarize, it is hypothesized that a higher R_C of one manure compared to another indicates that TAN has infiltrated to a lesser degree or that the emitting manure surface area is larger.

Since in this study, we have uniquely measured ESA, the surface areas of the slurries can be normalized by dividing R_C with the fraction of ESA to obtain a surface-area-normalized value, $R_{C,ESA}$, to account for differences in emitting manure surface area. Differences in $R_{C,ESA}$ between manure types/applications can then be ascribed solely to differences in TAN infiltration.

2.4 Manure and soil

Untreated and separated manure samples were taken from a commercial organic dairy farm (Otterslätten Lantbruk AB, Sweden). The untreated manure was collected from a small pumping unit situated between the livestock house and a screw press separator (CRI-MAN SM 260/75 FA DM). The screw press separator removed approximately 50% of the dry matter concentration. The liquid fraction was stored in an open storage tank with a naturally formed cover crust, from where the separated manure was collected. The digested manure was collected from a biogas plant in which manure from approximately 20 different farms in the local area (Vårgårda municipality, Sweden) was processed with other substrates. The fraction of cattle manure (conventional and organic) in the substrate mix was 66%. The second largest fraction was conventional pig manure, accounting for 20% of the substrate. The untreated manure was fresh from the livestock house at collection. The digested manure was taken directly from the biogas digester. Both untreated and digested manure was then stored for 3.5 months before the experiments. The separated manure was collected from a tank to which manure had been continuously added for 6 months, and was then subsequently stored for 3.5 months before the experiments.

Manure viscosities were measured with a rotational viscometer (DV-II+P Viscometer, Brookfield) with a LV2 spindle at 12 RPM and a manure temperature of 20±2°C, with and without addition of AY7. Adding AY7 to the manure did not change the viscosities. Particle distribution of the manure was measured in triplicate with laser diffraction (Master sizer 2000, Malvern Instruments Ltd., Worcestershire, United Kingdom). The results are given as percentage of a samples particle volume and can be found in Figure S3.

Surface pH of the manure was measured in the field with a flat surface pH electrode (OrionTM 8135BN ROSSTM, Combination Flat Surface pH Electrode). The electrode was rinsed with deionized water between experiments. Measurements with the flat tip electrode were compared to measurements with a conventional pH electrode in a separate experiment where measurements were taken at different times during drying of cattle manure; for more information see section S4 in the supporting materials. During experiment A, the surface pH was measured nine to ten times during the first four hours after application. During experiment B, the surface pH was measured 16 times, with two measurements the second day after application and one the third day after application.

Manure was applied at an application rate of 35 metric ton ha^{-1}, resulting in 0.7 L of manure applied in three bands in the wind tunnel frames, and 0.35 L manure applied in two bands in the dark chambers. For measurements of manure surface pH, manure bands were applied next to the other plots. Due to periodically light rainfall, the bands were covered with a bent metal sheet that allowed ventilation from the sides when pH was not being measured. All the

Table 1: *Soil and manure properties. Standard deviations are displayed in parentheses (n = 4 for soil analysis and n = 3 for manure analysis).*

Experiment	Soil Type	Dry bulk density [g cm^{-3}]	Water content [g g^{-1}]	1:1 water pH	Manure	Application rate [g NH_4-N m^{-2}]	Dry matter [%]	Total N [g L^{-1}]	Ammoniacal N [g L^{-1}]	Viscosity [cP]
A	Silty clay	1.11 (0.06)	0.21 (0.01)	6.11	Digested	11.6 (0.01)	4.36 (0.03)	4.69 (0.01)	3.30 (<0.01)	64 (15)
					Separated	6.6 (0.2)	4.36 (0.01)	3.20 (0.02)	1.89 (0.06)	125 (14)
					Untreated	6.8 (<0.01)	8.69 (<0.01)	3.75 (0.02)	1.95 (<0.01)	1300 (69)
B	Sandy loam	1.39 (0.09)	0.16 (0.003)	5.95	Digested	11.7 (0.03)	4.66 (0.03)	4.77 (0.04)	3.34 (<0.01)	84 (19)
					Separated	6.7 (0.2)	4.32 (0.04)	3.20 (0.05)	1.92 (0.06)	117 (19)
					Untreated	6.7 (0.11)	8.51 (0.01)	3.55 (0.04)	1.90 (0.03)	1371 (124)

manure was applied manually with a watering can with a hose. The manure was applied at the soil surface.

The experiments were performed on two different fields, both with spring oat stubble with an approximate height of 10 cm and a soil organic matter content of 3.1%. Experiment A was performed on a silty clay (43% clay and 11% sand) with a cereal dominated crop rotation and no manure addition during the past 50 years. Experiment B was performed on a sandy loam (14% clay and 71% sand) with a crop rotation involving both 3-4 year mixed ley as well as cereal crops. For the measurements of ESA, the crop was cut to an approximate height of 5 cm. The total area used for wind tunnels, ESA dark chambers, and surface pH measurements was approximately 20 x 20 meters. It is assumed that differences in soil within this area were insignificant.

Soil and manure data can be found in Table 1.

3 Results

3.1 Ammonia emission

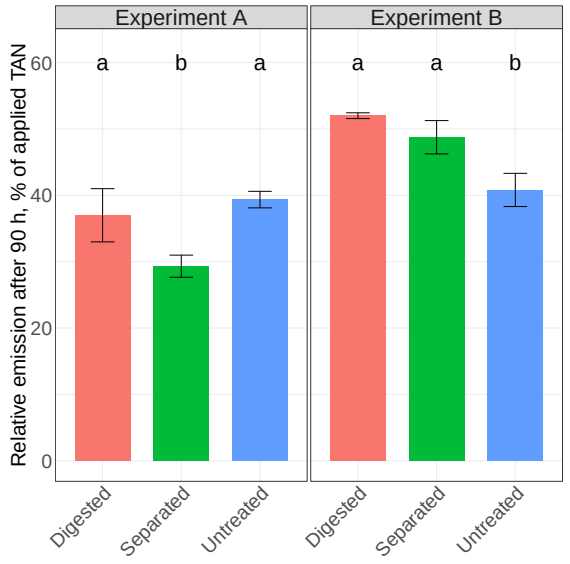

Figure 2: *Cumulative NH_3 emission as a percentage of applied TAN 90 hours after field application of 35 metric ton ha^{-1} digested, separated, and untreated cattle manure to silty clay (A) and sandy loam (B) with winter wheat stubble by trailing hoses (n = 3). Different letters within each experiment indicate that there is a significant difference between the cumulative emission based on Tukey's HSD test.*

Table 2: *Exposed surface area fit parameters and fraction of soil area covered by manure right after (0 h) and 24 h after field application of 35 metric ton ha^{-1} digested, separated, and untreated cattle manure to silty clay (A) and sandy loam (B) with spring oats stubble by trailing hoses (n = 3). a is the total reduction in ESA from the initial area after application until stagnation in ESA, b is a parameter that describes how fast the ESA changes after manure application, and c is the area of manure at the soil surface when ESA stagnates.*

Experiment	Manure	ESA fit parameter			Areas after application	
		a [m^2 m^{-2}]	b [h^{-1}]	c [m^2 m^{-2}]	0 h	24 h
A	Digested	0.12	0.33	0.41	0.53	0.41
	Separated	0.23	0.19	0.31	0.54	0.32
	Untreated	0.04	0.35	0.36	0.40	0.36
B	Digested	0.16	0.54	0.66	0.82	0.66
	Separated	0.26	0.32	0.57	0.83	0.57
	Untreated	0.09	0.51	0.46	0.55	0.46

During experiment A, a significantly (P=0.0067) lower NH_3 emission was found from separated manure compared to digested and untreated manure with relative lower TAN loss of 20±12% and 26±5% respectively (Figure 2). During experiment B, significantly (P<0.0001) higher NH_3 emission was found from separated and digested manure compared to untreated of 21±8% and 28±6% respectively (Figure 2). The NH_3 emission from untreated manure was approximately the same during the two experiments, whereas a higher emission from digested and separated manure was observed during experiment B compared to experiment A.

3.2 Exposed surface area

From the parameters of the ESA fits (Table 2), it can be seen that the untreated manure had a relatively fast but small change in ESA (large b and small a). The digested manure had a relatively fast and large change in ESA (large b and a), whereas the separated had the slowest but biggest change in ESA (smallest b and largest a). The initial ESA from separated and digested manure was larger than untreated in both experiments due to more spreading out on the soil surface compared to untreated manure (Table 2 and Figure 3).

3.3 Manure surface pH

The surface pH of all three manure types increased after application (Figures 4 and S4). For digested and separated cattle manure, pH increased by approximately one pH unit during the first 9 and 21 hours after manure application respectively, before it dropped. For digested manure, pH ended slightly below the starting point after 47 hours, whereas for separated manure pH only dropped slightly from the maximum reading, and after 47 hours pH it was half a unit higher than initially. For untreated manure, surface pH started at 6.7, and con-

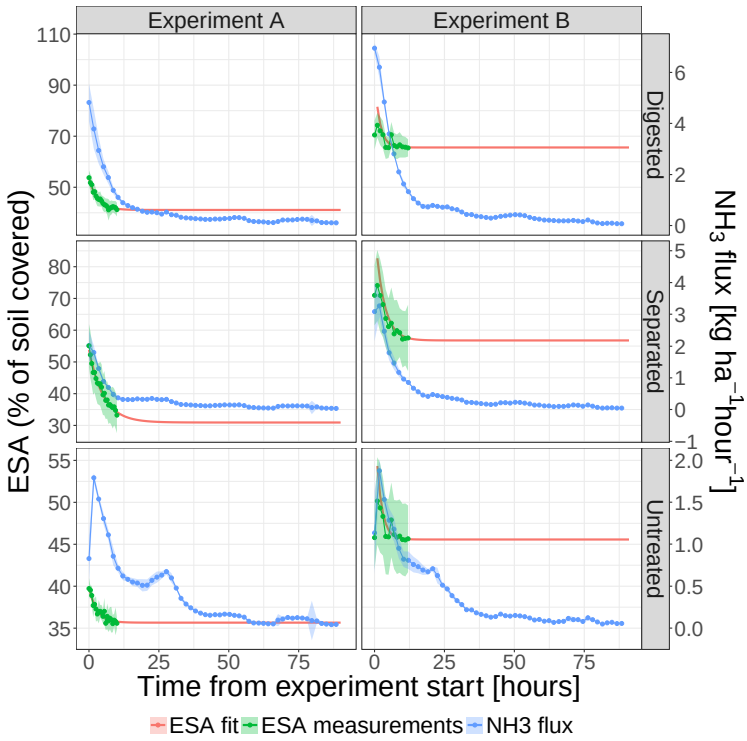

Figure 3: *Ammonia emission rates, ESA raw data, and fitted ESA curves after field application by trailing hoses of 35 metric ton ha^{-1} untreated, separated, and digested cattle manure on silty clay (A) and sandy loam (B) with spring oats stubble. Standard deviations are displayed in bands NH_3 flux and raw data points used for ESA modelling ($n = 3$).*

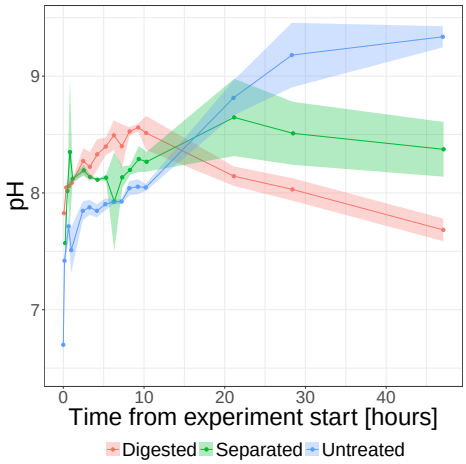

Figure 4: *Manure surface pH after field application by trailing hoses of 35 metric ton* ha^{-1} *untreated, separated, and digested cattle manure on sandy loam (B) with spring oats stubble. Standard deviations are displayed in bands (n = 3). The initial pH at the time of application was 7.82, 7.57, and 6.7 for digested, separated, and untreated manure respectively. pH measurements for experiment A can be found in Figure S2.*

stantly increased during the 47 hours to a final value of 9.3.

4 Discussion

4.1 Effect of infiltration based on normalized ammonia emissions

There was not a clear consistent effect of manure type on the NH_3 emissions, even though both separated and digested manures are expected to infiltrate faster due to the lower dry matter content (de Jonge et al., 2004; Misselbrook et al., 2005b). For digested manure, lower dry matter content is expected to compensate for the higher pH. It is challenging to compare NH_3 emission from different slurries on different soil types as many parameters will have an interactive effect. By calculating R_C it is possible to compare NH_3 emissions regardless of differences in pH, TAN, and temperature. The use of flat surface pH electrodes may not necessarily provide the true surface pH (which is very complicated to measure for manure slurry placed on soil), but the measured values and increases over time seem realistic in comparison to model calculations of surface pH as well as manure surface pH measurements by microelectrodes (Hafner et al., 2017, 2013; Petersen et al., 2014). From plots of R_C as a function of time (Figure 5a), it is seen that the temporal manure profiles are quite similar. If the infiltration rates of separated and digested manure were higher than of untreated manure (as

expected), a higher R_C of untreated manure would be expected because the effect of lower pH of untreated manure has been taken into account in the calculation of R_C. However, ESA is also lower for untreated manure, which needs to be accounted for. By including ESA ($R_{C,ESA}$) it is possible to normalize by the differences in the exposed area and it is indeed observed that $R_{C,ESA}$ is higher for untreated manure (Figure 5b). The differences between the manure types as seen in Figure 5b are interpreted as being due to differences in infiltration.

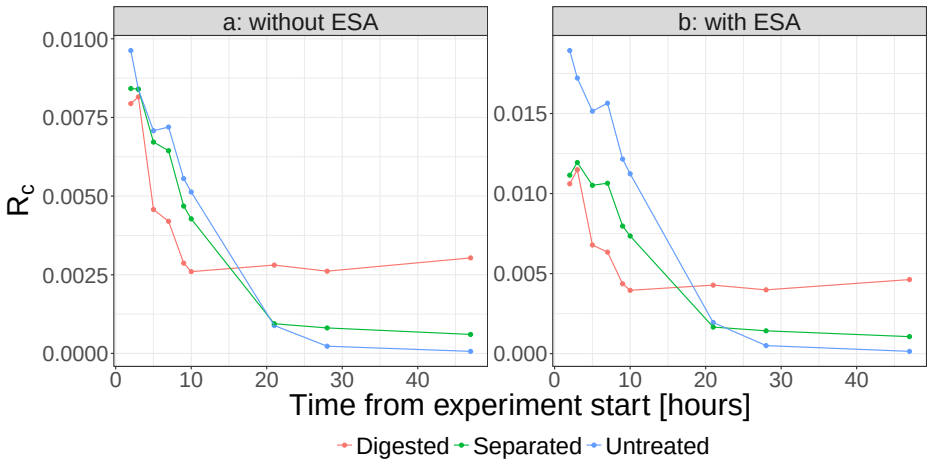

Figure 5a-b: *R_C with and without ESA after field application by trailing hoses of 35 metric ton ha^{-1} untreated, separated, and digested cattle manure on sandy loam with spring oats stubble.*

In comparison to digested manure and separated manure, the band applied untreated manure stays at the soil surface for a longer time, but is less spread out. The higher TAN and pH of the digested manure has been thought not to be of importance due to the lower viscosity (Rubæk et al., 1996; Wulf et al., 2002), presumably leading to faster infiltration. These experiments shows, however, that a large initial ESA will neutralize or even counteract the effect of fast infiltration, as most of the emissions occur during the first couple of hours after application (Figure 3). Therefore, it is important to consider the interaction between the manure and soil, with an increased focus on the very top layer of the soil where the infiltration takes place.

In both experiments, the ESA from untreated cattle manure right after application was 23-34% lower compared to the ESA of separated and digested manure (Table 2 and Figure 3). As the high viscosity, dry matter, and amount of particles and higher fraction of larger particles of the untreated cattle manure allowed for

it to be applied in liquid bands, the band application radically decreased ESA compared to the less viscous digested and separated manures that spread out on the relatively wet soils (Table 1). Hence, the effect of band application as a general strategy for NH_3 emission mitigation might be lower for less viscous manure, as is the case for the digested manure in both experiments, and separated manure during experiment B.

The separated and digested manure had approximately the same dry matter content and viscosity, but digested manure had a higher amount of particles in the range from 250 – 1000 μm. The dry matter and particles in digested and separated manure might have very different characteristics, which can be the cause of different behavior when applied to soil. Even though the ESA of digested manure changed faster compared to untreated and separated manure, the high emissions indicates that even faster changes in ESA is needed in order to compensate for the higher TAN and pH. The time to reach half of the cumulative NH_3 emission was approximately 14 hours for untreated manure, whereas it was between 6 and 7 hours for separated and digested manure in both experiments (Figure 3). This indicates that a thick layer on top of the soil surface results in emissions for a longer period compared to the thin layers of separated and digested manure.

It should be emphasized that the calculation of R_c is based on several simplifications and assumptions and that the approach should be further investigated and verified in future studies aimed specifically at separating effects of pH, TAN, ESA and infiltration. However, for relative comparison of emissions from applied manure types with different characteristics, R_C and $R_{C,ESA}$ are still useful for normalization and interpretation of experimental results that are otherwise difficult to explain.

4.2 Soil and temperature effect on ammonia emissions

The emissions from untreated manure are similar in both experiments, whereas differences can be observed for separated and digested manures. This indicates that the emission from manure with higher ESA right after application is more affected by soil conditions. The higher dry bulk soil density during experiment B might have caused less infiltration and thereby higher potential for NH_3 loss, compared to experiment A. In the first 10 hours after application high NH_3 flux is observed from digested and separated manure in experiment B, corresponding to the higher ESA right after application (Figure 3). ESA of untreated manure is also higher in experiment B compared to experiment A, but the relative difference is lower compared to digested and separated manure.

Another factor that could potentially cause generally higher NH_3 emission during experiment B compared to experiment A is the air temperature right after manure application. During the first two hours of both experiments, the ESA

was largest and 25% of the total NH_3 emission occurred for separated and digested manure in this period. At this time the ambient air temperature was 1.5 to 2°C higher during experiment B than experiment A (Table S1). During the complete measuring period the average temperatures were quite similar for both experiments being 17.1 and 16.4°C for experiment A and B, respectively (Table S1).

4.3 Differences in ammonia emission between manure types

During experiment B, a higher emission was found from digested manure compared to untreated. This is consistent with results from other studies (Amon et al., 2006; Dinuccio et al., 2011; Möller and Stinner, 2009) in which a higher emission is ascribed to higher pH and higher TAN content in the digested manure. In two studies (Amon et al., 2006; Clemens et al., 2006), the reported cumulative emissions are very low with emission ceasing within 48 hours. This is in contrast to other studies, and might be due to the method with a 27 m^2 dynamic chamber not being able to collect all NH_3 emissions, but it is assumed that the relative differences between the manure types are correct. Wulf et al. (2002) did not find any significant difference between NH_3 emission from digested and untreated manure, which corresponds with experiment A. They hypothesize that the lower viscosity of the digested manure gave a faster infiltration, which compensated for the increased emission potential due to higher TAN and pH compared to untreated manure. Our results highlight that in addition to infiltration, the influence of ESA needs to be considered as well. Rubæk et al. (1996) investigated digested and untreated cattle manure applied by trailing hoses on a ryegrass field, and found a significantly lower emission from digested manure during one experiment, and no significant difference during the other. They assigned the lack of difference in NH_3 emission to a high soil-water content in the field resulting in a lower infiltration of both untreated and digested manure. This corresponds with the findings in experiment A, where the high soil-water and high clay content could have lowered the infiltration rate. The results show that differences in emissions from digested manure compared to untreated manure are hard to predict because multiple variables may be important. The higher emissions in experiment B compared to A can be explained by higher ESA and pH right after application, leading to high emissions rates (Figure 3). When comparing untreated and digested manure, it should be emphasized that they do not have the same origin, which to some degree will influence the results.

Significant differences were found between NH_3 emissions from separated and untreated manure in both experiments. In experiment A, a lower emission of separated manure was found, in contrast to experiment B where the emission from separated manure was higher. The lower emissions from separated manure in experiment A is in agreement with literature (Amon et al., 2006; Fangueiro

et al., 2015). The contrasting results from experiment B is best explained by spreading out of the separated manure resulting in higher emission rates compared to experiment A (Table 1 and Figure 3).

4.4 Treatment effect on manure surface pH

Surface pH is influenced by emissions of carbon dioxide and NH_3, related acid-base reactions in manure (Hafner et al., 2013), and interactions between manure solution and soil, with soil pH being much lower than manure pH in both experiments (Table 1). Decreases in pH, as seen for the digested manure, are probably related to buffering by soil. Assuming separated and untreated manure had a similar manure solution composition, the larger increase in pH for untreated manure is likely to be related to less infiltration and less buffering by soil, due to a greater separation of manure and soil resulting from higher dry matter and fiber content. The pH increase for untreated manure (Figure 4) was large compared to other measurements and reaction-transport simulations. Bussink et al. (1994) and Sommer and Olesen (2000) measured manure surface pH after field application and found a maximum increase of ca. 1.5 pH units following manure application, with pH reaching 8.0 – 8.5. Chantigny et al. (2004) measured soil pH at different depths following manure application, and the upper (0 – 5 mm) layer increased to ca. 8.0 – 8.5. Predictions from a reaction-transport model (Hafner et al., 2017, 2013) for a thin layer (10 mm) manure shows that a pH increase from 6.7 to 9.5 is possible. While NH_3 emission generally increases with pH, pH differences alone are not sufficient for predicting differences in emission. For example, NH_3 emission rate was low for untreated manure in the period when pH was >8.5 (>20 h, Figures 3 and 4). Most likely, emission several hours after application is limited by TAN availability, due to depletion of TAN near the exposed surface by volatilization or sorption. Predicting effects of pH and infiltration on emission is therefore complex, but in general differences soon after application will be more important than differences long after application.

5 Conclusions

The results of this study clearly show that multiple factors have to be considered when evaluating whether a manure treatment will result in abatement of NH_3 emission after field application. It should not be assumed that slurries with lower dry matter and viscosity will necessarily have lower NH_3 emission. Furthermore, sandy soil does not always give lower emissions than clay soils, as many other factors need to be considered. The new method for quantification of ESA as a function of time can give new insight into the complex relation between the manure and soil and help explain why some types of manure and application techniques lead to successful abatement under some circumstances, but not under other. Therefore, these measurements, along with measurements of manure

surface pH, should be included in future experiments aimed at comparing abatement methods. Calculations of pH, TAN, temperature, and ESA-normalized NH_3 emission made it possible to identify the effects of infiltration on NH_3 emissions. Finally, it should be noted that further developing the ESA method to include quantification of infiltration rate and information about manure thickness would be very useful in order to assess strategies for abatement of NH_3 emission.

Acknowledgements: The authors would like to thank the technical staff Heidi Grønbæk, Jens Kr Kristensen, Per Wiborg Hansen, and Peter Storegård Nielsen from Aarhus University for their skillful assistance with development of the measuring system, carrying out measurements, and laboratory analysis. Furthermore, the authors would like to thank Mattias Gustafsson, Erik Zakrisson, and Håkan Svantesson from Swedish University of Agriculture for their important help with preparations and setting up the measuring system. The authors would like to express gratitude to Ida Maria Hiitola Pedersen for her invaluable help and expertise with camera techniques.

Funding: This work was funded by the Ministry of Environment and Food of Denmark as a Green Development and Demonstration Program (GUDP) with the project title New application method for slurry in growing crops, and by Region Västra Götaland and Cattle Foundation Skaraborg.

References

Aeby, P., Schultze, U., Braichotte, D., Bundt, M., Moser-Boroumand, F., Wydler, H., Flühler, H., 2001. Fluorescence imaging of tracer distributions in soil profiles. Environ. Sci. Technol. 35, 753–760. https://doi.org/10.1021/es000096x

Aeby, P.G., 1998. Quantitative fluorescence imaging of tracer distribution in soil profiles. Dr. Thesis, Res. Collect. Swiss Federal Insitute of Technology Zürich. https://doi.org/10.3929/ethz-a-010782581

Amon, B., Kryvoruchko, V., Amon, T., Zechmeister-Boltenstern, S., 2006. Methane, nitrous oxide and ammonia emissions during storage and after application of dairy cattle slurry and influence of slurry treatment. Agric. Ecosyst. Environ. 112, 153–162. https://doi.org/10.1016/j.agee.2005.08.030

Aneja, V.P., Schlesinger, W.H., Erisman, J.W., 2009. Effects of agriculture upon the air quality and climate: Research, policy, and regulations. Environ. Sci. Technol. 43, 4234–4240. https://doi.org/10.1021/es8024403

Bell, M.J., Hinton, N.J., Cloy, J.M., Topp, C.F.E., Rees, R.M., Williams, J.R., Misselbrook, T.H., Chadwick, D.R., 2015. How do emission rates and emission factors for nitrous oxide and ammonia vary with manure type and time of application in a Scottish farmland? Geoderma 264, 81–93. https://doi.org/10.1016/j.geoderma.2015.10.007

Bussink, D.W., Huijsmans, J.F., Ketelaars, J.J., 1994. Ammonia volatilization from nitric-acid-treated cattle slurry surface applied to grassland. Netherlands J. Agric. Sci.

Chantigny, M.H., Rochette, P.R., Angers, D.A., Masse, D., Cote, D., 2004. Ammonia volatilization and selected soil characteristics following application of anaerobically digested pig slurry. Soil Sci. Soc. Am. J. 68, 306–312. https://doi.org/10.2136/sssaj2004.3060

Clemens, J., Trimborn, M., Weiland, P., Amon, B., 2006. Mitigation of greenhouse gas emissions by anaerobic digestion of cattle slurry. Agric. Ecosyst. Environ. 112, 171–177. https://doi.org/10.1016/j.agee.2005.08.016

de Jonge, L.W., Sommer, S.G., Jacobsen, O.H., Djurhuus, J., 2004. Infiltration of slurry liquid and ammonia volatilization from pig and cattle slurry applied to harrowed and stubble soils. Soil Sci. 169, 729–736. https://doi.org/10.1097/01.ss.0000146019.31065.ab

Dinuccio, E., Berg, W., Balsari, P., 2011. Effects of mechanical separation on GHG and ammonia emissions from cattle slurry under winter conditions. Anim. Feed Sci. Technol. 166–167, 532–538. https://doi.org/10.1016/j.anifeedsci.2011.04.037

Fangueiro, D., Pereira, J., Bichana, A., Surgy, S., Cabral, F., Coutinho, J., 2015. Effects of cattle-slurry treatment by acidification and separation on nitrogen dynamics and global warming potential after surface application to an acidic soil. J. Environ. Manage. 162, 1–8. https://doi.org/10.1016/j.jenvman.2015.07.032

Feilberg, A., Bildsoe, P., Adamsen, A.P.S., 2015. Ramiran, in: Influence of Surface Processes on Gaseous Emissions from Manure Slurry - Surface Oxidation and PH Gradient. Hamburg, Germany, pp. 334–337.

Feilberg, A., Sommer, S.G., 2013. Ammonia and malodorous gases: Sources and abatement technologies, in: Animal Manure Recycling. John Wiley and Sons, Ltd., pp. 153–176. https://doi.org/10.1002/9781118676677

Hafner, S.D., Bisogni, J.J., 2009. Modeling of ammonia speciation in anaerobic digesters. Water Res. 43, 4105–4114. https://doi.org/10.1016/j.watres.2009.05.044

Hafner, S.D., Montes, F., Alan Rotz, C., 2013. The role of carbon dioxide in emission of ammonia from manure. Atmos. Environ. 66, 63–71.
https://doi.org/10.1016/j.atmosenv.2012.01.026

Hafner, S.D., Pacholski, A., Bittman, S., Burchill, W., Bussink, W., Chantigny, M., Carozzi, M., Génermont, S., Häni, C., Hansen, M.N., Huijsmans, J., Hunt, D., Kupper, T., Lanigan, G., Loubet, B., Misselbrook, T., Meisinger, J.J., Neftel, A., Nyord, T., Pedersen, S. V., Sintermann, J., Thompson, R.B., Vermeulen, B., Vestergaard, A. V., Voylokov, P., Williams, J.R., Sommer, S.G., 2018. The ALFAM2 database on ammonia emission from field-applied manure: Description and illustrative analysis. Agric. For. Meteorol. 258, 66–79.
https://doi.org/10.1016/j.agrformet.2017.11.027

Hafner, S.D., Pacholski, A., Bittman, S., Carozzi, M., Chantigny, M., Génermont, S., Häni, C., Hansen, M.N., Huijsmans, J., Kupper, T., Misselbrook, T., Neftel, A., Nyord, T., Sommer, S.G., 2019. A flexible semi-empirical model for estimating ammonia volatilization from field-applied slurry. Atmos. Environ. 199, 474–484. https://doi.org/S1352231018308069

Hafner, S.D., Sommer, S.G., Petersen, V., Markfoged, R., 2017. Effects of carbon dioxide hydration kinetics and evaporative convection on pH profile development during interfacial mass transfer of ammonia and carbon dioxide. Heat Mass Transf. und Stoffuebertragung 53, 1335–1342. https://doi.org/10.1007/s00231-016-1910-6

Hjorth, M., Christensen, K. V., Christensen, M.L., Sommer, S.G., 2010. Solid-liquid separation of animal slurry in theory and practice, Sustainable Agriculture. https://doi.org/10.1051/agro

Huijsmans, J.F.M., Vermeulen, G.D., Hol, J.M.G., Goedhart, P.W., 2018. A model for estimating seasonal trends of ammonia emission from cattle manure applied to grassland in the Netherlands. Atmos. Environ. 173, 231–238. https://doi.org/10.1016/j.atmosenv.2017.10.050

Martínez-Lagos, J., Salazar, F., Alfaro, M., Misselbrook, T., 2013. Ammonia volatilization following dairy slurry application to a permanent grassland on a volcanic soil. Atmos. Environ. 80, 226–231. https://doi.org/10.1016/j.atmosenv.2013.08.005

Masse, L., Massé, D.I., Beaudette, V., Muir, M., 2005. Size distribution and composition of particles in raw and anaerobically digested swine manure. Trans. Am. Soc. Agric. Eng. 48, 1943–1949. https://doi.org/10.13031/2013.20003

Misselbrook, T.H., Nicholson, F.A., Chambers, B.J., 2005a. Predicting ammonia losses following the application of livestock manure to land. Bioresour. Technol. 96, 159–168. https://doi.org/10.1016/j.biortech.2004.05.004

Misselbrook, T.H., Scholefield, D., Parkinson, R., 2005b. Using time domain reflectometry to characterize cattle and pig slurry infiltration into soil. Soil Use Manag. 21, 167–172. https://doi.org/10.1079/SUM2005316

Möller, K., Stinner, W., 2009. Effects of different manuring systems with and without biogas digestion on soil mineral nitrogen content and on gaseous nitrogen losses (ammonia, nitrous oxides). Eur. J. Agron. 30, 1–16. https://doi.org/10.1016/j.eja.2008.06.003

Nasir, I.M., Mohd Ghazi, T.I., Omar, R., 2012. Anaerobic digestion technology in livestock manure treatment for biogas production: A review. Eng. Life Sci. 12, 258–269. https://doi.org/10.1002/elsc.201100150

Pedersen, J.M., Feilberg, A., Kamp, J.N., Hafner, S., Nyord, T., 2020. Ammonia emission measurement with an online wind tunnel system for evaluation of manure application techniques. Atmos. Environ. 230. https://doi.org/10.1016/j.atmosenv.2020.117562

Petersen, V., Markfoged, R., Hafner, S.D., Sommer, S.G., 2014. A new slurry pH model accounting for effects of ammonia and carbon dioxide volatilization on solution speciation. Nutr. Cycl. Agroecosystems 100, 189–204. https://doi.org/10.1007/s10705-014-9637-6

R Core Team, 2018. R: A language and environment for statistical computing. R foundation for statistical computing, Vienna.

Rochette, P., Guilmette, D., Chantigny, M.H., Angers, D., MacDonald, J.D., Bertrand, N., Parent, L.-É., Côté, D., Gasser, M.O., 2008. Ammonia volatilization following application of pig slurry increases with slurry interception by grass foliage. Can. J. Soil Sci. 88, 585–593.

https://doi.org/10.4141/CJSS07083

Rosenbom, A.E., Ernstsen, V., Flühler, H., Jensen, K.H., Refsgaard, J.C., Wydler, H., 2008. Fluorescence imaging applied to tracer distributions in variably saturated fractured clayey till. J. Environ. Qual. 37, 448. https://doi.org/10.2134/jeq2007.0145

Rubæk, G.H., Henriksen, K., Petersen, J., Rasmussen, B., Sommer, S.G., 1996. Effect of application technique and anaerobic digestion on gaseous nitrogen loss from animal slurry applied to ryegrass. J. Agric. Sci. 126, 481–492.

Sakar, S., Yetilmezsoy, K., Kocak, E., 2009. Anaerobic digestion technology in poultry and livestock waste treatment - A literature review. Waste Manag. Res. 27, 3–18. https://doi.org/10.1177/0734242X07079060

Schwarzenbach, R.P., Sxchwend, P.M., Imboden, D.M., 2003. Environmental organic chemistry, second edi. ed. Wiley-Interscience, John Wiley Sons, Inc. Canada.

Sommer, S.G., Hansen, M.N., Søgaard, H.T., 2004. Infiltration of slurry and ammonia volatilisation. Biosyst. Eng. 88, 359–367. https://doi.org/10.1016/j.biosystemseng.2004.03.008

Sommer, S.G., Hutchings, N.J., 2001. Ammonia emission from field applied manure and its reduction - Invited paper. Eur. J. Agron. 15, 1–15. https://doi.org/10.1016/S1161-0301(01)00112-5

Sommer, S.G., Jacobsen, O.H., 1999. Infiltration of slurry liquid and volatilization of ammonia from surface applied pig slurry as affected by soil water content. J. Agric. Sci. 132, 297–303. https://doi.org/10.1017/S0021859698006261

Sommer, S.G., Olesen, J.E., 2000. Modelling ammonia volatilization from animal slurry applied with trail hoses to cereals. Atmos. Environ. 34, 2361–2372. https://doi.org/10.1016/S1352-2310(99)00442-2

Stadler, D., Stähli, M., Aeby, P., Flühler, H., 2000. Dye tracing and image analysis for quantifying water infiltration into frozen soils. Soil Sci. Soc. Am. J. 64, 505. https://doi.org/10.2136/sssaj2000.642505x

Vanderborght, J., Gahwiller, P., Wydler, H., Schultze, U., Fluhler, H., 2002. Imaging fluorescent dye concentrations on soil surfaces uncertainty of concentration estimates. Soil Sci. Soc. Am. J. 66, 760–773.

Walker, J.T., Robarge, W.P., Shendrikar, A., Kimball, H., 2006. Inorganic PM2.5at a U.S. agricultural site. Environ. Pollut. 139, 258–271. https://doi.org/10.1016/j.envpol.2005.05.019

Webb, J., Pain, B., Bittman, S., Morgan, J., 2010. The impacts of manure application methods on emissions of ammonia, nitrous oxide and on crop response-A review. Agric. Ecosyst. Environ. 137, 39–46. https://doi.org/10.1016/j.agee.2010.01.001

Wulf, S., Maeting, M., Clemens, J., 2002. Application technique and slurry co-fermentation effects on ammonia, nitrous oxide, and methane emissions after spreading. J. Environ. Qual. 31, 1789. https://doi.org/10.2134/jeq2002.1795

Supporting Information

The effect of exposed surface area on ammonia emission from untreated, separated, and digested cattle manure

Johanna Pedersen[a], Karin Andersson[b], Anders Feilberg[a], Sofia Delin[b], Sasha Hafner[c], Tavs Nyord[a]*

[a]Aarhus University, Dept. of Engineering, Denmark
[b]Swedish University of Agricultural Sciences, Sweden
[c]Hafner Consulting LLC, Reston, VA, USA 20191
*Corresponding author email: tavs.nyord@eng.au.dk, Address: Aarhus University, Finlandsgade 12, 8200 Aarhus N, Denmark, +45 20605533

S1 Acid yellow 7 and calibration curve

S1.1 Information about Acid yellow 7

Acid yellow 7 (AY7, $C_{20}H_{15}N_2NaO_5S$, 418 g mol^{-1}, also known as Brilliant Sulfaflavine, Lissamine, Flavine FF, and Brilliant acid yellow 8G) has been used in several studies for quantification of water flows (Aeby et al., 2001; Aeby, 1998; Cai and Stark, 1997; Garcerá et al., 2017; Rosenbom et al., 2008; Stadler et al., 2000; Vanderborght et al., 2002).

AY7 has a low toxicity (Field et al., 1995), a high solubility in water (20 g L^{-1}) (Aeby et al., 2001; Aeby, 1998), low fluorescence quenching by soil constitutes, and the background fluorescence of the soil does not interfere significantly with the dye emissions (Aeby et al., 2001; Aeby, 1998; Smart and Laidlaw, 1977). As the compound is ionic it is only slightly sorbed by clay minerals and dissolved organic matter in soil (Field et al., 1995; Stadler et al., 2000). It has a low pH dependency in the range of 4 to 9 (Smart and Laidlaw, 1977), and is highly temperature independent (Smart and Laidlaw, 1977). It is mobile in a broad range of soils (Finkner and Gilley, 1986; Smart and Laidlaw, 1977; Smettem and Trudgill, 1983; Trudgill, 1987). The excitation wavelength maximum of AY7 is 418 nm and the emission maximum is found at 547 nm (Aeby et al., 2001; Aeby, 1998).

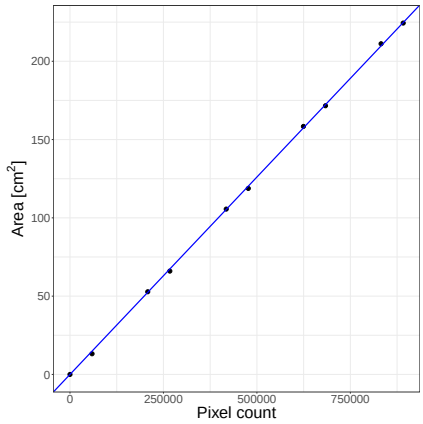

Figure S1: *Fit between measured area and pixel count with ESA method.*

S1.2 Calibration curve

In order to calculate the exposed surface area (ESA) based on the number of pixels with manure, a calibration curve was made. Five round containers, one with a surface area of 13.2 cm^2 and the other four with an area of 52.8 cm^2, were filled with cattle manure treated with 25 mmol L^{-1} of Acid yellow 7 dye. A

picture was taken with the same camera settings as the intensity pictures in the field. The picture was treated with steps a-e (Section 2.2.1 Data treatment) with different masks so that different combinations of the five containers with manure resulted in nine different areas. The known area and count of pixels were plotted against each other and a standard curve and conversion factor (the slope) was calculated (Figure S1).

S2 Manure surface pH

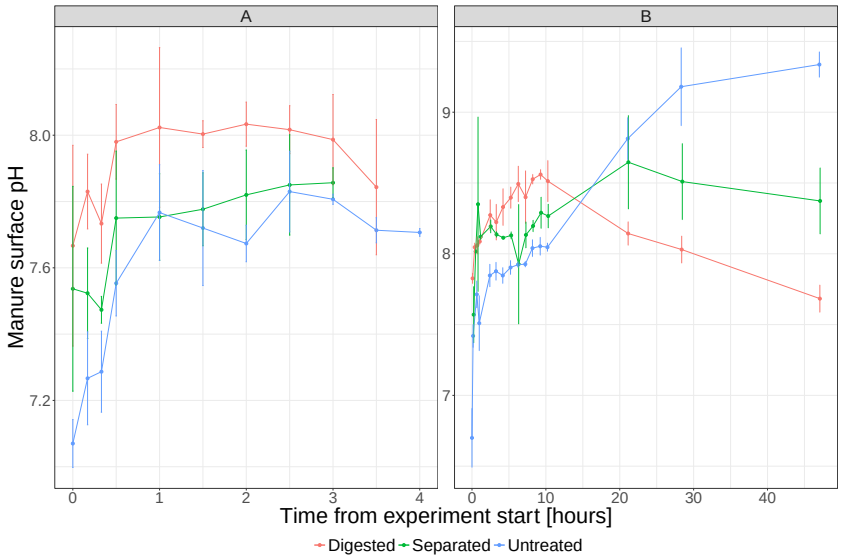

Figure S2: *pH of manure surface after application after field application by trailing hoses of 35 metric ton ha^{-1} untreated, separated, and digested cattle manure on silty clay (A) and sandy loam (B) with winter wheat stubble. Standard deviations are displayed as errorbars (n = 3).*

S3 Particle size distribution

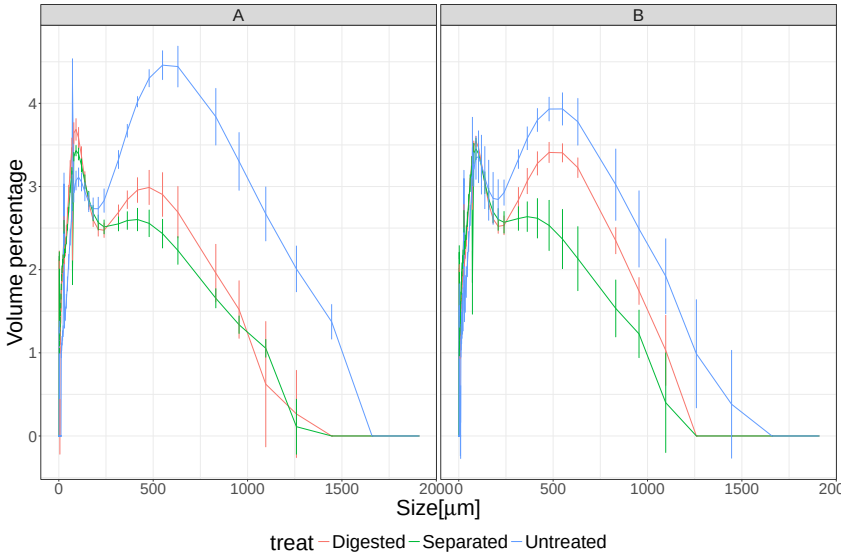

Figure S3: *Particle distribution in the range from 0.1 to 2000 µm of digested, separated, and untreated cattle manure used in experiment A and B. Standard deviations are displayed as errorbars (n = 3).*

S4 Test of flat surface pH electrode

The accuracy of the flat tip electrode (OrionTM 8135BN ROSSTM, Combination Flat Surface pH Electrode) and the effect of dilution on the pH measurements were tested. Untreated cattle manure (not the same manure as the one used for emission and ESA measurements) was poured into aluminum foil containers to a layer of approximately 3-5 mm. The manure was allowed to dry in a laboratory with an approximate temperature of 22°C during the experiment. At different times the pH of the manure was measured with the flat tip electrode in the containers. Three 5 g samples were taken and diluted with 5 mL deionized water, pH was measured in the samples with the flat tip electrode and a normal tip electrode (Portamess™ 911 pH, Knick). The samples were diluted two times more, and pH was measured with both electrodes in both dilutions.

Figure S4 shows the average pH measurement of both electrodes and all dilution steps at different dry matter contents. There is no systematic effect of dilution, and the measurements from the different pH electrodes are in agreement.

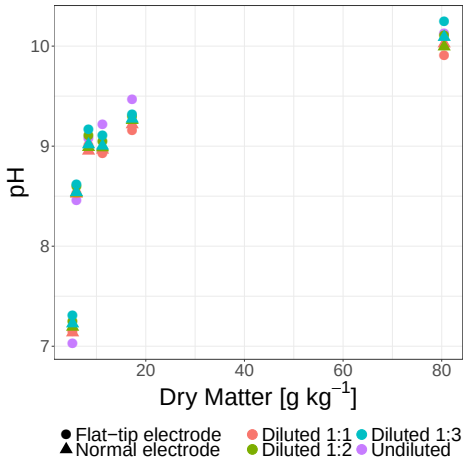

Figure S4: *pH measurements of untreated manure with flat tip electrode and normal electrode in three different dilutions and undiluted (only flat tip) at different dry matter concentrations. Measuring points is an average of three samples.*

S5 Average ambient air temperatures

Table S1: *Average ambient air temperature one, two, three, six, 24 and 90 hours after manure application.*

	Average ambient air temperature [°C]					
Experiment	1 h	2 h	3 h	6 h	24 h	90 h
A	18.6	18.6	18.8	19.0	15.8	17.1
B	21.0	20.8	20.4	19.6	16.0	16.4

References:

Aeby, P., Schultze, U., Braichotte, D., Bundt, M., Moser-Boroumand, F., Wydler, H., Flühler, H., 2001. Fluorescence imaging of tracer distributions in soil profiles. Environ. Sci. Technol. 35, 753–760. https://doi.org/10.1021/es000096x

Aeby, P.G., 1998. Quantitative fluorescence imaging of tracer distribution in soil profiles. Dr. Thesis, Res. Collect. Swiss Federal Insitute of Technology Zürich. https://doi.org/10.3929/ethz-a-010782581

Cai, S.S., Stark, J.D., 1997. Evaluation of five fluorescent dyes and triethyl phosphate as atmospheric tracers of agricultural sprays. J. Environ. Sci. Heal. - Part B Pestic. Food Contam. Agric. Wastes 32, 969–983. https://doi.org/10.1080/03601239709373123

Field, M.S., Wilhelm, R.G., Quinlan, J.F., Aley, T.J., 1995. An Assessment of the Potential Adverse Properties of Fluorescent Tracer Dyes Used for Groundwater Tracing. Open access is tiring out peer 38, 75–96.

Finkner, S.C., Gilley, J.E., 1986. Sediment and Dye Concentration Effects on Fluorescence. Appl. Eng. Agric. 2, 104–107. https://doi.org/10.13031/2013.26721

Garcerá, C., Moltó, E., Chueca, P., 2017. Spray pesticide applications in Mediterranean citrus orchards: Canopy deposition and off-target losses. Sci. Total Environ. 599–600, 1344–1362. https://doi.org/10.1016/j.scitotenv.2017.05.029

Rosenbom, A.E., Ernstsen, V., Flühler, H., Jensen, K.H., Refsgaard, J.C., Wydler, H., 2008. Fluorescence Imaging Applied to Tracer Distributions in Variably Saturated Fractured Clayey Till. J. Environ. Qual. 37, 448. https://doi.org/10.2134/jeq2007.0145

Schwarzenbach, R.P., Sxchwend, P.M., Imboden, D.M., 2003. Environmental organic chemistry, second edi. ed. Wiley-Interscience, John Wiley Sons, Inc. Canada.

Smart, P.L., Laidlaw, I.M.S., 1977. An Evaluation of Some Fluorescent Dyes for Water Tracing. Water Resour. Res. 13, 15–33. https://doi.org/10.1029/WR013i001p00015

Smettem, K.R.J., Trudgill, S.T., 1983. An evaluation of some fluorescent and non-fluorescent dyes in the identification of water transmission routes in soils. J. Soil Sci. 34, 45–56. https://doi.org/10.1111/j.1365-2389.1983.tb00811.x

Stadler, D., Stähli, M., Aeby, P., Flühler, H., 2000. Dye Tracing and Image Analysis for Quantifying Water Infiltration into Frozen Soils. Soil Sci. Soc. Am. J. 64, 505. https://doi.org/10.2136/sssaj2000.642505x

Trudgill, S.T., 1987. Soil water dye tracing, with special reference to the use of rhodamine WT, lissamine FF and amino G acid. Hydrol. Process. 1, 149–170. https://doi.org/10.1002/hyp.3360010204

Vanderborght, J., Gahwiller, P., Wydler, H., Schultze, U., Fluhler, H., 2002. Imaging

Fluorescent Dye Concentrations on Soil Surfaces Uncertainty of Concentration Estimates. Soil Sci. Soc. Am. J. 66, 760–773.

Chapter 6

Paper IV (Draft)

J. Pedersen, T. Nyord, A. Feilberg, R. Labouriau, D. Hunt, S. Bittman. Effect of reduced exposed surface area and enhanced infiltration on ammonia emission from untreated and separated cattle slurry.

Effect of reduced exposed surface area and enhanced infiltration on ammonia emission from untreated and separated cattle slurry

Johanna Pedersen[a]*, Tavs Nyord[a], Anders Feilberg[a], Rodrigo Labouriau[b], Derek Hunt[c], Shabtai Bittman[c]

[a]Aarhus University, Dept. of Engineering, Denmark
[b]Aarhus University, Dept. of Mathematics, Denmark
[c]Agassiz Research and Development Center, BC, Canada

*Corresponding author email: jp@eng.au.dk, Address: Aarhus University, Finlandsgade 10, 8200 Aarhus N, Denmark, +45 93508869

Keywords: Ammonia emission, Application method, Exposed surface area, Slurry surface crust

Abstract

Ammonia (NH_3) loss during field application of liquid manure (slurry) cause loss of nutrients for the crops and contributes to contamination of the environment. The emission can be mitigated by different low emission application technologies and slurry treatment prior to application. Generally, it is assumed that a lower area for air-slurry interaction will lower the emission. The NH_3 emission mitigation potential of the following technologies was investigated for cattle slurry applied on grassland: 1) solid-liquid separation of the slurry, 2) reduced slurry exposed surface area (ESA), and 3) application with a sub-surface-deposition (SSD) slurry application (creating aeration slots). No correlation between ESA and NH_3 emission for untreated cattle slurry was found, but application over aeration slots resulted in a significantly decreased emission. Reduced ESA by band application reduced emission from separated slurry compared to splash-plate applied slurry, but no further reduction was obtained by using the SSD technique. Generally, lower emission was observed from separated slurry compared to untreated for all application methods. This study shows that a reduction in NH_3 emission is not necessarily obtained solely by reducing the ESA. It is hypothesized that rapid crust formation of the untreated slurry in the relative warm conditions mitigated NH_3 emission, thereby counteracting a larger ESA.

1 Introduction

Valuable nutrients in liquid manure (slurry) can be utilized when it is applied as fertilizer for crops. A substantial amount of the inorganic nitrogen available in the

slurry can be lost through ammonia (NH_3) emissions. These must be mitigated, to ensure maximum use of the nutrients in the slurry, and reduce contamination of the environment (Aneja et al., 2009; Sommer et al., 2003).

Extensive research has shown that application techniques reducing the contact area between the applied slurry and the atmosphere, as well as methods than enhance slurry infiltration into the soil, reduce the NH_3 emission (Sommer and Hutchings, 2001; Webb et al., 2010). When slurry is applied in fields, the ammoniacal nitrogen (TAN) is hypothesized to be divided into a fast and slow pool (Hafner et al., 2019). Total ammoniacal nitrogen from the fast pool is exposed to the atmosphere, and will thereby be available for emission. The slow pool represents TAN that has a lower exposure to the atmosphere as a result of incorporation, infiltration into the soil, distance from the exposed surface or crust formation (Chantigny et al., 2004; Rodhe et al., 2004; Sommer et al., 2004, 2003; Webb et al., 2013). It is the slow pool that can be protected by infiltration and incorporation which may be too slow for the fast pool.

Several studies have found that the dry matter (DM) of the slurry is one of the most important parameters affecting NH_3 emission after field application of slurry. A lower DM content of the slurry has been found to yield lower NH_3 emission (de Jonge et al., 2004; Häni et al., 2016; Misselbrook et al., 2005; Smith et al., 2000; Sommer and Olesen, 1991). This effect is assigned to higher infiltration of the slurry and thereby shorter time the slurry is exposed to the atmosphere provided the soil is not saturated and is reasonably porous.

Solid-liquid separation of slurry can be used as a strategy to lower the DM content, and has been observed to reduce the NH_3 emission from field-application of the liquid fraction (Hjorth et al., 2010; Webb et al., 2013). It can be achieved by mechanically removing solids from the slurry or by letting the solids settle in a tank and subsequently taking the liquid fraction from the top. Both methods gives a thick solid-rich- and a thin liquid fraction, the former having a higher P:N ratio than the latter. Separation often gives a higher nutrient utilization of field applied slurry and a higher flexibility in slurry management and storage capacity (Hjorth et al., 2010).

Efficient NH_3 emission reduction can be achieved by rapid and complete incorporation of the slurry into the soil (Hansen et al., 2003; Holly et al., 2017). Hansen et al. (2003) found that the reduction correlated with the injection depth and volume of injection furrows (slots) when cattle slurry was applied on grassland. The higher reductions also correlated with higher energy demands making the application much more expensive compared to splash-plate application. Furthermore, the higher energy demand increase the carbon dioxide emission during application (Hansen et al., 2003; Huijsmans et al., 2004). Injection has also been found to reduce yields on grass fields (Rees et al., 1993; Rodhe and Halling, 2015), therefore other strategies for abatement that also increase yield are needed.

To reduce NH_3 emission without disturbing the soil or existing vegetation, slurry application techniques that reduce the contact area between slurry and atmosphere can be used. Slurry application in bands by trailing hoses or trailing shoes reduce the exposed surface area compared to broadcasting with a splash-plate or similar applicators. Band application of cattle slurry on grass fields has been found to give an average reduction in NH_3 emission of 26-51% compared to splash-plate application from studies with a broad variety of slurry and soil parameters and crop canopy (Bittman et al., 2005; Häni et al., 2016; Misselbrook et al., 2002; Smith et al., 2000). Even though banding on average reduce the NH_3 emission, the technique has under some conditions been found not to reduce the emission (Bhandral et al., 2009; Bittman et al., 2005; Häni et al., 2016), such as on saturated soils or where there is rapid drying and where there is limited canopy to intercept the slurry before it contacts the soil.

Sub-surface deposition (SSD) slurry application applying slurry over aeration slots made by rolling tines, has been proposed as a NH_3 mitigation strategy (Bittman et al., 2005; Chen et al., 2001) as it assists infiltration (Ai et al., 2012) and consequently is expected to lower the emission. The application technique has been tested in two studies (Bhandral et al., 2009; Bittman et al., 2005), where it showed great promise as a low emission application technique. The aim of this study was to further investigate the potential of SSD, both alone and in combination with separation of the slurry, and to determine if the potentially reduced emission can be explained by differences in exposed surface area (ESA) of the slurry after application.

The objectives of this study were to (i) asses the effect of ESA of slurry on NH_3 emission, and investigate if it can be used as a predictor for emission from cattle slurry applied at high ambient air temperatures, (ii) evaluate solid-liquid separation, SSD and the combined effect of these as mitigation strategies for NH_3 emission.

2 Materials and methods

Four experiments were conducted to investigate the relationship between the ESA of slurries and NH_3 emission, and the efficiency of two reduction techniques: mechanical aeration and solids removal by settling and decantation of the slurry as well as the combination of these measures.

Each experiment (A, B, C, and D) had four treatments. One treatment (band applied untreated slurry, U-band) was present in all experiments. For an overview of the treatments in the different experiments, see Table 1.

Ammonia emission was measured with 16 wind tunnels (4 treatments x 4 replicates). The ESA was measured with 12 dark chambers (4 treatments x 3 replicates) using a new technique, based on imaging, for detecting the area of slurry on the soil surface using slurry doped with a fluorescence dye. The

Table 1: *Overview of experiments and treatments. U: untreated, S: separated, splash: splash-plate, line: 20 cm wide line, band: narrow bands, SSD: band applied over sub-surface deposition aeration slots.*

Experiment	Treatments
A & C	U-band, U-line, U-splash, S-splash
B & D	U-band, U-SSD, S-band, S-SSD

NH_3 measurements spanned approximately 94 hours when most of the emissions took place and the ESA measurements spanned over 8 hours since no additional changes were observed.

2.1 Site

The experiments were performed at the Agassiz Research and Development Centre, Agriculture and AgriFood Canada, in south coastal British Columbia, Canada (49°24′ N, 121°76′ W) from May to July 2019. The soil was a silty loam with a 10 year old stand of Kentucky bluegrass and white clover. Care was taken to locate the wind tunnels and dark chambers on areas in the field with uniform soil and crop. The plots in each trial were kept as close as possible to minimize soil and crop variation. The grass was trimmed in the experimental area the day before each experiment. For experiment A and C a block design was used for the tunnels. For experiment B and D a block design was not possible due to practicalities regarding the mechanical aeration. After plots were chosen for aeration and no aeration the treatments where distributed with as much variance as possible. The layout of the wind tunnels and dark chambers for all four experiments can be seen in Supplementary materials, Figure S1.

2.2 Slurry and slurry application

The slurry was collected in late fall from a slurry tank on a typical British Colombian commercial high producing dairy farm using saw-dust bedding. The slurry was stored for three months in two in-ground 2.5 m deep concrete storage cylinders. The tanks were uncovered but had a roof to keep out rainwater, which is typical of many farms in the area. The raw slurry was thoroughly mixed before pumping for use in each experiment (hereafter called untreated). The separated slurry (hereafter called separated) was decanted from the top one-third of the second tank located next to the first. The untreated and separated slurries were analyzed for TAN by steam distillation (KjeltecTM 2400, Foss, Hillerød, Denmark) followed by titration (Rutherford et al., 2008) and for total N by Kjeldahl method (Rutherford et al., 2008). Dry matter was determined after oven drying at 105°C for 24 h (American Public Health Association, 1999). Slurry properties and application rates for each experiment can be found in Table 2.

Table 2: *Slurry properties. Standard deviations are displayed in parenthesis (n = 2).*

Experiment	Slurry	Application rate [g NH_4-N m^{-2}]	DM [%]	Total N [g kg^{-1}]	TAN [g kg^{-1}]	pH
A	Untreated	10.52 (0.59)	7.5	2.90 (0.08)	1.75 (0.10)	6.8
B		10.76 (0.09)	7.9	3.03 (0.03)	1.79 (0.01)	6.8
C		10.86 (0.03)	7.2	3.04 (0.01)	1.81 (<0.01)	7.0
D		10.62 (0.16)	6.7	3.07 (0.03)	1.77 (0.03)	7.5
A	Separated	7.48 (0.144)	4.4	2.22 (0.01)	1.25 (0.02)	6.9
B		4.61 (0.00)	1.8	1.23 (0.01)	0.77 (<0.01)	7.2
C		4.76 (0.12)	1.5	1.21 (0.02)	0.79 (0.02)	7.2
D		4.48 (0.05)	1.5	1.15 (0.07)	0.75 (0.01)	7.6

For application with a rolling tine the AerWay^{TM} SSD^{TM} slurry applicator (Holland Canada, Norwich, ON) was used to make the intermittent vertical injection pockets (Bittman et al., 2005). The distance between the rows of rolling tines was 20 cm and the distance between the centers of the aeration slots in a row was 40 cm. The average width and depth of each aeration slot was 15.1±2.3 cm and 12.3±1.4 cm, respectively. The SSD was passed over the appropriate field plots before the wind tunnel frames were inserted. The frames were positioned so that each frame had two rows of five aeration slots along the length of the frame, giving 10 slots per m^2. The imaging chambers had an experimental area of 0.14 cm^2, and were positioned so that each chamber encompassed two complete aeration slots.

A slurry application rate of 6 kg m^{-2} was used for all treatments, resulting in 6 L per tunnel and 0.87 L per dark chamber. As it was the goal to investigate the effect of ESA, the same volume of untreated and separated slurry were applied. All the slurry was applied by hand with a watering can. In quick succession, the slurry was applied, tunnel covers were placed over the frames and measurements begun so that less than 10 minutes lapsed between slurry spreading and the start of NH_3 collection. To simulate broadcasting with a splash-plate, a wooden plate (15 x 10 cm) was attached at the nozzle of the watering can.

For slurry spread in the dark chambers Acid Yellow 7 (AY7, Brilliant Sulfaflavine, 404.37 M, 100± 3%, MP Biomedics, USA) was added. The dye was first diluted into 1 L sample of the slurry, which was then mixed thoroughly with the rest of the slurry giving a final concentration of 25 mmol AY7 L^{-1}.

For all experiments, slurry was applied in the morning beginning at 9AM starting with the dark chambers followed by the tunnels. All treatments were completed before 11AM.

2.3 Conditions during the trial

At the beginning of each experiment three soil cores of 495 cm^3 were taken across the experimental site to gravimetrically determine the soil-water content and dry

bulk density to a depth of 6.5 cm. An additional sample was taken for soil pH. The dry bulk density over the four trials was 1.08 (0.02) g cm^{-3} (n = 12) and the soil pH (1:1 water pH) was 5.3 (0.2) (n = 4). Sorptivity and water infiltration at steady state was measured with a Cornell Sprinkle Infiltrometer (Cornell University, Department of Crop and Soil Sciences, NY, USA) (van Es and Schindelbeck, 2006). Soil properties can be found in Supplementary materials Table S1.

Ambient air temperature and relative humidity was logged by a weather station located next to the field each hour. Soil temperature was measured at 5 cm depth. Due to an error soil data was not logged for experiment A. Average temperature data for each shift and the total period can be found in Supplementary materials Table S2.

2.4 Exposed surface area

Exposed surface area of the slurry for several hours after application was quantified with a method developed by Pedersen et al. (n.d.). The method quantifies the slurry area by the light emitted from a fluorescent compound (AY7) added to the slurry immediately prior to application.

In order to exclude extraneous light, cylinders with a diameter of 56 cm and a height of 80 cm (barrels with bottoms cut out) were used as dark chambers. A round plywood sheet (68 cm diameter) with a square opening (37 x 37 cm) was sealed to the bottom of the barrels so that no light could enter form the sides. All interior surfaces were painted with a black matte paint. Immediately after the slurry containing the dye was applied on the soil, the dark chambers were positioned. The procedure was carried out within a few moments to avoid photodecomposition of the dye molecules. To take images of the fluorescing slurry a camera with a long pass filter and UV light source was mounted to the top of the chamber. Pictures were taken of the slurry covering at 0, 2, 4, 6, and 8 h after slurry application to detect changes in ESA. In addition a reference photo of a pink florescence cardboard (Tutein & Koch ApS, Denmark) was taken to correct for light intensity differences in the pictures (Aeby et al., 2001; Rosenbom et al., 2008).

To test for photodecomposition of the dye during the experiments, black beakers (1.3 cm in diameter) with the dyed slurry were positioned in the chamber prior to photographing.

The pictures were first corrected for non-uniform lighting using the reference photo (Aeby et al., 2001; Rosenbom et al., 2008). A mask was then applied around the slurry to avoid influence from the crops. The color images were converted to a greyscale and a threshold of 0.7 was used to convert the greyscale pictures to two tone black and white pictures. The number of white pixels (pixels with slurry) was counted. For each dark chamber the white pixel values were fitted to

an exponential model (Equation 1).

$$ESA = a*e^{-b*t}+c \qquad \text{Equation 1}$$

ESA is the fraction of soil area covered by slurry (m^2 m^{-2}), a (m^2 m^{-2}) is the total reduction in ESA from the initial area after application until stagnation in ESA, b (h^{-1}) is a parameter that describes how fast the ESA changes after slurry application, t is time (h), and c is the area of slurry at the soil surface at $t = \infty$ (m^2 m^{-2}). Fitting was done using nonlinear regression (nls()) function in R (version 3.4) (R Core Team, 2018).

For the standardization beakers, the area detected with the imaging method was compared with the area of the beaker (data not shown).

The grass crop lid up to some extent in the ESA pictures. Even though only the area with slurry was used for calculations of ESA, it was impossible exclude all of the fluorescent grass in the pictures; hence the slurry area was slightly overestimated for all treatments and times. As the grass canopy structure was uneven, any slurry adhering to the sides of vertically oriented grass was not be seen from above. This could lead to a small underestimation of ESA. While it was not possible to quantify these sources of error, it was assumed that they tended to balance out.

2.5 Ammonia emission

2.5.1 Wind tunnels

The wind tunnels used to measure NH_3 volatilization were based on the design of Lockyer et al. (1984). For a detailed description of the tunnels, see Bhandral et al. (2009). Each tunnels consisted of a 2 x 0.5 m meter frame, which was inserted the soil to a depth of about 5 cm prior to the experiment. A flexible polycarbonate sheet was attached to the side of a frame to form a tunnel with a semi-circular cross section with a height of 0.45 m. A blower was attached to the outlet end of the tunnel while the inlet side remained open. Air was drawn through the tunnel into a round orifice (0.15 m in diameter) situated at the center of a concave funnel. The air flow through the tunnel was measured with a rotating anemometer and the data was collected continuously with a datalogger (CR10 data logger, Campbell Scientific Inc., Logan, UT). Air flow was also measured periodically in the tunnel with a portable hot wire anemometer to ensure consistency over time.

Air samples from both the inlet and the outlet of the tunnels were drawn continuously throughout the trials through PTFE coated tubing into an impinger assembly. The volume of air collected in each impinger stream between shift changes was quantified with a volumetric gas meter (Gallus 2000, Norgas Controls, Inc., Burlington, KY) which were tested before and after the trials. The sample air stream was bubbled through solutions of phosphoric acid (0.01 mol

L^{-1}) to trap the NH_3. For the tunnel outlet air samples, two 100-mL bubbler units was arranged in series in order to ensure that all NH_3 was trapped although very little NH_3 was found in the second cylinder. A single cylinder was used for inlet air. The acid solutions were changed first at two and four hours after slurry application, and thereafter each morning and afternoon until a total of nine shifts had been measured. The data from the flowmeters was recorded at the end of each shift. After collection, the acid samples were sealed and stored for a few days at 5°C. Before analysis, the volumes were increased to exactly 150 mL with distilled water. The 150-mL samples were frozen and later analyzed with a spectrophotometer based autoanalyser (ADVIA 1800, Siemens, Germany).

Ammonia emissions were calculated from the difference of outlet and inlet concentrations, the air flow through the tunnel and the flow rate of the sample air (Bhandral et al., 2009).

2.5.2 Statistical analysis

A generalized linear mixed model (GLMM) defined with the Gamma distribution was used to describe and compare the emission of the treatments together. The GLMM used was defined with the logarithm link function and contained two independent Gaussian random components, representing the experiment and the tunnel nested in each experiment, respectively, in this way taking into consideration the dependence between observations induced by the experimental design. The GLMM was adjusted using the package "lmer4" of the software R (R Core Team, 2018) and the post-hoc analyses were performed using the package "postHoc" (Labouriau, 2020) adjusting the p-values for multiple comparisons using the method of controlled false discovery rates (Benjamini and Yekutieli, 2001).

3 Results

3.1 Ammonia emission

The emission is highest in the beginning right after slurry application in all four experiments for all treatments (Figure 1). The flux quickly decreases, and after 25 hours, only minor fluxes are measured. The cumulative emission ranged from 7.8% (4.55-13.21) to 35% (20.36-59.02) (Figure 2 and Table S3) of applied TAN, with the highest emissions being observed from U-line and the lowest from S-SSD. No significant differences were observed between U-splash, U-line, U-band, and S-splash, but U-SSD had a lower cumulative emission than U-line and U-band. Emission from S-splash were significantly higher than S-band and S-SSD (Figure 2 and Table S3).

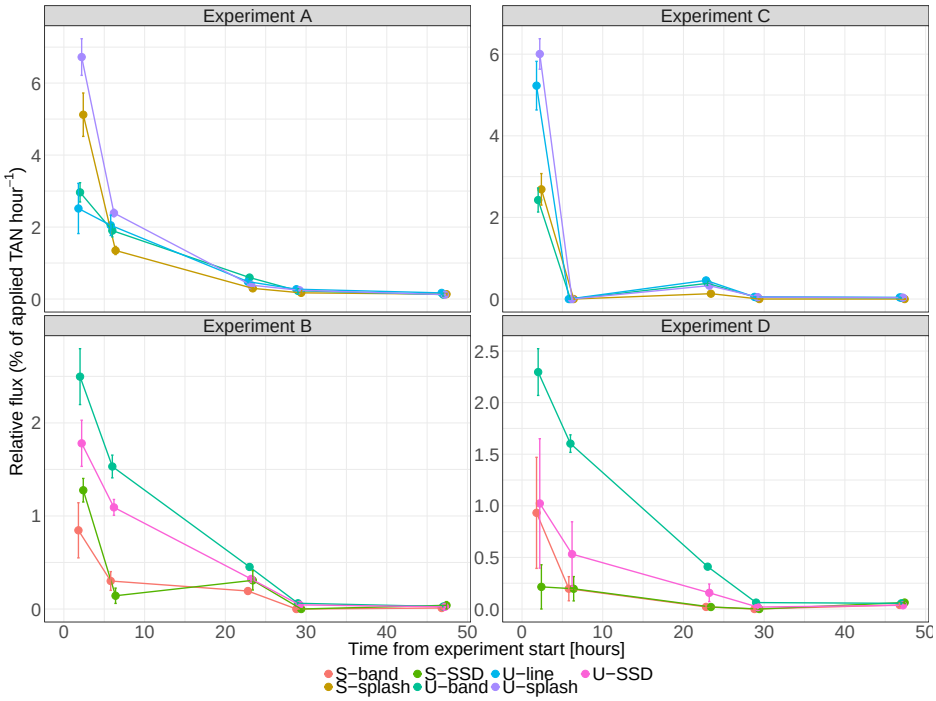

Figure 1: *Ammonia flux after application of 60 metric ton ha^{-1} untreated and separated cattle slurry to bluegrass and white clover with different application techniques. U: untreated, S: separated, splash: splash-plate, line: 20 cm wide line, band: narrow bands, SSD: band applied over subsurface deposition aeration slots. Standard errors are displayed as vertical error bars (n = 4). Flux for 48 hours shown, for full measuring period see Figure S2 in supplementary materials.*

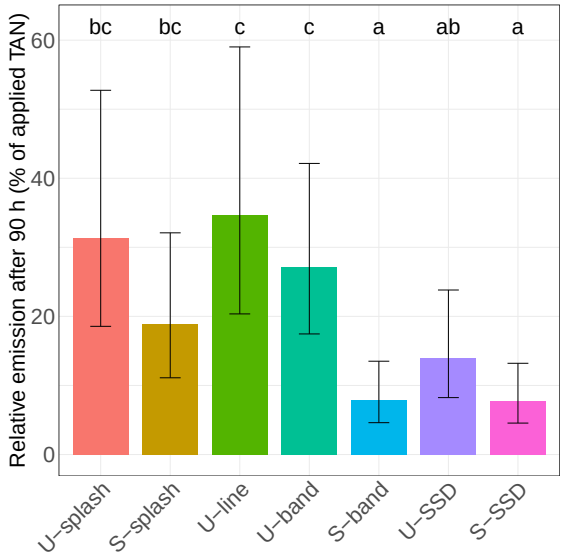

Figure 2: *Calculated cumulative NH_3 emission after application of 60 metric ton ha^{-1} untreated and separated cattle slurry to bluegrass and white clover with different application techniques. U: untreated, S: separated, splash: splash-plate, line: 20 cm wide line, band: narrow bands, SSD: band applied over subsurface deposition aeration slots. Confidence intervals with 95% coverage are displayed as error bars; pairs of emissions containing a common letter in their labels do not statistically differ at a 5% significance level. The means and confidence intervals can be found in Table S3 in supplementary materials.*

3.2 Exposed surface area

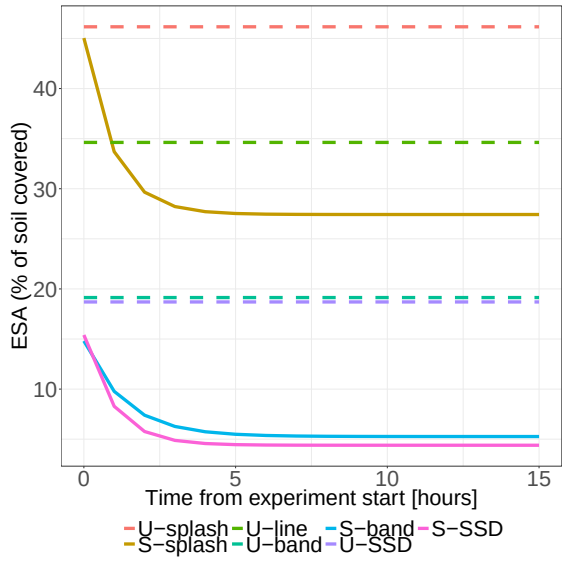

Figure 3: *Exposed surface area after field application of 60 metric ton ha^{-1} separated and untreated cattle slurry to bluegrass and white clover with different application techniques. U: untreated, S: separated, splash: splash-plate, line: 20 cm wide line, band: narrow bands, SSD: band applied over subsurface deposition aeration slots. Area for untreated slurry estimated to be unchanged over time.*

A large decrease (23-81%, average 42±14%) in ESA of untreated slurry was measured during all four experiments (data not shown). This decrease is extremely high compared to previous observations by Pedersen et al. (2020), of 10% and 16%, for untreated cattle slurry. The raw pictures showed that the dry slurry in this study did not show enough fluorescence for detection. Using more dye may have produced better results as in the previous study. The assumption that the decrease in area observed for untreated slurry was incorrect is supported by the reference sample. For separated slurry, the measured areas were above 95% of the true area of the reference sample, whereas the area calculated for the untreated slurry decreased very fast after application, and in some cases dropped below 10%. Therefore, only the ESA pictures right after application were used for untreated cattle slurry. Based on previous studies, the maximum change in the ESA would be in the range of 10-16% (Pedersen et al., n.d.).

The change in ESA from separated slurry showed a very similar pattern for all application techniques. The rate of change (b) was approximately the same

Table 3: *Exposed surface area fit parameters after field application of 60 metric ton ha^{-1} separated and untreated cattle slurry to bluegrass and white clover with different application techniques. a is the total reduction in ESA from the initial area after application until stagnation in ESA, b is a parameter that describes how fast the ESA changes after slurry application, and c is the area of slurry at the soil surface at $t = \infty$. As ESA was assumed to be constant for untreated slurry ($ESA_{t=0} = ESA_{t=\infty} = c$) only c is provided. U: untreated, S: separated, splash: splash-plate, line: 20 cm wide line, band: narrow bands, SSD: band applied over subsurface deposition aeration slots.*

	Parameters from ESA fit		
Treatment	a [m^2 m^{-2}]	b [m^2 m^{-2}]	c [m^2 m^{-2}]
S-splash	0.18	1.03	0.27
S-SSD	0.11	1.04	0.04
S-band	0.10	0.75	0.05
U-splash			0.46
U-line			0.35
U-band			0.19
U-SSD			0.19

(0.75 – 1.03 h^{-1}, Table 3). The change in area over time (a) and finial area (c) were almost identical for S-SSD and S-band, whereas the change over time for S-splash was twice as big compared to S-SSD and S-band, but the final area was almost six times as high (Figure 3 and Table 3).

4 Discussion

4.1 Ammonia emission

The flux pattern with high initial emission and a fast decrease (Figure 1) is in agreement with other studies (Bhandral et al., 2009; Misselbrook et al., 2002; Smith et al., 2000). The cumulative emission reported from field application of cattle slurry with characteristics similar to the untreated and separated slurry used in this study, varies from 10% to 150% of applied TAN after application with splash-plate, trailing hoses or band application over aeration slots (Hafner et al., 2018). This variation is caused by the many factors affecting the emission. The focus in the discussion will therefore be on the relative differences observed in the present study and the comparison with relative differences observed by others.

4.2 Effect of exposed surface area

No significant differences in NH_3 emission were observed for U-splash, U-line and U-band (Figure 2) despite of the big differences in initial ESA, which ranged from 19% for U-band to 46% for U-splash (Figure 3 and Table 3). This is in contrast to the general assumption that a lower area of slurry-air interaction will lower the emission (Sommer and Hutchings, 2001; Webb et al., 2010). It is only in the

first measurement, that the flux is higher from U-splash compared to U-line and U-band (Figure 1). Similar results were obtained by Smith et al. (2000), who found a general reduction by band-applied slurry compared to splash-plate, but in the one experiment (out of 16) that had a slurry DM similar to the one in the present study, they did not observe any difference between the two application methods. In their experiments with slurries with lower DM, a lower emission was observed from band-applied slurry compared to splash-plate. Misselbrook et al. (2002) also found that band application of cattle slurry on grass reduced NH_3 emissions compared to splash-plate, but the DM of the slurry in these experiments was approximately half of the DM content of the untreated slurry in the present study. Furthermore, the ambient air temperature was lower. It is speculated, that the lack of differences in emission between U-splash, U-line and U-band in the present study is caused by fast drying out of the slurry creating a surface crust, which has been hypothesized to reduce emission by Misselbrook et al. (2005). As the splash-plate applied slurry will be applied in a thin layer, it will dry fast at temperatures around 20°C (Table S2), whereas the lower temperatures in Misselbrook et al. (2002) and lower DM in Smith et al. (2000) might have delayed drying or prevented crust formation of the splash-plate applied slurry, allowing for high emission for a longer period.

Another study by Bittman et al. (2005) with similar temperatures, DM content of slurry and application rate obtained a 40% emission reduction after surface banding of untreated slurry compared to splash-plate applied slurry, and assigned this to a lower observed ESA. The slurry used in the study by Bittman et al. (2005) had a pH that was 0.5 higher on average than the slurry used in the present study and the grass canopy was thinner (Bittman, unpublished). If everything else is equal, an increase in pH of 0.5 will approximately give a threefold increase in emission. As the flux is generally highest immediately after application, the higher pH might have given higher emission in this period, which in turn gave higher differences between splash-plate and band applied slurry.

For separated slurry the emission from S-band was significantly lower than S-splash (Figure 2). This corresponds with findings by Bell et al. (2015) who found a 40% reduction after band application of cattle slurry with comparable DM content as the separated slurry in the present study, compared to splash-plate applied slurry. The emission from S-band were very low, and can most likely be assigned to a combination of low final ESA of only 5% (Figure 3 and Table 3) and a presumably fast infiltration into the dry soil with relatively low bulk density (Table S1) due to the low DM content of the slurry.

Reducing the area has been hypothesized to lower emission, but these results show that under warm conditions and with high DM slurries, the effect of rapid drying and crust formation might have more influence on emission mitigation than reduced areas. Comparing these results with other studies highlights the

importance of taking DM of the slurry, temperature, pH and crop canopy into consideration, as other studies have shown great emission reductions with band application compared to splash-plate application under other experimental conditions and slurry characteristics (Bittman et al., 2005; Misselbrook et al., 2002; Smith et al., 2000).

4.3 Effect of slurry type

Comparing the emission from separated and untreated slurry (splash, band and SSD), separated slurry resulted in lower emission in all three cases (Figure 2), but the difference was only significant between U-band and S-band. This result is consistent with a study by Amon et al. (2006), who found a big reduction in NH_3 emission after band application of separated slurry compared to untreated. No significant differences were observed between emission from S-SSD and U-SSD (Figure 2). The SSD did not lower the emission from separated slurry, whereas it lowered the emission from untreated, resulting in emission closer to separated slurry. This is in contrast to results from Bhandral et al. (2009) who observed higher emissions from S-SSD compared to U-SSD. The soil-water content and application rate of slurry in the study by Bhandral et al. (2009) were higher than the present study. Higher soil-water content has been identified to lower infiltration (Sommer et al., 1997; Sommer and Jacobsen, 1999), which consequently will increase the emission (de Jonge et al., 2004). In the present study not all slurry could be contained in the aeration slots, hence higher application rates and shallower injection slots would cause lager amounts of slurry at the soil surface. These things combined might have caused the differences in emission reduction by the SSD.

The emission from S-splash is lower than from U-splash, but the difference is not significant (Figure 2). The initial ESA is approximately the same for the two slurries (46% for U-splash and 47% for S-splash) (Figure 3 and Table 3), but ESA of S-splash quickly decreases to 27%, which is assumed to be caused by infiltration that is expected to lower emission. In the study by Bhandral et al. (2009) S-splash and U-splash was also compared. They found that the emission from S-splash was higher than U-splash and assigned this to a rapid crust formation of the untreated slurry. This has been discussed in the preceding section as an explanatory factor for the relatively low emissions from U-splash in the present study.

Several studies have assigned DM content as an important factor in relation to NH_3 emission (de Jonge et al., 2004; Häni et al., 2016; Sommer et al., 2003; Sommer and Olesen, 1991). The explanation is commonly that a higher DM content reduces infiltration and thereby increase emission. The results in the present study supports the hypothesis made by Bhandral et al. (2009) and Misselbrook et al. (2005) that surface crusting might have an important influence

on emission. Higher DM could potentially under warm conditions result in lower emission if a crust is formed relatively rapidly. More research linking the interaction between crust formation, DM content, and temperature to NH_3 emission is needed in order to make further conclusions on the significance. In order to do this, a method for measuring the rate of crust formation and the crust thickness after field application of slurry should be developed.

4.4 Effect of sub-surface deposition slurry applicator

The SSD did not reduce emission from separated slurry (Figure 2). As the separated slurry had a low DM ESA quickly decreases from 15% to 4% for S-SSD and from 15% to 10% for S-band (Table 3 and Figure 3). Hence, there was no difference in ESA between the two treatments. Likewise, it is hypothesized that there was no difference in infiltration, as this was presumably already very rapid for the separated slurry under the conditions of dry soil and high permeability (Table S1) of the present study.

For untreated slurry, SSD reduced the emission significantly (Figure 2). This is in agreement with findings by Bittman et al. (2005) who also tested U-SSD and U-band under similar conditions and with similar DM contents. Exposed surface area of U-SSD and U-band were both 19% (Table 3 and Figure 3), but it is assumed that some of the liquid part of the U-SSD infiltrated more quickly due to the aeration slots.

The results in the present study indicates that SSD is an efficient emission abatement technique for slurry with higher DM content, but using it with separated slurry (low DM) and fast reduction in ESA following application will not give an additional emission reduction on permeable soils. With separated slurries the SSD might provide other benefits, such as reduced runoff (Harrigan et al., 2006; Rotz et al., 2011).

5. Conclusion

The results from this study underlines the importance of the interactions between slurry and soil characteristics, application technique and ambient weather conditions on NH_3 emission of field applied slurry. Reducing the contact area between slurry and air can be insufficient to reduce NH_3 emission under warm temperatures with high DM slurries applied to grass land. Under these conditions, additional measurements need to be considered. The combination of band application and separation significantly reduces the emission due to reduction of ESA and increased infiltration. An emission reduction for untreated slurry can be obtained with band application over aeration slots, which is hypothesized to enhance infiltration of the liquid part of the slurry. This study highlights the importance of surface crust formation under warm conditions and the possibility

that this counteracts expected emission increases at higher temperatures.

Acknowledgements: The authors would like to acknowledge the technical staff Andrew Friesen and Frederic Bounaix from AAFC for their skillful assistance with preparation, setting up the measuring system, carrying out measurements and laboratory analysis. The authors would like to thank Peter Storegaard Nielsen from AU for his skillful help with development of the dark chambers used for the exposed surface area measurements.

Funding: This work was funded by the Ministry of Environment and Food of Denmark as a green development and demonstration program (GUDP) with the project title *New application method for slurry in growing crops.*

References

Aeby, P., Schultze, U., Braichotte, D., Bundt, M., Moser-Boroumand, F., Wydler, H., Flühler, H., 2001. Fluorescence imaging of tracer distributions in soil profiles. Environ. Sci. Technol. 35, 753–760. https://doi.org/10.1021/es000096x

Ai, S., Chen, Y., Zhang, Q., 2012. Simulation of liquid movement in soil following pocket injection. Am. Soc. Agric. Biol. Eng. 55, 85–92.

American Public Health Association, 1999. Standard methods for the examination of water and wastewater.

Amon, B., Kryvoruchko, V., Amon, T., Zechmeister-Boltenstern, S., 2006. Methane, nitrous oxide and ammonia emissions during storage and after application of dairy cattle slurry and influence of slurry treatment. Agric. Ecosyst. Environ. 112, 153–162. https://doi.org/10.1016/j.agee.2005.08.030

Aneja, V.P., Schlesinger, W.H., Erisman, J.W., 2009. Effects of agriculture upon the air quality and climate: Research, policy, and regulations. Environ. Sci. Technol. 43, 4234–4240. https://doi.org/10.1021/es8024403

Bell, M.J., Hinton, N.J., Cloy, J.M., Topp, C.F.E., Rees, R.M., Williams, J.R., Misselbrook, T.H., Chadwick, D.R., 2015. How do emission rates and emission factors for nitrous oxide and ammonia vary with manure type and time of application in a Scottish farmland? Geoderma 264, 81–93. https://doi.org/10.1016/j.geoderma.2015.10.007

Benjamini, Y., Yekutieli, D., 2001. The control of the false discovery rate in multiple testing under dependency. Ann. Stat. 29, 1165–1188. https://doi.org/10.1214/aos/1013699998

Bhandral, R., Bittman, S., Kowalenko, G., Buckley, K., Chantigny, M.H., Hunt, D.E., Bounaix, F., Friesen, A., 2009. Enhancing soil infiltration reduces gaseous emissions and improves N uptake from applied dairy slurry. J. Environ. Qual. 38, 1372. https://doi.org/10.2134/jeq2008.0287

Bittman, S., van Vliet, L.J.P., Kowalenko, C.G., McGinn, S., Hunt, D.E., Bounaix, F., 2005. Surface-banding liquid manure over aeration slots: A new low-disturbance method for

reducing ammonia emissions and improving yield of perennial grasses. Agron. J. 97, 1304–1313. https://doi.org/10.2134/agronj2004.0277

Chantigny, M.H., Rochette, P.R., Angers, D.A., Masse, D., Cote, D., 2004. Ammonia volatilization and selected soil characteristics following application of anaerobically digested pig slurry. Soil Sci. Soc. Am. J. 68, 306–312. https://doi.org/10.2136/sssaj2004.3060

Chen, Y., Zhang, Q., Petkau, D.S., 2001. Evaluation of different techniques for liquid manure application og grassland. Appl. Eng. Agric. 17, 489–496.

de Jonge, L.W., Sommer, S.G., Jacobsen, O.H., Djurhuus, J., 2004. Infiltration of slurry liquid and ammonia volatilization from pig and cattle slurry applied to harrowed and stubble soils. Soil Sci. 169, 729–736. https://doi.org/10.1097/01.ss.0000146019.31065.ab

Hafner, S.D., Pacholski, A., Bittman, S., Burchill, W., Bussink, W., Chantigny, M., Carozzi, M., Génermont, S., Häni, C., Hansen, M.N., Huijsmans, J., Hunt, D., Kupper, T., Lanigan, G., Loubet, B., Misselbrook, T., Meisinger, J.J., Neftel, A., Nyord, T., Pedersen, S. V., Sintermann, J., Thompson, R.B., Vermeulen, B., Vestergaard, A. V., Voylokov, P., Williams, J.R., Sommer, S.G., 2018. The ALFAM2 database on ammonia emission from field-applied manure: Description and illustrative analysis. Agric. For. Meteorol. 258, 66–79. https://doi.org/10.1016/j.agrformet.2017.11.027

Hafner, S.D., Pacholski, A., Bittman, S., Carozzi, M., Chantigny, M., Génermont, S.,

Häni, C., Hansen, M.N., Huijsmans, J., Kupper, T., Misselbrook, T., Neftel, A., Nyord, T., Sommer, S.G., 2019. A flexible semi-empirical model for estimating ammonia volatilization from field-applied slurry. Atmos. Environ. 199, 474–484. https://doi.org/S1352231018308069

Häni, C., Sintermann, J., Kupper, T., Jocher, M., Neftel, A., 2016. Ammonia emission after slurry application to grassland in Switzerland. Atmos. Environ. 125, 92–99. https://doi.org/10.1016/j.atmosenv.2015.10.069

Hansen, M.N., Sommer, S.G., Madsen, N.P., 2003. Reduction of ammonia emission by shallow slurry injection: injection efficiency and additional energy demand. J. Environ. Qual. 32. https://doi.org/10.2134/jeq2003.1099

Harrigan, T.M., Bailey, B.B., Northcott, W.J., Kravchenko, A.N., Laboski, C.A.M., 2006. Field performance of a low-disturbance, rolling-tine, dribble-bar manure applicator. Appl. Eng. Agric. 22, 33–38.

Hjorth, M., Christensen, K. V., Christensen, M.L., Sommer, S.G., 2010. Solid-liquid separation of animal slurry in theory and practice, Sustainable Agriculture. https://doi.org/10.1051/agro

Holly, M.A., Larson, R.A., Powell, J.M., Ruark, M.D., Aguirre-Villegas, H., 2017. Greenhouse gas and ammonia emissions from digested and separated dairy manure during storage and after land application. Agric. Ecosyst. Environ. 239, 410–419. https://doi.org/10.1016/j.agee.2017.02.007

Huijsmans, J., Verwijs, B., Rodhe, L., Smith, K., 2004. Costs of emission-reducing manure application. Bioresour. Technol. 93, 11–19. https://doi.org/10.1016/j.biortech.2003.10.020

Labouriau, R., 2020. postHoc: Tools for Post-Hoc Analysis. Comprehensive R archive (CRAN).

Lockyer, D.R., 1984. A system for the measurement in the field of losses of ammonia through volatilisation. J. Sci. Food Agric. 35, 837–848. https://doi.org/10.1002/jsfa.2740350805

Misselbrook, T.H., Nicholson, F.A., Chambers, B.J., 2005. Predicting ammonia losses following the application of livestock manure to land. Bioresour. Technol. 96, 159–168. https://doi.org/10.1016/j.biortech.2004.05.004

Misselbrook, T.H., Smith, K.A., Johnson, R.A., Pain, B.F., 2002. Slurry application techniques to reduce ammonia emissions: Results of some UK field-scale experiments. Biosyst. Eng. 81, 313–321. https://doi.org/10.1006/bioe.2001.0017

Pedersen, J.M., Andresson, K., Feilberg, A., Delin, S., Hafner, S., Nyord, T., n.d. The effect of manure exposed surface area on ammonia emission from untreated, separated, and digested cattle manure. Submitt. to Biosyst. Eng.

R Core Team, 2018. R: A language and environment for statistical computing. R foundation for statistical computing, Vienna.

Rees, Y.J., Pain, B.F., Phillips, V.R., Elbrook, T.H., 1993. The influence of surface and sub-surface application methods for pig slurry on herbage yields and nitrogen recovery. Grass Forage Sci. 48, 38–44. https://doi.org/10.1111/j.1365-2494.1993.tb01834.x

Rodhe, L., Halling, M.A., 2015. Grassland yield response to knife/tine slurry injection equipment - benefit or crop damage? Grass Forage Sci. 70, 255–267. https://doi.org/10.1111/gfs.12106

Rodhe, L., Rydberg, T., Gebresenbet, G., 2004. The influence of shallow injector design on ammonia emissions and draught requirement under different soil conditions. Biosyst. Eng. 89, 237–251. https://doi.org/10.1016/j.biosystemseng.2004.07.001

Rosenbom, A.E., Ernstsen, V., Flühler, H., Jensen, K.H., Refsgaard, J.C., Wydler, H., 2008. Fluorescence imaging applied to tracer distributions in variably saturated fractured clayey till. J. Environ. Qual. 37, 448. https://doi.org/10.2134/jeq2007.0145

Rotz, C.A., Kleinman, P.J.A., Dell, C.J., Veith, T.L., Beegle, D.B., 2011. Environmental and economic comparisons of manure application methods in farming systems. J. Environ. Qual. 40, 438–448. https://doi.org/10.2134/jeq2010.0063

Rutherford, P.M., McGill, W.B., Arocena, J.M., Figueiredo, C.T., 2008. Total nitrogen, in: Carter, M.R., Gregorich, E.G. (Eds.), Soil Sampling and Methods of Analysis. CRC Press, Taylor & Francis Group, LLC.

Smith, K.A., Jackson, D.R., Misselbrook, T.H., Pain, B.F., Johnson, R.A., 2000. Reduction of ammonia emission by slurry application techniques. J. Agric. Eng. Res. 78, 233–243. https://doi.org/10.1006/jaer.2000.0639

Sommer, S.G., Friis, E., Bach, A., Schjørring, J.K., 1997. Ammonia volatilization from pig slurry applied with trail hoses or broadspread to winter wheat: Effects of crop developmental

stage, microclimate, and leaf ammonia absorption. Ecosyst. Process. 26, 1153–1160.

Sommer, S.G., Génermont, S., Cellier, P., Hutchings, N.J., Olesen, J.E., Morvan, T., 2003. Processes controlling ammonia emission from livestock slurry in the field. Eur. J. Agron. 19, 465–486. https://doi.org/10.1016/S1161-0301(03)00037-6

Sommer, S.G., Hansen, M.N., Søgaard, H.T., 2004. Infiltration of slurry and ammonia volatilisation. Biosyst. Eng. 88, 359–367. https://doi.org/10.1016/j.biosystemseng.2004.03.008

Sommer, S.G., Hutchings, N.J., 2001. Ammonia emission from field applied manure and its reduction - Invited paper. Eur. J. Agron. 15, 1–15. https://doi.org/10.1016/S1161-0301(01)00112-5

Sommer, S.G., Jacobsen, O.H., 1999. Infiltration of slurry liquid and volatilization of ammonia from surface applied pig slurry as affected by soil water content. J. Agric. Sci. 132, 297–303. https://doi.org/10.1017/S0021859698006261

Sommer, S.G., Olesen, J.E., 1991. Effects of dry matter content and temperature on ammonia loss from surface-applied cattle slurry. J. Environ. Qual. 20, 679–683. https://doi.org/doi:10.2134/jeq1991.00472425002000030029x

van Es, H., Schindelbeck, R., 2006. Field procedures and data analysis for the cornell sprinkle infiltrometer.

Webb, J., Pain, B., Bittman, S., Morgan, J., 2010. The impacts of manure application methods on emissions of ammonia, nitrous oxide and on crop response-A review. Agric. Ecosyst. Environ. 137, 39–46. https://doi.org/10.1016/j.agee.2010.01.001

Webb, J., Sørensen, P., Velthof, G., Amon, B., Pinto, M., Rodhe, L., Salomon, E., Hutchings, N., Burczyk, P., Reid, J., 2013. An assessment of the variation of manure nitrogen efficiency throughout Europe and an appraisal of means to increase manure-N efficiency. Adv. Agron. 119, 371–441. https://doi.org/10.1016/B978-0-12-407247-3.00007-X

Supporting Information

Effect of reduced exposed surface area and enhanced infiltration on ammonia emission from untreated and separated cattle slurry

Johanna Pedersen[a]*, Tavs Nyord[a], Anders Feilberg[a], Rodrigo Labouriau[b], Derek Hunt[c], Shabtai Bittman[c]

[a]Aarhus University, Dept. of Engineering, Denmark
[b]Aarhus University, Dept. of Mathematics, Denmark
[c]Agassiz Research and Development Center, BC, Canada

S1 Soil data

Table S1: *Soil water content (n = 3), sorptivity and infiltration at steady state (n = 2 for experiment A and B and n = 3 for experiment C and D). Standard deviations are displayed in parenthesis.*

Experiment	Soil water content [g g^{-1}]	Sorptivity	Infiltration at steady state [cm min^{-1}]
A	0.35 (0.03)	1.02 (0.05)	0.32 (0.01)
B	0.19 (0.01)	1.16 (0.05)	0.22 (0.03)
C	0.14 (0.01)	1.13 (0.34)	0.42 (0.28)
D	0.19 (0.03)	0.92 (0.15)	0.27 (0.12)

S2 Weather data

Table S2: *Air and soil temperature during all experiments. Averages of each shift and total experimental period. Soil temperature is measured at 5 cm depth.*

	Air temperature [°C]				Soil temperature [°C]			
Shift	A	B	C	D	A	B	C	D
1	22.4	16.5	20.2	18.5	NA	24.4	21.1	17.4
2	24.9	18.9	23.7	21.7	NA	26.1	25.6	21.7
3	17.1	14.8	20.4	15.5	NA	18.5	21.9	18.1
4	17.5	15.0	20.3	21.5	NA	19.9	20.8	19.7
5	16.3	10.9	16.1	15.8	NA	15.8	20.3	19.7
6	18.9	15.3	15.5	15.8	NA	22.7	17.7	18.0
7	17.0	13.0	12.2	14.3	NA	17.8	16.8	17.9
8	21.5	14.9	15.7	16.4	NA	22.1	18.4	18.6
9	17.5	13.2	13.7	14.6	NA	17.6	16.8	17.8
Total	17.8	13.7	16.3	15.8	NA	18.77	19.23	18.56

S3 Layout of experiments

Figure S1: *Experimental layout.*

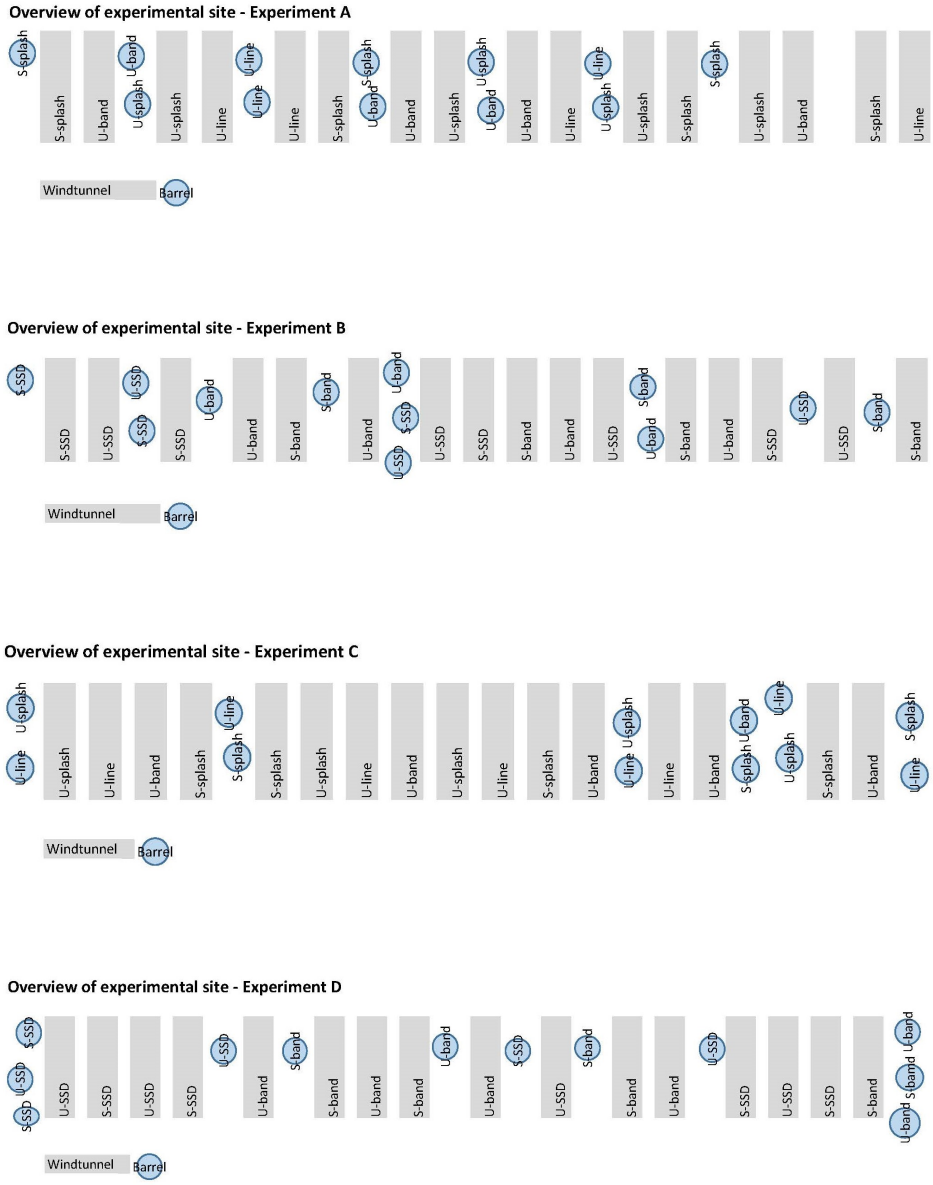

S4 Ammonia flux

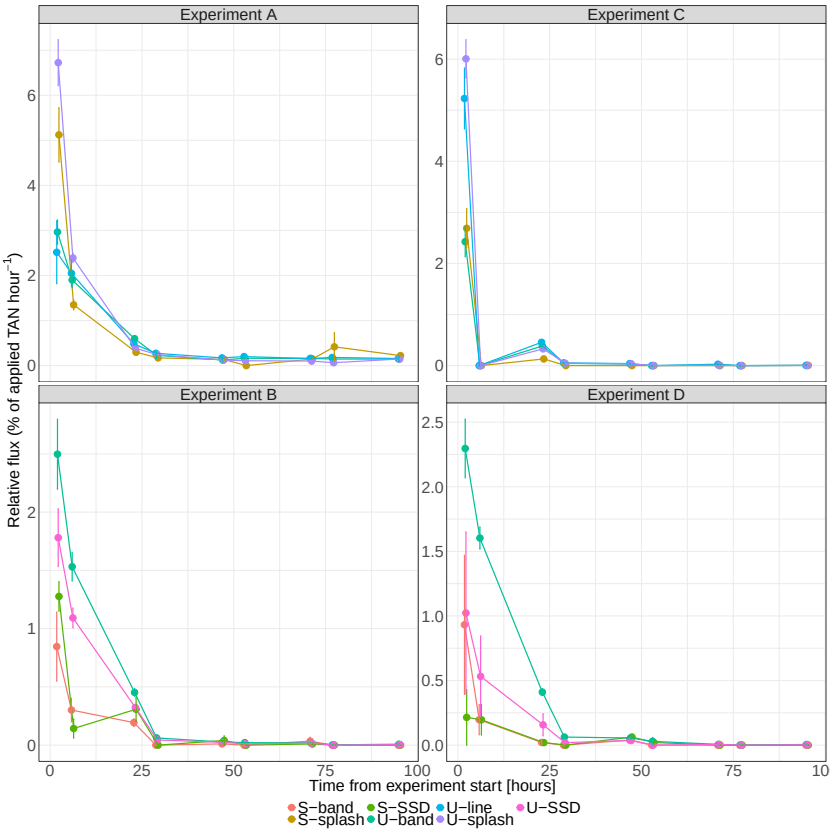

Figure S2: *Ammonia flux after application of 60 metric ton ha^{-1} untreated and separated cattle slurry to bluegrass and white clover with different application techniques. U: untreated, S: separated, splash: splash-plate, line: 20 cm wide line, band: narrow bands, SSD: band applied over subsurface deposition aeration slots. Standard errors are displayed as vertical error bars (n = 4).*

S5 Post hoc analysis results

Table S3: *Post hoc analysis results. Values followed by the same letter are not significantly different.*

Treatment	Mean and confidence interval
U-line	34.67 (20.36-59.02) c
S-splash	18.89 (11.11-32.1) bc
U-band	27.13 (17.46-42.15) c
U-splash	31.29 (18.56-52.74) bc
S-band	7.89 (4.61-13.51) a
U-SSD	14.01 (8.24-23.82) ab
S-SSD	7.75 (4.55-13.21) a

Chapter 7

Paper V (Draft)

J. Pedersen, T. Nyord, A. Feilberg, R. Labouriau. Analysis of the effect of air temperature on ammonia emission from band application of slurry.

Analysis of the effect of air temperature on ammonia emission from band application of slurry

Johanna Pedersen[a]*, Tavs Nyord[a], Anders Feilberg[a], Rodrigo Labouriau[b]

[a]Aarhus University, Dept. of Engineering, Denmark
[b]Aarhus University, Dept. of Mathematics, Denmark
*Corresponding author email: jp@eng.au.dk, Address: Aarhus University, Finlandsgade 10, 8200 Aarhus N, Denmark, +45 93508869

Keywords: Slurry, Field application, Temperature effect, Ammonia, Statistical model

1 Introduction

Field application of liquid animal manure (slurry) is a significant source of ammonia (NH_3) emission to the atmosphere (Aneja et al., 2009). Ammonia emission should be mitigated as it contributes to nitrogen deposition, acidification, and particle formation (Aneja et al., 2009; Walker et al., 2006).

Over the last decades, extensive research has contributed to increased knowledge about the factors controlling and effecting the NH_3 emission and thereby which measurements can be used in order to mitigate these (Hafner et al., 2018; Sommer and Hutchings, 2001; Webb et al., 2010). It is well established that application technique and rate, slurry pH and dry matter (DM), soil and crop type and conditions, and application timing are important parameters that affect NH_3 emission rate after field application of slurry (Bell et al., 2015; de Jonge et al., 2004; Hafner et al., 2019; Huijsmans et al., 2018; Martínez-Lagos et al., 2013; Misselbrook et al., 2005; Rochette et al., 2008; Rodhe et al., 2004; Smith et al., 2000; Sommer and Olesen, 1991). Due to interactions between the parameters, it is challenging to determine the effects of the individual parameters on NH_3 emission.

Timing of application include several factors, such as wind speed, rainfall rate, solar radiation and air temperature. The positive correlation between temperature in the measuring period and NH_3 emission has been recognized in several studies (Beauchamp et al., 1982; Bell et al., 2015; Génermont and Cellier, 1997; Hafner et al., 2019, 2018; Huijsmans et al., 2018; Martínez-Lagos et al., 2013; Sommer et al., 1991). Huijsmans et al. (2018) and Sommer and Olesen (1991) suggested that the temperature right after slurry application is the most important temperature, as the NH_3 emission potential is highest in this period. The effect of temperature on NH_3 emission is well supported by theory.

Theoretical calculations of NH_3 in the gas phase from a solution, shows that

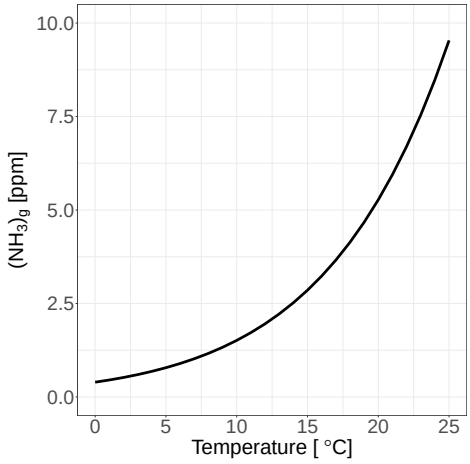

Figure 1: *Equilibrium gas phase NH_3 concentration for a solution with 0.1 M NH_4^+ and a pH of 7 at temperatures ranging from 0 to 25°C.*

a 1°C increase in temperature results in an approximately 13% increase in the gas-phase NH_3 (Hafner et al., 2018; Hafner and Bisogni, 2009) (Figure 1). This relatively high increase in theoretical gas-phase NH_3 caused by small changes in temperature is the results of the equilibrium constant (determining the ratio between NH_4^+ and NH_3) and Henry's law constant (determining the ratio between NH_3 in solution and NH_3 in the gas phase) both are temperature dependent. Increasing temperature increase the potential for NH_3 loss due to a shift of the NH_4^+/NH_3 equilibrium in solution towards NH_3. Additionally the amount of NH_3 in the gas phase compared to NH_3 in solution increase with temperature (Misselbrook et al., 2005; Sommer et al., 2003).

The effect of temperature has been predicted in previous models. The Vol't Air model by Genermont et al. (1997) found a positive correlation between air temperature and cumulative emission, and describe that a 2°C or 4°C increase in air temperature can increase NH_3 emission by 10% and 20%. These findings were contradicted by Smith et al. (2009) who tested the Vol't Air model and only found a 1% increase in cumulative NH_3 emission after an increase in air temperature of 5°C in a model sensitivity evaluation under certain conditions. Neither Genermont et al. (1997) or Smith et al. (2009) provide the other input parameters for their examples, so it is assumed that the differences regarding the temperature effect on cumulative emission are caused by differences in these. The first ALFAM model (Ammonia Loss from Field-Applied Manure) by Søgaard et al. (2002) predicted that 1°C increase in temperature would increase

the cumulative NH_3 emission by 2% (for illustrative example, see Figure S1 in supplementary materials). In the semi-empirical ALFAM2 model (Hafner et al., 2019), the emission has an increasing response to temperature. Due to the structure of the model, meant to be a simple representation of the physical emission system, the effect of temperature depends on the value of other predictor variables (e.g., slurry DM, application method, application rate, incorporation (shallow or deep), air temperature, wind speed, and rainfall rate) (for illustrative example, see Figure S2 in supplementary materials).

As the parameters affecting NH_3 emission interact, the temperature effect anticipated from air-water equilibrium is not always found in field experiments. Braschkat et al. (1997) and Misselbrook et al. (2005) did not find the expected effect of temperature on cumulative NH_3 emission and hypothesized that a surface crust formation of the slurry caused by drying counteracted it. A surface crust on the field-applied slurry is expected to increase the surface resistance of NH_3 transport with the results of a lower NH_3 transport from the slurry to the atmosphere (Sommer et al., 2003). Other studies also discuss the possible effect of crust formation and its mitigating effect on NH_3 emission (Hafner et al., 2018; Pedersen et al., n.d.[a]; Salazar et al., 2014; Sommer et al., 1991; Vandré et al., 1997).

Field measurements are very limited in the number of replications possible and commonly the results have a high variation. As several parameters cannot be controlled but only observed during field measurements (e.g. parameters depending on application timing, and to some extend soil and slurry parameters) these will vary between experiments, making it difficult to make inter-comparisons. Furthermore, a high variation between test organizations has been observed in the ALFAM2 database (Hafner et al., 2018), which has to be considered when comparing results from different studies and different institutes.

In the present study, data from 19 different experiments measured with the same system of dynamic chambers and online measurements will be used to statistically analyze the effect of temperature. The system, which is presented in detail by Pedersen et al. (2020), allows for a high time resolution in NH_3 flux measurements and low variability. By using data measured with the same system, the high variation observed between test organizations recognized by Hafner et al. (2018) is removed. Furthermore, other factors linked to the timing of application (wind speed, rainfall rate, and solar radiation) will be constant in the wind tunnels throughout all experiments, giving a unique possibility to isolate the effect of ambient air temperature. The aim was to model the effect of temperature on cumulative NH_3 emission from band-applied slurry. The specific objectives were to (i) evaluate the effect of ambient air temperature on NH_3 emission from band-applied slurry, (ii) examine the response on cumulative NH_3 emission of air temperature and (iii) derived from the studies the effect of DM and the inter-

action between soil type and application technique on cumulative NH_3 emission will be investigated.

2 Materials and methods

2.1 Ammonia measurements

Ammonia emission after field application of manure was measured with a system consisting of nine wind tunnels. A detailed description and evaluation of the system is presented in (Pedersen et al., 2020), and only a short description is given in the following. A stainless steel chamber (0.8 x 0.4 x 0.25 m) was used as the emission chamber. Air entered from a small air inlet and was passed through the chamber with a manually adjusted air exchange rate of 25 min^{-1}, corresponding to a calculated mean air speed of 0.33 m s^{-1}. The emission chamber was connected to a fan, motor, and frequency converter via a steel duct. Metal frames (0.293 x 0.674 m) was inserted into the soil for the tunnels to be mounted on, in order to control the amount of manure in each plot, giving a plot area for each tunnel of 0.2 m^2. Ammonia concentration in the air entering the tunnels was measured with three background measurements, equally distributed among the tunnels. From each tunnel and the three background measurements, air was drawn through heated PTFE tubing to a channel selection manifold. A Cavity Ring-Down Spectroscopy (CRDS) instrument (G2103 NH_3 Concentration Analyzer, Picarro, CA, USA) was used to measure the NH_3 concentrations in the air stream from the channel selection manifold continuously. Different measuring intervals for each tube was used, ranging from five to 12 minutes (Table S1).

The air flow through the tunnels was constant and there was no precipitation or solar radiation inside the emission chambers. As these parameters were eliminated, it was easier to isolate the effect of temperature. The air flow inside the emission chamber has been found to be the most critical operating parameter (Eklund, 1992; Smith and Watts, 1994; Sommer and Misselbrook, 2016). Experiments evaluating the air turbulence at the soil surface (caused by air exchange) inside the emission chamber and at ambient conditions were used to select the air flow that gave a turbulence at the soil surface closest to ambient conditions at different combinations of temperature and wind speed. Details of the experiments are provided in (Pedersen et al., 2020).

Recovery of NH_3 throughout the measuring system (from tube inlet on the tunnels to the CRDS instrument) was frequently tested, and always found to be minimum 90% within the measuring interval.

Average NH_3 emission flux F (g m^{-2} min^{-1}) in each measurement interval was calculated separately for each wind tunnel from the concentration C (g m^{-3}), the air flow q (m^3 min^{-1}) in the emission chamber, and the soil area covered by

the wind tunnel A (m^2) (Equation 1).

$$F_{NH3} = (C*q)/A \qquad \text{Equation 1}$$

Cumulative NH_3 emission was calculated using the trapezoidal rule. During all of the experiments, ambient air temperature was logged.

2.2 Data

The data used consisted of 108 observations from 19 different experiments were selected. To obtain a relatively homogeneous dataset and ensure that the data was representative for Danish conditions a set of criteria were used for data selection:

- Slurry: untreated pig or cattle slurry.
- Application techniques: trailing hoses or (Bomech) trailing shoes.
- Soil type: coarse sand, sandy loam, or loamy sand.
- Application rate [metric ton ha^{-1}] should be in within Danish standard practices.
- Minimum measuring period of 90 hours.

These criteria meant that all data was used (3 treatments x 3 replicates (wind tunnels)) for some of the experiments, whereas for other experiments only one or two of the treatments were included.

The data can be found in Table 1, additional information about soil, crops, and manure for the individual experiments can be found in Table S1 in supplementary materials.

Parts of the data has been published in previous publications (Foldager et al., 2019, Pedersen et al., 2020, n.d.[b]), for detailed overview, see Table S2 in supplementary materials.

2.3 Model description

The NH_3 emission was modelled using a generalized additive model (Hastie, 1991; Hastie and Tibshirani, 1990; Venables and Ripley, 2002) defined with a Gamma distribution, and a logarithmic link function. The model contained three additive effects, one representing a combination of the soil type and application method, a second representing the dichotomized dry matter (<=4 or >4), and a third given by a smooth function of the air temperature at slurry application estimated by a cubic B spline. Additionally, the model contained an offset given by the logarithm of the total ammoniacal nitrogen (TAN) applied. This model is equivalent to describing the expected NH_3 emission per unit of applied TAN as a smooth

Table 1: *Data used for the statistical analysis.*

ID[a]	Soil type[b]	Slurry DM [g kg^{-1}]	App. method[c]	Air temperature [°C] At application	6 h average	24 h average	90 h average.	TAN applied [kg N ha^{-1}]	NH_3 emission [kg N ha^{-1}][d]
A	CS	<=4	TS	24.4	25.1	18.9	15.1	100	12.33; 15.12; 8.83
A	CS	<=4	TH	24.4	25.1	18.9	15.1	100	18.83; 31.91; 27.55
B	LS	<=4	TS	22.8	22.7	17.6	18.1	99	26.92; 27.39; 26.90
B	LS	<=4	TH	22.8	22.7	17.6	18.1	99	15.15; 19.53; 27.17
C	SL	<=4	TS	19.2	21.8	20.2	20.4	101	32.70; 29.09; 22.41
C	SL	<=4	TH	19.2	21.8	20.2	20.4	101	28.96; 30.10; 29.03
D	CS	>4	TH	8.3	8.2	7.8	11.3	102	10.59; 17.51; 10.55
E	CS	>4	TH	20.0	22.1	17.3	15.3	102	14.21; 19.50; 21.57
F	LS	>4	TS	15.2	15.8	12.8	15.0	98	21.17; 20.05; 20.39
F	LS	>4	TH	15.2	15.8	12.8	15.0	98	26.38; 27.47; 31.6
G	LS	>4	TS	22.8	22.6	17.0	16.9	99	23.81; 28.58; 28.96
G	LS	>4	TH	22.8	22.6	17.0	16.9	99	29.39; 32.58; 33.60
H	LS	>4	TS	15.7	15.9	14.7	15.8	95	26.08; 24.69; 28.20
H	LS	>4	TH	15.7	15.9	14.7	15.8	95	31.69; 29.08; 24.11
I	CS	<=4	TS	20.9	21.6	19.3	17.6	52	8.56; 9.56; 9.73
I	LS	<=4	TS	20.9	21.6	19.3	17.6	52	11.26; 11.58; 10.48
I	SL	<=4	TS	20.9	21.6	19.3	17.6	52	12.68; 15.27; 18.79
J	CS	<=4	TH	23.1	23.6	19.6	15.6	56	15.18; 14.13; 13.84
J	LS	<=4	TH	23.1	23.6	19.6	15.6	56	16.77; 17.53; 15.49
J	SL	<=4	TH	23.1	23.6	19.6	15.6	56	16.60; 16.41; 19.70
K	SL	<=4	TS	18.6	18.9	16.5	15.1	60	8.80; 11.62; 10.86; 12.48; 14.88; 10.85; 10.52; 12.81; 9.23
L	LS	>4	TS	21.3	21.7	17.9	15.5	62	9.46; 7.77; 8.24; 8.25; 7.23; 7.74; 8.25; 8.91; 6.94
M	CS	<=4	TS	15.0	15.3	12.2	12.2	65	10.43; 8.39; 7.23; 9.83; 10.83; 10.38; 9.17; 8.17; 9.21
N	SL	<=4	TH	5.9	6.8	7.8	5.3	99	2.21; 3.53; 4.42
N	SL	<=4	TS	5.9	6.8	7.8	5.3	99	3.19; 3.38; 3.12
O	SL	<=4	TH	8.4	8.0	5.6	3.5	51	2.47; 1.46; 2.17
P	LS	>4	TH	21.0	19.6	16.1	16.4	67	27.26; 28.68; 25.49
Q	SL	<=4	TH	10.9	7.1	6.6	6.9	106	31.56; 35.14; 27.65
R	SL	>4	TH	17.2	12.9	10.2	8.2	113	48.42; 45.95; 43.44
S	CS	>4	TS	21.5	19.6	14.6	12.0	59	32.54; 32.93; 29.51

[a]Experiment ID. [b]CS: coarse sand, LS: loamy sand, SL: sandy loam. [c]TH: trailing hoses, TS: trailing shoes. [d]Cumulative emission 90 hours after application.

function of the temperature at slurry application (not necessarily linear). The details are given below.

Denote by Y_{smdr} the random variable representing the total NH_3 emission observed at the r^{th} replicate (combination of tunnel and experiment) of the observation from the s^{th} soil type (s = coarse sand, loamy sand, sandy loam) that received the d^{th} dosis (d = <=4, >4) applied using the m^{th} method (m = trailing hoses, trailing shoes). According to the model, for the $smdr^{th}$ observation Y_{smdr} is Gamma distributed (see (Jørgensen and Labouriau, 2012)) and have expectation given by Equation 2.

$$log[E(Y_{smdr})] = K_{sm}+H_d+f(T_{smdr})+log(TAN_{smdr}) \qquad \text{Equation 2}$$

Here the notation is constructed with the same indexing convention employed for defining Y_{smdr}, according to which K_{sm} is the additive effect of the combination of the s^{th} soil type and the m^{th} method; and H_d is the additive effect of the d^{th} dose. The function f is an estimated cubic B-spline so that $f(\mathrm{T}_{smdr})$ is an additive regression term representing a possibly non-linear effect the temperature at application. Additionally, TAN_{smdr} is the known TAN applied to the $smdr^{th}$ observation, which enters in the model as an offset, and E is the expectation operator (i.e., $E(X)$ denotes the expectation of the random variable X). Solving Equation 2 to $E(Y_{smdr})$ and passing the constant $1/\mathrm{TAN}_{smdr}$ to inside expectation operator yields Equation 3.

$$E(\frac{Y_{smdr}}{TAN_{smdr}}) = exp(K_{sm})exp(H_d)g(T_{smdr}) \qquad \text{Equation 3}$$

Here the expected emission per TAN unit, $E(Y_{smdr}/TAN_{smdr})$, is expressed as a smooth function $g(\cdot)= exp[f(\cdot)]$ (which is smooth because it is a composition of two smooth functions) that expresses the functional form of the regression term representing the temperature at the application; the exponential of the effects of the dose and the combination of soil type and application method enter in the model as multiplicative factors which will be reported in Table 2. The model above was adjusted using the software R version 6.3.6; in particular, the R-packages "gam" (Hastie and Tibshirani, 1990; Venables and Ripley, 2002), and "postHoc" (Labouriau, 2020) were used for performing post-hoc analyses. Model validation can be found in supplementary information, section S4.

The potential of the mean temperature in the periods 0-6h (Temp6h), 0-24h (Temp24h) and 0-90h (Temp90h) was assessed for predicting the total emission by using a graphical model (Abreu et al., 2010; Edwards et al., 2010; Lauritzen, 1999) as described below. In a graphical model, a group of variables in a study is represented as nodes of a graph with the following convention. Two nodes are connected by an edge (i.e., a line) if, and only if, the conditional covariance between the two corresponding variables given the other variables is different

than zero. The absence of an edge connecting two nodes indicates that the corresponding two variables are conditionally non-correlated given the other variables. According to the theory of graphical models, if a variable, say E, is isolated from a group of other variables, say T6, T24 and T60, in a graph representing a graphical model (in the sense that it is not possible to connect the nodes of E to any of the nodes representing T6, T24 or T60 by a sequence of edges), then the variables T6, T24 and T60, do not carry any information on the variable E (see (Whittaker, 1990)). We consider a graphical model constructed with the following four variables: the mean temperature in the periods 0-6h, 0-24h and 0-90h and the emission adjusted for the effects of the soil type, application method, temperature at application and slurry dry matter. The graphical model was estimated by searching for the graph the minimizes the BIC, using the R-package "gRapHD" (see (Abreu et al. 2009)). Moreover, we tested for the presence of edges using a bootstrap version of the conditional test described in (Anderson, 2003).

3 Results

There is a positive response of the cumulative NH_3 emission to the temperature at application when the temperature varies from 5°C to approximately 14°C. Thereafter, no significant raise in the emission is observed when the temperature increases (Figure 2). Indeed, according to the model, increasing the temperature at application from 5°C to 10°C or 15°C results in a predicted 5-fold and 10-fold increase in NH_3 emission respectively (fraction of applied TAN). An additional increase from 15°C to 20°C does not increase the predicted NH_3 emission additionally.

The model predicts that application by trailing shoes decrease the NH_3 emission by 18.5% (95% coverage CI, 13.8%-23.2%), 36.4% (95% coverage CI, 33.6%-39.2%) and 27.7% (95% coverage CI, 23.5%-31.9%) relative to trailing hoses for coarse sand, loamy sand and sandy loam respectively, with the NH_3 emission from sandy loam being significantly higher than coarse sand and loamy sand (p-value

Table 2: *Model parameters and confidence intervals with 95% coverage. Pairs containing a common letter do not statistically differ at a 5% significance level.*

Combination of application method and soil type	Parameter and confidence interval (with 95% coverage)
Trailing shoes - Coarse sand	0.1494 (0.1262-0.1768) a
Trailing shoes - Loamy sand	0.1248 (0.1031-0.1509) a
Trailing shoes - Sandy loam	0.2109 (0.1748-0.2546) b
Trailing hoses - Coarse sand	0.177 (0.1398-0.224) b
Trailing hoses - Loamy sand	0.1702 (0.1415-0.2047) b
Trailing hoses - Sandy loam	0.2693 (0.2244-0.3233) c
Slurry DM >4 [g kg^{-1}]	1.498 (1.2564-1.7861) d

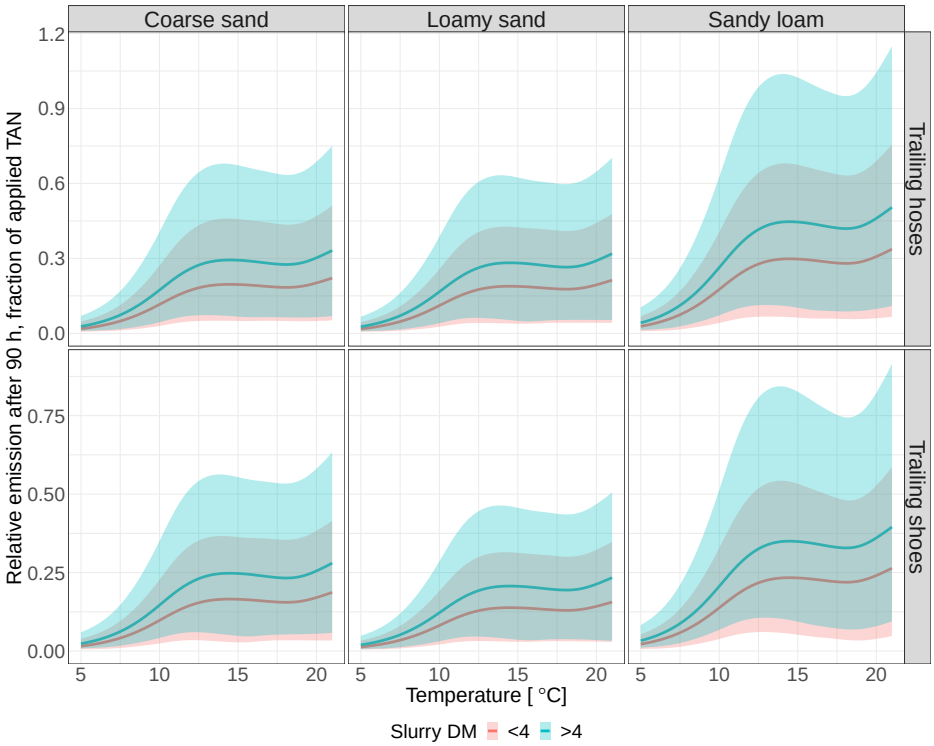

Figure 2: *Model predictions of cumulative NH_3 emission at temperatures between 5°C and 21°C after application of untreated pig or cattle manure on coarse sand, loamy sand or sandy loam by trailing hoses or trailing shoes. Pointwise confidence region with 90% coverage is displayed as highlighted bands.*

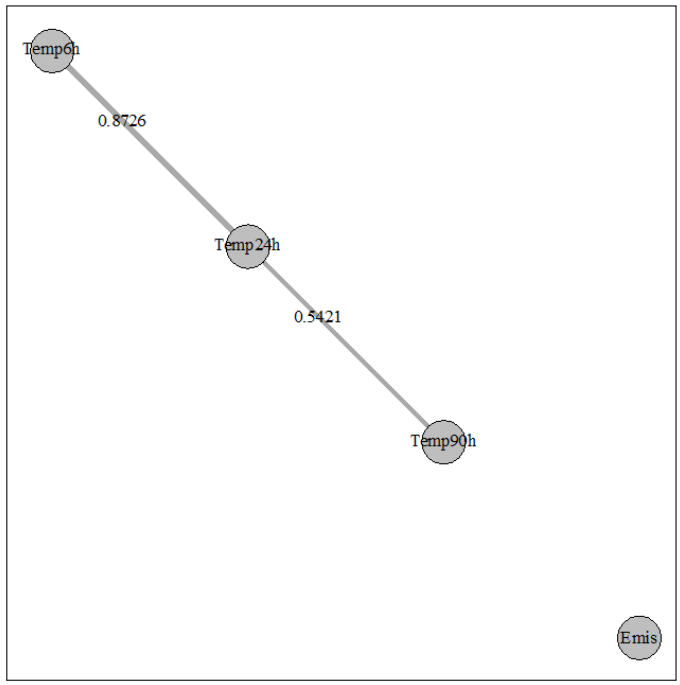

Figure 3: *Representation of the graphical model for the adjusted emission and the mean temperature observed in the periods 0-6h, 0-24h and 0-90h, labelled "Emis", "Temp6h", "Temp24h" and "Temp90h", respectively. Two nodes are connected by a vertice (a line in the figure) if, and only if, the conditional covariance between the two corresponding variables, given the other variables, is different than zero. The graph was estimated by searching for the graph that minimizes the BIC. The numbers over the lines are the estimated conditional correlations between the respective variables; the thickness of the lines are proportional to the conditional correlation.*

<0.0001) for both application techniques. The effect of DM on NH_3 emission was found to be significant, with the emission being 50% lower on average from slurries with DM <=4 g kg^{-1} compared to slurries with DM >4 g kg^{-1}.

Figure 3 displays a graphical model constructed with the adjusted emission and the mean temperature in the periods 0-6h, 0-24h and 0-90h. The graph was inferred by searching for the graph that minimizes the BIC. Additionally, all the possible vertices in the graph were tested and it was found that the corresponding conditional correlations to each of the vertices present in the graph were significantly different from zero ($P<0.05$). Moreover, each of the conditional correlations related to the vertices not present in the graph was not significantly different from zero ($P<0.05$). The node representing the adjusted emission is isolated from the other three nodes (in the sense that no edges are connecting the node representing the adjusted emission to any of the other nodes). This result indicates that none of the three mean-temperature-related variables carries information on the emission that is not already contained in the temperature at application (which enters in the adjustment of the emission).

4 Discussion

4.1 Model evaluation

The present study is an observational study, as no attempt was made to control temperature in the wind tunnels. The experiments were performed in order to investigate the effects of other parameters (e.g. soil type, application technique, manure treatment) on NH_3 emission, and were therefore not designed optimally for statistical modelling. This was partially accounted for by selecting observations from all experiments that meet the chosen criteria, thereby making the dataset more homogeneous. The observed temperatures were not evenly distributed and in some areas only a few observations were made. Consequently, the results should be interpreted as trends and indications.

The plateau observed (Figure 2) fluctuates slightly. It is assumed that this is caused by sparse data and unevenly distributed temperature observations. Therefore, it is suggested that there is a positive response on the cumulative NH_3 emission of the temperature at application, but at a certain temperature the emission increase levels off. Hereafter the temperature effect is small or not present. Due to the sparsity of the data, the exact point of the beginning of the plateau could not be determined based on the present study.

4.2 Effect of temperature

It is generally assumed and modelled that there is a positive correlation between NH_3 emission and temperature, but contradictory results have been observed. The lack of correlation has usually been ascribed to drying out of the surface leading to crust formation (Braschkat et al., 1997; Hafner et al., 2018; Misselbrook

et al., 2005; Salazar et al., 2014; Søgaard et al., 2002; Sommer et al., 1991; Vandré et al., 1997).

The theoretical exponential correlation between temperature and NH_3 emission can be described by Henry's law constant and the equilibrium constant (Figure 1). Both of these describe the chemical processes in a liquid and are not applicable in a slurry that has a high DM content. When the surface of the field-applied slurry dries out the DM content at the surface increase and crust formation can take place. It is hypothesized that the dry layer creates a physical barrier and hinders the diffusion of NH_3 to the soil surface (Sommer et al., 2003), and this process is assumed to cause the plateau observed in the model (Figure 2). Braschkat et al. (1997) did not see any differences in NH_3 emission from field applied manure at 8°C and 20°C and hypothesized that a crust formation at 20°C depressed the NH_3 emission, which is in agreement with the results from the present study.

The change in slurry DM at the surface and crust formation does not only depend on air temperature and slurry DM, but also on air flow right over boundary layer of the slurry as well as solar radiation. The air temperature inside the NH_3 emission chambers has been tested, and was found not to differ from ambient air temperature (Pedersen et al., n.d.[b]). The air flow and solar radiation are different in the wind tunnel than under ambient conditions. The air flow has been selected based on experiments, so that the average turbulence is close to the ambient one under a range of ambient air temperatures and ambient wind velocities (Pedersen et al., 2020). The slurry applied in the tunnels is not exposed to any solar radiation, which has been found to have an effect on NH_3 emission (Sommer et al., 2003, 2001). While it is not possible to quantify and account for the different environmental conditions inside the tunnels compared to ambient conditions, the conditions has been equal throughout all experiments. This provides the advantage that air speed and solar radiation can be eliminated as explanatory variables for the NH_3 emission in the present study.

Further research should be carried out in order to investigate the effect of temperature on slurry surface drying and crust formation of the field applied slurry, and the effect of these on NH_3 emission. Methods should be developed for quantification of these physical changes in the slurry over time after application. Additionally, the effects of air velocity/turbulence over the slurry surface on the slurry surface drying out and crust formation should also be considered and assessed. Determining the effect of slurry surface drying out and crust formation on NH_3 emission and the parameters affecting this can be used to improve current and future models of NH_3 emission from field-applied manure.

The temperature right after application was found to be an explanatory variable in the model, whereas mean temperatures in the periods 0-6 h, 0-24 h and 0-90 h (the whole measuring period) after application was not found to carry any

additional information on the total NH_3 emission that was not already explained by the model. The importance of the temperature at the time of application has been found in earlier studies (Beauchamp et al., 1982; Sommer et al., 1991; Sommer and Olesen, 1991), and the present study underlines the importance of reporting this in NH_3 emission studies.

4.3 Effect of dry matter and interaction between soil and application technique

Several studies ascribe slurry DM as an important parameter for NH_3 emission after field application of slurry (Braschkat et al., 1997; de Jonge et al., 2004; Hafner et al., 2019; Sommer et al., 1991). The effect is assigned to a decreased slurry infiltration into the soil at higher slurry DM levels. The predicted DM effect on NH_3 emission in ALFAM2 model are in the same range as found in the present study, though direct comparison cannot be made as the present study groups the DM in two categories, high (>4 g kg^{-1}) and low (<=4 g kg^{-1}).

The model of the present study show that there is an interaction between soil type and application technique (Table 1). Application by trailing shoes significantly lower the NH_3 emission compared to application by trailing hoses on all three soil types. Application by trailing hoses on sandy loam gives significantly higher NH_3 emission than the other combinations (Table 1). These results confirm the findings in a previous study by Pedersen et al. (2020) where some of the data included in the statistical model of the present study is presented. The present study includes data from several experiments not included in Pedersen et al. (2020), thereby further validating the conclusions found. The decrease in NH_3 emission by applying slurry by trailing shoes instead of trailing hoses were found to be 19±12% on average by Pedersen et al. (2020), the reductions found in the present study of 18.5% (95% coverage CI, 13.8%-23.2%), 36.4% (95% coverage CI, 33.6%-39.2%) and 27.7% (95% coverage CI, 23.5%-31.9%) for coarse sand, loamy sand and sandy loam respectively, is in the same range, but on average higher.

A reduction in NH_3 emission from application by trailing shoes instead of trailing hoses has been found in previous studies (Misselbrook et al., 2002; Webb et al., 2010; Wulf et al., 2002), but knowledge about the importance of interaction between application technique and soil type has not been investigated.

5 Conclusion

The results from this study shows that there is a positive response on the cumulative NH_3 emission after field application of slurry from the temperature at application between 5°C and 14°C, after which a plateauThese results contradict the general assumption and models which may overestimate NH_3 emission during warm periods. The temperature at slurry application was found to be the most

important, and average temperatures over the measuring period was not found to carry any additional information. The importance of the initial temperature on NH_3 emission should be considered to a higher extend when discussing NH_3 emission results, and the temperature should always be reported. The plateau that is reached is hypothesized to be a result of the slurry surface drying out and crust formation, but more research and techniques quantifying the physical changes are needed in order to make definitive conclusions.

The present study highlights the effect of slurry DM on NH_3 emission and underlines the important interaction between soil type and application technique. This relation should always be taken into account when low emission application technologies, such as trailing shoes, are considered as an NH_3 mitigation strategy.

Acknowledgements: The authors would like to acknowledge the technical staff Heidi Grønbæk, Jens Kr Kristensen, Per Wiborg Hansen, and Peter Storegård Nielsen for their skillful assistance with development of the measuring system, carrying out measurements and laboratory analysis. The authors would like to thank Sasha Hafner for helpful discussion of the temperature effect in the AL-FAM2 model.

Funding: This work was funded by the Ministry of Environment and Food of Denmark as a green development and demonstration program (GUDP) with the project title *New application method for slurry in growing crops*.

References

Abreu, G.C.G., Edwards, D., Labouriau, R., 2010. High-dimensional graphical model search with the gRapHD R package. J. Stat. Softw. 37, 1–18. https://doi.org/10.18637/jss.v037.i01

Anderson, T.W., 2003. An introduction to multivariate statistical analysis, Technometrics. John Wiley & Sons, Hoboken, New Jersey. https://doi.org/10.2307/1270458

Aneja, V.P., Schlesinger, W.H., Erisman, J.W., 2009. Effects of agriculture upon the air quality and climate: Research, policy, and regulations. Environ. Sci. Technol. 43, 4234–4240. https://doi.org/10.1021/es8024403

Beauchamp, E.G., Kidd, G.E., Thurtell, G., 1982. Ammonia volatilization from liquid dairy cattle manure in the field. Can. J. Soil Sci. 62, 11–19. https://doi.org/10.4141/cjss82-002

Bell, M.J., Hinton, N.J., Cloy, J.M., Topp, C.F.E., Rees, R.M., Williams, J.R., Misselbrook, T.H., Chadwick, D.R., 2015. How do emission rates and emission factors for nitrous oxide and ammonia vary with manure type and time of application in a Scottish farmland? Geoderma 264, 81–93. https://doi.org/10.1016/j.geoderma.2015.10.007

Braschkat, J., Mannheim, T., Marschner, H., 1997. Estimation of ammonia losses after application of liquid cattle manure on grassland. Pflanzenernähr. Bodenk. 160, 117–123.

de Jonge, L.W., Sommer, S.G., Jacobsen, O.H., Djurhuus, J., 2004. Infiltration of slurry liquid and ammonia volatilization from pig and cattle slurry applied to harrowed and stubble soils. Soil Sci. 169, 729–736. https://doi.org/10.1097/01.ss.0000146019.31065.ab

Edwards, D., de Abreu, G.C.G., Labouriau, R., 2010. Selecting high-dimensional mixed graphical models using minimal AIC or BIC forests. BMC Bioinformatics 11. https://doi.org/10.1186/1471-2105-11-18

Eklund, B., 1992. Practical guidance for flux chamber measurements of fugitive volatile organic emission rates. J. Air Waste Manag. Assoc. 42, 1583–1591. https://doi.org/10.1080/10473289.1992.10467102

Foldager, F.F., Pedersen, J.M., Skov, E.H., Evgrafova, A., Green, O., 2019. Lidar-based 3d scans of soil surfaces and furrows in two soil types. Sensors (Switzerland) 19, 1–13. https://doi.org/10.3390/s19030661

Génermont, S., Cellier, P., 1997. A mechanistic model for estimating ammonia volatilization from slurry applied to bare soil. Agric. For. Meteorol. 88, 145–167. https://doi.org/10.1016/S0168-1923(97)00044-0

Hafner, S.D., Bisogni, J.J., 2009. Modeling of ammonia speciation in anaerobic digesters. Water Res. 43, 4105–4114. https://doi.org/10.1016/j.watres.2009.05.044

Hafner, S.D., Pacholski, A., Bittman, S., Burchill, W., Bussink, W., Chantigny, M., Carozzi, M., Génermont, S., Häni, C., Hansen, M.N., Huijsmans, J., Hunt, D., Kupper, T., Lanigan, G., Loubet, B., Misselbrook, T., Meisinger, J.J., Neftel, A., Nyord, T., Pedersen, S. V., Sintermann, J., Thompson, R.B., Vermeulen, B., Vestergaard, A. V., Voylokov, P., Williams, J.R., Sommer, S.G., 2018. The ALFAM2 database on ammonia emission from field-applied manure: Description and illustrative analysis. Agric. For. Meteorol. 258, 66–79. https://doi.org/10.1016/j.agrformet.2017.11.027

Hafner, S.D., Pacholski, A., Bittman, S., Carozzi, M., Chantigny, M., Génermont, S., Häni, C., Hansen, M.N., Huijsmans, J., Kupper, T., Misselbrook, T., Neftel, A., Nyord, T., Sommer, S.G., 2019. A flexible semi-empirical model for estimating ammonia volatilization from field-applied slurry. Atmos. Environ. 199, 474–484. https://doi.org/S1352231018308069

Hastie, T.J., 1991. Generalized additive models, in: Chambers, J.M., Hastie, T.J. (Eds.), Statistical Models. Wadsworth & Brooks/Cole.

Hastie, T.J., Tibshirani, R., 1990. Generalized additive models. Chapman and Hall, London.

Huijsmans, J.F.M., Vermeulen, G.D., Hol, J.M.G., Goedhart, P.W., 2018. A model for estimating seasonal trends of ammonia emission from cattle manure applied to grassland in the Netherlands. Atmos. Environ. 173, 231–238. https://doi.org/10.1016/j.atmosenv.2017.10.050

Jørgensen, B., Labouriau, R., 2012. Exponential families and theoretical interference, 2nd ed. Springer, Rio de Janeiro.

Labouriau, R., 2020. postHoc: Tools for Post-Hoc Analysis. Comprehensive R archive (CRAN).

Lauritzen, S.L., 1999. Graphical models. Oxford University Press.

Martínez-Lagos, J., Salazar, F., Alfaro, M., Misselbrook, T., 2013. Ammonia volatilization following dairy slurry application to a permanent grassland on a volcanic soil. Atmos. Environ. 80, 226–231. https://doi.org/10.1016/j.atmosenv.2013.08.005

Misselbrook, T.H., Nicholson, F.A., Chambers, B.J., 2005. Predicting ammonia losses following the application of livestock manure to land. Bioresour. Technol. 96, 159–168. https://doi.org/10.1016/j.biortech.2004.05.004

Misselbrook, T.H., Smith, K.A., Johnson, R.A., Pain, B.F., 2002. Slurry application techniques to reduce ammonia emissions: Results of some UK field-scale experiments. Biosyst. Eng. 81, 313–321. https://doi.org/10.1006/bioe.2001.0017

Pedersen, J., Andresson, K., Feilberg, A., Delin, S., Hafner, S., Nyord, T., n.d.[b] The effect of manure exposed surface area on ammonia emission from untreated, separated, and digested cattle manure. Submitt. to Biosyst. Eng.

Pedersen, J., Feilberg, A., Kamp, J.N., Hafner, S., Nyord, T., 2020. Ammonia emission measurement with an online wind tunnel system for evaluation of manure application techniques. Atmos. Environ. 230. https://doi.org/10.1016/j.atmosenv.2020.117562

Pedersen, J., Nyord, T., Feilberg, A., Labouriau, R., Hunt, D., Bittman, S., n.d.[a] Effect of reduced exposed surface area and enhanced infiltratoin on ammonia emission from untreated and separated cattle slurry. under Prep.

Rochette, P., Guilmette, D., Chantigny, M.H., Angers, D., MacDonald, J.D., Bertrand, N., Parent, L.-É., Côté, D., Gasser, M.O., 2008. Ammonia volatilization following application of pig slurry increases with slurry interception by grass foliage. Can. J. Soil Sci. 88, 585–593. https://doi.org/10.4141/CJSS07083

Rodhe, L., Rydberg, T., Gebresenbet, G., 2004. The influence of shallow injector design on ammonia emissions and draught requirement under different soil conditions. Biosyst. Eng. 89, 237–251. https://doi.org/10.1016/j.biosystemseng.2004.07.001

Salazar, F., Martínez-Lagos, J., Alfaro, M., Misselbrook, T., 2014. Ammonia emission from a permanent grassland on volcanic soil after the treatment with dairy slurry and urea. Atmos. Environ. 95, 591–597. https://doi.org/10.1016/j.atmosenv.2014.06.057

Smith, E., Gordon, R., Bourque, C., Campbell, A., Génermont, S., Rochette, P., Mkhabela, M., 2009. Simulating ammonia loss from surface-applied manure. Can. J. Soil Sci. 89, 357–367. https://doi.org/10.4141/CJSS08047

Smith, K.A., Jackson, D.R., Misselbrook, T.H., Pain, B.F., Johnson, R.A., 2000. Reduction of ammonia emission by slurry application techniques. J. Agric. Eng. Res. 78, 233–243. https://doi.org/10.1006/jaer.2000.0639

Smith, R.J., Watts, P.J., 1994. Determination of odour emission rates from cattle feedlots: Part 2, Evaluation of two wind tunnels of different size. J. Agric. Eng. Res. 58, 231–240. https://doi.org/10.1006/jaer.1994.1053

Søgaard, H.T., Sommer, S.G., Hutchings, N.J., Huijsmans, J.F.M., Bussink, D.W., Nicholson, F., 2002. Ammonia volatilization from field-applied animal slurry-the ALFAM model. Atmos. Environ. 36, 3309–3319. https://doi.org/10.1016/S1352-2310(02)00300-X

Sommer, S.G., Génermont, S., Cellier, P., Hutchings, N.J., Olesen, J.E., Morvan, T., 2003. Processes controlling ammonia emission from livestock slurry in the field. Eur. J. Agron. 19, 465–486. https://doi.org/10.1016/S1161-0301(03)00037-6

Sommer, S.G., Hutchings, N.J., 2001. Ammonia emission from field applied manure and its reduction - Invited paper. Eur. J. Agron. 15, 1–15. https://doi.org/10.1016/S1161-0301(01)00112-5

Sommer, S.G., Misselbrook, T.H., 2016. A review of ammonia emission measured using wind tunnels compared with micrometeorological techniques. Soil Use Manag. 32, 101–108. https://doi.org/10.1111/sum.12209

Sommer, S.G., Olesen, J.E., 1991. Effects of dry matter content and temperature on ammonia loss from surface-applied cattle slurry. J. Environ. Qual. 20, 679–683. https://doi.org/doi:10.2134/jeq1991.00472425002000030029x

Sommer, S.G., Olesen, J.E., Christensen, B.T., 1991. Effects of temperature wind speed and air humidity on ammonia volatilization from surface applied cattle slurry. J. Agric. Sci. 117, 91–100.

Sommer, S.G., Søgaard, H.T., Møller, H.B., Morsing, S., 2001. Ammonia volatilization from sows on grassland. Atmos. Environ. 35, 2023–2032. https://doi.org/10.1016/S1352-2310(00)00428-3

Vandré, R., Clemens, J., Goldbach, H., Kaupenjohann, M., 1997. NH3 and N2O emissions after landspreading of slurry as influenced by application technique and dry matter-reduction. I. NH3 emissions. Zeitschrift für Pflanzenernährung und Bodenkd. 160, 303–307. https://doi.org/10.1002/jpln.19971600226

Venables, W.N., Ripley, B.D., 2002. Modern applied statistics. Springer, New York.

Walker, J.T., Robarge, W.P., Shendrikar, A., Kimball, H., 2006. Inorganic PM2.5at a U.S. agricultural site. Environ. Pollut. 139, 258–271. https://doi.org/10.1016/j.envpol.2005.05.019

Webb, J., Pain, B., Bittman, S., Morgan, J., 2010. The impacts of manure application methods on emissions of ammonia, nitrous oxide and on crop response-A review. Agric. Ecosyst. Environ. 137, 39–46. https://doi.org/10.1016/j.agee.2010.01.001

Whittaker, J., 1990. Graphical models in applied multivariate statistics. John Wiley & Sons, New York.

Wulf, S., Maeting, M., Clemens, J., 2002. Application technique and slurry co-fermentation effects on ammonia, nitrous oxide, and methane emissions after spreading. J. Environ. Qual. 31, 1789. https://doi.org/10.2134/jeq2002.1795

Supporting Information

Analysis of the effect of air temperature on ammonia emission from band application of slurry

Johanna Pedersen[a]*, Tavs Nyord[a], Anders Feilberg[a], Rodrigo Labouriau[b]

[a]Aarhus University, Dept. of Engineering, Denmark
[b]Aarhus University, Dept. of Mathematics, Denmark
*Corresponding author email: jp@eng.au.dk, Address: Aarhus University, Finlandsgade 10, 8200 Aarhus N, Denmark, +45 93508869

S1 ALFAM model

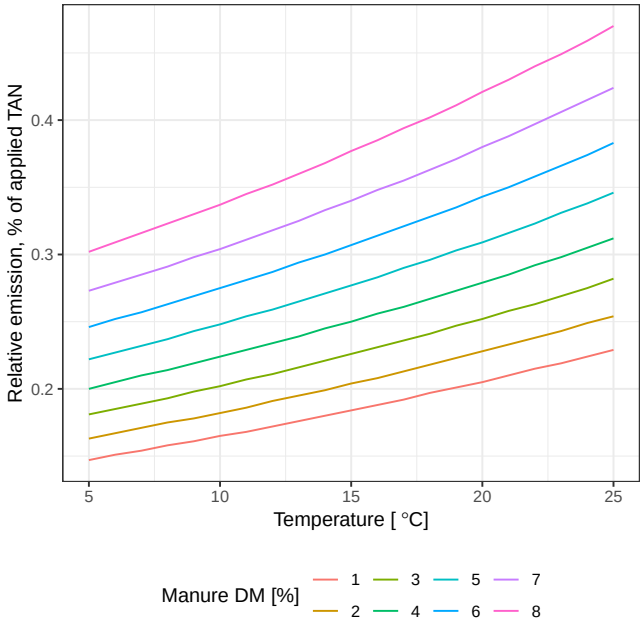

Figure S1: *The predicted effect of temperature and DM on cumulative NH_3 emission calculated with the ALFAM model (Søgaard et al., 2002). Other model parameters were set to: application by trailing hoses, application rate = 40 metric ton ha^{-1}, manure TAN concentration = 1 g kg^{-1}, wind speed = 3 m s^{-1}, no incorporation, soil moisture = dry, slurry type = pig, measuring technique: micrometeorological mass balance.*

S2 ALFAM2 model

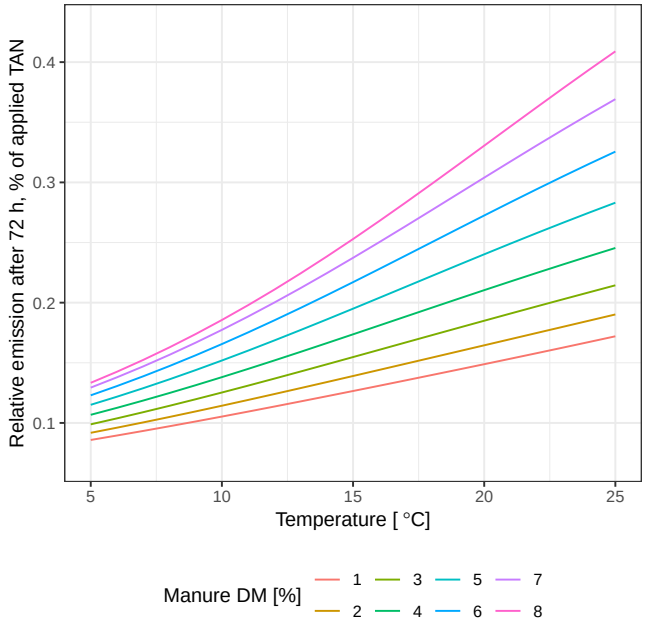

Figure S2: *The predicted effect of temperature (one mean temperature) and DM on cumulative NH_3 emission calculated with the ALFAM2 model (Hafner et al., 2019). Total ammoniacal nitrogen applied is set to 50 g kg^{-1} (as N). Other model parameters values were set to default values (reference conditions): application by trailing hoses, application rate = 40 metric ton ha^{-1}, manure TAN concentration = 1.2 g kg^{-1}, manure pH = 7.5, wind speed (2 m) = 2.7 m s^{-1}, crop height = 10 cm, no incorporation and no rainfall rate.*

S3 Data

Table S1: *Details of experiments used in the modelling.*

		Soil			Crop			Manure				Application rate		
ID[a]	App. tech.[b]	type[c]	Tunnel id	Water content [g g^{-1}]	Dry bulk density [g cm^{-3}]	Type[d]	Height [cm]	Type	DM [g kg^{-1}]	Total TAN [g kg^{-1}]	pH	[ton ha^{-1}]	[kg TAN ha^{-1}]	ET[e] [min]
A	TS	CS	5, 8, 12	0.09	0.09	ww	29	pig	3.78	2.22	7.2	45	100	109
	TH		1, 6, 10											
B	TS	LS	10, 6, 8	0.13	0.13	ww	12	pig	3.84	2.20	7.0	45	99	104
	TH		1, 12, 9											
C	TS	SL	6, 10, 12	0.17	0.17	ww	15	pig	3.40	2.25	7.1	45	101	104
	TH		2, 4, 9											
D	TH	CS	5, 8, 12	0.10	0.10	ww	16	cattle	6.28	2.61	7.7	50	131	90
E	TH	CS	1, 4, 5	0.07	0.07	ww	19	cattle	8.53	2.03	7.1	50	102	109
F	TS	LS	12, 2, 5	0.15	0.15	g	13	cattle	9.04	2.79	6.9	35	98	104
	TH		4, 8, 9											
G	TS	LS	1, 5, 12	0.21	0.21	g	14	cattle	8.96	2.83	6.9	35	99	104
	TH		2, 8, 10											
H	TS	LS	2, 5, 9	0.15	0.15	g	13	cattle	8.63	2.72	6.8	35	95	104
	TH		1, 8, 10											
	TS	CS	1, 2, 12	0.11	0.11									
I	TS	LS	4, 5, 6	0.18	0.18	-	-	pig	3.17	1.16	7.3	45	52	104
	TS	SL	8, 9, 10	0.18	0.18									
	TH	CS	1, 2, 12,	0.08	0.08									
J	TH	LS	4, 5, 6	0.13	0.13	-	-	pig	3.02	1.25	7.6	45	56	104
	TH	SL	8, 9, 10	0.14	0.14									
K	TS	SL	1, 2, 4, 5, 6, 8, 9, 10, 12	0.15	0.15	.	-	pig	2.93	1.34	7.5	45	60	104
L	TS	LS	1, 2, 4, 5, 6, 8, 9, 10, 12	0.15	0.15	-	-	pig	4.04	1.38	7.6	45	62	104
M	TS	CS	1, 2, 4, 5, 6, 8, 9, 10, 12	0.08	0.08	-	-	pig	3.12	1.45	7.7	45	65	104
N	TH	SL	2, 8, 10	0.23	1.29	wr	5	pig	2.27	2.20	7.0	45	99	156
	TS		4, 6, 9											
O	TH	SL	1, 2, 4	0.20	1.34	wr	5	pig	2.09	1.14	7.8	45	51	60
P	TH	LS	2, 6, 9	0.16	1.39	o	5	cattle	8.51	1.90	6.7	35	67	104
Q	TH	SL	1, 5, 10	0.15	1.70	ww	10	pig	3.27	3.52	7.8	30	106	104
R	TH	SL	10, 2, 8	0.13	1.54	ww	12	pig	6.46	3.76	7.5	30	113	104
S	TS	CS	1, 8, 10	0.10	1.27	g	10	cattle	5.79	2.37	7.7	25	59	104

[a]Experiment ID. [b]TH: trailing hoses, TS: (Bomech) trailing shoes. [c]CS: coarse sand, LS: loamy sand, SL: sandy loam. [d]ww: winter wheat, g: grass, NA: none, wr: winter rye, o: oat. [e]Elapsed time between measurement in each tunnel.

S4 Model validation

The appropriateness of the model was established by examining the residuals. Figure S3 (left) displays the scatter plot of the raw residuals against the fitted values. The cone-form pattern observed in that graph is what one would expect from a generalized additive model with Gamma distributed errors since the variance of Gamma distributed variables is proportional to the square of the theoretical means. Note that the pattern referred above disappeared in the scatter plot of the Pearson residuals against the fitted values, displayed in Figure S3 (right), which confirms that the Gamma error distribution is an adequate choice. As an additional model control the observed responses were transformed by the inverse of the theoretical cumulative distribution function and the adherence to the uniform distribution in the interval (0,1) was tested, which yielded a p-value of 0.79, indicating the absence of lack of fit (Figure S4).

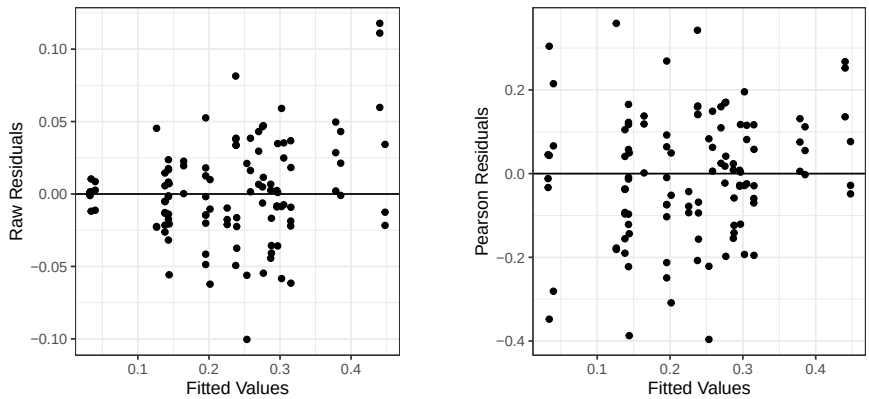

Figure S3: *Scatter plot of the raw residuals (left) and Pearson residuals (right) against the fitted values.*

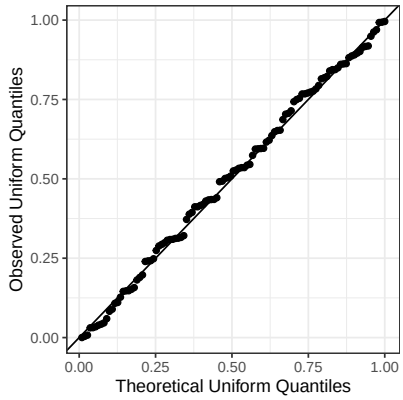

Figure S4: *Model control of the generalized additive model. The agreement of the responses transformed by the inverse of the cumulative distribution function with the uniform distribution indicates goodness of fitness.*

S5 Data included elsewhere

Table S2: *Overview of data included in the statistical dataset previously published.*

Experiment ID	Published in	Experimental ID in previous publication
A	Pedersen et al. (2020)	A
B	Pedersen et al. (2020)	B
C	Pedersen et al. (2020)	C
F	Pedersen et al. (2020)	D
G	Pedersen et al. (2020)	E
I	Pedersen et al. (2020)	F
J	Pedersen et al. (2020)	G
L	Foldager et al. (2019)	Sandy loam
M	Foldager et al. (2019)	Coarse sand
H	Pedersen et al. (2020)	H
P	Pedersen et al. (n.d.)	B

References

Foldager, F.F., Pedersen, J.M., Skov, E.H., Evgrafova, A., Green, O., 2019. Lidar-based 3d scans of soil surfaces and furrows in two soil types. Sensors (Switzerland) 19, 1–13. https://doi.org/10.3390/s19030661

Hafner, S.D., Pacholski, A., Bittman, S., Carozzi, M., Chantigny, M., Génermont, S., Häni, C., Hansen, M.N., Huijsmans, J., Kupper, T., Misselbrook, T., Neftel, A., Nyord, T., Sommer, S.G., 2019. A flexible semi-empirical model for estimating ammonia volatilization from field-

applied slurry. Atmos. Environ. 199, 474–484. https://doi.org/S1352231018308069

Pedersen, J., Andresson, K., Feilberg, A., Delin, S., Hafner, S., Nyord, T., n.d. The effect of manure exposed surface area on ammonia emission from untreated, separated, and digested cattle manure. Submitt. to Biosyst. Eng.

Pedersen, J., Feilberg, A., Kamp, J.N., Hafner, S., Nyord, T., 2020. Ammonia emission measurement with an online wind tunnel system for evaluation of manure application techniques. Atmos. Environ. 230. https://doi.org/10.1016/j.atmosenv.2020.117562

Søgaard, H.T., Sommer, S.G., Hutchings, N.J., Huijsmans, J.F.M., Bussink, D.W., Nicholson, F., 2002. Ammonia volatilization from field-applied animal slurry-the ALFAM model. Atmos. Environ. 36, 3309–3319. https://doi.org/10.1016/S1352-2310(02)00300-X

Chapter 8

Miscellaneous findings

8.1 Ammonia emission abatement with new slurry application aggregate

8.1.1 Background

A key aim of the NUGA project was to develop a new slurry application aggregate (called *NUGA tine(s)* here forth) for application of slurry in growing crops. The focus was on developing a tool that would surpass the current application techniques for spring application of slurry in winter cereal. Due to rainfall during the winter season, the soil hardens, and a soil-crust is created. Ideally, the NUGA tine should be able to break this soil-crust before slurry application, which expectedly will be enhancing slurry infiltration and thereby lowering NH_3 and odor emission. Another aim was to investigate whether the NUGA tine would function as mechanical weed control or increase germination of new weeds, due to soil disturbance.

8.1.2 Experimental overview

Five experiments were performed with the NUGA tines applying pig slurry in cereal crops. In all experiments, slurry application with trailing hoses was the control treatment. During the two first experiments (19D and 19E) NMVOC and H_2S were measured with the dynamic chambers and PTR-TOF-MS (detailed method description can be found in Chapter 4, Paper II, Sections 2.1 and 2.2) from a loamy sand soil with winter wheat. In the last three experiment (19G, 20A, 20B) NH_3 emission was measured with the dynamic chambers and CRDS (detailed method description can be found in Chapter 3, Paper I, Section 3.1),

using the trapezoid rule for calculation of cumulative emission instead of left Riemann sum. In 19G, slurry was applied on a loamy sand soil with spring barley and in 20A and 20B slurry was applied on a sandy loam soil with winter wheat. In parallel to the last three experiments, slurry was applied in other plots in the same field in order to measure nitrogen uptake by the plants and weed occurrence. The results of the nitrogen uptake and weed occurrence will be assessed by Ph.D. student Margaret Rose Mc Collough from Department of Agroecology, Aarhus University. A joint paper (with M. R. Mc Collough as first author) will be written, describing the performance of the new aggregate. During experiments 20A and 20B, ESA was measured in plots parallel to the dynamic chambers (detailed method description can be found in Chapter 5, Paper III, Section 2.2).

Experiment 19D, 19E, and 19G were performed in spring 2019 at Foulum Research Center, Aarhus University, whereas 20A and 20B were performed in spring 2020 at Flakkebjerg Research Center, Aarhus University.

Soil and slurry characteristics can be found in Tables 2.1 and 2.3 in Appendix 2.

8.1.3 Application aggregate

The NUGA tine was developed by Agricultural Technician Peter Storegård Nielsen and Senior Advisor Tavs Nyord from Institute of Engineering, Aarhus University in collaboration with Samson Agro A/S.

Figure 8.1: *Pictures of NUGA tines.*

The NUGA tine is constructed of a spring tine normally used for tine harrowing for mechanical weed control (hardened round steel bar with a diameter of 10 mm) attached to two springs made from tempered steel, each allowing 6-15 kg load on the aggregate (Figure 8.1). The vertical load on the NUGA tine when

used during the experiments was 23-24 kg. When the NUGA tine was worked across the soil surface it broke the soil-crust and created a narrow slot (Figure 8.2, left). Hereafter, the slurry was applied by Vogelsang trailing shoe directly in the slot. The Vogelsang trailing shoe was used for slurry application in order to control the application and avoid splashing of slurry, which can occur with trailing hose application and other types of trailing shoes.

8.1.4 Results

The NUGA tines successfully broke the surface crust, penetrated a few cm into the soil, and created a narrow slot, for some of the slurry to be contained in, even on a dry sandy loam soil with a hard surface crust (Figure 8.2, left).

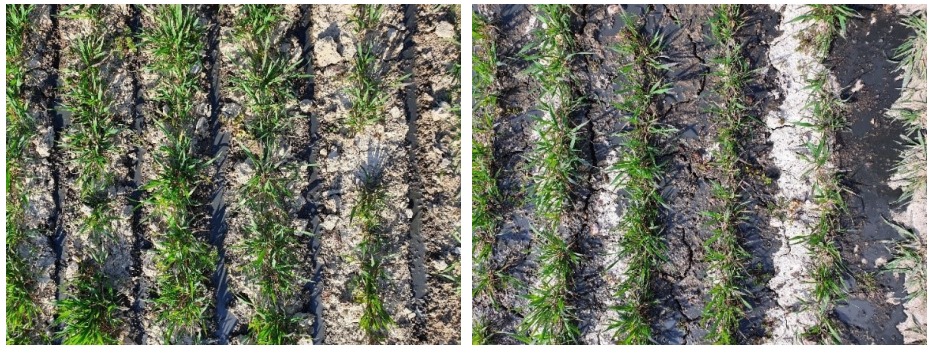

Figure 8.2: *Application of 30 metric ton ha^{-1} pig slurry on dry sandy loam soil with a hard surface crust with NUGA tines (left) and trailing hoses (right).*

In all three experiments measuring NH_3 emission, the emission following application with the NUGA tines were lower compared to application by trailing hoses. In experiments 20A and 20B the reduction was 8%, whereas the reduction was 27% in experiment 19G (Figure 8.3). It was only in experiment 19G that the difference was found to be significant different based on Tukey's HSD test ($p<0.05$)

During both experiments with measurements of ESA (20A and 20B), a large reduction in ESA was obtained when slurry was applied by the NUGA tines compared to trailing hoses (Figure 8.4). This reduction was also observed in the field in the plots for measurements of nitrogen uptake and weed control (Figure 8.2). In experiment 20A a considerable drop of 12% in ESA over time was observed for both application techniques. During experiment 20B the change in ESA over time was only 2% and 4% for NUGA tines and trailing hoses, respectively.

There were no significant differences based on Tukey's HSD test ($p<0.05$) in

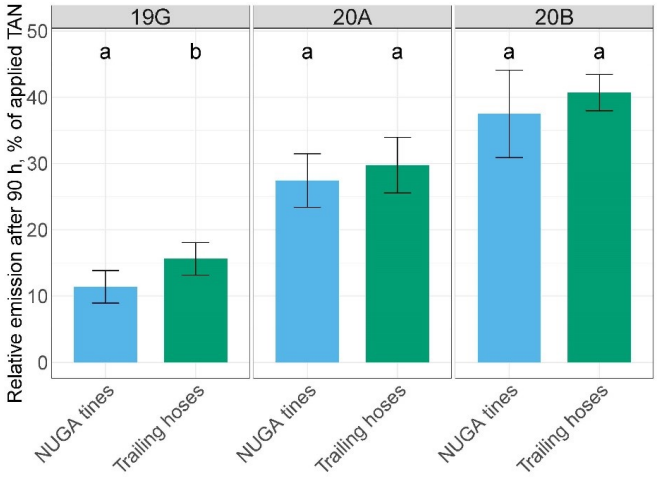

Figure 8.3: *Relative cumulative NH_3 emission 90 hours after field application of 22.8 metric ton ha^{-1} (19G) and 30 metric ton ha^{-1} (20A and 20B) pig slurry to loamy sand soil with spring barley (19G) and sandy loam soil with winter wheat (20A and 20B) by trailing hoses and NUGA tines (n = 3). The different letters within each experiment indicate that there is a significant difference between the cumulative emissions based on Tukey's HSD test ($p<0.05$) within one experiment.*

cumulative NMVOC and H_2S emission after slurry application by NUGA tines and trailing hoses in experiment 19D and 19E (data not shown). The measurements were in the same range as measured NMVOC and H_2S emissions from pig slurry measured in previous experiments (Chapter 4, Paper II).

8.1.5 Discussion

The small reduction of NH_3 emission when using the NUGA tines compared to trailing hoses, indicates that the NUGA tines can be used as a low emission application technique, and that the NUGA tines has potential to lower the emission further than trailing hoses. The reduction from using the NUGA tines compared to trailing hoses was lower than expected, especially considering the large decrease in ESA.

The reduction in NH_3 emission can most likely be assigned to the reduction in ESA by using the NUGA tines compared to trailing hoses (Figure 8.4). The narrow slot allowed some of the slurry to be contained, whereas the slurry applied by trailing hoses spread out to a great extent on the hard soil crust (Figures 8.2 and 8.4). Even though the NH_3 emission was reduced, the reduction was

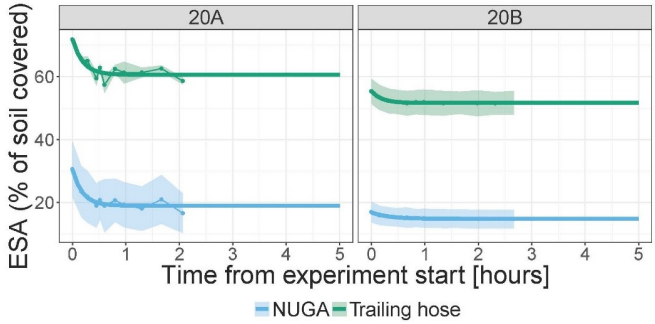

Figure 8.4: *Exposed surface area raw data and fitted ESA curves after field application of 30 metric ton ha^{-1} pig manure to sandy loam soil with winter wheat by trailing hoses and NUGA tines. Standard deviations are displayed in bands for raw data points used for ESA modelling (n = 3).*

smaller than what could be assumed from the great reduction in ESA. In both experiments ESA after application with NUGA tines was approximately one third of ESA from slurry applied by trailing hoses. It is speculated that the larger spread out of the slurry applied with trailing hoses allowed for faster infiltration of parts of the slurry, as it is more likely that a part of the slurry came near some of the large cracks in the soil (Figure 8.2) where almost instantaneous infiltration occurred.

The differences in ESA between experiment 20A and 20B was probably caused by differences in slurry characteristics. It was intended to use the same slurry for the two experiments, so after experiment 20A slurry was collected in buckets and stored at 4°C for six days until it was used during experiment 20B. Regardless of these efforts to have slurry with characteristics as similar as possible, the DM content and viscosity of the slurry used during experiment 20B is much higher than that of 20A (Table 2.3 in Appendix 2). It is speculated that proper mixing has not been performed before slurry collection for experiment 20B. This higher DM content and viscosity might have resulted in the lower spread out of the slurry right after application, resulting in a lower initial ESA. The change in ESA over time was also significantly lower during experiment 20B compared to 20A. The higher amount of dry matter in the slurry used in 20B might have blocked the small soil pores, resulting in a lower infiltration. Furthermore, the lower spread out of the slurry might have decreased slurry infiltration in the large cracks in the soil, which is speculated to have caused relatively quick infiltration of some of the slurry applied with trailing hoses during experiment 20A.

A generally higher emission from both application techniques was measured in experiment 20B compared to 20A. This can both be due to lower infiltration

due to the higher DM content and viscosity as discussed above, but it could also be caused by a higher ambient air temperature. The average temperature within the first six hours after application was 6°C higher during experiment 20B compared to 20A (Table 2.2 in Appendix 2).

The NH_3 reduction when using NUGA tines compared to trailing hoses was larger for the application in spring-sown (19G) cereal crops compared to winter-sown (20A and 20B), this was expected due to the newly tilled soil. It is speculated that at these conditions application with trailing shoes (e.g. Bomech) would result in NH_3 emissions in the same range as the NUGA tines, as it would create a slot in the soil containing the slurry (Chapter 3, Paper I). In the case of application on winter-sown cereal crops it is speculated that a trailing shoe (e.g. Bomech) would not create a slot in the soil due to the hard soil crust, and therefore not reduce the emissions further than trailing hoses (Chapter 3, Paper I). The rake angle for NUGA tines is higher than for Bomech trailing shoes, meaning that the NUGA tines operates more aggressive in the soil than Bomech trailing shoes and therefore actually breaks the soil surface instead of 'running on top' of the soil.

8.1.6 Conclusion

The results show that the NUGA tines has a potential as a low emission application technique in cases where it is assumed that infiltration will be slow due to a hard soil crust.

As only a limited number of experiments were conducted, further investigation is necessary before the potential of the NUGA tines can be established. Experiments with simultaneous measurements of NMVOC, H_2S and NH_3 would be beneficial, in order to investigate why no NMVOC and H_2S reduction was observed, as opposed to the reduction in NH_3.

The surprisingly low reduction in NH_3 compared to the large reduction in ESA demonstrates the importance of infiltration and underline the necessity of developing a quantitative measurement method that will work at near field-conditions, as this is expected to be the main explanatory variable.

8.2 Trailing shoe application of acidified digested cattle slurry on clover grass

8.2.1 Background

In Denmark, acidification of the slurry is an approved technology in order to mitigate NH_3 emission from field-applied slurry. The acidification can both be done in the livestock production facility, during storage or immediately before application. If slurry is applied in grass fields by trailing hoses or trailing shoes, the Danish law requires it to be acidified in order to lower NH_3 emissions. Un-acidified slurry must be applied by techniques that incorporate the slurry into the soil, such as disc injectors [155]. Several studies found a reduction in NH_3 emissions from acidified slurry [63, 73, 74, 76], but only two studies looked at acidification immediately before application to soil [75, 156]. When slurry is acidified in the field it is required that pH is below 6.4 [72]. Digestion of slurry is a common practice in Denmark for production of biogas. After digestion, the digestate is applied on to the fields and is subject to the same regulation as slurry.

The aim was to investigate the effect of acidification when applying digestate on a grass field with trailing shoes, as it is hypothesized that even a small amount of acid will lower the NH_3 emissions sufficiently, e.g. that the emission will be in the same range as the emission when using disc injection of untreated digestate.

8.2.2 Experimental overview

Two experiments (20C and 20D) were performed in collaboration with SEGES (SEGES, Landbrug & Fødevarer F.m.b.A., Aarhus N, Denmark) as a part of the experiment Techniques for application of digested and undigested slurry in clover grass (Danish: *Teknik til udbringing af afgasset og rågylle til kløvergræs*). SEGES were investigating the effect on crop yield after application of digested and separated cattle manure (slurry here forth) with Bomech trailing shoes, trailing hoses and disc injectors. The slurry applied by trailing hoses was acidified, and the slurry applied by disc injectors was un-acidified. Both acidified and non-acidified slurry was applied by trailing shoes. The experimental site was two different fields (near Holstebro, Denmark) with coarse sand soil.

In parallel to the SEGES experiments, in the same fields, NH_3 and ESA were measured from non-acidified and acidified slurry applied by trailing shoes with non-acidified slurry applied by disc injectors as a reference. Ammonia was measured with dynamic chambers and CRDS (detailed method description can be found in Chapter 3, Paper I, Section 3.1), using the trapezoidal rule for calculation of cumulative emission instead of left Riemann sum. Exposed surface area of the slurry was measured with imaging (detailed method description can be found in

Chapter 5, Paper III, Section 2.2). During experiment 20D some of the grass was cut with scissor by hand in the areas for ESA quantification. This was done to avoid the grass to overlap too much with the ESA and thereby disturb the measurements. The cutting was done with great care to not disrupt the soil surface.

To investigate the effect of a small addition of acid, it was chosen to add acid equivalent to the crop sulfur demand[1]. Therefore, one kg acid was added per metric ton slurry. The acidification was done with the 'SyreN system' (BIOCOVER A/S, Vejen, Denmark) that continuously pump sulfuric acid from an acid tank on the tractor to the manure spreader outlet where it is mixed with the slurry immediately before field application. Due to the design of the acidification system, slurry was collected in buckets from the trailing shoe outlets on the manure spreader, and stored until application in the experiments. The storing time was one and a half hour and three for experiment 20C and 20D, respectively.

Soil and slurry characteristics can be found in Tables 2.1 and 2.3 in Appendix 2.

8.2.3 Results

In both experiments disc injectors significantly reduced NH_3 emission of untreated slurry compared to application by trailing shoes (17% and 39% in experiment 20C and 20D, respectively) (Figure 8.5). In both experiments, the small amount of acid lowered the emission from slurry applied by trailing shoes (15% and 8% from experiment 20C and 20D, respectively) the difference was significant in experiment 20C.

In both experiments, the ESA of disc-injected slurry was lower than the ESA of acidified slurry applied with trailing shoes (Figure 8.6). In experiment 20C the un-acidified slurry applied by trailing shoes had a similar ESA over time as slurry applied by disc injectors. This is in contrast to experiment 20D acidified and un-acidified slurry applied by trailing shoes had similar ESA over time. During experiment 20C a reduction in ESA occurred within the first hour, whereas in experiment 20D ESA was almost constant.

The relatively small amount of acid added to the slurry lowered pH from 7.9 to 7.3 in the slurry bands after application. pH increased after application as expected (Section 2.1 and Chapter 5, Paper III, Section 4.4), but regardless of this, the pH difference between the acidified and non-acidified slurry remained in the pH measurements period (Figure 8.7).

[1]Assumption: three slurry applications over the season giving a total of 60-75 metric ton slurry ha^{-1} during the season. With 1 L H_2SO_4 per ton^{-1} slurry it gives 35-43 kg S ha^{-1}.

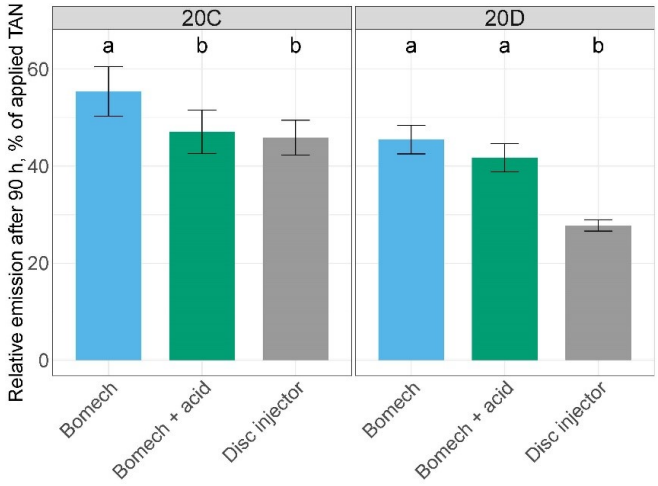

Figure 8.5: *Relative cumulative ammonia emission 113 hours after field application of 25 metric ton ha^{-1} digested and separated cattle manure to coarse sand soil with clover grass by Bomech trailing shoes, Bomech trailing shoes + acidification and disc injectors (n = 3). Different letter within each experiment indicate that there is a significant difference between the cumulative emissions based on Tukey's HSD test (p<0.05).*

8.2.4 Discussion

Disc injectors gave the lowest NH_3 emission, but during experiment 20C the acidification reduced the emission from slurry applied by trailing shoes to the same level as emission from un-acidified slurry applied by disc injectors, regardless of the higher ESA. The higher ESA was probably due to foaming caused by adding acid to the slurry. As this did not result in an increased emission, the lower pH must have sufficiently counteracted the bigger contact surface between air and slurry. The same effect of acidification was not observed in experiment 20C, where the reduction compared to un-acidified slurry applied by trailing shoes was only small.

In experiment 20D there was no difference in ESA between acidified and un-acidified slurry applied by trailing hoses. It is speculated that it was due to less foaming of the acidified slurry during experiment 20D where there was a time delay of three hours after acidification of the slurry before application, compared to 20C where the time delay was only approximately one and a half hour.

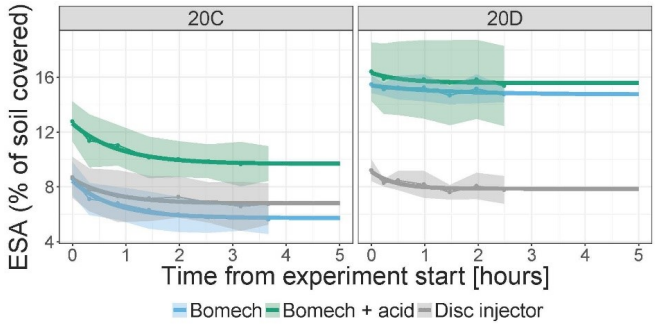

Figure 8.6: *Exposed surface area raw data and fitted ESA curves after field application of 25 metric ton ha^{-1} digested and separated cattle manure to coarse sandy soil with clover grass by Bomech trailing shoes, Bomech trailing shoes + acidification and disc injection. Standard deviations are displayed in bands for raw data points used for ESA modelling (n = 3).*

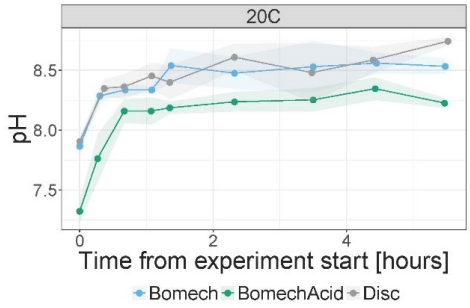

Figure 8.7: *Manure surface pH after field application of 25 metric ton ha^{-1} digested and separated cattle manure to coarse sandy soil with clover grass by Bomech trailing shoes, Bomech trailing shoes + acidification and disc injectors. Standard deviations are displayed in bands (n = 3).*

A difference between ESA of un-acidified slurry applied by trailing hoses and disc injectors was observed during experiment 20D, which was not observed during experiment 20C. In experiment 20D the soil had a higher dry bulk density and higher soil water content compared to the soil in 20C. These might have lead to a higher spread out of the slurry applied by trailing shoes. The slurry applied by disc injectors was contained in the slots created by the discs. Therefore, as long as the application rate is at a level where slurry is contained in the slot, additional spread out will not occur due to changes in soil conditions.

As the grass was cut in the ESA plots for 20D and not for 20C, it is uncertain if the results can be compared directly. The additional cutting might give rise to higher ESA, as there is less grass shading of the slurry.

The generally lower NH_3 emissions during experiment 20D compared to 20C is most likely caused by a difference in ambient air temperature following application. During experiment 20C the average temperature during the first five hours was approximately 5°C higher compared to experiment 20D (Table 2.2 in Appendix 2).

The pH measurements show that the pH difference between the acidified and un-acidified slurry was maintained during the first five hours. During this time most of the emission has occurred, hence, the acidification was effective in the period where the impact was highest. As no pH measurements were made during experiment 20D it is not possible to conclude if this is a general trend. pH measurements during 20D could potentially have helped enlighten why the difference in emission between acidified and non-acidified slurry applied by trailing hoses were low, it is possible that the pH of acidified slurry increased more rapidly than non-acidified, making the effect of acidification lesser.

8.2.5 Conclusion

These result show that acidification might have a small emission mitigation potential, even when using a higher target pH than required by the current legislation.

As this is based on only two experiments under less than ideal conditions (time delay from acidification to application and different treatment of crops in plots for ESA measurements), more experiments have to be conducted in order to make any conclusions. Furthermore, it would be interesting to make the same experiments with trailing hoses.

Chapter 9

Major findings, conclusions, and perspectives

The following is a presentation of the major findings and conclusions presented in the Ph.D. thesis, followed by perspectives. The findings from the scientific papers (Paper I, Paper II, Paper III, and Paper VI, Chapters 3-5 and Appendix 1), paper drafts (Paper IV, Paper V, and Paper VII, Chapters 6-7) and miscellaneous findings (Chapter 8) will be discussed. For details on the papers, please see Section 1.8.

9.1 Major findings and conclusions

Paper I presents the new system of dynamic chambers and online measurements of NH_3 with a CRDS instrument. The air flow through the system is carefully evaluated, as it has been found to be the most critical operating parameter of dynamic chambers. It is shown that the system allows for measurements with a high time resolution and relatively long measuring periods. The variability within triplicates is low with a coefficient of variance of 13±8%. The possibility to obtain high precision measurements with the system is further demonstrated with the results in Paper III, Paper VII, and Miscellaneous findings. The high precision makes it possible to investigate even small effects of low emission application techniques on NH_3 emission mitigation.

It was found that there was a significant interaction between soil type and application technique (Paper I), which was confirmed by LiDAR measurements of trailing shoe furrows in Paper VI. On average application by trailing shoes lowered NH_3 emission by 19±12% compared to trailing hoses (Paper I). Furthermore, the

importance of correct use of the low emission application techniques was proven to be of high importance. Application at the soil surface gave a reduction of 40±13% compared to trailing hoses applying the slurry 20 cm above the crop canopy (Paper I).

In Paper III a new method for quantification of ESA over time was presented, which relies on fluorescent dye added to the slurry and imaging. Initially, it was attempted to develop a method that would quantify slurry infiltration based on the decrease of fluorescence intensity of the slurry at the soil surface. This proved not to be possible with the design setup and fluorescent dye selected. Accurate measurements of ESA is however possible, where it relies on detection of fluorescence intensity above a threshold. Therefore, accurate quantification of the fluorescence intensity is not required. The ESA measurements can be used as an additional explanatory variable for the soil-slurry interaction after field application of slurry, and can help explain why some slurry treatments and application techniques leads to mitigation of NH_3 emission under certain conditions, while others do not. The method was subsequently used with success under a variety of soil, slurry, and crop conditions (Paper IV, Miscellaneous findings). It was found that ESA alone does not explain differences in NH_3 emission (Paper III, Paper IV, Miscellaneous findings), but is suitable as an explanatory variable in order to gain further insight into the soil-slurry interactions. As an approximation of infiltration effect a calculation of a pH-, TAN-, temperature-, and ESA-normalized NH_3 emission ($R_{C,ESA}$) was proposed in Paper III. For this calculation ESA measurements are important, as ESA from different slurries can have a high variation after field application, due to the spread of less viscous slurries, which needs to be considered when assessing infiltration.

A notable result from Paper IV was the lack of relation between ESA and NH_3 emission under warm conditions. The absence of correlation is hypothesized to be caused by rapid crust formation, as the temperature during slurry application was approximately 20°C during all experiments. In Paper V the mitigating effect of rapid change in DM content at the slurry surface after application at warm temperatures and possible crust formation was further elaborated. The rapid change can be caused by infiltration or evaporation of the liquid part of the slurry. A statistical analysis with data from 19 different experiments with the same measuring system was performed, thereby eliminating one of the main causes of the high variation observed between test organizations in [16] and the effect of air velocity and solar radiation on NH_3 emission. A positive response of the cumulative NH_3 emission to the temperature at application at temperatures between 5°C to approximately 14°C was found.Thereafter, no significant raise in the emission is observed when the temperature increases. This was hypothesized to be caused by changes of DM content and crust formation of the slurry after application at warm ambient air temperatures. This plateau is not included in

the ALFAM2 model [16], which therefore may overestimate emission at warm temperatures.

The findings of Paper II and Paper VII show that it is possible to use the measuring system with a PTR-TOF-MS for measurement, identification, and quantification of NMVOC and H_2S with a low variability and high precision after field application of slurry. The average variation of total NMVOC emission was 18±8% within treatments. These measurements provides new data to a field with limited data and knowledge. In Paper II high H_2S concentrations after application from pig slurry were found. 4-methylphenol accounted for most of the cumulative OAV, whereas carboxylic acids accounted for most of the long-term NMVOC emission and OAV. Using ratios of cumulated NMVOC emission divided by cumulated NH_3 emission based on this study, it is suggested as an update to the current methods for NMVOC emission calculation. The ratios 90 hours after application were found to be 1.15±0.55 and 0.72±0.26 for pig slurry applied by trailing hoses and trailing shoes respectively and is 0.43±0.11 and 0.18±0.04 for cattle slurry applied by trailing hoses and trailing shoes respectively.

9.2 Research perspectives

The present Ph.D. work demonstrates that the new measuring system combining dynamic chambers and online measurements with CRDS or PTR-TOF-MS is useful for quantitative measurements of NH_3 and NMVOC emission from field-applied slurry. The data has a low variance, making it possible to investigate differences in low emission application technologies. Data from 19 experiments were statistically modelled in order to investigate the effect of ambient air temperature on NH_3 emission mitigation. Furthermore, the link between NH_3 emission and ESA was investigated.

Several research questions needing further investigation were identified, through this Ph.D. research. Answering these questions would provide additional insight into the complexities of mitigating NH_3 and NMVOC emission from field applied slurry:

- Further optimization of dynamic chamber system.
  The dynamic chambers have proven useful, but one of their limitations is the need for manual 'hand-application' of the slurry by watering can. A key focus on improving this system should be to develop an approach to allow measurements from field application of slurry applied by real slurry application machinery. This could be obtained by e.g. adding filters to the air inlet of the emission chamber, or by drawing air into the emission chamber through an erected inlet or long inlet tube in order to provide non/low-contaminated air.

- Additional research into characterization of the slurry.
  Slurry parameters has a high influence on its emissions as they play a key role in the soil-slurry interaction, which influence slurry ESA and infiltration. It should be further investigated how quantitative, repeatable standard measurements of viscosity, stickiness, particle size and their distribution, and possible other parameters can be made, in order to use these as possible explanatory variables. Based on this it would be possible to target a potential treatment of manure on e.g. biogas plants and thereby ensure lower NH_3 emission potential.

- Additional research into slurry characterization at the soil surface after application.
  After application to soil slurry undergoes several physical and chemical changes. These are affected by slurry parameters, the slurry-soil interaction, and the climatic conditions. Though these changes, such as slurry surface pH and crust formation, have a high influence on the emission they are not well understood. Further development of measurement techniques linking the changes in slurry to NH_3 emission would be beneficial as some parameters are currently assumed to have a large effect (e.g. crust formation), but are not yet proven. Moreover, methods to characterize the physical changes of the slurry after field application in order to investigate what conditions cause changes in DM content or crust formation of the slurry surface should be developed. Furthermore, additional measurements of soil characteristics could be added as standard measurements when monitoring emissions following land application of slurry, such as penetrometer and descriptions of soil crust formation.

- Development of a quantitative method for infiltration measurements under field conditions.
  A central element of future work should be to develop a method for measurement of slurry infiltration into the soil, as it is speculated that many unanswered questions regarding NH_3 emissions can be answered by this parameter which is not well understood today. It could potentially be a further development of the ESA method using fluorescence dyes, or by combining ESA measurements with methods used to measure water infiltration into soil or new methods, for example optodes [157].

References

[1] V. P. Aneja, W. H. Schlesinger, and J. W. Erisman. Effects of agriculture upon the air quality and climate: Research, policy, and regulations. *Environmental Science and Technology*, 43(12):4234–4240, 2009. ISSN 0013936X. doi: 10.1021/es8024403.

[2] OECD. OECD-FAO Agricultural Outlook 2019-2028, 2019. ISSN 199911426596. URL `http://www.fao.org/3/a-i3818e.pdf`.

[3] E. Crist, C. Mora, and R. Engelman. The interaction of human population, food production, and biodiversity protection. *Science*, 356(6335):260–264, 2017. ISSN 10959203. doi: 10.1126/science.aal2011.

[4] OECD. Agriculture and the environment. (February), 2019.

[5] S. G. Sommer and T. H. Misselbrook. A review of ammonia emission measured using wind tunnels compared with micrometeorological techniques. *Soil Use and Management*, 32(June):101–108, 2016. ISSN 14752743. doi: 10.1111/sum.12209.

[6] F. Montes, R. Meinen, C. Dell, A. Rotz, A. N. Hristov, J. Oh, G. Waghorn, P. J. Gerber, B. Henderson, H. P. S. Makkar, and J. Dijkstra. Mitigation of methane and nitrous oxide emissions from animal operations: II. A review of manure management mitigation options. *American Society of Animal Science*, pages 5070–5094, 2013. ISSN 0146-0404. doi: 10.2527/jas2013-6584.

[7] A. Feilberg, P. Bildsoe, and T. Nyord. Application of PTR-MS for measuring odorant emissions from soil application of manure slurry. *Sensors (Switzerland)*, 15(1):1148–1167, 2015. ISSN 14248220. doi: 10.3390/s150101148.

[8] A. Feilberg, T. Nyord, M. N. Hansen, and S. Lindholst. Chemical evaluation of odor reduction by soil injection of animal manure. *Journal of environmental quality*, 40(5): 1674–82, 2011. ISSN 0047-2425. doi: 10.2134/jeq2010.0499. URL `http://www.ncbi.nlm.nih.gov/pubmed/21869529`.

[9] A. Feilberg, M. J. Hansen, D. Liu, and T. Nyord. Contribution of livestock H2S to total sulfur emissions in a region with intensive animal production. *Nature Communications*, 8(1):1–7, 2017. ISSN 20411723. doi: 10.1038/s41467-017-01016-2. URL `http://dx.doi.org/10.1038/s41467-017-01016-2`.

[10] J. B. Illerup, O.-K. Nielsen, M. Winther, M. H. Mikkelsen, M. Nielsen, P. Fauser, and S. Gyldenkærne. Projection of og SO2, NOX, NMVOC, NH3 and particle emissions - 2005 to 2030. Technical Report 655, University of Aarhus, Denmark, 2008.

[11] O.-K. Nielsen and M. Plejdrup. National emission inventories - Denmark 2020 submission, 2020.

[12] European Union. Directive (EU) 2016/2284 of the European Parliament and of the council - of 14 December 2016 - on the reduction of national emissions of certain atmospheric pollutants, amending Directive 2003/35/EC and repealing Directive 2001/81/EC, 2016. ISSN 1098-6596. URL https://eur-lex.europa.eu/legal-content/EN/TXT/PDF/?uri=CELEX:32016L2284{&}from=EN.

[13] Eurostat. Agri-environmental indicator - ammonia emissions, 2017.

[14] M. Sutton. Too much of a good thing. *Nature*, 472(159):5–7, 2011. ISSN 1476-4687. doi: 10.1038/472159a.

[15] D. P. Van Vuuren, L. F. Bouwman, S. J. Smith, and F. Dentener. Global projections for anthropogenic reactive nitrogen emissions to the atmosphere: An assessment of scenarios in the scientific literature. *Current Opinion in Environmental Sustainability*, 3(5):359–369, 2011. ISSN 18773435. doi: 10.1016/j.cosust.2011.08.014. URL http://dx.doi.org/10.1016/j.cosust.2011.08.014.

[16] S. D. Hafner, A. Pacholski, S. Bittman, M. Carozzi, M. Chantigny, S. Génermont, C. Häni, M. N. Hansen, J. Huijsmans, T. Kupper, T. Misselbrook, A. Neftel, T. Nyord, and S. G. Sommer. A flexible semi-empirical model for estimating ammonia volatilization from field-applied slurry. *Atmospheric Environment*, 199:474–484, 2019. ISSN 1352-2310. doi: S1352231018308069. URL https://www.sciencedirect.com/science/article/pii/S1352231018308069?dgcid=rss{_}sd{_}all.

[17] S. G. Sommer and N. J. Hutchings. Ammonia emission from field applied manure and its reduction - Invited paper. *European Journal of Agronomy*, 15(1):1–15, 2001. ISSN 11610301. doi: 10.1016/S1161-0301(01)00112-5.

[18] J. Webb, B. Pain, S. Bittman, and J. Morgan. The impacts of manure application methods on emissions of ammonia, nitrous oxide and on crop response-A review. *Agriculture, Ecosystems and Environment*, 137(1-2):39–46, 2010. ISSN 01678809. doi: 10.1016/j.agee.2010.01.001. URL http://dx.doi.org/10.1016/j.agee.2010.01.001.

[19] D. R. Jackson and K. A. Smith. Animal manure slurries as a source of nitrogen for cereals; effect of application time on efficiency. *Soil Use and Management*, 13(2):75–81, 1997. ISSN 02660032. doi: 10.1111/j.1475-2743.1997.tb00560.x.

[20] P. K. Mattila, E. Joki-Tokola, and R. Tanni. Effect of treatment and application technique of cattle slurry on its utilization by ley: I. Slurry properties and ammonia volatilization. *Nutrient Cycling in Agroecosystems*, 65(3):221–230, 2003. ISSN 13851314. doi: 10.1023/A:1022619304798.

[21] T. H. Misselbrook, J. A. Laws, and B. F. Pain. Surface application and shallow injection of cattle slurry on grassland: Nitrogen losses, herbage yields and nitrogen recoveries. *Grass and Forage Science*, 51(3):270–277, 1996. ISSN 01425242. doi: 10.1111/j.1365-2494.1996.tb02062.x.

[22] L. Rodhe and M. A. Halling. Grassland yield response to knife/tine slurry injection equipment - benefit or crop damage? *Grass and Forage Science*, 70(2):255–267, 2015. ISSN 13652494. doi: 10.1111/gfs.12106.

[23] SEGES Landbrug og Fødevarer. Kortlægning af udbringning af organisk gødning på grundlag af data i MO. Technical report, 2018.

[24] P. S. Monks, C. Granier, S. Fuzzi, A. Stohl, M. L. Williams, H. Akimoto, M. Amann, A. Baklanov, U. Baltensperger, I. Bey, N. Blake, R. S. Blake, K. Carslaw, O. R. Cooper, F. Dentener, D. Fowler, E. Fragkou, G. J. Frost, S. Generoso, P. Ginoux, V. Grewe, A. Guenther, H. C. Hansson, S. Henne, J. Hjorth, A. Hofzumahaus, H. Huntrieser, I. S.A. Isaksen, M. E. Jenkin, J. Kaiser, M. Kanakidou, Z. Klimont, M. Kulmala, P. Laj, M. G. Lawrence, J. D. Lee, C. Liousse, M. Maione, G. McFiggans, A. Metzger, A. Mieville, N. Moussiopoulos, J. J. Orlando, C. D. O'Dowd, P. I. Palmer, D. D. Parrish, A. Petzold, U. Platt, U. Pöschl, A. S.H. Prévôt, C. E. Reeves, S. Reimann, Y. Rudich, K. Sellegri, R. Steinbrecher, D. Simpson, H. ten Brink, J. Theloke, G. R. van der Werf, R. Vautard, V. Vestreng, Ch Vlachokostas, and R. von Glasow. Atmospheric composition change - global and regional air quality. *Atmospheric Environment*, 43(33):5268–5350, 2009. ISSN 13522310. doi: 10.1016/j.atmosenv.2009.08.021.

[25] IPCC. *2006 IPCC Guidelines for National Greenhouse Gas Inventories*. IGES, Japan, 2006.

[26] A. Feilberg, N. Dorno, and T. Nyord. Odour emissions following land spreading of animal slurry assessed by proton-transfer-reaction mass spectrometry (PTR-MS). *Chemical Engineering Transactions*, 23:111–116, 2010. doi: 10.3303/CET1023019.

[27] Dezhao Liu, Tavs Nyord, Li Rong, and Anders Feilberg. Real-time quantification of emissions of volatile organic compounds from land spreading of pig slurry measured by PTR-MS and wind tunnels. *Science of the Total Environment*, 639:1079–1087, 2018. ISSN 18791026. doi: 10.1016/j.scitotenv.2018.05.149. URL `https://doi.org/10.1016/j.scitotenv.2018.05.149`.

[28] D. Parker, J. Gilley, B. Woodbury, K. H. Kim, G. Galvin, S. L. Bartelt-Hunt, X. Li, and D. D. Snow. Odorous VOC emission following land application of swine manure slurry. *Atmospheric Environment*, 66:91–100, 2013. ISSN 13522310. doi: 10.1016/j.atmosenv.2012.01.001.

[29] B. L. Woodbury, J. E. Gilley, D. B. Parker, D. B. Marx, and R. A. Eigenberg. Emission of volatile organic compounds as affected by rate of application of cattle manure. *Transactions of the ASABE*, 59(3):885–895, 2016. ISSN 21510032. doi: 10.13031/trans.59.11374.

[30] European Environment Agency. National Emission Ceilings Directive. NEC Directive reporting status 2019. (April 2019):5–12, 2019. URL `https://www.eea.europa.eu/themes/air/national-emission-ceilings/nec-directive-reporting-status-2019/download.pdf.static{%}0Ahttps://www.eea.europa.eu/data-and-maps/dashboards/necd-directive-data-viewer`.

[31] H. M. Hanna, D. S. Bundy, J. C. Lorimor, S. K. Mickelson, S. W. Melvin, and D. C. Erbach. Manure incorporation equipment effects on odor, residue cover, and crop yield. *Applied Engineering in Agriculture*, 16(6):621–627, 2000. ISSN 08838542.

[32] S. G. Sommer and A. Feilberg. Gaseous emissions of ammonia and malodorous gases. In *Animal Manure Recycling*, chapter 8, pages 131–151. John Wiley and Sons, Ltd., 2013. doi: 10.1002/9781118676677.

[33] Y. Nagata. Measurement of odor threshold by triangle odor bag method. *Odor Measurement Review*, pages 118–127, 2003.

[34] M. J. Hansen, P. L. Kasper, A. P. S. Adamsen, and A. Feilberg. Key odorants from pig production based on improved measurements of odor threshold values combining olfactometry and proton-transfer-reaction mass spectrometry (PTR-MS). *Sensors (Switzerland)*, 18(3), 2018. ISSN 14248220. doi: 10.3390/s18030788.

[35] S. G. Sommer, S. Génermont, P. Cellier, N. J. Hutchings, J. E. Olesen, and T. Morvan. Processes controlling ammonia emission from livestock slurry in the field. *European Journal of Agronomy*, 19(4):465–486, 2003. ISSN 11610301. doi: 10.1016/S1161-0301(03)00037-6.

[36] J. Ni. Mechanistic models of ammonia release from liquid manure: A review. *Journal of Agricultural and Engineering Research*, 72(1):1–17, 1999. ISSN 00218634. doi: 10.1006/jaer.1998.0342.

[37] D. B. Parker, E. A. Caraway, M. B. Rhoades, N. A. Cole, R. W. Todd, D. Donnell, J. Spears, and K. D. Casey. Effect of wind tunnel air velocity on VOC flux rates from CAFO manure and wastewater. In *2008 Providence, Rhode Island, June 29 - July 2, 2008*, Providence, Rhode Island, 2008. ASABE. ISBN 9781605605364 (ISBN). doi: 10.13031/2013.25026. URL `http://elibrary.asabe.org/abstract.asp?JID=5{&}AID=25026{&}CID=prov2008{&}T=1`.

[38] S. D. Hafner, F. Montes, and C. Alan Rotz. The role of carbon dioxide in emission of ammonia from manure. *Atmospheric Environment*, 66:63–71, 2013. ISSN 13522310. doi: 10.1016/j.atmosenv.2012.01.026. URL `http://dx.doi.org/10.1016/j.atmosenv.2012.01.026`.

[39] R. P. Schwarzenbach, P. M. Sxchwend, and D. M. Imboden. *Environmental organic chemistry*. Wiley-Interscience, John Wiley & Sons, Inc. Canada, second edi edition, 2003.

[40] J. F. M. Huijsmans, G. D. Vermeulen, J. M. G. Hol, and P. W. Goedhart. A model for estimating seasonal trends of ammonia emission from cattle manure applied to grassland in the Netherlands. *Atmospheric Environment*, 173(2018):231–238, 2018. ISSN 18732844. doi: 10.1016/j.atmosenv.2017.10.050. URL `https://doi.org/10.1016/j.atmosenv.2017.10.050`.

[41] D. B. Parker, A. N. Cole, K. D. Casey, G. Galvin, R. Ormerod, C. S. Paris, E. A. Caraway, and M. B. Rhoades. Wind tunnels vs. flux chambers: Area source emission measurements and the necessity for VOC and odour correction factors. *Proc. 19th Int. Clean Air and Environ. Conf., Perth, Australia*, pages 6–9, 2009.

[42] S. G. Sommer and R. R. Sherlock. pH and buffer component dynamic in the surface layers of animal slurries. *Journal of Agricultural*, 127:109–116, 1996.

[43] L. W. de Jonge, S. G. Sommer, O. H. Jacobsen, and J. Djurhuus. Infiltration of slurry liquid and ammonia volatilization from pig and cattle slurry applied to harrowed and stubble soils. *Soil Science*, 169(10):729–736, 2004. ISSN 0038-075X. doi: 10.1097/01.ss.0000146019.31065.ab. URL `http://content.wkhealth.com/linkback/openurl?sid=WKPTLP:landingpage{&}an=00010694-200410000-00006`.

[44] T. H. Misselbrook, D. Scholefield, and R. Parkinson. Using time domain reflectometry to characterize cattle and pig slurry infiltration into soil. *Soil Use and Management*, 21(2):167–172, 2005. ISSN 02660032. doi: 10.1079/SUM2005316. URL `http://doi.wiley.com/10.1079/SUM2005316`.

[45] J. Braschkat, T. Mannheim, and H. Marschner. Estimation of ammonia losses after application of liquid cattle manure on grassland. *Pflanzenernähr. Bodenk.*, 160:117–123, 1997.

[46] S. D. Hafner, A. Pacholski, S. Bittman, W. Burchill, W. Bussink, M. Chantigny, M. Carozzi, S. Génermont, C. Häni, M. N. Hansen, J. Huijsmans, D. Hunt, T. Kupper, G. Lanigan, B. Loubet, T. Misselbrook, J. J. Meisinger, A. Neftel, T. Nyord, S. V. Pedersen, J. Sintermann, R. B. Thompson, B. Vermeulen, A. V. Vestergaard, P. Voylokov, J. R. Williams, and S. G. Sommer. The ALFAM2 database on ammonia emission from field-applied manure: Description and illustrative analysis. *Agricultural and Forest Meteorology*, 258(August 2017):66–79, 2018. ISSN 01681923. doi: 10.1016/j.agrformet.2017.11.027. URL `https://doi.org/10.1016/j.agrformet.2017.11.027`.

[47] A. Feilberg and S. G. Sommer. Ammonia and malodorous gases: Sources and abatement technologies. In *Animal Manure Recycling*, chapter 9, pages 153–176. John Wiley and Sons, Ltd., 2013. doi: 10.1002/9781118676677.

[48] S. G. Sommer, G. Q. Zhang, A. Bannink, D. Chadwick, T. Misselbrook, R. Harrison, N. J. Hutchings, H. Menzi, G. J. Monteny, J. Q. Ni, O. Oenema, and J. Webb. Algorithms determining ammonia emission from buildings housing cattle and pigs and from manure stores. *Advances in Agronomy*, 89(December 2006):261–335, 2006. ISSN 00652113. doi: 10.1016/S0065-2113(05)89006-6.

[49] C. J. Clanton, D. A. Nichols, R. L. Moser, and D. R. Ames. Swine manure characterization as affected by environmental temperature, dietary level intake, and dietary fat addition. *American Society of Agricultural Engineers*, 34(5):2164–2170, 1991.

[50] M. Hjorth, K. V. Christensen, M. L. Christensen, and S. G. Sommer. *Solid-liquid separation of animal slurry in theory and practice*, volume 2. 2010. ISBN 9789400703940. doi: 10.1051/agro.

[51] I. K. Hindrichsen, H. R. Wettstein, A. Machmüller, and M. Kreuzer. Methane emission, nutrient degradation and nitrogen turnover in dairy cows and their slurry at different milk production scenarios with and without concentrate supplementation. *Agriculture, Ecosystems and Environment*, 113(1-4):150–161, 2006. ISSN 01678809. doi: 10.1016/j.agee.2005.09.004.

[52] D. R. Chadwick, F. John, B. F. Pain, B. J. Chambers, and J. Williams. Plant uptake of nitrogen from the organic nitrogen fraction of animal manures: A laboratory experiment. *Journal of Agricultural Science*, 134(2):159–168, 2000. ISSN 00218596. doi: 10.1017/S0021859699007510.

[53] H. B. Møller, S. G. Sommer, and B. K. Ahring. Methane productivity of manure, straw and solid fractions of manure. *Biomass and Bioenergy*, 26(5):485–495, 2004. ISSN 09619534. doi: 10.1016/j.biombioe.2003.08.008.

[54] J. Webb, P. Sørensen, G. Velthof, B. Amon, M. Pinto, L. Rodhe, E. Salomon, N. Hutchings, Pi. Burczyk, and J. Reid. An assessment of the variation of manure nitrogen efficiency throughout Europe and an appraisal of means to increase manure-N efficiency. *Advances in Agronomy*, 119:371–441, 2013. ISSN 00652113. doi: 10.1016/B978-0-12-407247-3.00007-X. URL `http://dx.doi.org/10.1016/B978-0-12-407247-3.00007-X`.

[55] S. G. Sommer and J. E. Olesen. Effects of dry matter content and temperature on ammonia loss from surface-applied cattle slurry. *Journal of Environmental Quality*, 20: 679–683, 1991. doi: doi:10.2134/jeq1991.00472425002000030029x.

[56] S. D. Hafner, S. G. Sommer, V. Petersen, and R. Markfoged. Effects of carbon dioxide hydration kinetics and evaporative convection on pH profile development during interfacial mass transfer of ammonia and carbon dioxide. *Heat and Mass Transfer/Waerme- und Stoffuebertragung*, 53(4):1335–1342, 2017. ISSN 14321181. doi: 10.1007/s00231-016-1910-6.

[57] T. H. Misselbrook, F. A. Nicholson, and B. J. Chambers. Predicting ammonia losses following the application of livestock manure to land. *Bioresource Technology*, 96(2): 159–168, 2005. ISSN 09608524. doi: 10.1016/j.biortech.2004.05.004.

[58] K. A. Smith, D. R. Jackson, T. H. Misselbrook, B. F. Pain, and R. A. Johnson. Reduction of ammonia emission by slurry application techniques. *Journal of Agricultural Engineering Research*, 78(3):233–243, 2000. ISSN 00218634. doi: 10.1006/jaer.2000.0639. URL `http://linkinghub.elsevier.com/retrieve/pii/S0021863400906395`.

[59] S. G. Sommer, L. S. Jensen, S. B. Clausen, and H. T. Søgaard. Ammonia volatilization from surface-applied livestock slurry as affected by slurry composition and slurry infiltration depth. *Journal of Agricultural Science*, (April 2006):229–235, 2006. doi: 10.1017/S0021859606006022.

[60] H. Landry, C. Laguë, and M. Roberge. Physical and rheological properties of manure products. *Applied Engineering in Agriculture*, 20(3):277–288, 2004.

[61] O. Thygesen, J. M. Triolo, and S. G. Sommer. Indicators of physical properties and plant nutrient content of animal slurry and separated slurry. *Biological Engineering Transactions*, 5(3):123–135, 2012. ISSN 19342799.

[62] B. Amon, V. Kryvoruchko, T. Amon, and S. Zechmeister-Boltenstern. Methane, nitrous oxide and ammonia emissions during storage and after application of dairy cattle slurry and influence of slurry treatment. *Agriculture, Ecosystems and Environment*, 112(2-3): 153–162, 2006. ISSN 01678809. doi: 10.1016/j.agee.2005.08.030.

[63] J. P. Frost, R. J. Laughlin, and R. J. Stevens. Effect of separation and acidification of cattle slurry on ammonia volatilization and on the efficiency of slurry nitrogen for herbage production. *The Journal of Agricultural Science*, 115(1):49–56, 1990. ISSN 14695146. doi: 10.1017/S0021859600073901.

[64] T. Nyord, M. N. Hansen, and T. S. Birkmose. Ammonia volatilisation and crop yield following land application of solid-liquid separated, anaerobically digested, and soil injected animal slurry to winter wheat. *Agriculture, Ecosystems and Environment*, 160:75–81, 2012. ISSN 01678809. doi: 10.1016/j.agee.2012.01.002. URL `http://dx.doi.org/10.1016/j.agee.2012.01.002`.

[65] L. Masse, D. I. Massé, V. Beaudette, and M. Muir. Size distribution and composition of particles in raw and anaerobically digested swine manure. *Transactions of the American Society of Agricultural Engineers*, 48(5):1943–1949, 2005. ISSN 00012351. doi: 10.13031/2013.20003.

[66] I. M. Nasir, T. I. Mohd Ghazi, and R. Omar. Anaerobic digestion technology in livestock manure treatment for biogas production: A review. *Engineering in Life Sciences*, 12(3): 258–269, 2012. ISSN 16180240. doi: 10.1002/elsc.201100150.

[67] S. Sakar, K. Yetilmezsoy, and E. Kocak. Anaerobic digestion technology in poultry and livestock waste treatment - A literature review. *Waste Management and Research*, 27(1): 3–18, 2009. ISSN 0734242X. doi: 10.1177/0734242X07079060.

[68] G. H. Rubæk, K. Henriksen, J. Petersen, B. Rasmussen, and S. G. Sommer. Effect of application technique and anaerobic digestion on gaseous nitrogen loss from animal slurry applied to ryegrass. *Journal of Agricultural Science*, 126:481–492, 1996.

[69] S. Wulf, M. Maeting, and J. Clemens. Application technique and slurry co-fermentation effects on ammonia, nitrous oxide, and methane emissions after spreading. *Journal of Environment Quality*, 31(6):1789, 2002. ISSN 1537-2537. doi: 10.2134/jeq2002.1795. URL `https://www.agronomy.org/publications/jeq/abstracts/31/6/1789`.

[70] J. Clemens, M. Trimborn, P. Weiland, and B. Amon. Mitigation of greenhouse gas emissions by anaerobic digestion of cattle slurry. *Agriculture, Ecosystems and Environment*, 112(2-3):171–177, 2006. ISSN 01678809. doi: 10.1016/j.agee.2005.08.016.

[71] D. Fangueiro, M. Hjorth, and F. Gioelli. Acidification of animal slurry - a review. *Journal of environmental management*, 149:46–56, 2015. ISSN 10958630. doi: 10.1016/j.jenvman.2014.10.001.

[72] Miljø- og Fødevareministeriet. Lov om miljøgodkendelse m.v. af husdyrbrug, 2006.

[73] D. Fangueiro, S. Surgy, I. Fraga, F. Cabral, and J. Coutinho. Band application of treated cattle slurry as an alternative to slurry injection: Implications for gaseous emissions, soil quality, and plant growth. *Agriculture, Ecosystems and Environment*, 211:102–111, 2015. ISSN 01678809. doi: 10.1016/j.agee.2015.06.003. URL `http://dx.doi.org/10.1016/j.agee.2015.06.003`.

[74] P. Kai, P. Pedersen, J. E. Jensen, M. N. Hansen, and S. G. Sommer. A whole-farm assessment of the efficacy of slurry acidification in reducing ammonia emissions. *European Journal of Agronomy*, 28(2):148–154, 2008. ISSN 11610301. doi: 10.1016/j.eja.2007.06.004.

[75] T. Nyord, L. Liu, J. Eriksen, and A. P. S. Adamsen. Effect of acidification and soil injection of animal slurry on ammonia and odour emission. In *Ramiran*, 2013.

[76] B. F. Pain, T. H. Misselbrook, and Y. J. Rees. Effects of nitrification inhibitor and acid addition to cattle slurry on nitrogen losses and herbage yields. *Grass and Forage Science*, 49(2):209–215, 1994. ISSN 13652494. doi: 10.1111/j.1365-2494.1994.tb01994.x.

[77] D. W. Bussink, J. F. Huijsmans, and J. J. Ketelaars. Ammonia volatilization from nitric-acid-treated cattle slurry surface applied to grassland, 1994. ISSN 00282928.

[78] M. J. Bell, N. J. Hinton, J. M. Cloy, C. F. E. Topp, R. M. Rees, J. R. Williams, T. H. Misselbrook, and D. R. Chadwick. How do emission rates and emission factors for nitrous oxide and ammonia vary with manure type and time of application in a Scottish farmland? *Geoderma*, 264:81–93, 2015. ISSN 00167061. doi: 10.1016/j.geoderma.2015.10.007. URL `http://dx.doi.org/10.1016/j.geoderma.2015.10.007`.

[79] J. Martínez-Lagos, F. Salazar, M. Alfaro, and T. Misselbrook. Ammonia volatilization following dairy slurry application to a permanent grassland on a volcanic soil. *Atmospheric Environment*, 80:226–231, 2013. ISSN 13522310. doi: 10.1016/j.atmosenv.2013.08.005. URL `http://dx.doi.org/10.1016/j.atmosenv.2013.08.005`.

[80] D. Or, M. Tuller, and J. M. Wraith. Basic relationships and the soil phases under equilibrium conditions. In *Agricultural & environmental soil physics*, chapter 1, pages 3–6. 2009.

[81] H. P. Blume, G. W. Brümmer, H. Fleige, R. Horn, E. Kandeler, I Kögel-Knabner, R. Kretszchmar, K. Stahr, and M. B. Wilke. *Scheffer/Schachtschabel Soil Science*. Springer-Verlag, Berlin Heidelberg, 1st edition, 2016.

[82] S. G. Sommer, E. Friis, A. Bach, and J. K. Schjørring. Ammonia volatilization from pig slurry applied with trail hoses or broadspread to winter wheat: Effects of crop developmental stage, microclimate, and leaf ammonia absorption. *Ecosystem Processes*, 26: 1153–1160, 1997.

[83] S. G. Sommer and O. H. Jacobsen. Infiltration of slurry liquid and volatilization of ammonia from surface applied pig slurry as affected by soil water content. *Journal of Agricultural Science*, 132(1999):297–303, 1999. ISSN 0021-8596. doi: 10.1017/S0021859698006261. URL `isi:000081601400006{%}5CnC:{%}5Creference{%}5C452.pdf`.

[84] C. Häni, J. Sintermann, T. Kupper, M. Jocher, and A. Neftel. Ammonia emission after slurry application to grassland in Switzerland. *Atmospheric Environment*, 125:92–99, 2016. ISSN 18732844. doi: 10.1016/j.atmosenv.2015.10.069. URL `http://dx.doi.org/10.1016/j.atmosenv.2015.10.069`.

[85] T. H. Misselbrook, K. A. Smith, R. A. Johnson, and B. F. Pain. Slurry application techniques to reduce ammonia emissions: Results of some UK field-scale experiments. *Biosystems Engineering*, 81(3):313–321, 2002. ISSN 15375110. doi: 10.1006/bioe.2001.0017.

[86] P. Rochette, D. Guilmette, M. H. Chantigny, D. Angers, J. D. MacDonald, N. Bertrand, L.-É. Parent, D. Côté, and M. O. Gasser. Ammonia volatilization following application of pig slurry increases with slurry interception by grass foliage. *Canadian Journal of Soil Science*, 88(4):585–593, 2008. ISSN 0008-4271. doi: 10.4141/CJSS07083.

[87] L. Rodhe, M. Pell, and S. Yamulki. Nitrous oxide, methane and ammonia emissions following slurry spreading on grassland. *Soil Use and Management*, 22(3):229–237, 2006. ISSN 02660032. doi: 10.1111/j.1475-2743.2006.00043.x.

[88] L. Rodhe, T. Rydberg, and G. Gebresenbet. The influence of shallow injector design on ammonia emissions and draught requirement under different soil conditions. *Biosystems Engineering*, 89(2):237–251, 2004. ISSN 15375110. doi: 10.1016/j.biosystemseng.2004.07.001.

[89] E. G. Beauchamp, G. E. Kidd, and G. Thurtell. Ammonia volatilization from liquid dairy cattle manure in the field. *Canadian Journal of Soil Science*, 62(1):11–19, 1982. ISSN 0008-4271. doi: 10.4141/cjss82-002. URL `http://pubs.aic.ca/doi/abs/10.4141/cjss82-002`.

[90] T. Mannheim, J. Braschkat, and H. Marschner. Measurement of ammonia emission after liquid manure application: II. Comparison of the wind tunnel and the IHF method under field conditions. *Z. Pflanzenernähr. Bodenk.*, 158:215–219, 1995.

[91] R. Vandré, J. Clemens, H. Goldbach, and M. Kaupenjohann. NH3 and N2O emissions after landspreading of slurry as influenced by application technique and dry matter-reduction. I. NH3 emissions. *Zeitschrift für Pflanzenernährung und Bodenkunde*, 160(2): 303–307, 1997. ISSN 00443263. doi: 10.1002/jpln.19971600226.

[92] K. Cuddington, M. J. Fortin, L. R. Gerber, A. Hastings, A. Liebhold, M. O'connor, and C. Ray. Process-based models are required to manage ecological systems in a changing world. *Ecosphere*, 4(2):1–12, 2013. ISSN 21508925. doi: 10.1890/ES12-00178.1.

[93] H. T. Søgaard, S. G. Sommer, N. J. Hutchings, J. F.M. Huijsmans, D. W. Bussink, and F. Nicholson. Ammonia volatilization from field-applied animal slurry-the ALFAM model. *Atmospheric Environment*, 36(20):3309–3319, 2002. ISSN 13522310. doi: 10.1016/S1352-2310(02)00300-X.

[94] S. Génermont and P. Cellier. A mechanistic model for estimating ammonia volatilization from slurry applied to bare soil. *Agricultural and Forest Meteorology*, 88(1-4):145–167, 1997. ISSN 01681923. doi: 10.1016/S0168-1923(97)00044-0.

[95] E. Smith, R. Gordon, C. Bourque, A. Campbell, S. Génermont, P. Rochette, and M. Mkhabela. Simulating ammonia loss from surface-applied manure. *Canadian Journal of Soil Science*, 89(3):357–367, 2009. ISSN 00084271. doi: 10.4141/CJSS08047.

[96] P. J. Moseley, T. H. Misselbrook, B. F. Pain, R. Earl, and R. J. Godwin. The effect of injector tine design on odour and ammonia emissions following injection of bio-solids into arable cropping. *Journal of Agricultural and Engineering Research*, 71(4):385–394, 1998. ISSN 00218634. doi: 10.1006/jaer.1998.0337.

[97] T. H. Misselbrook, F. A. Nicholson, B. J. Chambers, and R. A. Johnson. Measuring ammonia emissions from land applied manure: An intercomparison of commonly used samplers and techniques. *Environmental Pollution*, 135(3 SPEC. ISS.):389–397, 2005. ISSN 02697491. doi: 10.1016/j.envpol.2004.11.012.

[98] T. Nyord, H. T. Søgaard, M. N. Hansen, and L. S. Jensen. Injection methods to reduce ammonia emission from volatile liquid fertilisers applied to growing crops. *Biosystems Engineering*, 100(2):235–244, 2008. ISSN 15375110. doi: 10.1016/j.biosystemseng.2008.01.013.

[99] A. Pacholski, G. Cai, R. Nieder, J. Richter, X. Fan, Z. Zhu, and M. Roelcke. Calibration of a simple method for determining ammonia volatilization in the field - Comparative measurements in Henan Province, China. *Nutrient Cycling in Agroecosystems*, 74(3):259–273, 2006. ISSN 13851314. doi: 10.1007/s10705-006-9003-4.

[100] B. F. Pain, V. R. Phillips, C. R. Clarkson, and J. V. Klarenbeek. Loss of nitrogen through ammonia volatilisation during and following the application of pig or cattle slurry to grassland. *Journal of the Science of Food and Agriculture*, 47(1):1–12, 1989. ISSN 10970010. doi: 10.1002/jsfa.2740470102.

[101] R. Bhandral, S. Bittman, G. Kowalenko, K. Buckley, M. H. Chantigny, D. E. Hunt, F. Bounaix, and A. Friesen. Enhancing soil infiltration reduces gaseous emissions and improves N uptake from applied dairy slurry. *Journal of Environment Quality*, 38(4):1372, 2009. ISSN 1537-2537. doi: 10.2134/jeq2008.0287. URL `https://www.agronomy.org/publications/jeq/abstracts/38/4/1372`.

[102] D. R. Lockyer. A system for the measurement in the field of losses of ammonia through volatilisation. *Journal of the Science of Food and Agriculture*, 35(8):837–848, 1984. ISSN 10970010. doi: 10.1002/jsfa.2740350805.

[103] E. C. C. Miola, P. Rochette, M. H. Chantigny, D. A. Angers, C. Aita, M.-O. Gasser, D. E. Pelster, and N. Bertrand. Ammonia volatilization after surface application of laying-hen and broiler-chicken manures. *Journal of Environment Quality*, 43(6):1864, 2014. ISSN 0047-2425. doi: 10.2134/jeq2014.05.0237. URL `https://dl.sciencesocieties.org/publications/jeq/abstracts/43/6/1864`.

[104] B. F. Pain, V. R. Phillips, C. R. Clarkson, T. H. Misselbrook, Y. J. Rees, and J. W. Farrent. Odour and ammonia emission following the spreading of aerobically-treated pig slurry on grassland. *Biological Wastes*, 34:149–160, 1990.

[105] B. F. Pain, T. H. Misselbrook, C. R. Clarkson, and Y. J. Rees. Odour and ammonia emissions following the spreading of anaerobically-digested pig slurry on grassland. *Biological Wastes*, 34(3):259–267, 1990. ISSN 02697483. doi: 10.1016/0269-7483(90)90027-P.

[106] P. Rochette, D. A. Angers, M. H. Chantigny, M.-O. Gasser, J. D. MacDonald, D. E. Pelster, and N. Bertrand. NH 3 volatilization, soil concentration and soil pH following subsurface banding of urea at increasing rates. *Canadian Journal of Soil Science*, 93(2): 261–268, 2013. ISSN 0008-4271. doi: 10.4141/cjss2012-095. URL `http://pubs.aic.ca/doi/abs/10.4141/cjss2012-095`.

[107] P. Rochette, D. A. Angers, M. H. Chantigny, J. D. MacDonald, M. O. Gasser, and N. Bertrand. Reducing ammonia volatilization in a no-till soil by incorporating urea and pig slurry in shallow bands. *Nutrient Cycling in Agroecosystems*, 84(1):71–80, 2009. ISSN 13851314. doi: 10.1007/s10705-008-9227-6.

[108] P. Rochette, M. H. Chantigny, D. Angers, N. Bertrand, and D. Côté. Ammonia volatilization and soil nitrogen dynamics following fall application of pig slurry on canola crop residues. *Canadian Journal of Soil Science*, 81(4):515–523, 2001. ISSN 0008-4271. doi: 10.4141/S00-044.

[109] S. G. Sommer and A. K. Ersbøll. Soil tillage effects on ammonia volatilization from surface-applied or injected animal slurry. *Journal of Environmental Quality*, 23(3):493–498, 1994. ISSN 0047-2425. doi: 10.2134/jeq1994.00472425002300030013x.

[110] D. E. Pelster, M. H. Chantigny, D. A. Angers, N. Bertrand, J. D. MacDonald, and P. Rochette. Can soil clay content predict ammonia volatilization losses from subsurface-banded urea in eastern Canadian soils? *Canadian Journal of Soil Science*, 98(3):556–565, 2018. ISSN 0008-4271. doi: 10.1139/cjss-2018-0036. URL `http://www.nrcresearchpress.com/doi/10.1139/cjss-2018-0036`.

[111] J. V. Klarenbeek, B. F. Pain, V. R. Phillips, and D. R. Lockyer. A comparison of methods for use in the measurement of ammonia emissions following the application of livestock wastes to land. *International Journal of Environmental Analytical Chemistry*, 53(3): 205–218, 1993. ISSN 10290397. doi: 10.1080/03067319308045990.

[112] S. B. Shah, P. W. Westerman, and J. Arogo. Measuring ammonia concentrations and emissions from agricultural land and liquid surfaces: a review. *Journal of the Air & Waste Management Association (1995)*, 56(7):945–960, 2006. ISSN 1096-2247. doi: 10.1080/10473289.2006.10464512.

[113] K. Smith, T. Cumby, J. Lapworth, T. Misselbrook, and A. Williams. Natural crusting of slurry storage as an abatement measure for ammonia emissions on dairy farms. *Biosystems Engineering*, 97(4):464–471, 2007. ISSN 15375110. doi: 10.1016/j.biosystemseng.2007.03.037.

[114] J. A. Businger. Evaluation of the accuracy with which dry deposition can be measured with current micrometeorological techniques. *Journal of Climate and Applied Meteorology*, 25(8):100–1124, 1985.

[115] B. Loubet, S. Génermont, R. Ferrara, C. Bedos, C. Decuq, E. Personne, O. Fanucci, B. Durand, G. Rana, and P. Cellier. An inverse model to estimate ammonia emissions from fields. *European Journal of Soil Science*, 61(5):793–805, 2010. ISSN 13510754. doi: 10.1111/j.1365-2389.2010.01268.x.

[116] J. C. Ryden and D. R. Lockyer. Evaluation of a system of wind tunnels for field studies of ammonia loss from grassland through volatilisation. *Journal of the Science of Food and Agriculture*, 36(9):781–788, 1985. ISSN 10970010. doi: 10.1002/jsfa.2740360904.

[117] C. K. Saha, W. Wu, G. Zhang, and B. Bjerg. Assessing effect of wind tunnel sizes on air velocity and concentration boundary layers and on ammonia emission estimation using computational fluid dynamics (CFD). *Computers and Electronics in Agriculture*, 78(1):49–60, 2011. ISSN 01681699. doi: 10.1016/j.compag.2011.05.011. URL `http://dx.doi.org/10.1016/j.compag.2011.05.011`.

[118] L. Hörtnagl, I. Bamberger, M. Graus, T. M. Ruuskanen, R. Schnitzhofer, M. Müller, A. Hansel, and G. Wohlfahrt. Biotic, abiotic, and management controls on methanol exchange above a temperate mountain grassland. *Journal of Geophysical Research: Biogeosciences*, 116(3):1–15, 2011. ISSN 01480227. doi: 10.1029/2011JG001641.

[119] N. Hudson and G. A. Ayoko. Odour sampling. 2. Comparison of physical and aerodynamic characteristics of sampling devices: A review. *Bioresource Technology*, 99(10):3993–4007, 2008. ISSN 09608524. doi: 10.1016/j.biortech.2007.03.043.

[120] B. Eklund. Practical guidance for flux chamber measurements of fugitive volatile organic emission rates. *Journal of the Air and Waste Management Association*, 42(12):1583–1591, 1992. ISSN 10473289. doi: 10.1080/10473289.1992.10467102.

[121] R. J. Smith and P. J. Watts. Determination of odour emission rates from cattle feedlots: Part 2, Evaluation of two wind tunnels of different size. *Journal of Agricultural Engineering Research*, 58(4):231–240, 1994. ISSN 00218634. doi: 10.1006/jaer.1994.1053.

[122] N. Hudson and G. A. Ayoko. Odour sampling 1: Physical chemistry considerations. *Bioresource Technology*, 99(10):3982–3992, 2008. ISSN 09608524. doi: 10.1016/j.biortech.2007.04.034.

[123] D. E. Kissel, H. L. Brewer, and G. F. Arkin. Design and test of a field sampler for ammonia volatilization. *Soil Science Society of America Journal*, 41(6):1133–1138, 1977. ISSN 0361-5995. URL `http://apps.isiknowledge.com/full{_}record.do?product=WOS{&}search{_}mode=GeneralSearch{&}qid=13{&}SID=3FE46IjkJoFH3g7aPLH{&}page=1{&}doc=1`.

[124] K. Jiang, P. J. Bliss, and T. J. Schulz. The development of a sampling system for determining odor emission rates from areal surfaces: Part 1. Aerodynamic performance. *Journal of the Air and Waste Management Association*, 45(10):831–832, 1995. ISSN 21622906. doi: 10.1080/10473289.1995.10467424.

[125] S. M. McGinn and H. H. Janzen. Ammonia sources in agriculture and their measurement. *Canadian Journal of Soil Science*, 78(1):139–148, 1998. ISSN 0008-4271. doi: 10.4141/S96-059.

[126] B. Nozière, M. Kalberer, M. Claeys, J. Allan, B. D'Anna, S. Decesari, E. Finessi, M. Glasius, I. Grgić, J. F. Hamilton, T. Hoffmann, Y. Iinuma, M. Jaoui, A. Kahnt, C. J. Kampf, I. Kourtchev, W. Maenhaut, N. Marsden, S. Saarikoski, J. Schnelle-Kreis, J. D. Surratt, S. Szidat, R. Szmigielski, and A. Wisthaler. The molecular identification of organic compounds in the atmosphere: state of the art and challenges. *Chemical Reviews*, 115(10): 3919–3983, 2015. ISSN 15206890. doi: 10.1021/cr5003485.

[127] E. Dinuccio, W. Berg, and P. Balsari. Effects of mechanical separation on GHG and ammonia emissions from cattle slurry under winter conditions. *Animal Feed Science and Technology*, 166-167(2011):532–538, 2011. ISSN 03778401. doi: 10.1016/j.anifeedsci.2011.04.037. URL `http://dx.doi.org/10.1016/j.anifeedsci.2011.04.037`.

[128] S. Shadman, C. Rose, and A. P. Yalin. Open-path cavity ring-down spectroscopy sensor for atmospheric ammonia. *Applied Physics B: Lasers and Optics*, 122(7):1–9, 2016. ISSN 09462171. doi: 10.1007/s00340-016-6461-5.

[129] J. Iqbal, M.J. Castellano, and T. B. Parkin. Evaluation of photoacoustic infrared spectroscopy for simultaneous measurement of N2O and CO2 gas concentrations and fluxes at the soil surface. *Global Change Biology*, 19(1):327–336, 2013. ISSN 13541013. doi: 10.1111/gcb.12021.

[130] D. Liu, L. Rong, J. Kamp, X. Kong, A. P. S. Adamsen, A. Chowdhury, and A. Feilberg. Photoacoustic measurement with infrared band-pass filters significantly overestimates NH3 emissions from cattle houses due to volatile organic compound (VOC) interferences. *Atmospheric Measurement Techniques*, 13(1):259–272, 2020. ISSN 18678548. doi: 10.5194/amt-13-259-2020.

[131] G. Berden, R. Peeters, and G. Meijer. Cavity ring-down spectroscopy: Experimental schemes and applications. *International Reviews in Physical Chemistry*, 19(4):565–607, 2000. ISSN 0144235X. doi: 10.1080/014423500750040627.

[132] K. Von Bobrutzki, C. F. Braban, D. Famulari, S. K. Jones, T. Blackall, T. E.L. Smith, M. Blom, H. Coe, M. Gallagher, M. Ghalaieny, M. R. McGillen, C. J. Percival, J. D. Whitehead, R. Ellis, J. Murphy, A. Mohacsi, A. Pogany, H. Junninen, S. Rantanen, M. A. Sutton, and E. Nemitz. Field inter-comparison of eleven atmospheric ammonia measurement techniques. *Atmospheric Measurement Techniques*, 3(1):91–112, 2010. ISSN 18678548. doi: 10.5194/amt-3-91-2010.

[133] M. J. Hansen, K.E. N. Jonassen, M. M. Løkke, A. P. S. Adamsen, and A. Feilberg. Multivariate prediction of odor from pig production based on in-situ measurement of odorants. *Atmospheric Environment*, 135:50–58, 2016. ISSN 18732844. doi: 10.1016/j.atmosenv.2016.03.060. URL `http://dx.doi.org/10.1016/j.atmosenv.2016.03.060`.

[134] P. L. Kasper, M. J. Hansen, and A. Feilberg. Impact of saturation effects during dynamic olfactometry on low-concentration environmental odour samples. *Chemical Engineering Transactions*, 68:37–42, 2018. ISSN 22839216. doi: 10.3303/CET1868007.

[135] P. L. Kasper, D. Mannebeck, A. Oxbøl, J. V. Nygaard, M. J. Hansen, and A. Feilberg. Effects of dilution systems in olfactometry on the recovery of typical livestock odorants determined by PTR-MS. *Sensors (Switzerland)*, 17(8), 2017. ISSN 14248220. doi: 10.3390/s17081859.

[136] P. L. Kasper, A. Oxbøl, M. J. Hansen, and A. Feilberg. Mechanisms of loss of agricultural odorous compounds in sample bags of Nalophan, Tedlar, and PTFE. *Journal of Environmental Quality*, 47(2):246–253, 2018. ISSN 15372537. doi: 10.2134/jeq2017.07.0289.

[137] J. V. Klarenbeek, N. W. M. Ogink, and H. van der Voet. Odor measurements according to EN 13725: A statistical analysis of variance components. *Atmospheric Environment*, 86:9–15, 2014. ISSN 13522310. doi: 10.1016/j.atmosenv.2013.12.032. URL `http://dx.doi.org/10.1016/j.atmosenv.2013.12.032`.

[138] R. S. Blake, P. S. Monks, A. M. Ellis, R. S. Blake, P. S. Monks, and A. M. Ellis. Proton-Transfer Reaction Mass Spectrometry. *Chemical Reviews*, 109(2):861–896, 2009. doi: 10.1021/cr800364q.

[139] J. Q. Ni, W. P. Robarge, C. Xiao, and A. J. Heber. Volatile organic compounds at swine facilities: A critical review. *Chemosphere*, 89(7):769–788, 2012. ISSN 00456535. doi: 10.1016/j.chemosphere.2012.04.061. URL `http://dx.doi.org/10.1016/j.chemosphere.2012.04.061`.

[140] D. Parker, J. Ham, B. Woodbury, L. Cai, M. Spiehs, M. Rhoades, S. Trabue, K. Casey, R. Todd, and A. Cole. Standardization of flux chamber and wind tunnel flux measurements for quantifying volatile organic compound and ammonia emissions from area sources at animal feeding operations. *Atmospheric Environment*, 66:72–83, 2013. ISSN 13522310. doi: 10.1016/j.atmosenv.2012.03.068. URL `http://dx.doi.org/10.1016/j.atmosenv.2012.03.068`.

[141] B. Yuan, A. R. Koss, C. Warneke, M. Coggon, K. Sekimoto, and J. A. De Gouw. Proton-Transfer-Reaction Mass Spectrometry: Applications in atmospheric sciences. *Chemical Reviews*, 117(21):13187–13229, 2017. ISSN 15206890. doi: 10.1021/acs.chemrev.7b00325.

[142] A. Feilberg, D. Liu, A. P. S. Adamsen, M. J. Hansen, and K. E. N. Jonassen. Odorant emissions from intensive pig production measured by online proton-transfer-reaction mass spectrometry. *Environmental Science and Technology*, 44(15):5894–5900, 2010. ISSN 0013936X. doi: 10.1021/es100483s.

[143] M. J. Hansen, D. Liu, L. B. Guldberg, and A. Feilberg. Application of proton-transfer-reaction mass spectrometry to the assessment of odorant removal in a biological air cleaner for pig production. *Journal of Agricultural and Food Chemistry*, 60(10):2599–2606, 2012. ISSN 00218561. doi: 10.1021/jf300182c.

[144] N. M. Ngwabie, G. W. Schade, T. G. Custer, S. Linke, and T. Hinz. Abundances and flux estimates of volatile organic compounds from a dairy cowshed in Germany. *Journal of Environmental Quality*, 37(2):565–573, 2008. ISSN 00472425. doi: 10.2134/jeq2006.0417.

[145] J. de Gouw and C. Warneke. Measurements of volatile organic compounds in the earth's atmosphere using proton-transfer-reaction mass spectrometry. *Mass Spectrometry REviews*, 26(26):223–257, 2007. ISSN 00195189. doi: 10.1002/mas.

[146] C. N. Hewitt, S. Hayward, and A. Tani. The application of proton transfer reaction-mass spectrometry (PTR-MS) to the monitoring and analysis of volatile organic compounds in the atmosphere. *Journal of environmental monitoring : JEM*, 5(1):1–7, 2003. ISSN 14640325. doi: 10.1039/b204712h.

[147] Picarro. Picarro, G2123 Analyzer for NH3/H2O, User's guide, 2017.

[148] N. A. Martin, V. Ferracci, N. Cassidy, and J. A. Hoffnagle. The application of a cavity ring-down spectrometer to measurements of ambient ammonia using traceable primary standard gas mixtures. *Applied Physics B: Lasers and Optics*, 122(8):1–11, 2016. ISSN 09462171. doi: 10.1007/s00340-016-6486-9.

[149] J. N. Kamp, A. Chowdhury, A. P. S. Adamsen, and A. Feilberg. Negligible influence of livestock contaminants and sampling system on ammonia measurements with cavity ring-down spectroscopy. *Atmospheric Measurement Techniques*, 12(5):2837–2850, 2019. ISSN 18678548. doi: 10.5194/amt-12-2837-2019.

[150] J. Sintermann, C. Ammann, U. Kuhn, C. Spirig, R. Hirschberger, A. Gärtner, and A. Neftel. Determination of field scale ammonia emissions for common slurry spreading practice with two independent methods. *Atmospheric Measurement Techniques*, 4(9):1821–1840, 2011. ISSN 18671381. doi: 10.5194/amt-4-1821-2011.

[151] M. Maasikmets, E. Teinemaa, A. Kaasik, and V. Kimmel. Measurement and analysis of ammonia, hydrogen sulphide and odour emissions from the cattle farming in Estonia. *Biosystems Engineering*, 139:48–59, 2015. ISSN 15375110. doi: 10.1016/j.biosystemseng.2015.08.002. URL `http://dx.doi.org/10.1016/j.biosystemseng.2015.08.002`.

[152] A. Jordan, S. Haidacher, G. Hanel, E. Hartungen, L. Märk, H. Seehauser, R. Schottkowsky, P. Sulzer, and T. D. Märk. A high resolution and high sensitivity proton-transfer-reaction time-of-flight mass spectrometer (PTR-TOF-MS). *International Journal of Mass Spectrometry*, 286(2-3):122–128, 2009. ISSN 13873806. doi: 10.1016/j.ijms.2009.07.005.

[153] T. Su and W. J. Chesnavich. Semiempirical calculation of diamagnetic susceptibilities of organogermanium compounds. *Journal of Chemical Physics*, 76(10), 1982. doi: 10.112/1.421275. URL `http://www.ncbi.nlm.nih.gov/pubmed/3883696`.

[154] A. Hansel, A. Jordan, R. Holzinger, P. Prazeller, W. Vogel, and W. Lindinger. Proton transfer reaction mass spectrometry: on-line trace gas analysis at the ppb level. *International Journal of Mass Spectrometry and Ion Processes*, 149-150(C):609–619, 1995. ISSN 01681176. doi: 10.1016/0168-1176(95)04294-U.

[155] Miljøstyrelsen. Bekendtgørelse om miljøregulering af dyrehold og om opbevaring og anvendelse af gødning. BEK nr. 760 af 30/07/2019, 2019.

[156] A. Seidel, A. Pacholski, T. Nyord, A. Vestergaard, I. Pahlmann, A. Herrmann, and H. Kage. Effects of acidification and injection of pasture applied cattle slurry on ammonia losses, N2O emissions and crop N uptake. *Agriculture, Ecosystems and Environment*, 247(May):23–32, 2017. ISSN 01678809. doi: 10.1016/j.agee.2017.05.030. URL `http://dx.doi.org/10.1016/j.agee.2017.05.030`.

[157] T. Merl and K. Koren. Visualizing NH3 emission and the local O2 and pH microenvironment of soil upon manure application using optical sensors. *Environment International*, 144(August):106080, 2020. ISSN 18736750. doi: 10.1016/j.envint.2020.106080. URL `https://doi.org/10.1016/j.envint.2020.106080`.

AARHUS
UNIVERSITY

Ph.D. Thesis

Mitigating gaseous emissions following land application of manure slurry in growing crops

Appendix

Johanna Pedersen
Department of Engineering
Aarhus University

September 2020

Johanna Pedersen
Aarhus University
Department of Engineering
Finlandsgade 12, 8200 Aarhus N.
Denmark
jp@eng.au.dk

Thesis submitted:
September 30 $^{\text{th}}$ 2020

Main Supervisor:
Anders Feilberg
Associate Professor
Department of Engineering
Aarhus University
af@eng.au.dk

Co-supervisors:
Tavs Nyord
Senior Advisor
Department of Engineering
Aarhus University
tavs.nyord@eng.au.dk

Sasha Hafner
Honorary Associate Professor
Department of Engineering
Aarhus University
sasha@hafnerconsulting.com

Contents

Chapter 1

Paper VI

Frederik F. Foldager, Johanna M. Pedersen, Esben Haubro Skov, Alevtina Evgrafova, Ole Green. LiDAR-Based 3D Scans of Soil Surfaces and Furrows in Two Soil Types *Sensors*, volume 19, 24 January 2019.

sensors

MDPI

Article

LiDAR-Based 3D Scans of Soil Surfaces and Furrows in Two Soil Types

Frederik F. Foldager [1,2,*], Johanna Maria Pedersen [1], Esben Haubro Skov [2], Alevtina Evgrafova [2] and Ole Green [2]

[1] Department of Engineering, Aarhus University, Inge Lehmanns Gade 10, 8000 Aarhus C, Denmark; jp@eng.au.dk

[2] Agro Intelligence ApS, Agro Food Park 13, 8200 Aarhus N, Denmark; ehs@agrointelli.com (E.H.S.); aev@agrointelli.com (A.E.); olg@agrointelli.com (O.G.)

* Correspondence: ffo@eng.au.dk; Tel.: +45-9189-2291

Received: 30 November 2018; Accepted: 24 January 2019; Published: date

Abstract: Soil surface measurements play an important role in the performance assessment of tillage operations and are relevant in both academic and industrial settings. Manual soil surface measurements are time-consuming and laborious, which often limits the amount of data collected. An experiment was conducted to compare two approaches for measuring and analysing the cross-sectional area and geometry of a furrow after a trailing shoe sweep. The compared approaches in this study were a manual pinboard and a Light Detection and Ranging (LiDAR) sensor. The experiments were conducted in coarse sand and loamy sand soil bins exposed to three levels of irrigation. Using the LiDAR, a system for generating 3D scans of the soil surface was obtained and a mean furrow geometry was introduced to study the geometrical variations along the furrows. A comparison of the cross-sectional area measurements by the pinboard and the LiDAR showed up to 41% difference between the two methods. The relation between irrigation and the resulting furrow area of a trailing shoe sweep was investigated using the LiDAR measurements. The furrow cross-sectional area increased by 11% and 34% under 20 mm and 40 mm irrigation compared to non-irrigated in the coarse sand experiment. In the loamy sand, the cross-sectional area increased by 17% and 15% by irrigation of 20 mm and 40 mm compared to non-irrigated measured using the LiDAR.

Keywords: 3D soil surface; microtopography; pinboard; furrow cross-section; trailing shoe; precision agriculture; SICK

1. Introduction

A wide range of sensors are used to describe various properties in arable ecosystems. Weed detection can be performed using high precision cameras [1], soil organic carbon stocks and many soil properties can be obtained using spectroscopic techniques [2], as well as soil surface roughness can be evaluated using scanners [3] and digital cameras [4]. Soil surface roughness is an important measure in agricultural research and engineering as it affects properties such as soil water interaction [5] and the risk of soil erosion [6,7]. The soil roughness and cross-sectional shapes of furrows have been determined to develop and assess the performance of tillage tools by measuring the resulting soil disturbance of tillage operations [8,9]. Several methods exist for evaluating the cross-sectional area and geometry of a furrow such as a pinboard [10] and a chain method [11]. These methods are manually operated and thus limited to assess only a finite number of cross-sectional profiles along a furrow. Digital and automated measurements of soil surface roughness illustrated a better description of the spatial variations in both natural and agro-ecosystems [12]. The automated measurement methods also allow for on-the-go measurements of soil roughness as shown in [3] for site-specific cultivation using a Light Detection and Ranging (LiDAR) sensor. The

LiDAR has the advantage of being a non-contact, high-resolution technique for spatial data acquisition [13]. Another method for surface detection is the camera-based Structure from Motion (SfM) method [14], where maps are created from a series of pictures. The method has shown its applicability in different scales from mapping landscapes [15] as well as in measuring soil roughness using a commercial grade camera [16].

The aim of this study was to use the 2D LiDAR sensor to assess the furrow geometry and area of a trailing shoe sweep. The trailing shoe is applied to establish a soil furrow to contain the liquid slurry during a slurry application. The use of the trailing shoes is expected to lower emissions in comparison to the slurry application by trailing hoses. The former reduces the surface contact between the slurry and the surrounding atmosphere, which is recognised as a significant factor [17–19]. Therefore, accurate measurements of how furrow geometry varies with soil texture and soil moisture content can support predictions of when application by trailing shoe is an efficient emission reduction technique. The objectives were (i) to compare two methods for evaluating soil surface and furrow cross-sectional profiles after a trailing shoe operation using a digital LiDAR sensor and an analogue pinboard and (ii) to measure the changes in furrow geometry and the spatial variations along furrows in coarse sand and loamy sand soils with three different amounts of irrigation.

1.1. Background

1.1.1. Manual Soil Surface Measurements

The relief meter, which was an early version of the pinboard was presented for measuring the soil roughness between cultivation and seedbed preparation [10]. The pinboards vary in size, numbers of pins, spacing between those, materials used, and method of collecting data, but the principle of the measurements is the same. The method is commonly used as it is cost effective and easy to operate. Since the early development, the pinboard method has been used to measure soil surface variations for different purposes [20,21]. Further development of the pinboard for measuring soil surface roughness and soil variations at the microscale was presented [22]. The pinboard has also been used for evaluating soil loss from quarter-drains by quantifying the changes of the cross-sectional area before and after rain events [23].

1.1.2. LiDAR and Camera-Based Soil Surface Sensing

In agricultural engineering, LiDAR-based systems have been applied for various applications such as obstacle detection for autonomous field-robots [24], 3D imaging of crop development [25], and soil surface analysis [6]. The automated systems for soil surface detection have been presented since the 1980s [26]. Moreover, sensor-based systems have been applied for studying microtopography and soil roughness on different scales, from point samples [27,28] to larger areas [29] as well as for airborne applications [30]. The laser-based method performs within the accuracy of the pin displacement unit [31], which made the laser a feasible tool for researching erosion [32]. In addition, microtopography effects of rainfall has been studied using both a photogrammetric technique and a high-resolution laser scanner [33] as well as 1D distance sensors [34,35] and 2D scanners [36] have been applied for soil roughness estimations [37,38]. Besides the use of scanners, camera-based techniques have also been applied to determine soil surface roughness, from hand-held cameras [39] to modern commercial grade cameras [40]. In addition, stereo photogrammetry was also used for mapping soil surfaces [41] and estimating microtopography and soil roughness [42]. Many stationary LiDAR and camera-based systems have been presented for automated soil surface measurements. However, LiDAR was mentioned as a feasible choice for stationary use as well as for on-the-go sensing of soil roughness in the field [3].

2. Materials and Methods

2.1. Experimental Settings

In order to compare two methods such as the pinboard and LiDAR, an experiment consisting of 18 trailing shoe furrows which were obtained in two semi-field soil bins at three irrigation amounts was conducted (Figure 1). For each furrow, a 3D scan and a pinboard measurement of the geometry and area were obtained.

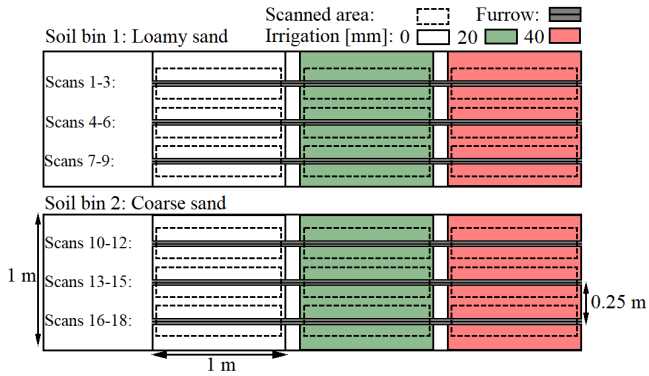

Figure 1. Experimental design sketch. 18 furrows were obtained and measured using the pinboard and LiDAR within six plots of two soil types and three irrigation amounts.

The experiment was conducted in the semi-field facility at Aarhus University Foulum Research Center, Tjele. The semi-field facility was established in 1993 [43], consisting of three soil bins under a moveable roof that allows for controlling the precipitation. Three weeks prior to and during the experiment, the roof was kept over the studied soil bins and the soil was kept bare during the experiments. Two out of three semi-field soil bins were used in this research, coarse sand and loamy sand [44–47]. The coarse sand (Ortic Haplohumod) had 4% clay (<0.002 mm), 5% silt (0.002–0.063 mm), and 2.0% soil organic matter, while loamy sand (Typic Hapludult) was characterized by 9% clay, 24% silt, and 2.5% soil organic matter [48]. Approximately 24 hours prior to the experiment, six plots (1 x 1 m) were irrigated with three different amounts of tap water: 0, 20 and 40 mm. The soil water contents were determined gravimetrically [49] using a soil core of 100 cm^3 (Table 1). The dry bulk densities were 1.28 $\pm$ 0.09 g cm^{-3} for loamy sand and 1.39 $\pm$ 0.07 g cm^{-3} for coarse sand. Due to an unusually dry and hot period prior to the experiments, no significantly different soil water contents were obtained except for the coarse sand soils with 40 mm of irrigation compared to the non-irrigated coarse sand soils (Table 1).

Table 1. Soil water content [g/g] (n = 3) with the standard deviation after three irrigation amounts such as 0, 20, and 40 mm were measured in the topsoils (0–10 cm). The letters indicate significance based on the Tukey's HDS test, $P \leq 0.05$.

Irrigation Level, mm	Loamy Sand		Coarse Sand	
0	0.13 (0.02)	a	0.06 (0.00)	a
20	0.16 (0.00)	a	0.08 (0.01)	ab
40	0.15 (0.03)	a	0.10 (0.02)	b

In order to study soil displacements of the furrows, three Bomech trailing shoes (Bomech B.V., Albergen, The Netherlands) were attached to a metal frame on wheels with a distance of 25 cm between each trailing shoe (Figure 2a,b). A vertical load of 117.7 N (12.0 kg) was exerted on each trailing shoe. Three sweeps were conducted for each soil bin at a constant speed of approximately 2.0 km h^{-1}. In

total, 18 furrows were obtained and measured using the analogue pinboard and the digital LiDAR approaches.

(**a**) (**b**)

Figure 2. Frame with three of the Bomech trailing shoes (**a**) and three furrows in coarse sand at 40 mm irrigation (**b**).

2.2. LiDAR-Based Soil Surface Measurement Unit

A soil surface measurement unit was assembled to obtain high-resolution and continuous scans of the soil surface. The 2D LiDAR sensor (SICK LMS511-20100 PRO) was chosen based on the indicated applicability for roughness measurements in the field [50]. The LiDAR operates from a minimum distance to the target at 0.70 m. According to the operating instructions, the statistical error is ± 7 mm at 1–10 m distance. The LiDAR was mounted on a linear rail system (Figure 3a) that allowed to obtain the 3D scans of the soil surface by moving the scanner at an elevation of 0.75 m above the surface and parallel to the direction of the furrow while monitoring the position of the scanner. The scans were conducted with an angular resolution of 0.167° and an angular frequency of 25 Hz, while the linear speed of the scanner ($\dot{y}$) (Figure 3b) was constant at 0.003 m s^{-1}, driven by a stepper motor. The distance between two line scans along the furrow (y-direction) was 0.33 mm. Each line scan was 37 cm wide and consisted of 166 data points with a maximum distance between two points of 2.3 mm. The beam diameter increases from 13 mm at the front screen of the sensor to approximately 16.5 mm in diameter at the soil surface of this elevation using the high resolution setting of the LiDAR.

The raw sensor data was collected using the software, SOPAS Engineering Tool ver. 2018.2 (SICK, Germany). No automatic filtering was applied during data sampling. However, the data points were transformed from polar coordinates into cartesian coordinates to study the vertical distances from the scanner to the soil surface in the post-processing and to assemble the 3D scans. A low-pass Gaussian filter ($\sigma = 1.5$) was applied in order to remove sensor noise before generating 3D scans using the package: *scipy.ndimage.filters.gaussian_filter* of SciPy ver. 2.0 in Python 3.6.5.

(**a**) (**b**)

Figure 3. The LiDAR-based soil surface measurement unit in the semi-field facility (**a**); Sketch of the furrow geometry that includes the reference frame of the cross-sectional profile (**b**), solid line indicates the soil surface and dashed lines indicate the vertical and horizontal axis of the origin.

The x and z coordinates were obtained using the LiDAR sensor, whereas the y coordinates were monitored through the stepper drive (Figure 3b).

2.3. Furrow Cross-Sectional Geometry and Area Measurements

2.3.1. LiDAR Measurements

3D scans of the furrows were obtained using LiDAR measurements and generated based on the filtered data. In order to compare the results of the 3D scanned furrows, a reference frame was introduced to each measured furrow profile. A coordinate system was located in the xz-plane of the furrow. The horizontal xy-plane was located at the elevation of the undisturbed soil. The yz-plane was intersecting with the deepest point of the furrow (Figure 3b). A *mean furrow* geometry was introduced to express 3D scans as 2D profiles and, hence, to visualise the spatial variations along furrows. The mean furrow was defined for each scan as the mean of the vertical distance measurements (z) for each value of (x) in the relative coordinate systems along the furrow (y). The mean furrow geometries were generated based on 3D scans of which the area was calculated using the package *sklearn.metrics.auc ver. 0.19.1* in Python 3.6.5 by integrating the elevations measurements (z) over the distance x_l to x_r using the trapezoidal rule (Figure 3b). The 2D mean furrow and standard deviations were obtained based on one scan per centimetre of the furrows.

2.3.2. Pinboard Measurements

The analogue measurements of the furrow geometries and areas were performed using pinboard (Figure 4). The pinboard consists of pins (width of 3 mm) that moves freely in the vertical direction. The device was operated by levelling the pins on the soil surface. The contour of the surface was then drawn on paper based on the position of the pins. Subsequent to this operation, the areas were obtained by moving a Digitizing Area-line Meter (Super PLANIX b, Tamaya Technics Inc., Tokyo, Japan) along the drawn contour of the furrow profile, hence referred to as the analogue area measurements. This procedure was done three times for each analogue cross-sectional measurement, and the mean value of these were used for further analysis. In this study, the Computer Aided Design (CAD) software, SOLIDWORKS 2018 SP1 (Dassault Systémes, Paris, France) was applied to digitalise the drawn pinboard-based contours.

Figure 4. The analogue measurement using pinboard of the furrow in loamy sand at 40 mm irrigation.

3. Results and Discussion

3.1. 2D and 3D Soil Surface Profiles

The 3D scans allowed to evaluate furrow geometries as a result of different irrigation amounts as well as to estimate the variation along furrows within a larger area. The LiDAR gave a more representative description of the furrow compared to analogue measurements as only a limited

number of manual measurements can be conducted along the furrow due to the time-consuming process [6]. The cross-sectional geometry, such as width, depth and shape, varied in the two soil types, where the loamy sand plots with no irrigation were characterized with a more well-defined edge and a narrower furrow-width compared to the non-irrigated coarse sand plots (Figures 5 and 6). The furrow geometry in the coarse sand was affected by the increased soil water content. However, in the loamy sand it was not possible to conclude on furrow geometry changes as a factor of soil water content due to the fact that the latter was not significantly different (Table 1). Although, the experiments were performed in semi-field conditions under controlled irrigation, the LiDAR will provide similar results under field conditions. The soil surface in the semi-field is comparable to soil surface conditions in fields, however, a limitation of the LiDAR is the need for bare soil to obtain an uninterrupted line of sight between the sensor and the soil surface.

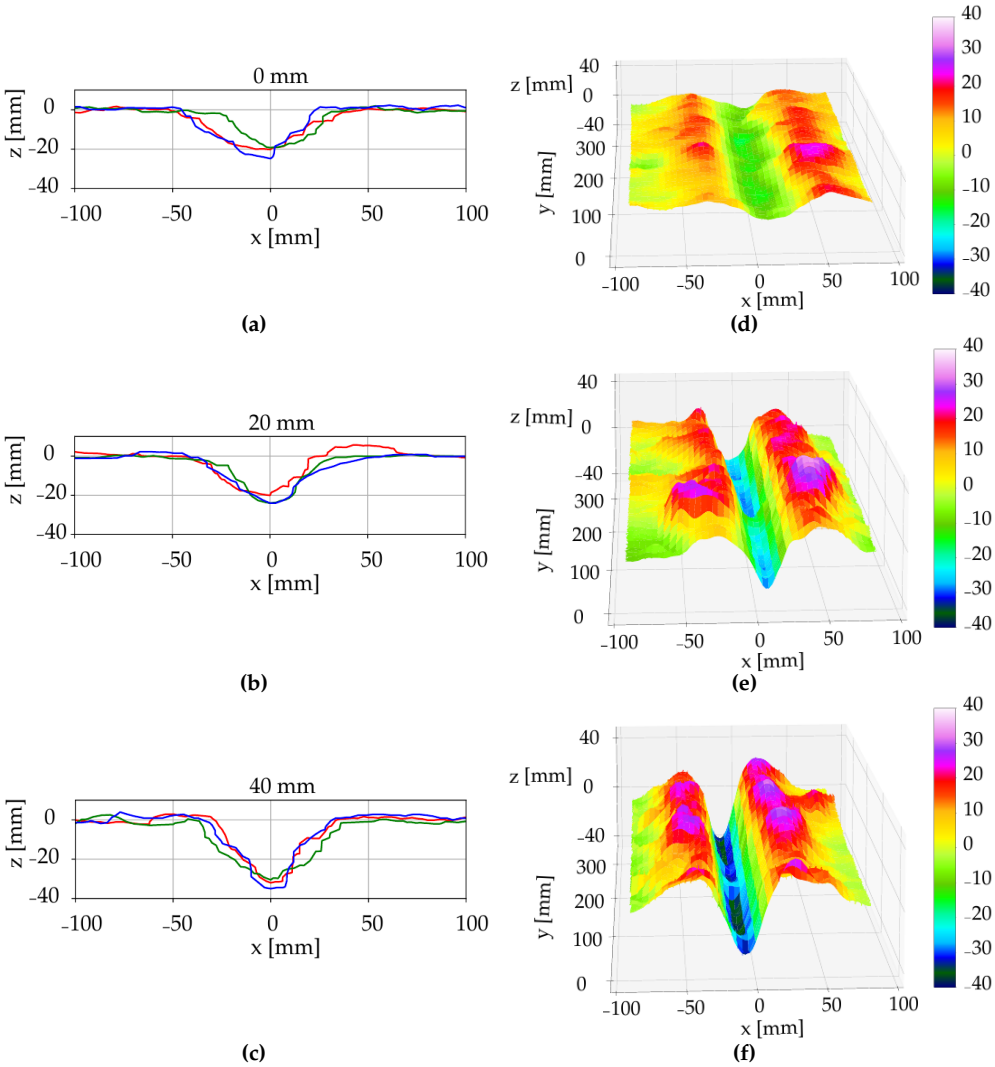

Figure 5. The cross-sectional measurements in coarse sand after irrigation of 0 mm **(a,d)**, 20 mm **(b,e)**, and 40 mm **(c,f)**. Pinboard measurements **(a-c)**, where three repetitions are shown as red, blue and green lines and LiDAR measurements **(d-f)**, where the colourbar represent elevation (z) in mm.

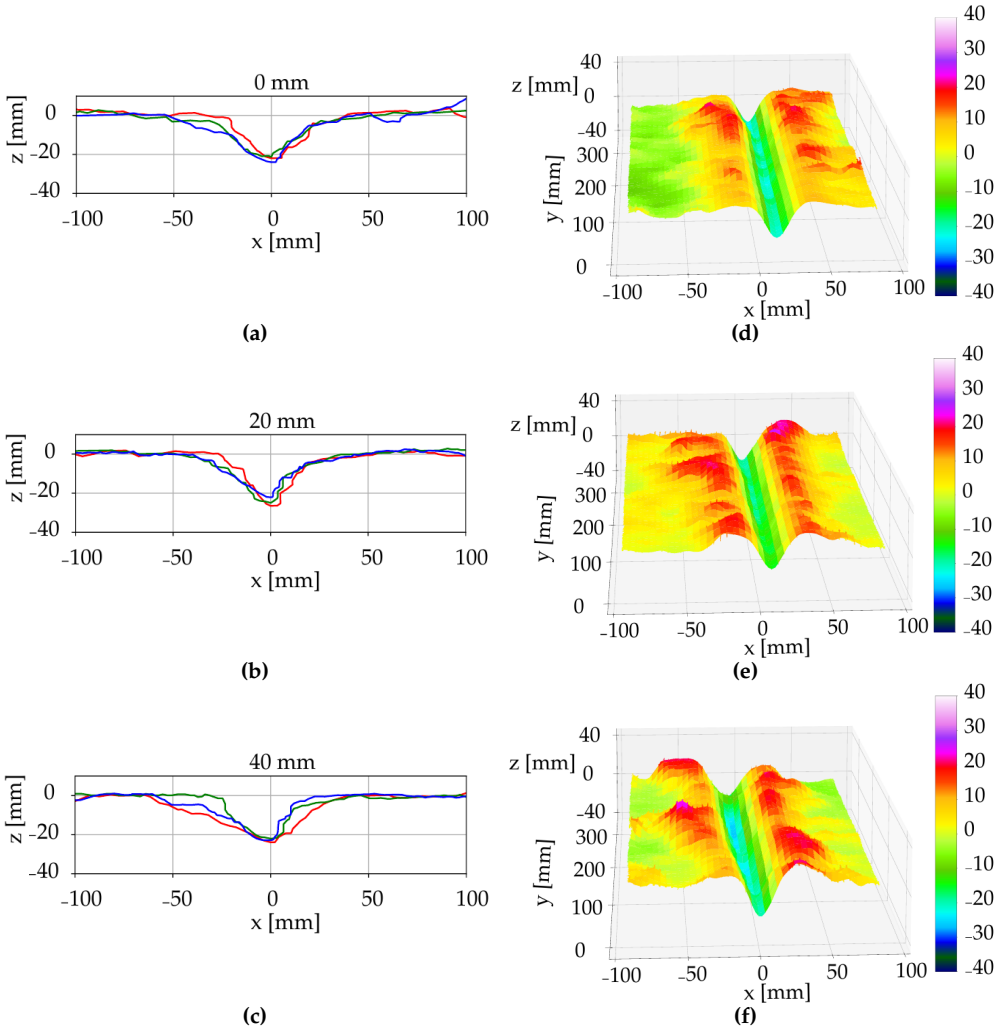

Figure 6. The cross-sectional measurements in loamy sand after irrigation of 0 mm **(a,d)**, 20 mm **(b,e)**, and 40 mm **(c,f)**. Pinboard measurements **(a-c)**, where three repetitions are shown as red, blue and green lines and LiDAR measurements **(d-f)**, the colourbar represent elevation (z) in mm.

The furrow profiles of the two soil types under the three irrigation amounts were illustrated in Figures 5 and 6. The subfigures, (a-c) present the 2D profiles of the pinboard measurements, three repetitions each, digitalised using CAD software. The subfigures (d-f) present a subset of the furrow 3D scans and was generated based on the stepper position and LiDAR measurements. In the coarse sand plots, a visual effect of the irrigation was observed by leaving a deeper furrow compared to the non-irrigated soil (Figure 5). This indicates that the resulting furrow geometry was dependent on the water content. Hence, water content and soil type should be considered when the trailing shoe is used for the liquid slurry application.

The mean furrows and the standard deviations of the elevation measurements in the direction of the furrows were determined as the spatial variation along the furrows was observed. Using the mean furrow, it was possible to present 3D scans as 2D cross-sectional plots, which allowed to compare the digital mean furrow plots with the analogue pinboard measurements of the furrow (Figure 7) as the common reference frame was applied (Figure 3b). The location of the common reference frame was a

feasible choice for the soil bin study. However, in a field setting, another choice of reference frame could be introduced, *e.g.* the deepest point of a furrow.

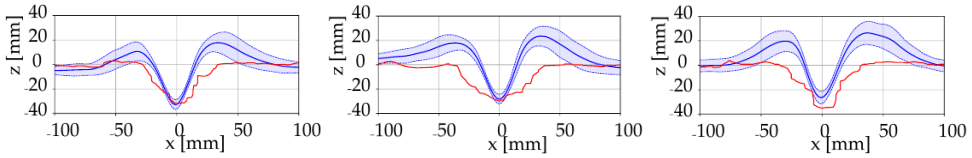

Figure 7. Mean profiles (solid blue lines), standard deviation on the elevation measurement (light blue area), analogue pinboard measurement (red line). Results are shown for all repetitions in coarse sand at 40 mm irrigation.

The ability to visualize and take into account the variation along the furrow is needed for research and development purposes related to soil and tillage tools [51]. The magnitude of the standard deviation provides an insight into the variation of the furrow geometry. By evaluating the 3D scans, the three-dimensional soil displacement become available in the assessment of tillage tools [52]. The pinboard has previously been applied for comparing results of simulations-based and measured soil-tool interactions [48]. By considering the variations along the furrow, it is possible to include a physics-based error tolerance when validating numerical models of corresponding soil-tool interactions [53].

The non-contact and automated approach of the LiDAR ensures consistent test results independent from soil conditions, which is an advantage for research purposes. The LiDAR has previously shown applicability in a field setting performing on-the-go measurements of soil surface [50]. This indicates that this technology can be further developed for applications in a field setting as a method for increasing the site-specific treatments based on LiDAR measurements. With respect to the slurry application using trailing shoes, on-board measurements of the furrow geometry and furrow area could act as an input for controlling the pressure on the trailing shoe to obtain the desired furrow area, which is shown to be dependent on the soil type and water content.

3.2. Furrow Area Measurements

The cross-sectional area of the furrow is important due to the application of the trailing shoe, namely to establish a furrow in which the liquid slurry is contained. Furthermore, high variations in the reported effect of trailing shoe on emission reduction were observed [54–57]. The inconsistencies in reported emission reduction by trailing shoe are often attributed to the soil properties, particularly, soil moisture content [17,56], as this affects the furrow cross-sectional area. Hereby, accurate and consistent methods for assessing the cross-sectional area under different conditions are important as well as being able to correlate the volume of the furrow with the volume of the slurry. The cross-sectional area was a subject for the comparison between the digital and analogue soil surface measurement techniques. Other parameters as width and depth could in a similar way have been considered as the measure for comparison. The cross-sectional areas were measured in every soil plot (Figure 1) in order to determine the change in area due to various irrigation amounts in the two soils. The digital cross-sectional areas were determined using the mean furrow geometry of the 3D scans (Figure 7). A comparison between the analogue profiles and the closest line scan as well as an example of the areas applied for the pinboard measurements are shown in Figure 8.

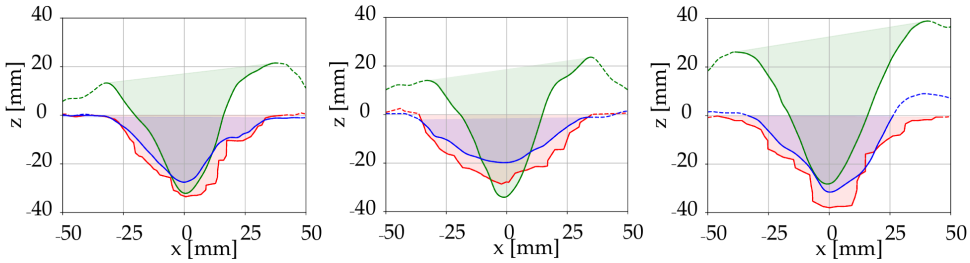

Figure 8. Cross-sectional geometries in coarse sand at irrigation amount of 40 mm. Line scans prior to the pinboard measurement (green line), line scan subsequent to the pinboard measurement (blue), and analogue pinboard measurement (red).

The analogue cross-sectional area measurements and the LiDAR-based mean furrow areas were shown in Figure 9. The values are based on the mean of the three repetitions for each plot *i.e.* combination of soil type and irrigation amount. As an example, for the coarse sand at 40 mm irrigation, the analogue area was calculated as the mean of the area above the red curves of Figure 7, whereas the digital area corresponds to the average area above the three solid blue curves.

There was no significant difference in the areas measured by the digital and analogue methods, except for the non-irrigated coarse sand and coarse sand irrigated at 40 mm (Tukey's HSD, $P < 0.05$). However, by comparing the areas of the digital and analogue methods in the coarse sand, it was found that the analogue pinboard predicted lower than the estimations of the digital approach by 7%, 15% and 8% for the 0, 20, and 40 mm irrigation amounts. In the loamy sand plots, all the analogue measurements provided larger cross-sectional areas compared to the digital measurements of 41%, 3% and 16%, respectively. This inconsistency indicated that the results of the analogue measurements was affected by the process of first measuring the surface contour using the pinboard and then calculating the area. By comparing the magnitude of the standard deviations of the analogue area measurements and the standard deviation based on the scanned area, it was found that the standard deviation was lower when LiDAR scans were used, compared to the analogue approach. Hence, the scanner provided more consistent results than the analogue method due to the non-contact and automated process. It was also expected as that the number of data points collected for 3D scans and the mean furrows was higher than the data points collected for the pinboard measurements. By comparing the digital cross-sectional area estimations for the dry coarse sand soil with the irrigated coarse sand of 20 and 40 mm, an increase in furrow cross-sectional area was obtained by 11% and 34%. For the loamy sand, the cross-sectional area increased 17% and 15% by irrigation of 20 and 40 mm. Nevertheless, more experiments under different soil conditions and irrigation amounts are needed to fully evaluate these effects.

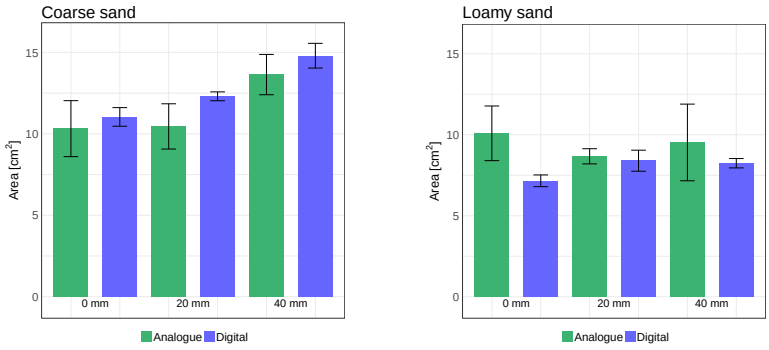

Figure 9. Cross-sectional area measurements based on pinboard (Analogue) and LiDAR scans (Digital) in the two soils.

3.3. Impact Analysis of Pinboard Measurement

The disturbance of the surface in loose soils during the application of the pinboard [58] was studied by comparing the digital 2D mean furrow geometries and the analogue pinboard measurements. Differences in the furrow geometry between the analogue and digital measurements were observed in the coarse sand plots as a result of the analogue measurement. The impacts were measured by scanning the surface prior to and after the pinboard measurements. In Figure 10, a 3D scan of the soil after the analogue measurement is shown. The positions where the pinboard measurements were taken are marked with arrows (Figure 10). 2D line scans of the furrows in coarse sand with 40 mm irrigation were compared to the corresponding pinboard measurement.

It was observed that the analogue measurements did not accurately capture the geometry of the furrow. Particularly, the features of the furrow for values $z > 0$, using the notation of Figure 3b, were not captured. Furthermore, it was observed that the analogue measurements provide a wider representation of the furrow cross-sectional geometry compared to the scan conducted before the pinboard measurements (Figure 8).

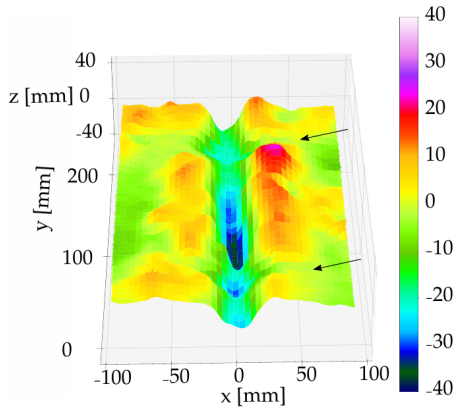

Figure 10. 3D scan subsequent to a pinboard measurement. The arrows indicate the location of two pinboard measurements. Experiments conducted in coarse sand, irrigation 40 mm.

By the means of the LiDAR, an assessment of the pinboard performance was accessible and an issue of the pinboard was identified, namely, the pinboard approach was challenged in capturing small cross-sectional geometries in loose sand due to disturbance of the soil. This issue has previously been reported as an uncertainty when using the pin-based methods in sandy soil [31].

4. Conclusions

Two methods were compared to evaluate the soil surface and furrow cross-sectional area after a trailing shoe sweep in two soils. A 2D mean profile of the furrow was constructed to compare the digital LiDAR-based results with the results of the analogue pinboard. From the experiments it was concluded:

(i) The geometric variations in the direction of the furrow were observed by increasing the resolution from 2D pinboard measurements to 3D scans.
(ii) The results indicated the importance of applying a non-contact method for accurate soil surface measurements in loose soils. The analogue furrow areas were below the LiDAR-based areas in coarse sand by up to 15% and for loamy sand, the analogue areas were above the LiDAR-based areas by up to 41%.
(iii) An increase in the cross-sectional areas was measured using the LiDAR-based method, in coarse sand the area increased by 11% and 34% for the 20 and 40 mm irrigation compared to the dry

coarse sand. In the loamy sand, the cross-sectional area of the furrow increased 17% and 15% by irrigation of 20 and 40 mm. However, more experiments are needed to fully evaluate these effects.

Author Contributions: Conceptualization, F.F.F. and J.M.P.; Methodology, F.F.F. and J.M.P.; Software, E.H.S. and F.F.F.; Experiment design and execution, E.H.S., J.M.P. and F.F.F.; Investigation, F.F.F., J.M.P. and A.E.; Resources, O.G. and J.M.P.; Data Curation, F.F.F., E.H.S. and J.M.P.; Writing—Original Draft Preparation, F.F.F., J.M.P. and A.E.; Writing—Review & Editing, F.F.F., J.M.P., A.E., E.H.S., and O.G.; Visualization, E.H.S.; Supervision, F.F.F. and O.G.; Project Administration, F.F.F.; Funding Acquisition, F.F.F. and O.G.

Funding: This work is partly funded by the Danish Innovation Fund under grant number 7038-00231B and by the Ministry of Environment and Food of Denmark as a green development and demonstration program (GUDP) with the project title *New application method for slurry in growing crops.*

Acknowledgments: We would like to acknowledge all the technical staff for the support in and contributions to the performance of the tests and Henri Bonnart for assisting in assembling the test setup.

Conflicts of Interest: The authors declare no conflict of interest.

References

1. Tellaeche, A.; BurgosArtizzu, X.P.; Pajares, G.; Ribeiro, A.; Fernández-Quintanilla, C. A new vision-based approach to differential spraying in precision agriculture. *Comput. Electron. Agric.* **2008**, *60*, 144–155.
2. Viscarra Rossel, R.A.; Lobsey, C.R.; Sharman, C.; Flick, P.; McLachlan, G. Novel proximal sensing for monitoring soil organic C stocks and condition. *Environ. Sci. Technol.* **2017**, *51*, 5630–5641.
3. Jensen, T.; Karstoft, H.; Green, O.; Munkholm, L.J. Assessing the effect of the seedbed cultivator leveling tines on soil surface properties using laser range scanners. *Soil Tillage Res.* **2017**, *167*, 54–60. doi:10.1016/j.still.2016.11.006.
4. Moreno, R.G.; Álvarez, M.C.; Alonso, A.T.; Barrington, S.; Requejo, A.S. Tillage and soil type effects on soil surface roughness at semiarid climatic conditions. *Soil Tillage Res.* **2008**, *98*, 35–44. doi:10.1016/j.still.2007.10.006.
5. Bauer, T.; Strauss, P.; Grims, M.; Kamptner, E.; Mansberger, R.; Spiegel, H. Long-term agricultural management effects on surface roughness and consolidation of soils. *Soil Tillage Res.* **2015**, *151*, 28–38. doi:10.1016/j.still.2015.01.017.
6. Thomsen, L.M.; Baartman, J.E.M.; Barneveld, R.J.; Starkloff, T.; Stolte, J. Soil surface roughness: comparing old and new measuring methods and application in a soil erosion model. *Soil* **2015**, *1*, 399–410. doi:10.5194/soil-1-399-2015.
7. Jester, W.; Klik, A. Soil surface roughness measurement - Methods, applicability, and surface representation. *Catena* **2005**, *64*, 174–192. doi:10.1016/j.catena.2005.08.005.
8. Milkevych, V.; Munkholm, L.J.; Chen, Y.; Nyord, T. Modelling approach for soil displacement in tillage using discrete element method. *Soil Tillage Res.* **2018**, *183*, 60–71. doi:10.1016/j.still.2018.05.017.
9. Zhang, X.; Chen, Y. Soil disturbance and cutting forces of four different sweeps for mechanical weeding. *Soil Tillage Res.* **2017**, *168*, 167 – 175. doi:10.1016/j.still.2017.01.002.
10. Kuipers, H. A relief meter for soil cultivation studies. *Neth. J. Agric. Sci.* **1957**, *5*, 255–262.
11. Saleh, A. Soil roughness measurement: chain method. *J. Soil Water Conserv.* **1993**, *48*, 527–529.
12. Wolock, D.M.; Price, C.V. Effects of digital elevation model map scale and data resolution on a topography-based watershed model. *Water Resour. Res.* **1994**, *30*, 3041–3052.
13. Oz, I.; Arav, R.; Filin, S.; Assouline, S.; Furman, A. High-Resolution Measurement of Topographic Changes in Agricultural Soils. *Vadose Zone J.* **2017**, *16*. doi:10.2136/vzj2017.07.0138.
14. Westoby, M.J.; Brasington, J.; Glasser, N.F.; Hambrey, M.J.; Reynolds, J.M. 'Structure-from-Motion' photogrammetry: A low-cost, effective tool for geoscience applications. *Geomorphology* **2012**, *179*, 300–314. doi:10.1016/j.geomorph.2012.08.021.
15. Eltner, A.; Maas, H.G.; Faust, D. Soil micro-topography change detection at hillslopes in fragile Mediterranean landscapes. *Geoderma* **2018**, *313*, 217–232. doi:10.1016/j.geoderma.2017.10.034.
16. Snapir, B.; Hobbs, S.; Waine, T.W. Roughness measurements over an agricultural soil surface with Structure from Motion. *ISPRS J. Photogramm. Remote Sens.* **2014**, *96*, 210–223. doi:10.1016/j.isprsjprs.2014.07.010.

17. Smith, K.A.; Jackson, D.R.; Misselbrook, T.H.; Pain, B.F.; Johnson, R.A. Reduction of ammonia emission by slurry application techniques. *J. Agric. Eng. Res.* **2000**, *77*, 277–287. doi:10.1006/jaer.2000.0604.
18. Wulf, S.; Maeting, M.; Clemens, J. Application technique and slurry co-fermentation effects on ammonia, nitrous oxide, and methane emissions after spreading. *J. Environ. Qual.* **2002**, *31*, 1795–1801.
19. Webb, J.; Sørensen, P.; Velthof, G.; Amon, B.; Pinto, M.; Rodhe, L.; Salomon, E.; Hutchings, N.; Burczyk, P.; Reid, J. An assessment of the variation of manure nitrogen efficiency throughout Europe and an appraisal of means to increase manure-N efficiency. In *Advances in Agronomy*; Elsevier, 2013; Volume 119, pp. 371–442.
20. Ram, D.N.; Zwerman, P.; A convenient soil compaction integrator. *Agron. J.* **1960**, *52*.
21. Burwell, R.E.; Allmaras, R.R.; Amemiya, M. A field measurement of total porosity and surface microrelief of soils. *Soil Sci. Soc. Am. Proc.* **1963**, *27*, 697–700.
22. Moreno, R.G.; Álvarez, M.C.D.; Requejo, A.S.; Tarquis, A.M. Multifractal Analysis of Soil Surface Roughness. *Vadose Zone J.* **2008**, *7*, 512. doi:10.2136/vzj2007.0016.
23. Kornecki, T.S.; Fouss, J.L.; Prior, S.A. A portable device to measure soil erosion/deposition in quarter-drains. *Soil Use Manag.* **2008**, *24*, 401–408. doi:10.1111/j.1475-2743.2008.00181.x.
24. Foldager, F.F.; Larsen, P.G.; Green, O. *Development of a Driverless Lawn Mower Using Co-Simulation*; Lecture Notes in Computer Science (including subseries Lecture Notes in Artificial Intelligence and Lecture Notes in Bioinformatics); Springer, 2018; Volume 10729 LNCS, pp. 330–344. doi:10.1007/978-3-319-74781-1_23.
25. Garrido, M.; Paraforos, D.S.; Reiser, D.; Arellano, M.V.; Griepentrog, H.W.; Valero, C. 3D maize plant reconstruction based on georeferenced overlapping lidar point clouds. *Remote Sens.* **2015**, *7*, 17077–17096. doi:10.3390/rs71215870.
26. Harral, B.B.; Cove, C.A. Development of an optical displacement transducer for the measurement of soil surface profiles. *J. Agric. Eng. Res.* **1982**, *27*, 421–429. doi:10.1016/0021-8634(82)90080-4.
27. Frede, H.G.; Gäth, S. Soil surface roughness as the result of aggregate size distribution 1. report: Measuring and evaluation method. *Z. Pflanzenernähr. Bodenkd.* **1995**, *158*, 31–35.
28. Darboux, F.; Huang, C.H. An Instantaneous-Profile Laser Scanner to Measure Soil Surface Microtopography. *Soil Sci. Soc. Am. J.* **2003**, *67*, 92. doi:10.2136/sssaj2003.9200.
29. Verhoest, N.E.; Lievens, H.; Wagner, W.; Álvarez-Mozos, J.; Moran, M.S.; Mattia, F. On the soil roughness parameterization problem in soil moisture retrieval of bare surfaces from synthetic aperture radar. *Sensors* **2008**, *8*, 4213–4248. doi:10.3390/s8074213.
30. Turner, R.; Panciera, R.; Tanase, M.A.; Lowell, K.; Hacker, J.M.; Walker, J.P. Estimation of soil surface roughness of agricultural soils using airborne LiDAR. *Remote Sens. Environ.* **2014**, *140*, 107–117. doi:10.1016/j.rse.2013.08.030.
31. Rice, C.; Wilson, B.N.; Appleman, M. Soil topography measurements using image processing techniques. *Comput. Electron. Agric.* **1988**, *3*, 97–107. doi:10.1016/0168-1699(88)90015-4.
32. Eltz, F.L.F.; Norton, L.D. Surface roughness changes as affected by rainfall erosivity, tillage, and canopy cover. *Soil Sci. Soc. Am. J.* **1997**, *61*, 1746–1755.
33. Nouwakpo, S.K.; Huang, C.H. A Simplified Close-Range Photogrammetric Technique for Soil Erosion Assessment. *Soil Sci. Soc. Am. J.* **2012**, *76*, 70. doi:10.2136/sssaj2011.0148.
34. Raper, R.L.; Grift, T.E.; Tekeste, M.Z. A Portable Tillage Profiler for Measuring Subsoiling Disruption. *Trans. ASAE* **2004**, *47*, 23–27. doi:10.13031/2013.15861.
35. Arvidsson, J.; Bölenius, E. Effects of soil water content during primary tillage - laser measurements of soil surface changes. *Soil Tillage Res.* **2006**, *90*, 222–229. doi:10.1016/j.still.2005.09.005.
36. Jensen, T.; Green, O.; Munkholm, L.J.; Karstoft, H. Fourier and granulometry methods on 3D images of soil surfaces for evaluating soil aggregate size distribution. *Appl. Eng. Agric.* **2016**, *32*, 609–615. doi:10.13031/aea.32.10938.
37. Huang, C.H.; Bradford, J.M. Portable Laser Scanner for Measuring Soil Surface Roughness. *Soil Sci. Soc. Am. J.* **1990**, *54*, 1402. doi:10.2136/sssaj1990.03615995005400050032x.
38. Huang, C.; Bradford, J. Applications of a laser scanner to quantify soil microtopography. *Soil Sci. Soc. Am. J.* **1992**, *56*, 14–21. doi:10.2136/sssaj1992.03615995005600010002x.
39. Warner, W.S. Mapping a three-dimensional soil surface with hand-held 35 mm photography. *Soil Tillage Res.* **1995**, *34*, 187–197. doi:10.1016/0167-1987(95)00462-2.
40. Rieke-Zapp, D.H.; Nearing, M.A. Digital close range photogrammetry for measurement of soil erosion. *Photogramm. Rec.* **2005**, *20*, 69–87. doi:10.1111/j.1477-9730.2005.00305.x.

41. Taconet, O.; Ciarletti, V. Estimating soil roughness indices on a ridge-and-furrow surface using stereo photogrammetry. *Soil Tillage Res.* **2007**, *93*, 64–76. doi:10.1016/j.still.2006.03.018.
42. Gilliot, J.M.; Vaudour, E.; Michelin, J. Soil surface roughness measurement: A new fully automatic photogrammetric approach applied to agricultural bare fields. *Comput. Electron. Agric.* **2017**, *134*, 63–78. doi:10.1016/j.compag.2017.01.010.
43. Nyord, T.; Kristensen, E.F.; Munkholm, L.J.; Jørgensen, M.H. Design of a slurry injector for use in a growing cereal crop. *Soil Tillage Res.* **2010**, *107*, 26–35. doi:10.1016/j.still.2010.01.001.
44. Manevski, K.; Børgesen, C.D.; Andersen, M.N.; Kristensen, I.S. Reduced nitrogen leaching by intercropping maize with red fescue on sandy soils in North Europe: A combined field and modeling study. *Plant Soil* **2015**, *388*, 67–85. doi:10.1007/s11104-014-2311-6.
45. Olesen, J.E.; Askegaard, M.; Rasmussen, I.A. Design of an organic farming crop-rotation experiment. *Acta Agric. Scand. Sect. B Soil Plant Sci.* **2000**, *50*, 13–21. doi:10.1080/090647100750014367.
46. Pandey, A.; Li, F.; Askegaard, M.; Rasmussen, I.A.; Olesen, J.E. Nitrogen balances in organic and conventional arable crop rotations and their relations to nitrogen yield and nitrate leaching losses. *Agric. Ecosyst. Environ.* **2018**, *265*, 350–362. doi:10.1016/j.agee.2018.05.032.
47. De Jonge, L.W.; Sommer, S.G.; Jacobsen, O.H.; Djurhuus, J. Infiltration of slurry liquid and ammonia volatilization from pig and cattle slurry applied to harrowed and stubble soils. *Soil Sci.* **2004**, *169*, 729–736. doi:10.1097/01.ss.0000146019.31065.ab.
48. Chen, Y.; Munkholm, L.J.; Nyord, T. A discrete element model for soil–sweep interaction in three different soils. *Soil Tillage Res.* **2013**, *126*, 34–41. doi:10.1016/j.still.2012.08.008.
49. Soil Survey Staff. 2009. *Soil Survey Field and Laboratory Methods Manual. Soil Survey*; Investigations Report No. 51, Version 1.0. R. Burt (ed.). U.S. Department of Agriculture, Natural Resources Conservation Service.
50. Jensen, T.; Munkholm, L.; Green, O.; Karstoft, H. A mobile surface scanner for soil studies. In Proceedings of the Second International Conference on Robotics, Associated High-Technologies and Equipment for Agriculture and Forestry—RHEA 2014, pp. 187–194.
51. Znova, L.; Melander, B.; Lisowski, A.; Klonowski, J.; Chlebowski, J.; Edwards, G.T.; Kirkegaard Nielsen, S.; Green, O. A new hoe share design for weed control: measurements of soil movement and draught forces during operation. *Acta Agric. Scand. Sect. B Soil Plant Sci.* **2018**, *68*, 139–148. doi:10.1080/09064710.2017.1367837.
52. Solhjou, A.; Fielke, J.M.; Desbiolles, J.M. Soil translocation by narrow openers with various rake angles. *Biosyst. Eng.* **2012**, *112*, 65–73.
53. Shmulevich, I. State of the art modeling of soil-tillage interaction using discrete element method. *Soil Tillage Res.* **2010**, *111*, 41–53. doi:10.1016/j.still.2010.08.003.
54. Hafner, S.D.; Pacholski, A.; Bittman, S.; Burchill, W.; Bussink, W.; Chantigny, M.; Carozzi, M.; Génermont, S.; Häni, C.; Hansen, M.N.; et al. The ALFAM2 database on ammonia emission from field-applied manure: Description and illustrative analysis. *Agric. Forest Meteorol.* **2018**, *258*, 66–79. doi:10.1016/j.agrformet.2017.11.027.
55. Webb, J.; Pain, B.; Bittman, S.; Morgan, J. The impacts of manure application methods on emissions of ammonia, nitrous oxide and on crop response—A review. *Agric. Ecosyst. Environ.* **2010**, *137*, 39–46. doi:10.1016/j.agee.2010.01.001.
56. Rochette, P.; Guilmette, D.; Chantigny, M.H.; Angers, D.A.; MacDonald, J.D.; Bertrand, N.; Parent, L.É.; Côté, D.; Gasser, M.O. Ammonia volatilization following application of pig slurry increases with slurry interception by grass foliage. *Can. J. Soil Sci.* **2008**, *88*, 585–593. doi:10.4141/CJSS07083.
57. Häni, C.; Sintermann, J.; Kupper, T.; Jocher, M.; Neftel, A. Ammonia emission after slurry application to grassland in Switzerland. *Atmos. Environ.* **2016**, *125*, 92–99. doi:10.1016/j.atmosenv.2015.10.069.
58. Khorashahi, J.; Byler, R.K.; Dillaha, T.A. An opto-electronic soil profile meter. *Comput. Electron. Agric.* **1987**, *2*, 145–155. doi:10.1016/0168-1699(87)90025-1.

Chapter 2

Miscellaneous findings

Experiment	Soil type	Crops	Dry bulk density [g cm^{-3}]	Water content [g g^{-1}]	1:1 water pH
19D	Loamy sand	Winter wheat	1.28 (0.03)	0.13 (0.01)	5.94
19E				0.12 (0.01)	
19G		Spring barley	1.47 (0.07)	0.16 (0.01)	NA
20A	Sandy loam	Winter wheat	1.62 (0.1)	0.15 (0.01)	6.52
20B				0.13 (0.02)	6.62
20C	Coarse sand	Clover grass	1.27 (0.03)	0.10 (0.02)	5.94
20D			1.39 (0.06)	0.18 (0.02)	6.01

Table 2.1: *Soil properties. Standard deviations are displayed in parentheses (n = 3).*

	5 h average [°C]	24 h average [°C]	Total average [°C]
19D	6.9	5.0	10.5
19E	13.9	12.0	12.0
19G	14.4	11.5	11.4
20A	10.4	6.5	7.4
20B	16.4	10.4	8.4
20C	18.92	14.28	11.99
20D	13.74	16.24	14.28

Table 2.2: *Average ambient air temperature.*

Experiment	Acidified	Application rate [kg m^{-2}]	Application rate [g NH_4-N m^{-2}]	Dry matter [%]	Total N [g L^{-1}]	Ammoniacal N [g L^{-1}]	Viscosity [cP]	pH
19D	No	3	8.40 (0.24)	6.45 (0.01)		2.80 (0.08)	NA	6.11 (0.02)
19E	No	3	8.87 (0.92)	6.14 (0.09)		2.96 (0.31)	NA	6.06 (<0.01)
19G	No	2.28	3.53 (1.59)	4.93 (0.37)		1.55 (0.07)	NA	7.77 (0.04)
20A	No	3	10.57 (0.77)	3.27 (<0.01)	4.16 (0.05)	3.52 (0.26)	106 (14)	7.82 (0.06)
20B	No	3	11.28 (0.46)	6.46 (0.04)	4.85 (0.06)	3.76 (0.15)	1004 (79)	7.51 (0.03)
20C	No	2.5	5.92 (0.03)	5.79 (0.03)	3.50 (0.14)	2.37 (0.17)	1280 (38)	7.66 (0.01)
20C	Yes	2.3	5.99 (0.05)	5.99 (0.05)	3.53 (0.03)	2.50 (0.19)	1231 (49)	7.30 (0.07)
20D	No	2.5	5.87 (0.04)	5.87 (0.04)	3.54 (0.07)	2.41 (<0.01)	1946 (43)	7.56 (0.01)
20D	Yes	2.5	5.96 (0.12)	5.96 (0.12)	3.66 (0.03)	2.45 (<0.01)	2311 (174)	7.28 (0.04)

Table 2.3: *Slurry properties of pig manure. Standard deviations are displayed in parenthesis (n = 2)*